

---

# Transcriptional regulation of *RAM1*, a central regulator of arbuscule branching in arbuscular mycorrhiza symbiosis

---

Priya Pimprikar

Dissertation an der Fakultät für Biologie der  
Ludwig-Maximilians-Universität München



München, 2018



Dissertation eingereicht am: 15.02.2018

Tag der mündlichen Prüfung: 19.07.2018

**Erstgutachter: Prof. Dr. Caroline Gutjahr**

**Zweitgutachter: Prof. Dr. Martin Parniske**



### Eidesstattliche Versicherung

Ich versichere hiermit an Eides statt, dass die vorgelegte Dissertation von mir selbstständig und ohne unerlaubte Hilfe angefertigt ist.

München, den

Priya Pimprikar

14.02.18

### Erklärung

Hiermit erkläre ich, dass die Dissertation nicht ganz oder in wesentlichen Teilen einer anderen Prüfungskommission vorgelegt worden ist. Ich habe nicht versucht, anderweitig eine Dissertation einzureichen oder mich einer Doktorprüfung zu unterziehen.

München, den

Priya Pimprikar

14.02.18



## Table of Contents

I.	List of Abbreviations	8
II.	List of Publications	10
III.	Declaration of contribution as co-author	11
IV.	Summary	14
V.	Zusammenfassung	16
VI.	Introduction	
	1. Arbuscular mycorrhiza (AM) symbiosis	19
	2. AM development	
	i. Pre-contact phase	20
	ii. Hyphopodium formation	20
	iii. Formation of intraradical hyphae	21
	iv. Arbuscule development and degeneration	22
	3. Function of AM	24
	4. Cellular changes during AM development	26
	5. Signal transduction during AM development	27
	6. Transcriptional changes during AM development	32
	7. Genes required during AM development	
	i. Genes required for hyphopodium formation	33
	ii. Genes required for mature arbuscule development	33
	iii. Genes required for arbuscule degeneration	35
	iv. Genes regulating the amounts of colonization	36
VII.	Aims of the Thesis	39
VIII.	Results	
	1. Paper I:	40
	A CcMK-CYCLOPS-DELLA complex activates transcription of <i>RAM1</i> to regulate arbuscule branching	
	2. Paper II:	80
	Lipid transfer from plants to arbuscular mycorrhiza fungi	
IX.	General Discussion	145
X.	Outlook	156
XI.	References	158
XII.	List of figures	176
XIII.	List of Tables	176
XIV.	Acknowledgements	177
XV.	Curriculum Vitae	180
XVI.	Permission for republishing	185

## I. List of Abbreviations

ABC	ATP Binding Cassette
AM	Arbuscular Mycorrhiza
AMT	Ammonium Transporter
BCP1	Blue Copper Protein 1
BiFC	Bimolecular Fluorescence Complementation
CaMV	Cauliflower Mosaic Virus
CaM	Calmodulin
Ca <sup>2+</sup>	Calcium ion
CCaMK	Calcium- and Calmodulin-dependent protein Kinase
CNGC	Cyclic Nucleotide-Gated Channels
COs	Chitin Oligomers
CoIP	Co immunoprecipitation
ChIP	Chromatin immunoprecipitation
CP3	Cysteine Protease 3
<i>dis</i>	<i>disorganized</i>
DIP	DELLA INTERACTING PROTEIN
D14L	DWARF 14 LIKE
D53	DWARF 53
ER	Endoplasmic Reticulum
EXO	Exocyst
FAS	Fatty Acid Synthase
FA	Fatty Acid
GA	Gibberellic Acid
GFP	Green Fluorescent Protein
GID1	Gibberellin-Insensitive Dwarf-1
GPAT	Glycerol 3-phosphate Acyl Transferase
GSE	Geminating Spore Exudates
HMGR	3-Hydroxy-3-Methylglutaryl coenzyme A Reductase
KAI	Karrikin Insensitive
LCOs	Lipo-chito-oligosaccharides
LOM	Lost Meristems
Lj	<i>Lotus japonicus</i>
LYK10	LysM Receptor-like Kinase 10
MAMI	Meristem And Mycorrhiza Induced
MAX	More Axillary Growth
MAG	Monoacylglycerol

MCA	Medicago truncatula calcium ATPase
MIG1	Mycorrhiza Induced GRAS 1
miR	microRNA
MST	Monosaccharide Transporter
Mt	<i>Medicago truncatula</i>
NARK	Nodulation Autoregulation Receptor Kinase
NFP	Nod Factor Protein
NFR	Nod Factor Receptor
NIN	Nodule Inception
NLS	Nuclear Localization Signal
NMR	Nuclear Magnetic Resonance
NSP	Nodulation Signaling Pathway
NUP	Nucleoporins
Os	<i>Oryza sativa</i>
PAM	Peri-arbuscular Membrane
PAS	Peri-arbuscular Space
PLT	Polyol Transporter
Ph	<i>Petunia hybrida</i>
PPA	Pre-penetration Apparatus
PT	Phosphate Transporter
qPCR	quantitative Polymerase Chain Reaction
RAD	Required for Arbuscule Development
RAM	Reduced Arbuscular Mycorrhiza
<i>red</i>	<i>reduced and degenerate</i>
RNS	Root Nodule Symbiosis
RNAi	RNA interference
SLs	Strigolactones
SMAX	Suppressor of MAX2
STP	Monosaccharide Transporter
SYMRK	Symbiosis Receptor Kinase
TAG	Triacylglycerol
VAMP	Vesicle-Associated Membrane Protein
Vpy	Vapyrin
YFP	Yellow Florescent Protein
Y2H	Yeast-2-Hybrid assay

## II. List of Publications

### Research Papers

- Keymer A#, **Pimprikar P**#, Wewer V, Huber C, Brands M, Bucerius SL, Delaux PM, Klingl V, von Roepenack-Lahaye E, Wang TL, Eisenreich W, Dörmann P, Parniske M, Gutjahr C (2017). Lipid transfer from plants to arbuscular mycorrhiza fungi. *eLife* 6. pii: e29107.

# equal contribution

- **Pimprikar P**, Carbonnel S, Paries M, Katzer K, Klingl V, Bohmer MJ, Karl L, Floss DS, Harrison MJ, Parniske M, Gutjahr C (2016). A CCaMK-CYCLOPS-DELLA complex activates transcription of *RAM1* to regulate arbuscule branching. *Current Biology* 26: 987-998

### Reviews

- **Pimprikar P** and Gutjahr C (2018). Transcriptional regulation of arbuscular mycorrhiza development. *Plant Cell Physiology*.  
[doi.org/10.1093/pcp/pcy024](https://doi.org/10.1093/pcp/pcy024)

### III. Declaration of contribution as co-author

**Paper I:** A CCaMK-CYCLOPS-DELLA complex activates transcription of *RAM1* to regulate arbuscule branching

Reference: **Pimprikar P**, Carbonnel S, Paries M, Katzer K, Klingl V, Bohmer MJ, Karl L, Floss DS, Harrison MJ, Parniske M, Gutjahr C (2016). A CCaMK-CYCLOPS-DELLA complex activates transcription of *RAM1* to regulate arbuscule branching. *Current Biology* 26: 987-998

Priya Sunil Pimprikar

-designed, performed and analysed most of the experiments, created the figures and contributed to the conception of the study except the following

- Samy Carbonnel performed experiments corresponding to figure 3B, S2, and S3
- Samy Carbonnel performed all the statistics wherever required throughout the paper
- Leonhard Karl generated preliminary data for Figure 6A.
- Monica J. Bohmer contributed transgenic roots and cloning of promoter deletion plasmids and one biological replicate for the left graph of Figure 7A under the supervision of Priya S. Pimprikar
- Michael Paries performed hairy root transformation and analysis for figure 2D and 5E, transactivation assay and analysis for 7A and S7 under the supervision of Priya S. Pimprikar.
- Dr. Katja Katzer performed and analyzed the experiment corresponding to figure 7C
- Verena Klingl performed yeast transformation and drop test for Figure 6C and S6A and supported some other experiment by cloning, hairy root transformation and cDNA preparation under the supervision of Priya S. Pimprikar.
- Dr. Daniela S. Floss and Prof. Dr. Maria J. Harrison contributed Figure S6B.
- Prof. Dr. Martin Parniske contributed materials and contributed to the conception of the study and editing the manuscript.
- Prof. Dr. Caroline Gutjahr identified the *ram1-3* mutation in NGS data, conceived the study, designed experiments, supervised the study, and wrote the manuscript.

Signature of first author,  
Priya Pimprikar  
14.02.18

Signature of the Supervisor,  
Prof. Dr. Caroline Gutjahr  
14.02.18

## **Paper II: Lipid transfer from plants to arbuscular mycorrhiza fungi**

Reference: Keymer A#, **Pimprikar P#**, Wewer V, Huber C, Brands M, Bucerius SL, Delaux PM, Klingl V, von Roepenack-Lahaye E, Wang TL, Eisenreich W, Dörmann P, Parniske M, Gutjahr C (2017). Lipid transfer from plants to arbuscular mycorrhiza fungi. eLife 6. pii: e29107.

# equal contribution

Priya Sunil Pimprikar:

-designed, performed, analyzed and created figures for the following experiments

- Identification of mutation in the *RAM2* gene by map-based cloning and Sanger sequencing (Figure supplement 3 and 4 corresponding to Figure 1)
- Arbuscule phenotype of *ram2-1* and *ram2-2* and complementation of *ram2-1* mutant (Figure 1B)
- Activity of *DIS* and *RAM2* promoter (Figure 2A and 2B; Video 1, 2, 3, 4, 5 and 6)
- *DIS* and *RAM2* promoter activity in the wild type, *dis* and *ram2* mutants (Figure supplement 2B, 2C and 2D corresponding to Figure 2)

-Provided cDNA samples for the quantitative PCR analysis of Figure 6

-wrote materials and methods corresponding to the following section

- Identification of *RAM2* by map-based cloning and Sanger sequencing
- Microscopy

Signature of co-first author,  
Andreas Keymer  
14.02.18

Signature of co-first author,  
Priya Pimprikar  
14.02.18

Signature of the Supervisor,  
Prof. Dr. Caroline Gutjahr  
14.02.18

#### IV. Summary

Arbuscular mycorrhiza (AM) is an ancient symbiosis, established between 80% of land plants and obligate biotrophic fungi belonging to the class glomeromycotina. AM is an essential component in natural ecosystems, as it plays a major role in the global carbon cycle, enhances plant growth in nutrient deficient soil and is thus believed to sustain whole environ such as tropical rain forests. It also has a great fertilizing potential for sustainable practices in agriculture. Crucial for this symbiosis is the formation of highly branched tree-like structures called arbuscules by the fungus, inside root cortical cells of the host plant. These fungal structures deliver mineral nutrients after taking them up from the soil via extraradical hyphae, mainly phosphate and nitrogen, which are difficult to access for the plant. In turn, the fungus receives up to 20% of photosynthetically fixed carbon. Arbuscule formation is accompanied by massive transcriptional changes in the colonized cell. In addition, the cell undergoes subcellular rearrangements to accommodate the arbuscule. This is associated with the formation of a plant-derived membrane, called peri-arbuscular membrane, which surrounds the arbuscule and separates the fungal hyphae from the plant cytoplasm. The well-ordered and complex AM developmental steps, are regulated by the plant and depend on its nutritional status.

Although arbuscule development is crucial for this symbiosis, the molecular basis of its development is poorly understood. A *Lotus japonicus* plant mutant *reduced and degenerate arbuscules (red)* found in a former study by forward genetics screen is perturbed in arbuscule development. To identify plant genes essential for arbuscule development, we investigated genes perturbed in *red*. Rough mapping indicated presence of two mutations in *red*, causative for the arbuscule phenotype. Complementation analysis confirmed causative mutations in a gene encoding a GRAS-type transcription factor named REDUCED ARBUSCULAR MYCORRHIZA 1 (RAM1) and in a gene encoding a lipid biosynthesis enzyme GLYCEROL 3-PHOSPHATE ACYL TRANSFERASE 6 (GPAT6/RAM2).

In this doctoral thesis, I found that the AM symbiosis-specifically induced gene *RAM1*, is a principal regulator of arbuscule development. It is directly regulated by a complex of CYCLOPS and DELLA. CYCLOPS, is a DNA-binding transcription factor and a central regulator of symbiotic signaling and DELLA is a negative regulator of hormonal gibberellic acid (GA) signaling. The CYCLOPS-DELLA complex activates *RAM1* expression via binding of CYCLOPS to a novel *cis*-element in the *RAM1* promoter. Thus, we presented for the first time a target gene of CYCLOPS in AM symbiosis and a regulatory node integrating symbiosis

(CYCLOPS) and hormonal GA signaling (DELLA). This direct connection may be important for the plant to connect symbiosis with its nutritional and therefore physiological status. Further, I revealed that RAM1 acts as a transcriptional activator of genes required for AM development, downstream of *CCaMK* and *CYCLOPS*. Ectopic expression of *RAM1* induced AM-specific genes such as *RAM2* in absence of AM-fungi. In frame of another thesis, they showed that *RAM2* participate in an AM-specific lipid biosynthesis pathway and is essential for arbuscule development. *RAM2* acts downstream of another lipid biosynthetic gene *DIS* (encoding  $\beta$ -keto-acyl ACP synthase I), which is also indispensable for arbuscule development. *RAM2* uses C16:0 fatty acids synthesized by *DIS* as substrates for synthesis of  $\beta$ -monoacylglycerol. C16:0 is the predominant form of fatty acid found in AM fungi. Textbook knowledge exhibited carbohydrate as the only form of carbon supplied to the AM fungus, which is subsequently used to synthesis lipids. However, whole genome sequence analysis indicated that AM fungi lack genes encoding protein responsible for the *de novo* synthesis of C16:0 fatty acid. They further showed that the lipid containing C16:0 fatty acid synthesized by *RAM2* is supplied to AM-fungi as a plant-derived carbon source.

Arbuscule development can be conceptually divided into distinct steps by plant mutants, indicating that the respective gene product regulates the step-wise development of arbuscule. Accumulating evidences indicate transcriptional changes during arbuscule development occurs in successive but overlapping waves. For example, genes upregulated in the arbuscule containing cells might be also activated in neighboring cells preparing to accommodate arbuscule. These cells undergoing subcellular rearrangement forming a pre-penetration apparatus (PPA) do not have visible fungal structures. Transcriptomic analysis from cells containing only visible fungal structure, limit to relate the gene activation to individual stages of arbuscule development and PPA formation. To correlate the promoter activity of genes with the precise stages of arbuscule development, I designed a construct which allows visualization of the fungus in living roots due to accumulation of fluorescent protein mCherry in the apoplastic space surrounding the fungal hyphae. AM specific *SbtM1* promoter used to drive *mCherry* is active across all stages of arbuscule development including cells undergoing rearrangement to form PPA. Using this construct, I showed that *DIS* and *RAM2* promoters are activated during all the stages of arbuscule maturation, but become inactive during arbuscule degeneration.

## V. Zusammenfassung

Arbuskuläre Mykorrhiza (AM) ist eine evolutionär alte Symbiose, die zwischen 80% aller Landpflanzen und den obligat-biotrophen Pilzen der *Glomeromycotina* ausgebildet wird. Sie leistet einen entscheidenden Beitrag für natürliche Ökosysteme indem sie eine wichtige Rolle im globalen Kohlenstoffkreislauf einnimmt und Pflanzenwachstum in nährstoffarmen Böden verbessert. Somit wird angenommen, dass die arbuskuläre Mykorrhiza Symbiose ganze Lebensräume, wie zum Beispiel Regenwälder, aufrechterhält. Darüber hinaus bietet AM ein großes Potential für die zusätzliche Nährstoffzufuhr in der nachhaltigen Landwirtschaft. Entscheidend für die Symbiose ist die Ausbildung der Arbuskel. Hierbei handelt es sich um stark-verzweigte baumförmige Strukturen des Pilzes, welche in den Wurzeln der Wirtspflanze - im Inneren der Kortexzellen - ausgebildet werden. Jene Strukturen liefern der Pflanze Mineralstoffe - insbesondere Phosphat und Nitrat – nachdem diese von den extraradikalen Hyphen aus dem Boden aufgenommen wurden. Im Gegenzug erhält der Pilz bis zu 20% des mittels Photosynthese gebundenen pflanzlichen Kohlenstoffs. Die Ausbildung der Arbuskel geht mit drastischen transkriptionellen Veränderungen der kolonisierten Zellen einher. Zusätzlich findet eine subzelluläre Umstrukturierung der Zelle statt, um den Arbuskel zu beherbergen. Diese Umstrukturierung steht in Verbindung mit dem Aufbau der periarbuskulären Membran. Diese Membran pflanzlichen Ursprungs umhüllt den Arbuskel und separiert die Hyphen des Pilzes vom Zytoplasma der Pflanzenzelle. Die wohlgeordneten und komplexen Entwicklungsabschnitte der arbuskulären Mykorrhiza innerhalb der Wurzel werden von der Pflanze reguliert und hängen von deren Nährstoffbedarf ab.

Wenngleich die Entwicklung der Arbuskel entscheidend für diese Symbiose ist, sind ihre molekularen Grundlagen bisher kaum verstanden. Eine *Lotus japonicus* Mutante „*reduced and degenerate arbuscules*“ (*red*), welche in einem vorwärts gerichteten genetischen Screen gefunden wurde, ist in der Arbuskelverzweigung beeinträchtigt. Um Gene zu identifizieren, die entscheidend für die Arbuskelentwicklung sind, suchte ich nach den Mutationen in *red*. Eine grobe Genkartierung weist auf zwei Mutationen in *red* hin, die den Arbuskelphänotyp der Mutante verantworten. Komplementierungsstudien bestätigten die verursachenden Mutationen. Eines der Gene kodiert für REDUCED ARBUSCULAR MYCORRHIZA 1 (RAM1), aus der Familie der GRAS-Transkriptionsfaktoren. Das andere kodiert für das Lipidbiosynthese Enzym GLYCEROL 3-PHOSPHATE ACYL TRANSFERASE 6 (GPAT6) RAM2.

In dieser Doktorarbeit fand ich heraus, dass das symbiose-spezifisch induzierte Gen *RAM1* einen bedeutenden Regulator der Arbuskelentwicklung darstellt und direkt durch einen Komplex aus *CYCLOPS* und *DELLA* reguliert wird. *CYCLOPS* ist ein DNA-bindender Transkriptionsfaktor und ein zentrales Mitglied der symbiotischen Signaltransduktionskette. *DELLA* stellt einen negativen Regulator der Signalübertragung des Pflanzenhormons Gibberellin (GA) dar. Der *CYCLOPS-DELLA* Komplex aktiviert die *RAM1* Expression mittels Bindung von *CYCLOPS* an ein neues *cis*-Element innerhalb des *RAM1* Promoters. Damit gelang es uns nicht nur erstmals ein Zielgen von *CYCLOPS* in der AM Symbiose zu entdecken, sondern auch einen regulatorischen Knotenpunkt, der den Symbiose-Signalweg (*CYCLOPS*) mit einem Hormonsignalweg (*DELLA*) verknüpft, zu finden. Diese unmittelbare Verknüpfung ist womöglich für die Pflanze relevant, um die Symbiose auf die Nährstofflage und somit auf den physiologischen Zustand der Pflanze abzustimmen. Darüber hinaus konnte ich herausfinden, dass *RAM1* als transkriptioneller Aktivator für AM-entwicklungsbestimmende Gene fungiert, welche *CCaMK* und *CYCLOPS* nachgelagert sind. Ektopische Expression von *RAM1* induziert AM-spezifische Gene wie zum Beispiel *RAM2* in Abwesenheit des Pilzes. In Rahmen einer anderen Arbeit konnte gezeigt werden, dass *RAM2* Teil des AM-spezifischen Lipidbiosynthesewegs und unerlässlich für die Arbuskelentwicklung ist. *RAM2* agiert unterhalb eines weiteren Lipidbiosynthesegens *DIS* (kodierend für eine  $\beta$ -keto-acyl ACP Synthase I), welches ebenfalls für die Arbuskelentwicklung wesentlich ist. *RAM2* verwendet von *DIS* hergestellte C16:0 Fettsäuren als Substrat für die Synthese von  $\beta$ -Monoacylglycerol. In AM-Pilzen sind vorwiegend C16:0 Fettsäuren zu finden. Jedoch deuteten Genomsequenzierungen darauf hin, dass arbuskulären Mykorrhizapilzen die Gene fehlen, welche Proteine für die *de novo* Synthese von C16:0 Fettsäuren kodieren. Fachbuchwissen führte bisher Kohlenhydrate als einzige Form des Kohlenstoffs an, welcher dem Pilz zur Verfügung gestellt und im Pilz als Kohlenstoffquelle für die Lipidsynthese verwendet wird. Darüber hinaus konnte in jener Arbeit gezeigt werden, dass C16:0 Fettsäuren enthaltende Lipide, die von *RAM2* hergestellt werden, AM-Pilzen als zusätzliche Kohlenstoffquelle pflanzlichen Ursprungs dienen.

Die Entwicklung der Arbuskeln kann mit Hilfe von Pflanzenmutanten konzeptionell in getrennte Abschnitte eingeteilt werden. Dies weist darauf hin, dass das Produkt eines entsprechenden Genes die stufenweise Entwicklung des Arbuskels kontrolliert. Sich häufende Hinweise legen nahe, dass sich während der Arbuskelentwicklung transkriptionelle Änderungen in Zellen des inneren Kortexes in aufeinanderfolgenden aber dennoch überlappenden Wellen ereignen. Beispielsweise können Gene, die in einer Arbuskel-beherbergenden Zelle

hochreguliert sind, auch in benachbarten Zellen aktiviert sein um auf die bevorstehende Kolonisierung vorzubereiten. Die Zellen, welche diese Umstrukturierung und Ausbildung des Prä-Penetrationsapparats (PPA) erfahren, zeigen keinerlei Anwesenheit von erkennbaren pilzlichen Strukturen. Transkriptomanalysen von erkennbar Pilz-bergenden Zellen, limitieren die Aussagekraft der Verknüpfung von Genaktivierung mit den einzelnen Abschnitten der Arbuskelentwicklung, unter Einbezug der PPA Ausbildung. Um die Promoteraktivität von Genen auf einzelne Entwicklungsabschnitte der Arbuskel beziehen zu können, habe ich zum ersten Mal ein Konstrukt angewandt, das die Visualisierung des Pilzes in lebenden Wurzeln ermöglicht. Dies geschieht durch die Akkumulation des Fluorophors mCherry im Appoplasten, welcher die Pilzhyphen umgibt. Der AM-spezifische *SbtM1* Promoter, der verwendet wurde um *mCherry* zu exprimieren, ist in allen Teilabschnitten der Arbuskelentwicklung aktiviert - auch in jenen Zellen, die für die PPA-Ausbildung umstrukturiert werden. Unter Verwendung dieses Konstrukts zeigte ich, dass sowohl der *DIS* als auch der *RAM2* Promotor in allen Abschnitten der Arbuskelreifung aktiviert wird. Während der Degeneration der Arbuskeln sind jedoch beide Promotoren inaktiv.

## **VI. Introduction**

### **1. Arbuscular mycorrhiza symbiosis**

Arbuscular mycorrhiza (AM) symbiosis is established between 70-90% of land plants and fungi belonging to monophyletic phylum glomeromycotina (Parniske 2008, Spatafora et al. 2016). AM is one of the plant adaptations to enhance the mineral nutrients acquisition, mainly phosphate, from the poor nutrient soil via the vast fungal network (Carbonnel and Gutjahr 2014). The AM structures were discovered in a fossil of an early Devonian land plant suggesting AM existed more than 400 million years ago and might have played a role in the origin of land plants (Remy et al. 1994). In exchange of mineral nutrients, the plant provide up to 20% of photosynthetically fixed carbon (Bago et al. 2000, Smith and Read 2008, Smith and Smith 2011, Jiang et al. 2017, Keymer et al. 2017, Luginbuehl et al. 2017, Roth and Paszkowski 2017). Phosphate is a macronutrient essential for the plant growth and development (Carbonnel and Gutjahr 2014). The total pool of phosphate available in the soil may be high, often present in inaccessible form or not reachable by the plant roots. Up to 20 to 80% of phosphate available in soil is found in organic form (Richardson 1994). The concentration of inorganic phosphate rarely exceeds 10 $\mu$ M, the most readily accessed by plants (Bielecki 1973). After nitrogen, phosphate is second major limiting macronutrient for plant growth and development. In addition to AM symbiosis, to enhance the uptake of the available phosphate in deficient condition, plants have inducible high-affinity phosphate transporters (Smith 2002) and can change the root architecture (Watt and Evans 1999, Williamson et al. 2001). AM symbiosis also plays a vital role in global carbon cycle as approximately, 5 billion tons of carbon per year is anticipated to be consumed by AM fungi (Parniske 2008) thereby sequestering the atmospheric carbon dioxide to the soil organic carbon (Bago et al. 2000). In addition to the nutrient supply, the mycorrhizal fungus enhances the fitness of the host plant by enhancing the abiotic (drought, salinity or heavy metals) and biotic (leaf pathogens) stress resistance (Augé 2001, Ruiz-Lozano 2003, Göhre and Paszkowski 2006, Liu et al. 2007, Gianinazzi et al. 2010).

### **2. Arbuscular mycorrhiza development**

The host plant controls the development of AM depending on its phosphate status (Carbonnel and Gutjahr 2014). For example, at high phosphate availability, plant favors direct and non-symbiotic uptake by the root system and inhibits symbiotic

uptake of phosphate via AM symbiosis (Balzergue et al. 2010, Breuillin et al. 2010, Carbonnel and Gutjahr 2014). Thus, it is a plant strategy to limit plant derived carbon consumption of the AM fungi by inhibiting its development in the roots in a phosphate sufficient condition. Despite of broad range of plant and fungal species involved, the AM development stages are relatively similar. Extensive forward and reverse genetic studies in the model legumes *Medicago truncatula* and *Lotus japonicus* led to discovery of the genes and stages involved in the AM development (MacLean et al. 2017). The AM development can be divided into four distinct stages: Pre-contact stage, hyphopodium formation, intraradical hyphae formation, arbuscule development and degeneration (Gutjahr and Parniske 2013). However, AM development being an asynchronous process, different AM development steps exists in the same root system simultaneously.

#### **i. Pre-contact phase**

A reciprocal exchange of diffusible signaling molecule between the host plant and AM fungi takes place in the pre-symbiotic stage (MacLean et al. 2017) (Figure 1). Plant roots exude strigolactones (SLs) in phosphate deficient conditions (Yoneyama et al. 2007, Kretschmar et al. 2012, Yoneyama et al. 2012) (Figure 1). SLs induces fungal spore germination, enhance metabolic activity and hyphal growth and branching (Buée et al. 2000, Akiyama et al. 2005, Besserer et al. 2006, Yoneyama et al. 2007, Besserer et al. 2008). SLs are carotenoid-derived plant phytohormones discovered to act as germination stimulants for a parasitic weeds such as *Striga lutea* (Cook et al. 1966, Cook et al. 1972). In return, the AM fungi growing towards the host root, secrete diffusible signaling molecule(s) called Myc Factors (MacLean et al. 2017) (Figure 1). Myc Factors activates certain plant responses, such as transcriptional activation of plant genes (Kosuta et al. 2003, Navazio et al. 2007, Kuhn et al. 2010, Mukherjee and Ané 2010, Ortu et al. 2012), nuclear calcium spiking (Kosuta et al. 2008, Chabaud et al. 2011, Sun et al. 2015), starch accumulation (Gutjahr et al. 2009) and lateral root formation (Olah et al. 2005, Mukherjee and Ané 2010, Sun et al. 2015). The Myc Factors are shown to be a mixture of short-chain chitin oligomers (Myc-COs) and lipochitooligosaccharides (Myc-LCOs) (Maillet et al. 2011, Genre et al. 2013). The Myc-LCOs are structurally very similar to Nod Factors, secreted by the rhizobial bacteria that forms root nodule symbiosis (RNS) with legumes (Oldroyd and Downie 2004, Maillet et al. 2011).

#### **ii. Hyphopodium formation**

Upon reaching the host root surface, the fungal hypha differentiates to form an attachment structure called hyphopodium (Figure 1) (Gutjahr and Parniske 2013). Hyphopodium formation was triggered by isolated cell wall fragment of the host plant *D. carota* but not by the non-host plant *B. vulgaris* (Nagahashi and Douds 1997). Thus, a cell wall signal was sufficient and does not require an intact host root or a host-root secreted signal for hyphopodium formation (Nagahashi and Douds 1997). Cell wall composition seems to be a key factor for fungal recognition, however very little is known.

### iii. Formation of intraradical hyphae

From the hyphopodia, the fungus forms a peg-like structure in order to penetrate outer epidermal cell intracellularly as shown in *M. truncatula* (Figure 1) or between two anticlinal cell walls of two adjacent epidermal cells as shown in *M. truncatula* and *L. japonicus* (Bonfante et al. 2000, Genre et al. 2005, Genre et al. 2008). However, it has been observed that the fungal hyphae passing intercellularly, transverse intracellularly either the exodermis or the outer cortical cell layer to reach the inner cortex in *M. truncatula*, *D. carota* and *L. japonicus* (Bonfante et al. 2000, Demchenko et al. 2004, Genre et al. 2008). This obligatory step to cross intracellularly at least once, might be a check point held by the plant for controlling the root colonization. Once the fungal hyphae reach the inner cortex, it spread longitudinally in the apoplastic space and differentiate to form arbuscules in the inner cortical cells (MacLean et al. 2017) (Figure 1).

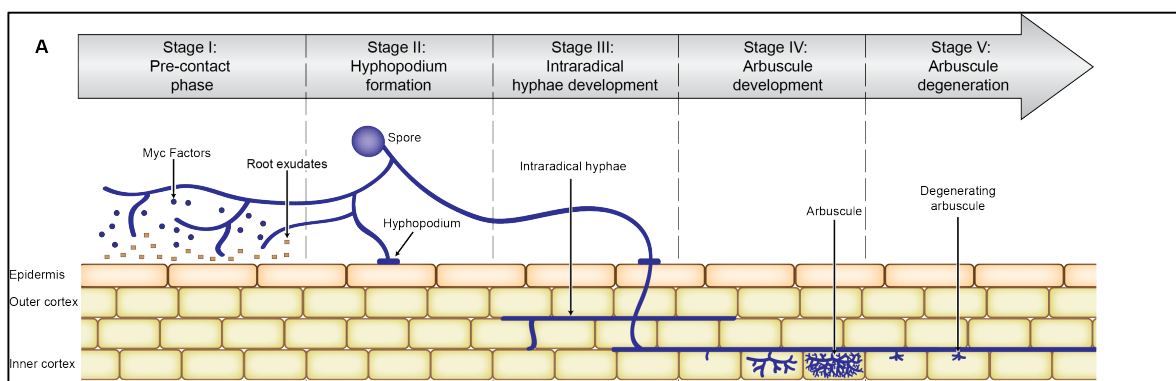


**Figure 1. Schematic representation of cell and stage specific gene expression corresponding to AM developmental stages (Figure from Pimprikar and Gutjahr 2018).**

#### iv. Arbuscule development and degeneration

The arbuscule is the primary site, where mineral nutrients are transferred to the host plant by the fungus in exchange of plant-derived carbon (Luginbuehl and Oldroyd 2017, MacLean et al. 2017) and therefore is at the heart of AM symbiosis. Fungal hyphae in the inner cortical cell layer colonize in two morphological types, called *Arum*- and *Paris*- type (Bonfante and Genre 2008). The type of colonization depends on the AM fungal and host genotype. In *Arum*-type, the hyphae spread intercellular in the apoplastic space and differentiate to forms highly branched tree-like structures termed terminal arbuscules (Bonfante and Genre 2008). The *Arum*-type colonization is found in most of the legumes, including *Lotus japonicus* (Figure 1). In *Paris*-type, the hyphae spread intracellularly and subsequently differentiate to form coils and intercalary arbuscule (Bonfante and Genre 2008). The Paris-type colonization is found in carrot (Bonfante and Genre 2008). Several intermediate morphologies ranging between *Arum*- to *Paris*- type were observed by Dickson and co-workers depending on the host plant and fungus combination (Dickson 2004). The mechanism underlying the formation of different types of arbuscule morphologies in the cortical cell layers is still unknown.

The most studied *Arum*-type arbuscule development, can be divided into six different genetically separable steps (Gutjahr and Parniske 2013, Pimprikar and Gutjahr 2018, In press) (Figure 2): (0) Unchanged cortex cell prior to PPA formation; (I) formation of the pre-penetration apparatus (PPA) in inner cortical cell; (II) the intercellular fungal hypha enters the cell and forms arbuscule trunk; (III) the arbuscule trunk subsequently differentiates to form coarse and low-order branching, forming an immature arbuscule; (IV) the immature arbuscule further undergoes branching to form thin and high-order branches, developing a mature arbuscule; (V) the mature arbuscule collapses and is subsequently degraded. The collapsed arbuscule is separated by formation of septa from the other fungal network in the root (Gutjahr and Parniske 2013, Pimprikar and Gutjahr 2018).

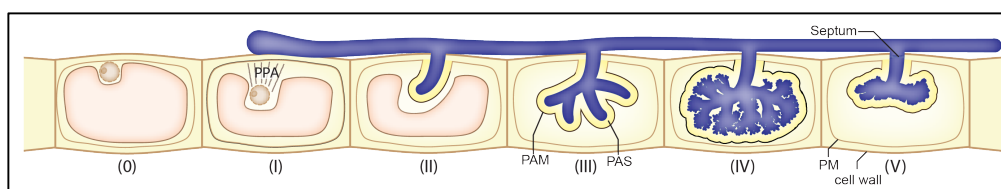


**Figure 2. Schematic representation of stages of arbuscule development (modified from Pimprikar and Gutjahr, 2018 modified from Gutjahr and Parniske., 2013). Six different stages (0 to V) of arbuscule development.**

The hyphal entry into the cortical cell at stage II of arbuscule development takes place by invagination of plant plasma membrane which is then *de novo* extended by exocytosis to envelop every hyphal branching during stage III and IV of mature arbuscule development, termed as peri-arbuscular membrane (PAM) (Figure 2) (Gutjahr and Parniske 2013). *De novo* plant synthesized PAM, prevents direct contact of the fungal hyphae with the plant cytoplasm and serves as a symbiotic interface for the nutrient exchange between the symbionts (Gutjahr and Parniske 2013) (Figure 2). The space between the fungal plasma membrane and the PAM creates an apoplastic compartment called as peri-arbuscular space (PAS) (Figure 2) (Gutjahr and Parniske 2013). Thus, the metabolites transferred between the fungus and the plant have to cross the two membranes via the PAS (Parniske 2008). Accumulation of several transporters such as; a PHOSPHATE TRANSPORTER 4 (PT4) and the heterodimer of the two half-size ATP binding cassette (ABC) transporters STR1 and -2 localize to the branch domain of the PAM in *M. truncatula* (Pumplin and Harrison 2009, Zhang et al. 2010). Revolutionary work carried out by Pumplin and co-worker showed that although the PAM is in continuum with the plant plasma membrane, it consists of the two distinct domain depending on the protein composition within the arbuscule containing cell; PAM surrounding (i) the arbuscule trunk called as trunk domain and (ii) arbuscule branching called as branch domain (Pumplin and Harrison 2009, Pumplin et al. 2012). The plant plasma membrane and the trunk domain has similar protein composition (Pumplin and Harrison 2009, Pumplin et al. 2012). For example, GFP tagged proteins localization studies during arbuscule development in *M. truncatula* revealed that BLUE COPPER PROTEIN 1 (BCP1) was exclusively localized to plant plasma membrane and trunk domain whereas the PT4 was specifically localized to the branch domain (Pumplin and Harrison 2009). Promoter and protein-GFP fusion studies revealed that the plant plasma membrane localized transporter proteins: a PHOSPHATE TRANSPORTER 1 (PT1), a monosaccharide transporter (STP) and a POLYOL TRANSPORTER (PLT) were redirected to the branch domain when driven under the control of the *PT4* promoter from *Medicago*, which is active in cells containing arbuscule with branches (Pumplin et al. 2012). While, all three proteins PT1, STP and PLT localized to plasma membrane when expressed under the *Cauliflower mosaic virus (CaMV) 35S* promoter in the non-colonized cells (Pumplin et al. 2012). Thus, these results together suggest that the precise temporal regulation of the gene is critical for the protein subcellular localization during arbuscule development resulting in a differential composition of the PAM as compared to the plasma membrane (Pumplin et al. 2012). Temporal regulation of the promoter determining the subcellular localization of the protein can be achieved by coupling

with transient redirected secretion of newly synthesized protein predominantly towards the developing PAM during arbuscule formation (Pumplin et al. 2012). Consistent with this, *SbtM1* promoter driving a signal peptide fused to Venus localizes to PAS (Takeda et al. 2009). An *Arabidopsis* aquaporin PIP2a and *Medicago* PHOSPHATE TRANSPORTER 1 (PT1) are normally localized to the plasma membrane (Cutler et al. 2000, Pumplin et al. 2012). However, PIP2a was retained in the endoplasmic reticulum while PT1 localized to PAM when driven by the *PT4* promoter (Pumplin et al. 2012). In contrast, PT4 was retained in the endoplasmic reticulum whereas PT1 and PIP2a localized to the plasma membrane when expressed ectopically under *CaMV 35S* promoter (Pumplin et al. 2012). These observations indicate that there should be an additional signal resident in the protein sequence required for cargo selection, which enables entry into the secretion pathway during arbuscule development (Pumplin et al. 2012). Thus, together it can be concluded that the timing of expression coupled with cargo selection enabling entry into the transient redirected secretion predominant towards developing arbuscule, determines the subcellular localization of the newly synthesized protein during arbuscule development.

### 3. Function of AM

The exchange of nutrients is the foundation of the symbiosis, which occurs at the symbiotic interface (MacLean et al. 2017). The extraradical fungal hyphae acquire phosphate from the soil and transport it in the form of polyphosphate to the arbuscule site (Ezawa et al. 2002, Parniske 2008). The phosphate is then released from polyphosphate in the intraradical hyphae by polyphosphate catabolism (Ezawa et al. 2002, Parniske 2008). The phosphate is then discharged into the common apoplast via phosphate transporters localized in the fungal plasma membrane (Figure 3) (Ezawa et al. 2002, Karandashov and Bucher 2005, Javot et al. 2007a, Parniske 2008). Subsequently, the plant phosphate transporters, such as PT4, localized to the PAM import the phosphate into the cytoplasm of the host cell (Figure 3) (Javot et al. 2007b). AM fungi not only supply phosphate but also nitrogen to the host root. The AM fungi can acquire nitrogen from organic material (Hodge et al. 2001). Similarly to the Phosphate uptake, AM-fungal ammonium transporters are predicted to be involved in the uptake of nitrogen by extraradical hyphae (López-Pedrosa et al. 2006). The long distance transport of the nitrogen probably takes place in the form of arginine (Figure 3) (Govindarajulu et al. 2005, Cruz et al. 2007). The nitrogen is then released to the plant in carbon-free form probably such as ammonium (Figure 3) (Govindarajulu et al. 2005). An AM-specific ammonium

transporter situated on the PAM is predicted to involve in the uptake of ammonium or nitrate (Guether et al. 2009b, Kobae et al. 2010, Breuillin-Sessoms et al. 2015). AM fungi being obligate biotrophs, depends on the photoautotrophic partner for completing their life cycle and produce next generation spores (Smith and Read 2008). <sup>13</sup>C-labelled tracer based Nuclear magnetic resonance (NMR) studies indicated hexose sugar as the major form of carbon supplied to the fungus by plants (Figure 3) (Shachar-Hill et al. 1995). Reduction in expression of the high affinity *monosaccharide transporter 2 (MST2)* from *Glomus* by host induced gene silencing results in malformed arbuscule (Helber et al. 2011). This designates the importance of hexose transfer to the intraradical hyphae. AM fungi store carbon essentially in the form of lipids, mainly triacylglycerol (TAG). The major form of fatty acids (FAs) found in AM fungi are 16:0 (palmitic acid) and 16:1 $\omega$ 5 (palmitvaccenic acid). The 16:1 $\omega$ 5 FAs is specific to AM fungi and certain bacteria and therefore used for detection of AM fungi (Graham et al. 1995, Bentivenga and Morton 1996, Madan et al. 2002, Trépanier et al. 2005). It was predicted that the hexose sugars supplied by the host plant are directly metabolized by the AM fungi or used as a precursor molecule for the lipid biosynthesis (Pfeffer et al. 1999). Interestingly, *de novo* FA biosynthesis was only observed inside the host root and not in the extraradical mycelia or spores. These observations led to the conclusion that the fungus can biosynthesize lipid only in colonized roots (Pfeffer et al. 1999, Trépanier et al. 2005). However, recent sequencing of whole genome of the AM fungi *Rhizophagus irregularis*, *Gigaspora margarita* and *Gigaspora rosea* revealed the absence of genes encoding the multidomain cytosolic fatty acid synthase (FAS) subunit responsible for *de novo* synthesis of 16:0 FA. However, genes encoding enzymes required for the 16:0 FA elongation to higher chain length and for FA desaturation, are present (Trépanier et al. 2005, Wewer et al. 2014, Ropars et al. 2016, Salvioli et al. 2016, Tang et al. 2016). Lipids are the major form of carbon storage in AM fungi and important for their growth and reproduction (Trépanier et al. 2005). However, the source of 16:0 FA in AM fungi was for a long time mysterious. Recent studies showed that plant host not only provide carbohydrate but also lipids to the AM fungi (Jiang et al. 2017, Keymer et al. 2017, Luginbuehl et al. 2017).

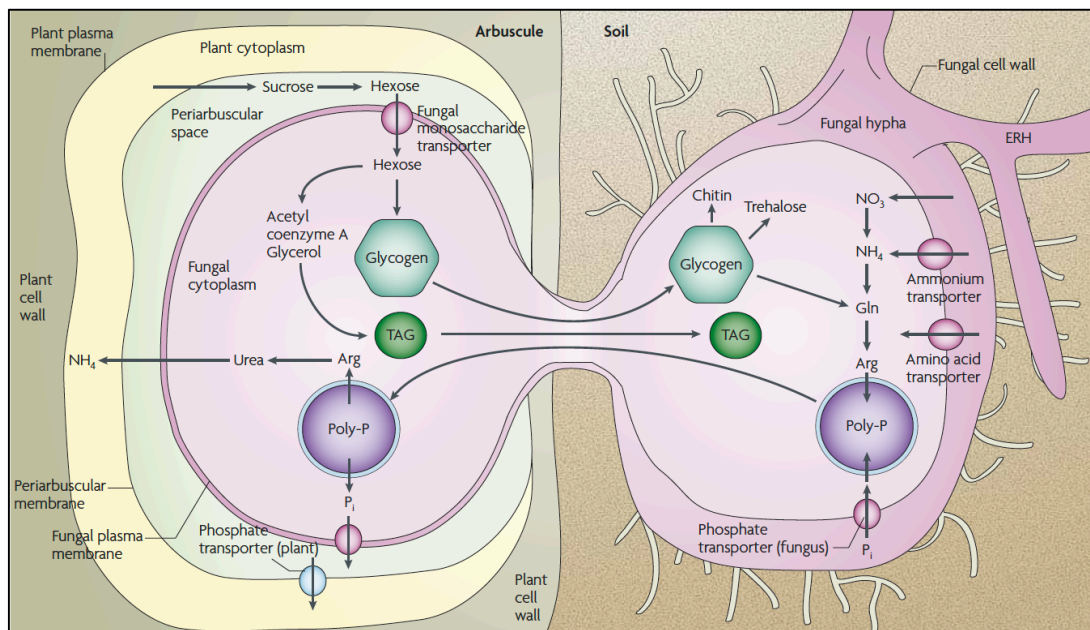


**Figure 3. Nutrients transport and exchange between the two symbionts in AM symbiosis (Figure from Parniske 2008).**

#### 4. Cellular changes during AM development

The host root cell undergoes distinct cellular changes to accommodate the fungal structures. Live imaging of AM colonized *Medicago* hairy root clones expressing appropriate GFP-labelled cellular markers for monitoring cytoskeleton and ER revolutionized the understanding about the host cellular changes during AM development (Genre et al. 2005, Genre et al. 2008). The epidermal cell nucleus migrates to position itself directly below the hyphopodium formation. The nucleus moves across the cell towards the opposite side of the cell, forming a tunnel-like structure called pre-penetration apparatus (PPA) (Genre et al. 2005). The PPA is a cytoplasmic bridge and surrounded by the plant plasma membrane and cellular components (Genre et al. 2005). The fungal hyphae grow through the PPA once it is fenced by the plant plasma membrane forming a symbiotic interface. Outer cortical cells below the epidermal cell in contact with the hyphopodium respond even before the physical contact by the fungal hyphae (Genre et al. 2008, Sieberer et al. 2012). The adjacent outer cortical cells below the colonized epidermal cell undergo low-frequency peri-nuclear calcium spiking followed by the nuclear migration and forms reversible transcellular PPA formation (Sieberer et al. 2012). However, the underlying cortical cell, which will subsequently get colonized, switches to high-frequency perinuclear calcium spiking before colonization (Sieberer et al. 2012). The PPA and the plant plasma membrane encapsulation escort the intracellular fungal growth traversing several cell layers, to reach the inner cortex of the root (Genre et

al. 2005, Genre et al. 2008, Gutjahr and Parniske 2013). The PPA dismantles, the nucleus migrates to the cell periphery, and the calcium spiking disappears once the fungal hyphae have reached the cell (Genre et al. 2005, Genre et al. 2008, Sieberer et al. 2012, Gutjahr and Parniske 2013). PPAs are also observed prior to arbuscule development in the inner cortical cell and it proceeds in a similar fashion as during initial fungal penetration through the epidermal cell (Genre et al. 2008).

Drastic cellular rearrangement takes place in the inner cortical cell to accommodate the highly branched arbuscule. The arbuscule development is accompanied by the fragmentation of the large central vacuole resulting in the formation of a tubular network (Pumplin and Harrison 2009). Massive cytoskeleton rearrangement takes place not only in the arbuscule containing cell but also in cells adjacent to the intercellular hyphae or arbuscule containing cell (Blancaflor et al. 2001). In arbuscule containing cells, actin filaments and microtubules form a dense network bounding the arbuscule branches and enclosing the arbuscule (Genre and Bonfante 1998, Blancaflor et al. 2001). The plastids and mitochondria increase in number and plastidial stromules form interconnected networks around the arbuscule (Fester et al. 2001, Hans et al. 2004, Lohse et al. 2005). Similarly, aggregates of mitochondria, endoplasmic reticulum, and Golgi bodies are observed nearby the arbuscule (Cox and Sanders 1974, Scannerini and Bonfante-Fasolo 1983, Lohse et al. 2005). The nucleus moves from the periphery of the cell to the center of the arbuscule. The nucleus increases in size, which might indicate endoreduplication or chromatin decondensation for the massive transcriptional reprogramming observed prior to and during arbuscule formation (Balestrini et al. 1992, Genre et al. 2008).

## 5. Signal transduction during AM development

AM development in the plant root requires a conceptual signaling cascade called common symbiotic signaling pathway, which is shared with another root endosymbiosis, the root nodule symbiosis (RNS) formed between legumes and rhizobia bacteria converting atmospheric nitrogen into ammonia (Kistner and Parniske 2002, Kistner et al. 2005). The rhizobia bacteria are accommodated in a specialized organ known as the root nodule (Held et al. 2010). Genes such as *SYMRK*, *CASTOR*, *POLLUX*, *CNGC15*, *MCA8*, *NUP85*, *NUP133*, *NENA*, *VAPYRIN*, *CCAMK*, *CYCLOPS* and *DELLA* are classified as common symbiotic genes, required for both endosymbiosis (Endre et al. 2002, Stracke et al. 2002, Ane et al. 2004, Levy et al. 2004, Mitra et al. 2004, Imaizumi-Anraku et al. 2005, Kanamori et al. 2006, Tirichine et al. 2006, Saito et al. 2007, Charpentier et al. 2008, Yano et al. 2008, Groth

et al. 2010, Capoen et al. 2011, Murray et al. 2011, Venkateshwaran et al. 2012, Floss et al. 2013, Charpentier et al. 2016, Fonouni-Farde et al. 2016, Jin et al. 2016).

The Myc Factors released by the AM fungi in the pre-contact phase are perceived by plant plasma membrane localized receptor(s), most probably belonging to class LysM receptor kinases (Antolín-Llovera et al. 2012), although, the bona-fide Myc Factor-specific receptor is still unidentified (Figure 4). In *M. truncatula*, the treatment with sulphated and non-sulphated Myc-LCO lead to partially specific transcriptional response indicating that more than one receptor is required for the perception of Myc Factor (Czaja et al. 2012, Camps et al. 2015). Several studies using knockout or knockdown of a gene encoding receptor-like kinase in different species, revealed their role in early AM developmental step. Downregulation of *LysM receptor-like kinase 10 (LYK10)* in *S. lycopersicum* resulted in complete absence of colonization or in rare cases spores or extraradical hyphae were observed around the root without penetration in tomato (Buendia et al. 2016). Also, RNAi knockdown of *NOD FACTOR PROTEIN (NFP)* in *Parasponia andersonii* perturbed colonization by AM fungi (Op den Camp et al. 2011). It has been shown in rice that silencing or knockout of the *LysM Receptor-Like Kinase 1 (OSCKER1)* leads to a delay in fungal penetration (Miyata et al. 2014, Zhang et al. 2015a). Also, the *Oscerk1* mutant failed to induce nuclear calcium spiking upon treatment with Myc-CO supporting its role in the perception of one or more Myc Factors (Carotenuto et al. 2017). Thus, several receptors or co-receptor (AM specific and non-specific) might act in concert to induce AM-specific signaling responses, upon perception of Myc Factor for the establishment of AM (Figure 4). The receptor like kinase SYMBIOSIS RECEPTOR KINASE (SYMRK) required for microbial entry in both endosymbiosis, has been shown to interact with the NOD FACTOR RECEPTOR 1 (NFR1) and NFR5 in *Lotus* (Stracke et al. 2002, Antolín-Llovera et al. 2014). It is also required for the generation of calcium spiking upon Myc Factor treatment (Sun et al. 2015) and likely acts as a co-receptor in Nod- and Myc Factor perception. SYMRK/DMI2 interacts with a 3-hydroxy-3-methylglutaryl coenzyme A reductase 1 (HMGR1), involved in the production of mevalonate (Figure 4) (Kevei et al. 2007). Application of mevalonate was sufficient to induce nuclear calcium spiking in response to Myc Factor in wild-type and *dmi2* mutant in *Medicago* indicating that mevalonate or a downstream metabolite could act as a second messenger upon perception of Myc Factor in the common symbiotic pathway (Venkateshwaran et al. 2015). Calcium spiking in the nucleus is generated by three recently discovered three cyclic nucleotide-gated channels 15 (CNGC15s) (Charpentier et al. 2016) and the pump MCA8 (Capoen et al. 2011). Knockdown of *MCA8* or *CNGC15s* using RNAi method, perturbed calcium spiking and root colonization by AM fungi

(Capoen et al. 2011, Charpentier et al. 2016). CASTOR and POLLUX are potassium channels likely acting as counter ion channels (Imaizumi-Anraku et al. 2005, Charpentier et al. 2008, Venkateshwaran et al. 2012). The precise role of NUP85, NUP133 and NENA in calcium spiking is still not well understood (Kanamori et al. 2006, Saito et al. 2007, Groth et al. 2010, Binder and Parniske 2013). They are predicted to be involved directly or indirectly in the generation or maintenance of calcium spiking (Binder and Parniske 2013).

The nuclear calcium spiking is deciphered by a nuclear-localized CALCIUM- AND CALMODULIN-DEPENDENT KINASE (CCaMK) in both endosymbiosis (Levy et al. 2004). CCaMK contains a calmodulin binding domain and three EF-hands in addition to a kinase domain. The kinase activity is de-inhibited upon binding of calcium ( $\text{Ca}^{2+}$ ) and calmodulin (CaM) (Miller et al. 2013). CCaMK is considered to be a master regulator of both endosymbiosis. In AM, the *ccamk* mutant fails to allow formation intraradical hyphae and arbuscule in *Medicago*, *Lotus* and *Rice* (Levy et al. 2004, Mitra et al. 2004, Kistner et al. 2005, Gutjahr et al. 2008). In addition, expression of the gain-of-function CCaMK<sup>T265D</sup> (Thr is substituted by Asp at the auto-phosphorylation site in the kinase domain confers  $\text{Ca}^{2+}$  independent activation) under 35S promoter restored AM development in the common symbiotic mutants perturbed in the genes required to generate the calcium spiking such as *symrk*, *castor*, *pollux*, *nup85* and *nup133* (Hayashi et al. 2010). Thus, auto-active CCaMK can compensate for the loss of the upstream genes required for generation of calcium spiking and can activate the downstream symbiotic responses. Furthermore, an auto-active CCaMK<sup>314(T265D)</sup>, which solely contains the kinase domain under the 35S promoter was sufficient to induce cytoplasmic aggregations resembling to PPA-like structures in cortical cells, in the absence of the AM fungi (Takeda et al. 2012). In addition, the deregulated CCaMK<sup>314(T265D)</sup> was able to induce AM-specific marker genes such as *SbtM1*, *RAM1*, *RAM2* and *Vpy* upon overexpression in the absence of AM fungi (Takeda et al. 2015). However, CCaMK-independent transcriptional responses were observed indicating parallel signaling pathways (Czaja et al. 2012, Camps et al. 2015).

One of the transcription factors essential for both endosymbiosis is CYCLOPS (Gutjahr et al. 2008, Yano et al. 2008) (Figure 4). CYCLOPS encodes a nuclear coiled-coil DNA-binding transcription factor (Messinese et al. 2007, Yano et al. 2008, Singh et al. 2014). In AM, the *cyclops* mutant fails to allow arbuscule formation but permits establishment of intraradical hyphae in *L. japonicus* and *O. sativa* (Gutjahr et al. 2008, Yano et al. 2008, Singh et al. 2014). CCaMK physically interact with CYCLOPS and form a CCaMK-CYCLOPS complex in the nucleus (Messinese et al. 2007, Yano et al. 2008). This complex appears to be preassembled

as the interaction was shown in the absence of the calcium spiking (Yano et al. 2008). The genes induced during arbuscule development such as *SbtM1* and *PT4* are dependent on *CYCLOPS* (Takeda et al. 2011). *CYCLOPS* binds DNA in a sequence-specific manner and transactivates a nodulation-specific gene *NIN* upon phosphorylation by CCaMK (Singh et al. 2014). A phosphomimetic version of *CYCLOPS* was able to transactivate *NIN* in transactivation assay in *Nicotiana benthamiana* leaves and was able to induce spontaneous root nodule organogenesis in the absence of rhizobia and CCaMK (Singh et al. 2014). Although *CYCLOPS* is essential for induction of several AM-specific genes, the direct targets of *CYCLOPS* in AM development were unknown when I started my Ph.D. thesis.

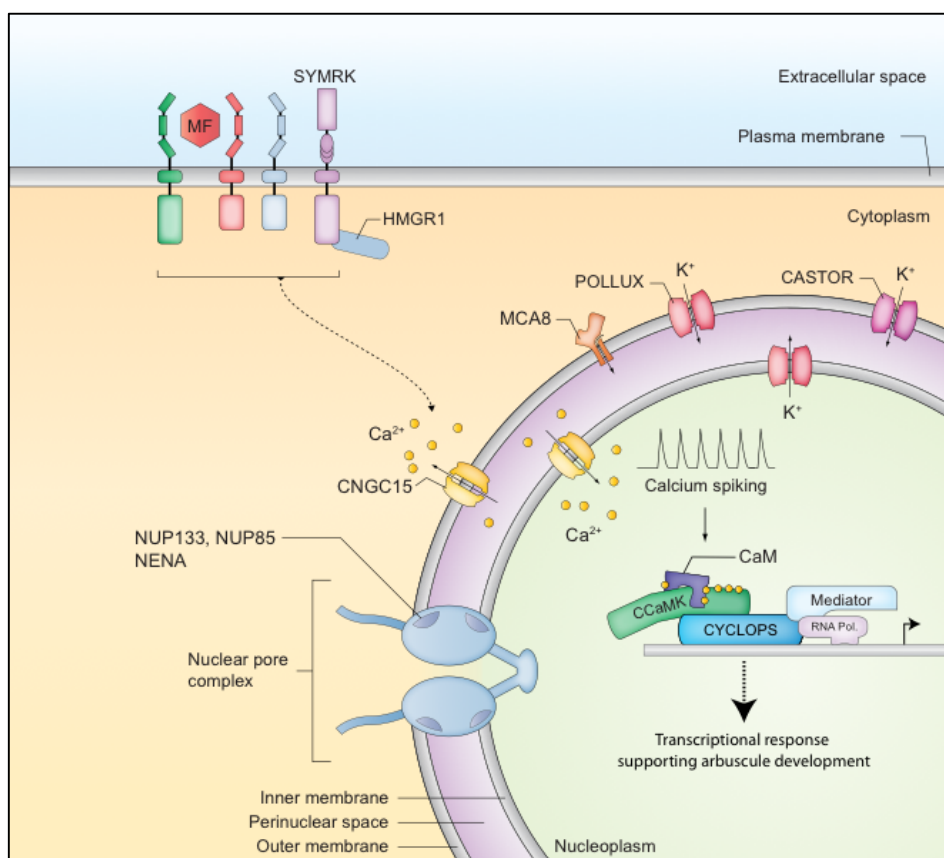


**Figure 4. Overview of signal transduction via common symbiosis signaling upon perception of Myc Factor in the root cell (Modified from Singh and Parniske 2012).**

DELTA protein is the most downstream component known so far in common symbiotic signaling. *DELTA* is classified as a common symbiotic gene because it is also required for establishment of both endosymbiosis (Floss et al. 2013, Floss et al. 2016, Fonouni-Farde et al. 2016, Jin et al. 2016, Pimprikar et al. 2016). *DELTA* protein belongs to family of GRAS-type (for GA<sub>3</sub> insensitive, GAI; Repressor of GAI, RGAI; And Scarecrow, SCR) transcription factors and acts as repressor of GA signaling (Hauvermale et al. 2012). The stability of *DELTA* proteins depends on the hormone

gibberellin (GA) (Davière and Achard 2016). GA is involved in regulation of plant growth and development (Fleet and Sun 2005). GAs are biosynthesized from carotenoid precursors and the bioactive GA pool is regulated by biosynthesis and metabolism (Yamaguchi 2008, Hedden and Thomas 2012). At low GA condition, DELLA modulate the transcription activation of genes by interacting with DNA binding transcription factors (Davière and Achard 2016) (Figure 5). GA is perceived by the soluble alpha/beta hydrolase receptor GIBBERELLIN-INSENSITIVE DWARF-1 (GID1), subsequently interacts with DELLA via the N-terminus of DELLA, which contains the DELLA and TVHYNP domain (Davière and Achard 2016). The GID1-GA-DELLA complex interacts with the SCF<sup>SLY1</sup> complex, which polyubiquitylates DELLA (Davière and Achard 2016). Upon polyubiquitylation, DELLA is degraded via the 26S proteasome (Silverstone et al. 2001, Davière and Achard 2013, Davière and Achard 2016) (Figure 5). It is known for a long time that GA treatment perturbs AM development and specifically arbuscule formation (El Ghachtouli et al. 1996). Treatment with bioactive GA to colonized wild-type roots of *M. truncatula* and *L. japonicus* roots showed intraradical hyphae formation but lack of arbuscules, suggesting a positive role of DELLA protein in arbuscule development (Floss et al. 2013, Takeda et al. 2015, Pimprikar et al. 2016). Similarly, *della* mutants in *Medicago* display intraradical hyphae formation but hardly any arbuscule (El Ghachtouli et al. 1996, Floss et al. 2013, Foo et al. 2013, Yoshida et al. 2014, Takeda et al. 2015, Floss et al. 2017), indicating DELLA proteins are essential for arbuscule formation. However, the arbuscule formed in rare cases in these mutant showed wild-type degree of branching indicating the role of DELLA proteins in arbuscule initiation (Floss et al. 2013, Floss et al. 2017). The exact arbuscule developmental stage at which DELLA proteins are required is still unclear. DELLA proteins might be required for PPA formation, arbuscule trunk formation or first order arbuscule branching during arbuscule development (Pimprikar and Gutjahr, 2018. In press). However, upon inoculation with AM fungi, the plant cell showed nucleus enlargement and movement underneath the fungal hypha prior to hyphal entry in the *della* mutant suggesting DELLA proteins are not required for PPA formation (Ivanov and Harrison 2014). Interestingly, this cellular response is also not dependent on CCaMK (Genre et al. 2009) and thus might be independent of CCaMK-CYCLOPS and DELLA, possibly because it does not require transcriptional regulation. Removal of the DELLA or the TVHYNP domain from the DELLA protein makes DELLA insensitive to degradation even in presence of GA and leads to its accumulation (Willige et al. 2007). Also, the AM development in *M. truncatula* and *L. japonicus* roots became insensitive to GA treatment upon ectopic expression of *della-Δ18*, a resistant to degradation DELLA protein lacking 18

amino acids including the DELLA domain (Floss et al. 2013, Takeda et al. 2015, Pimprikar et al. 2016). However, the exact mode of action of GA/DELLA module in AM development was not understood when I started my doctoral thesis work.

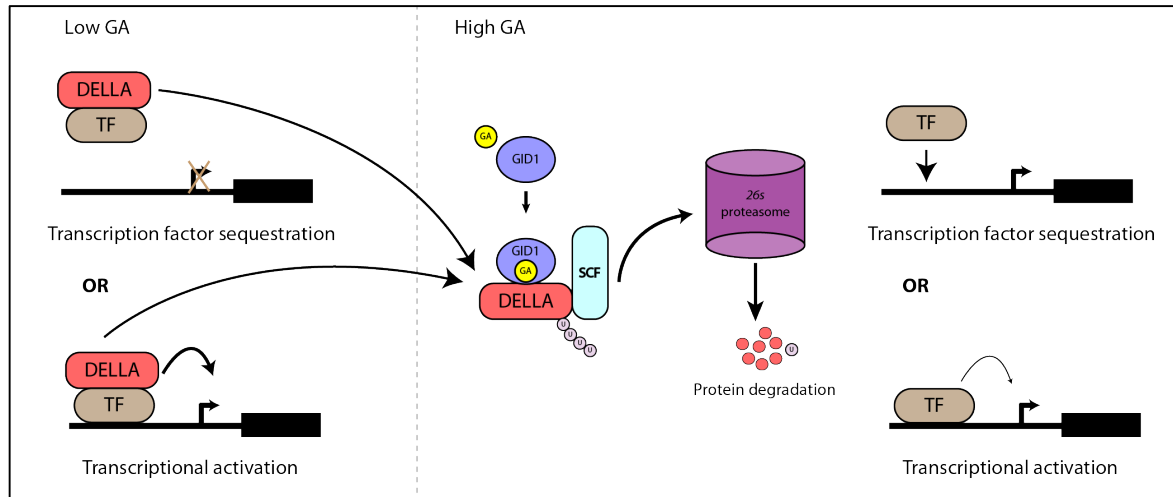


**Figure 5. A schematic representation of the GA perception (Adopted from Davière and Achard 2016).**

## 6. Transcriptional changes during AM development

AM colonization is accompanied by immense transcriptional changes (Liu et al. 2003, Güimil et al. 2005, Hohnjec et al. 2005, Liu et al. 2007, Fiorilli et al. 2009, Guether et al. 2009a, Gaude et al. 2012, Schaarschmidt et al. 2013, Handa et al. 2015). The genes activated during the AM development are involved in signaling, transcriptional regulation, protein biosynthesis, nutrient transport, cell wall synthesis, plant metabolite biosynthesis and lipid metabolism (Liu et al. 2003, Frenzel et al. 2005, Güimil et al. 2005, Hohnjec et al. 2005, Fiorilli et al. 2009, Guether et al. 2009a). These sets of genes confirm host root cellular reprogramming towards AM symbiotic nutrient uptake. The distinctive transcriptional changes to the specific stages of AM development are still not well understood as it is an asynchronous process, with several developmental stages (hyphopodium, intracellular hyphae, vesicles and arbuscules) simultaneously present in the root system. However, in the recent years, application of fungal signaling molecule to non-colonized roots and by laser microdissection of root cells containing different fungal structures has partially circumvented this problem. The transcriptional regulation during the pre-contact phase has been studied by application of germinating spore exudates (GSE) or synthetically isolated Myc-LCOs or Myc-COs (Czaja et al. 2012, Miyata et al. 2014, Camps et al. 2015, Giovannetti et al. 2015, Gutjahr et al. 2015, Hohnjec et al. 2015). The first transcriptome associated with

hyphopodium formation was studied by manual dissection of the hyphopodia containing root pieces from the hairy root culture of *Medicago* and using suppressive-subtractive cDNA library sequencing (Siciliano et al. 2007). Further, the transcriptional changes in arbuscule containing cells were investigated using laser microdissection in combination with qPCR or microarray hybridization (Fiorilli et al. 2009, Gomez et al. 2009, Gaude et al. 2012, Hogeekamp and Küster 2013). Hogeekamp and Küster (2013) carried out the most comprehensive comparative transcriptomic study. The largest number of transcripts found were related to arbuscule containing cells, which is in line with drastic the developmental changes required to host an arbuscule. The transcriptional changes during arbuscule development are divided into at least two waves of cell autonomous gene expression changes. The first wave consists of genes induced prior to and during arbuscule development such as *SbtM1* and *BCP1*. The second wave consists of genes induced during arbuscule development and specific to arbuscule containing cells such as *PT4* and *AMT2.2* (Gutjahr and Parniske 2013).

## **7. Genes required during AM development**

### **i) Genes required for hyphopodium formation**

A *DWARF 14 LIKE (D14L)* gene encoding a receptor alpha/beta hydrolase is shown to be essential for recognition of the AM fungi as the *d14l* mutant is perturbed in formation of hyphopodia in rice (Gutjahr et al. 2015). Consistent with the AM phenotype, the transcript profile of the *Osd14l* compared to wild-type upon treatment with germinating spore exudate indicates that D14L-mediated signaling plays a role in pre-contact stage (Gutjahr et al. 2015). D14L is predicted to be the receptor of an unknown endogenous signaling molecule. D14L-mediated signaling require the F-box protein MORE AXILLARY GROWTH 2 (MAX2). Knockout of MAX2 in rice have been shown to have strong reduction of AM colonization. Further, it remains to be studied that if this pathway required for hyphopodia formation crosstalk with the common symbiotic pathway.

### **ii) Genes required for mature arbuscule formation**

Several targeted or non-targeted approaches led to the discovery of number of genes required for the development of arbuscule. *CYCLOPS* encodes a transcription factor, required for the development of arbuscule in *L. japonicus* and *O. sativa* (Gutjahr et al. 2008, Yano et al. 2008, Singh et al. 2014). DELLA acting as a central

regulator of GA signaling by repressing GA response (described in detail above), was shown to be required for the arbuscule initiation as discussed above (Floss et al. 2013, Floss et al. 2017). In the last few years, several studies reported genes encoding GRAS-type transcription factors other than *DELLA* such *REDUCED ARBUSCULAR MYCORRHIZA 1 (RAM1)*, *REQUIRED FOR ARBUSCULE DEVELOPMENT 1 (RAD1)* and *MYCORRHIZA INDUCED GRAS 1 (MIG1)* are required for arbuscule development (Gobbato et al. 2012, Park et al. 2015, Rich et al. 2015, Xue et al. 2015, Heck et al. 2016, Pimprikar et al. 2016). Role of *RAM1* and *RAD1* during arbuscule development are discussed in detail in the discussion part of this thesis. Downregulation of *MIGs* in *Lotus* by RNAi resulted in smaller and distorted arbuscule, although the total colonization remained unchanged (Heck et al. 2016). Overexpression of *Δ18-DELLA* restored the arbuscule development in the hairy root co-expressing RNAi construct targeting *MIGs* indicating that *DELLA* can compensate for the reduction in *MIG* expression when stabilized (Heck et al. 2016). *MIG1* interacts physically with *DELLA* in Y2H and bimolecular fluorescence complementation assay (BiFC) in *N. benthamiana* leaves (Heck et al. 2016). Overexpression of *MIG1* and *DELLA1* was shown to increase the cell width and number of cortex cell layers and therefore root diameter. Thus, it is possible that *MIG* interacts with *DELLA* to regulate the cortex cell development during arbuscule development (Heck et al. 2016). However, overexpression of *MIG1* did not induce genes required for arbuscule development in absence of fungus (Park et al. 2015, Floss et al. 2016, Heck et al. 2016). Thus, it is still not well understood how *MIG1* can control the arbuscule branching by regulating the cell size.

*RAM2* is shown to be one of the targets of *RAM1* and required for arbuscule development (discussed in detail in the discussion part of this thesis) (Wang et al. 2012). Two *M. truncatula* genes, *STR* and *STR2* encoding half ABC transporters are essential for arbuscule development as the downregulation of the respective genes led to a developmental arrest at the bird foot stage (Zhang et al. 2010). *STR* and *STR2* form heterodimers in the branch domain of the PAM. Because of its PAM localization, the *STR/STR2* complex is predicted to export a small molecule into the PAS, although the nature of this molecule is still not known (Zhang et al. 2010). Another transporter localizing to PAM is *PT4*, which belongs to the Pht1 subfamily I (Harrison et al. 2002). *PT4* is known to import phosphate delivered by the AM fungi into the plant cell cytoplasm containing arbuscule (Harrison et al. 2002, Javot et al. 2007b, Pumplun and Harrison 2009). The Medicago *pt4* mutant displayed premature death of arbuscules and the total root length colonization was strongly reduced (Javot et al. 2007b). However, the *pt4* phenotype was restored by nitrogen starvation indicating that nitrogen delivery can promote arbuscule maintenance

(Guether et al. 2009b, Kobae et al. 2010, Javot et al. 2011, Breuillin-Sessoms et al. 2015). The *AMMONIUM TRANSPORTER 2.2* (*AMT2.2*) in *L. japonicus* is one of the highly upregulated genes during AM colonization, specifically in arbuscule containing cells, and is involved in symbiotic nitrogen uptake (Guether et al. 2009a, Guether et al. 2009b). Consistent with its predicted function, *AMT2.2* also localizes to the PAM (Kobae et al. 2010, Breuillin-Sessoms et al. 2015)

The plant derived membrane around the arbuscule harbors AM specific proteins such as PT4 (as described above). However, these proteins must be secreted and incorporated into the newly synthesized PAM. Exocytotic pathway has been shown to play an important role in arbuscule development (Genre et al. 2012). For example, *VAMP721d* and *VAMP712e* localizing to the PAM, are indispensable for the arbuscule development (Ivanov et al. 2012). Downregulation of *L. japonicus* gene *LjVTI12* by RNAi, displayed stunted arbuscule formation. *LjVTI12* encodes a Qb-SNARE family protein, which is thought to be involved in vesicle docking (Lota et al. 2013). Similarly, silencing of *SYP132A* encoding a t-SNARE protein displayed significant reduction in arbuscule formation (Pan et al. 2016). Subsequently, Zhang and co-worker showed that the *EXO70I* subunit of the exocyst complex is necessary for the arbuscule formation as the *exo70i* mutant displayed stunted arbuscules in *Medicago* (Zhang et al. 2015b). *EXO70I* was also shown to be essential for the incorporation of *STR* and *STR2* into the PAM (Zhang et al. 2015b). It is predicted that the *EXO70I* might be also important in incorporation of other PAM localized proteins or expansion of the PAM. Several other *EXO70s* are transcriptionally induced in arbuscule containing cells, indicating that several *EXO70* subunits might act in concert to support the development of arbuscules (Zhang et al. 2015b). *EXO70I* physically interacts and partially co-localizes with a plant-specific protein called *VAPYRIN* (Zhang et al. 2015b). *VAPYRIN* was shown to be required for the epidermal entry by AM fungi in *M. truncatula* and *P. hybrida*. The fungus was able to form intraradical hyphae in rare cases when it managed to enter the root but could not form arbuscule indicating role of *VAPYRIN* in cell penetration during AM development (Reddy et al. 2007, Feddermann et al. 2010, Pumplin et al. 2010, Murray et al. 2011).

### iii) Genes required for arbuscule degeneration

Arbuscules are regularly turned over with a life span of around 2-3 days in rice (Kobae and Hata 2010). However, the life span of arbuscules differs among individual arbuscule and also depends on plant and fungal species involved in the symbiosis (Brown and King 1982, Alexander et al. 1989, Kobae and Hata 2010). The

biological relevance of arbuscule turnover has not been well understood but from the phenotype of nutrient transporter mutants such as *pt4* in *Medicago*, it has been suggested a regulatory mechanism to control efficient delivery of nutrients and avoid fungal parasitism (Javot et al. 2007b, Gutjahr and Parniske 2017). In 2017, Floss and co-worker found that the transcription factor MYB1 plays an important role in arbuscule degeneration. Arbuscule life is restored to normal in the *pt4 myb1* double mutant in *M. truncatula*, indicating that MYB1 accelerates the transcriptional program for the degeneration of the arbuscule in the *pt4* mutant background (Floss et al. 2017). However, the *myb1* mutant in *Medicago* did not show increase in life span of the arbuscule. The *Mtpt4* mutant upon colonization displayed increased expression of genes involved in degradative processes such as a range of hydrolases (proteases, lipases, chitinases) and ripening-related proteins, indicating that plant cells play an important role in the arbuscule degeneration. Consistently, *MYB1* overexpression induced the expression of marker genes for arbuscule degeneration such as *CYSTEINE PROTEASE 3 (CP3)* in the absence of fungus whereas upon colonization, it increased arbuscule degeneration and affected root length colonization. However, the induction of arbuscule degeneration marker genes upon overexpression of *MYB1* was absent in *nsp1* and *della* double mutants. Subsequently, it was shown that MYB1 interact with NSP1 and DELLA1 in Y2H and co-immunoprecipitation (CoIP) from *N. benthamiana* leaves indicating that MYB1 might form a complex with NSP1 and DELLA1 to activate the arbuscule degeneration program (Floss et al. 2017). Although, in the *myb1* mutant, induction of the arbuscule degeneration marker by colonization was only mildly affected indicating redundancy at the level of *MYB1* in the presence of *PT4* (Floss et al. 2017). However, it is still not well understood what triggers the arbuscule degeneration. The putative homolog of MYB1 in *Lotus* was described to be induced in arbuscule containing cells and root meristem, named *MERISTEM AND MYCORRHIZA INDUCED (MAMI)* (Volpe et al. 2013). However, the RNAi construct targeting *MAMI* showed no AM phenotype but significant reduction in lateral root branching of hairy root culture, which is consistent with the Floss et al 2017 results (Volpe et al. 2013). In contrast to the *Medicago MYB1*, overexpression of *MAMI* did not led to premature arbuscule degeneration in *Lotus*. This discrepancy can be due to weak 35S promoter activity in *Lotus* roots or the two copies of *MAMI* in *Lotus* might have gained specialized function, one specifically induced and essential for arbuscule degeneration and the other for the lateral root development (Volpe et al. 2013, Floss et al. 2017).

#### iv) Genes regulating the amount of colonization

GRAS protein NODULATION SIGNALING PATHWAY 1 (NSP1) and NSP2 have been shown to regulate the quantitative colonization (Liu et al. 2011, Lauressergues et al. 2012, Delaux et al. 2013, Takeda et al. 2013). They were initially implicated in root nodule symbiosis (Kaló et al. 2005, Smit et al. 2005). In *M. truncatula*, mutation in *NSP1* and *NSP2* lead to significant reduction in colonization (Lauressergues et al. 2012, Delaux et al. 2013) but in *L. japonicus* only *nsp1* showed decrease in colonization but not *nsp2* mutants. However, this discrepancy within the species is surprising based on interaction studies in yeast and *N. benthamiana*, NSP1 and NSP2 are shown to interact physically (Hirsch et al. 2009, Jin et al. 2016) indicating that this interaction might not be crucial for AM symbiosis. NSP1 and NSP2 are shown to form homodimer as well as heterodimer with other proteins (Hirsch et al. 2009). NSP2 interact with proteins such as RAM1, RAD1, DELLA and NSP1 whereas NSP1 interacts with NSP2, MIG1 and MYB1. These protein complexes might be involved in induction of specific set of genes (Hirsch et al. 2009, Gobbato et al. 2012, Park et al. 2015, Xue et al. 2015, Fonouni-Farde et al. 2016, Heck et al. 2016, Jin et al. 2016, Floss et al. 2017). Both *NSP1* and *NSP2* are predicted to be involved in strigolactones biosynthesis as the *nsp1* and *nsp2* mutants are affected in the expression of strigolactones biosynthesis genes and strigolactones production (Liu et al. 2011). Strigolactones are important plant root exudates which activate AM fungi in the pre-contact phase and thus AM development is strongly reduced in mutants perturbed in strigolactones biosynthesis or exudation (Waters et al. 2017). However, full colonization was not restored in *nsp1* mutant by exogenous application of strigolactones (Takeda et al. 2013) indicating that additional factors reduce the colonization in *nsp1* in *L. japonicus*. NSP1 is activated by Myc-LCO and is important for the induction of several genes in response to Myc-LCO perception (Delaux et al. 2013, Camps et al. 2015, Hohnjec et al. 2015). Some of these genes might be participating in the promotion of root length colonization. An apoplastic localized plant protease, SbtM1 belonging to subtilase family, is required for AM colonization as suppression of *SbtM1* via RNAi caused decrease in total root length colonization in *L. japonicus* (Takeda et al. 2009). *SbtM1* is induced upon colonization and SbtM1 signal peptide fused to fluorophore driven by *SbtM1* promoter, indicated SbtM1 localization to PAS in *Lotus* (Takeda et al. 2009). Together these results suggest that SbtM1 cleaves of specific substrate present in the PAS essential for AM development (Takeda et al. 2009).

The *NSP2* transcript is post transcriptionally regulated by a microRNA called miR171h (Lauressergues et al. 2012, Hofferek et al. 2014). According to the *in silico* analysis, miR171h and its binding site in NSP2 are conserved across AM competent

plant species (Lauressergues et al. 2012). Consistent with these observations, miR171h overexpression causes reduction in colonization whereas overexpression of *NSP2* gene resistant to miR171h leads to significant increase in colonization. In non-manipulated roots, miR171h is predicted to downregulate *NSP2* in the root tip, which is generally not colonized. Consistent with this hypothesis, overexpression of *NSP2* resistant to miR171h leads to colonization in the root tip (Lauressergues et al. 2012). miR171h accumulation is regulated by the physiological status of the plant as it accumulates in high phosphate and low nitrogen, whereas it decreases in low phosphate and high nitrogen (Hofferek et al. 2014). Together, this results indicates that miR171h and *NSP2* are responsible for quantitative colonization of the root depending on the nutrient availability. The other members of the miR171 family are known to target the *LOST MERISTEMS (LOM)* gene, encoding a GRAS-type transcription factor and required for the maintenance of shoot and root indeterminacy by regulating meristem cell differentiation (Stuurman et al. 2002, Engstrom et al. 2010, Schulze et al. 2010). In *M. truncatula*, *LOM1* is known to regulate the quantitative colonization as RNAi construct targeting *LOM1* resulted in decrease root length colonization. *LOM1* and *LOM2* in *Medicago* are targeted by miR171a-f except miR171b (Couzigou et al. 2017). Expression of *LOM1* resistant to miR171 members results in *LOM1* transcript accumulation and thereby increase in colonization level under its native promoter (Couzigou et al. 2017). miR171b is assumed to protect the *LOM1* from cleavage by the other miR171 family members, as *miR171b* is able to anneal with *LOM1* transcript but is unable to cleave the transcript via DICER due to presence of a mismatch at the cleavage site. This mismatch is conserved across AM competent species but not in *A. thaliana* indicating a strategy to fine tune the spatio-temporal expression of *LOM1* via mi171-target mimicry pair and may be advantageous for AM (Couzigou et al. 2017). Indeed, the promoter of *LOM1* and other member of miR171a-f except miR171b are active throughout the root and the *miR171b* promoter shows activity only in the colonized root areas. This expression pattern of the promoters indicates that miR171b protect *LOM1* transcript and leads to its accumulation in the colonized area while in non-colonized part of the root, *LOM1* is downregulated by the other members of miR171 (Couzigou et al. 2017).

## VII. Aims of the thesis

At the start of my doctoral thesis the majority of plant genes known to be required for AM development were essential for intracellular accommodation of the fungus in the epidermis. They represent a subset of genes required for root nodule symbiosis in legumes. However, specific responses have to be generated downstream or in parallel of common symbiotic signaling for the induction of a specific developmental program to allow either AM or RNS. Very few candidate genes involved specifically in AM development were known. These were required for the development and maintenance of arbuscules. In the past, a forward genetic screen was carried out in the *L. japonicus* ecotype Gifu (Groth et al. 2013). This led to the identification of an AM-specific plant mutant called *reduced and degenerate arbuscules* (*red*), which is perturbed in matured development of arbuscule branching leading to formation of stunted arbuscule (Groth et al. 2013). Co-segregation analysis along with positional mapping and next generation sequencing revealed two mutations in *red* located on chromosome 1 and 6 (Groth et al. 2013).

The first aim of this doctoral thesis was to identify the causative mutation(s) in *red* by fine-mapping using SSR markers and next generation sequencing technology. I found a mutation on chromosome 1 in *REDUCED ARBUSCULAR MYCORRHIZA 1* (*RAM1*), encoding a protein belonging to GRAS-type transcription factors family and on chromosome 6 in *RAM2*, encoding a glycerol 3-phosphate acyl transferase 6. *RAM1* was specifically and strongly induced upon colonization by AM fungi in wild-type roots. Therefore, the second aim of my thesis was to determine how the promoter of *RAM1* is regulated. I found that *RAM1* is transcriptionally activated by a complex of CCaMK-CYCLOPS and DELLA via binding of CYCLOPS to a novel *cis*-element in the *RAM1* promoter. *RAM1* appears to act as a transcription factor, inducing genes required for arbuscule development such as *RAM2*. *RAM2* is also strongly induced upon colonization by AM fungi. Thus, the third aim of my thesis was to investigate the promoter activity of *RAM2* using a promoter-reporter system during root colonization. *RAM2* promoter is specifically active in the cortical cells of root containing arbuscule. To further correlate *RAM2* promoter activity with the precise stage(s) of arbuscule development, I designed a construct which enabled for the first time visualization of the different developmental stages of arbuscule including pre-penetration apparatus formation in live roots.

## VIII. Results

**Paper I:** A CCaMK-CYCLOPS-DELLA complex activates transcription of *RAM1* to regulate arbuscule branching

Reference: **Pimprikar P**, Carbonnel S, Paries M, Katzer K, Klingl V, Bohmer MJ, Karl L, Floss DS, Harrison MJ, Parniske M, Gutjahr C (2016). A CCaMK-CYCLOPS-DELLA complex activates transcription of *RAM1* to regulate arbuscule branching. *Current Biology* 26: 987-998.

# Current Biology

## A CCaMK-CYCLOPS-DELLA Complex Activates Transcription of *RAM1* to Regulate Arbuscule Branching

### Highlights

- *Lotus japonicus* *RAM1* is required for arbuscule branching
- *RAM1* acts downstream of the CCaMK-CYCLOPS complex and DELLA
- The *RAM1* promoter is transactivated by a complex of CCaMK-GOF, CYCLOPS, and DELLA
- CYCLOPS binds to a *cis* element in the *RAM1* promoter

### Authors

Priya Pimprikar, Samy Carbonnel, Michael Paries, ..., Maria J. Harrison, Martin Parniske, Caroline Gutjahr

### Correspondence

caroline.gutjahr@lmu.de

### In Brief

Pimprikar et al. identify *Lotus japonicus* *RAM1* as a central regulator of arbuscule branching and related gene expression. *RAM1* is activated by a complex of CCaMK, CYCLOPS, and DELLA, which emerges as a major regulatory hub interconnecting symbiosis and gibberellin signaling during arbuscule development.

### Accession Numbers

KU557503

# A CCaMK-CYCLOPS-DELLA Complex Activates Transcription of *RAM1* to Regulate Arbuscule Branching

Priya Pimprikar,<sup>1</sup> Samy Carbonnel,<sup>1</sup> Michael Paries,<sup>1</sup> Katja Katzer,<sup>1</sup> Verena Klingl,<sup>1</sup> Monica J. Bohmer,<sup>1</sup> Leonhard Karl,<sup>1</sup> Daniela S. Floss,<sup>2</sup> Maria J. Harrison,<sup>2</sup> Martin Parniske,<sup>1</sup> and Caroline Gutjahr<sup>1,\*</sup>

<sup>1</sup>Faculty of Biology, Genetics, Biocenter Martinsried, LMU Munich, Großhaderner Strasse 2-4, 82152 Martinsried, Germany

<sup>2</sup>Boyce Thompson Institute for Plant Research, 533 Tower Road, Ithaca, NY 14853, USA

\*Correspondence: [caroline.gutjahr@lmu.de](mailto:caroline.gutjahr@lmu.de)

<http://dx.doi.org/10.1016/j.cub.2016.01.069>

## SUMMARY

Intracellular arbuscular mycorrhiza symbiosis between plants and glomeromycotan fungi leads to formation of highly branched fungal arbuscules that release mineral nutrients to the plant host. Their development is regulated in plants by a mechanistically unresolved interplay between symbiosis, nutrient, and hormone (gibberellin) signaling. Using a positional cloning strategy and a retrotransposon insertion line, we identify two novel alleles of *Lotus japonicus* *REDUCED ARBUSCULAR MYCORRHIZA1* (*RAM1*) encoding a GRAS protein. We confirm that *RAM1* is a central regulator of arbuscule development: arbuscule branching is arrested in *L. japonicus ram1* mutants, and ectopic expression of *RAM1* activates genes critical for arbuscule development in the absence of fungal symbionts. Epistasis analysis places *RAM1* downstream of *CCaMK*, *CYCLOPS*, and *DELLA* because ectopic expression of *RAM1* restores arbuscule formation in *cyclops* mutants and in the presence of suppressive gibberellin. The corresponding proteins form a complex that activates *RAM1* expression via binding of *CYCLOPS* to a *cis* element in the *RAM1* promoter. We thus reveal a transcriptional cascade in arbuscule development that employs the promoter of *RAM1* as integrator of symbiotic (transmitted via *CCaMK* and *CYCLOPS*) and hormonal (gibberellin) signals.

## INTRODUCTION

In arbuscular mycorrhiza (AM) symbioses, fungi of the glomeromycota deliver mineral nutrients, especially phosphate and nitrogen, to the plant in exchange for organic carbon [1]. Mineral nutrient release occurs via highly branched fungal structures, the arbuscules, that develop inside root cortex cells [2]. Arbuscule formation is determined by preceding developmental changes in the host cell and progresses in distinct steps that can be genetically dissected with plant mutants [3]. Although several plant genes required for these distinct steps have been

identified, it remains unknown how plant cell developmental changes during arbuscule development are regulated and executed mechanistically and how the individual encoded proteins are functionally connected.

In legumes, AM and root nodule symbioses development require a set of common symbiosis genes [4, 5], some of which encode signal transduction proteins. Signaling is initiated upon perception of microbial N-acetyl-glucosamine-containing molecules such as lipochito-oligosaccharides or chitin oligomers by receptor-like kinases [6], which triggers nuclear calcium spiking [7]. A nuclear localized calcium and calmodulin-dependent kinase (CCaMK) [8] interacts with and phosphorylates the transcription factor *CYCLOPS* that directly activates the nodulation-specific gene *NODULE INCEPTION* (*NIN*) [9, 10]. In AM symbiosis, *CYCLOPS* is required for arbuscule initiation [9, 11] and expression of colonization marker genes such as *SbtM1*, *PT4* in *Lotus japonicus*, or *AM10* and *PT11* in rice [12, 13]. Overexpression of a dominant active version of CCaMK (CCaMK<sup>314</sup>) can induce transcription of AM-related marker genes such as *SbtM1*, *RAM1*, *RAM2*, and *Vapyrin* in the absence of AM fungi and calcium spiking [14], and the expression of *SbtM1*, *RAM1*, and *Vapyrin* was shown to depend on CCaMK [12, 15, 16]. Taken together, this suggests that the CCaMK-CYCLOPS complex regulates genes during AM symbiosis. However, its precise hierarchical placement and its direct target promoters in the AM transcriptional regulatory cascade have been elusive.

An important physiological signal that inhibits arbuscule formation is the plant hormone gibberellin (GA) [17–20]. Conversely, arbuscule formation requires the presence of DELLA proteins [18–20], repressors of GA signaling that are stable in the absence of GA and degraded upon GA perception [21]. Although the DELLA/GA module is a key player in the regulation of arbuscule development and therefore a major determinant of quantitative nutrient transfer, its mechanistic function and its position in the interplay with symbiosis signaling remain unknown. GA-mediated degradation of DELLA requires an N-terminal DELLA domain, and deletion of this domain confers stability of the resulting ΔDELLA version toward the presence of GA [22]. 35S promoter-driven DELLA<sup>Δ18</sup> can restore arbuscule formation in the presence of GA and in roots of a *cyclops* mutant [20]. Furthermore, ectopic expression of DELLA<sup>Δ18</sup> can induce *RAM1* and other genes required for arbuscule development, in the absence of the symbiotic fungus [23]. This suggests that DELLA might act downstream of or at the same hierarchy level as *CYCLOPS* [20]

and upstream of *RAM1* and other arbuscule-related genes [23]. However, the mechanistic relationship between CYCLOPS and DELLA as well as the direct targets of these proteins in AM development remained unresolved. *RAM1* encodes a GRAS protein that is required for arbuscule branching and induction of marker genes related to arbuscule development in *Medicago truncatula*, *L. japonicus*, and *Petunia hybrida* [23–25]. Ectopic expression of *RAM1* can induce arbuscule-development-related genes, indicating that it might act as a transcriptional regulator [23].

A forward genetics screen in *L. japonicus* has been performed to find novel host regulators and executors of arbuscule development [26]. Here, we identified a novel allele of *L. japonicus ram1* as causal for perturbation in arbuscule branching in one of the mutants. We discovered that *RAM1* is transcriptionally regulated by a complex comprising CCaMK, CYCLOPS, and DELLA and CYCLOPS directly binds to the *RAM1* promoter. The CCaMK-CYCLOPS-DELLA complex therefore constitutes a major regulatory hub interconnecting symbiosis and GA signaling during arbuscule development.

## RESULTS

### *red* Carries a Nonsense Mutation in *RAM1*, Encoding a GRAS Protein

The *L. japonicus* mutant *reduced and degenerate arbuscules* (*red*; SL0181-N), found in a forward genetics screen, displays reduced root colonization and a strong defect in arbuscule branching. Rough mapping had identified two loci containing causal mutations on chromosome 1 and 6 segregating in the progeny of SL0181-N [26]. The mutation on chromosome 6 appeared to be heterozygous in individual mutants in the M2 generation because we could retrieve single mutants of the mutation on chromosome 1 in subsequent generations that displayed the aberrant arbuscule phenotype (Figures 1B and 2A). This was confirmed by outcrossing an M6 individual of the SL0181-N line (M1619) to ecotype MG20 and segregation analysis of the AM phenotype in the resulting F2 population. Using a combination of classical mapping and next-generation sequencing, we identified two nonsense mutations in open reading frames in the mapping interval between the markers TM1666 and TM0356 on chromosome 1 (Figure S1A). One candidate mutation was a C to T transition at position 115 of chr1.CM1852.30.r2.m, replacing the codon for amino acid 39 of the encoded GRAS protein with a stop codon (Figure S1). It represents a novel *L. japonicus* allele of the previously identified *M. truncatula* *REDUCED ARBUSCULAR MYCORRHIZA 1* (*RAM1*) and *P. hybrida* *ATYPICAL ARBUSCULE* (*ATA*) [15, 25] (Figure S2). Because two retrotransposon (LORE1) insertion mutants of *L. japonicus RAM1* have previously been described by reverse genetics [24], we named the mutant carrying the novel *ram1* allele *ram1-3* (Figures 1A and 1B). Transformation of *ram1-3* hairy roots with the wild-type *RAM1* gene including its own promoter restored arbuscule branching, confirming that the nonsense mutation in the *RAM1* gene caused the stunted arbuscule phenotype. An independent additional mutant (*ram1-4*) carrying a retrotransposon (LORE1) insertion in exon 2 phenocopied *ram1-3* with respect to arbuscule branching (Figures 1A and 1B) and extent of root colonization (Figure 2A).

### *RAM1*-Dependent Gene Regulation

To assess at which stage of arbuscule development *L. japonicus ram1* mutants are perturbed, we examined the expression of marker genes associated with arbuscule initiation (*SbtM1*, *BCP1*, and *Vapyrin A* and *B*) and branching (*RAM2*, *STR*, *PT4*, and *AMT2.2*) [3]. Of these, *STR* and *RAM2* are similarly to *RAM1* required for the development of fine arbuscule branches [27–29]. All marker genes except *Vapyrin A* and *AMT2.2* were induced in both *ram1* mutants upon AM colonization (Figure 2B). Nonetheless, overexpression of *RAM1* driven by the ubiquitously active *L. japonicus ubiquitin* promoter (*pUbi:RAM1*) induced all marker genes with the exception of *BCP1*, *Vapyrin A*, and *Vapyrin B* in the absence of AM fungi (Figure 3B). Thus, *RAM1* is sufficient to induce arbuscule-development-related genes, even for some that do not require *RAM1* for induction.

### AM-Induced *RAM1* Transcription Depends on CYCLOPS

Consistent with an important role of *RAM1* in AM development, *RAM1* transcripts strongly accumulated in colonized roots (Figures 1C–1E) whereas only background levels were detectable in control roots, stems, leaves, and flowers (Figure 1C). To detect the activity pattern of the *RAM1* promoter, the same 2-kb *RAM1* promoter fragment (including the 5' UTR) used to successfully restore wild-type-like colonization in *ram1-3* (Figure 1A) was coupled to the *uidA* gene (*pRAM1:GUS*). Strong GUS activity was detected specifically in colonized, but not in non-inoculated roots (Figure 1F). *RAM1* promoter activity was restricted to colonized root segments, in which it was detected in all tissue layers independently of whether the fragments contained arbuscules or intraradical hyphae (Figures 1G–1I). In *ram1* mutants, transcript accumulation from the *ram1* mutant alleles as well as *pRAM1:GUS* expression was also observed in response to AM colonization (Figures 2B–2D), indicating that *RAM1* transcription does not depend on *RAM1* itself. However, as previously reported for *Medicago* [15], *RAM1* was not induced by AM fungi in a *ccamk-13* mutant that does not allow intraradical colonization (Figures 1D and 1E). Induction was also absent from two allelic *cyclops* mutants (*cyclops-3* and *-4*; Figures 1D–1F and 1J), although they were colonized by intraradical hyphae (Figure 1D), which in the wild-type were associated with *RAM1* promoter activity (Figure 1I). This indicates that *RAM1* transcriptional activation depends on the CCaMK-CYCLOPS complex (Figure 1D).

### *RAM1* Expression Is Sufficient to Trigger Symbiotic Transcriptional Regulation Downstream of CCaMK and CYCLOPS

To investigate whether *RAM1* acts downstream of CCaMK and CYCLOPS, we examined whether ectopic *RAM1* expression could restore arbuscule formation in hairy roots of the *ccamk-13* mutant and the two allelic *cyclops* mutants. Indeed, numerous arbuscules formed in hairy roots of *cyclops-3* and *-4* transformed with *pUbi:RAM1*, whereas none of the mutants allowed arbuscule development when transformed with the empty vector control. This demonstrates that *RAM1* expression independent of CYCLOPS is sufficient to restore arbuscule development in *cyclops* (Figure 3A). However, in *ccamk-13* mutant roots, *RAM1* overexpression did not restore arbuscule formation (Figure 3A).

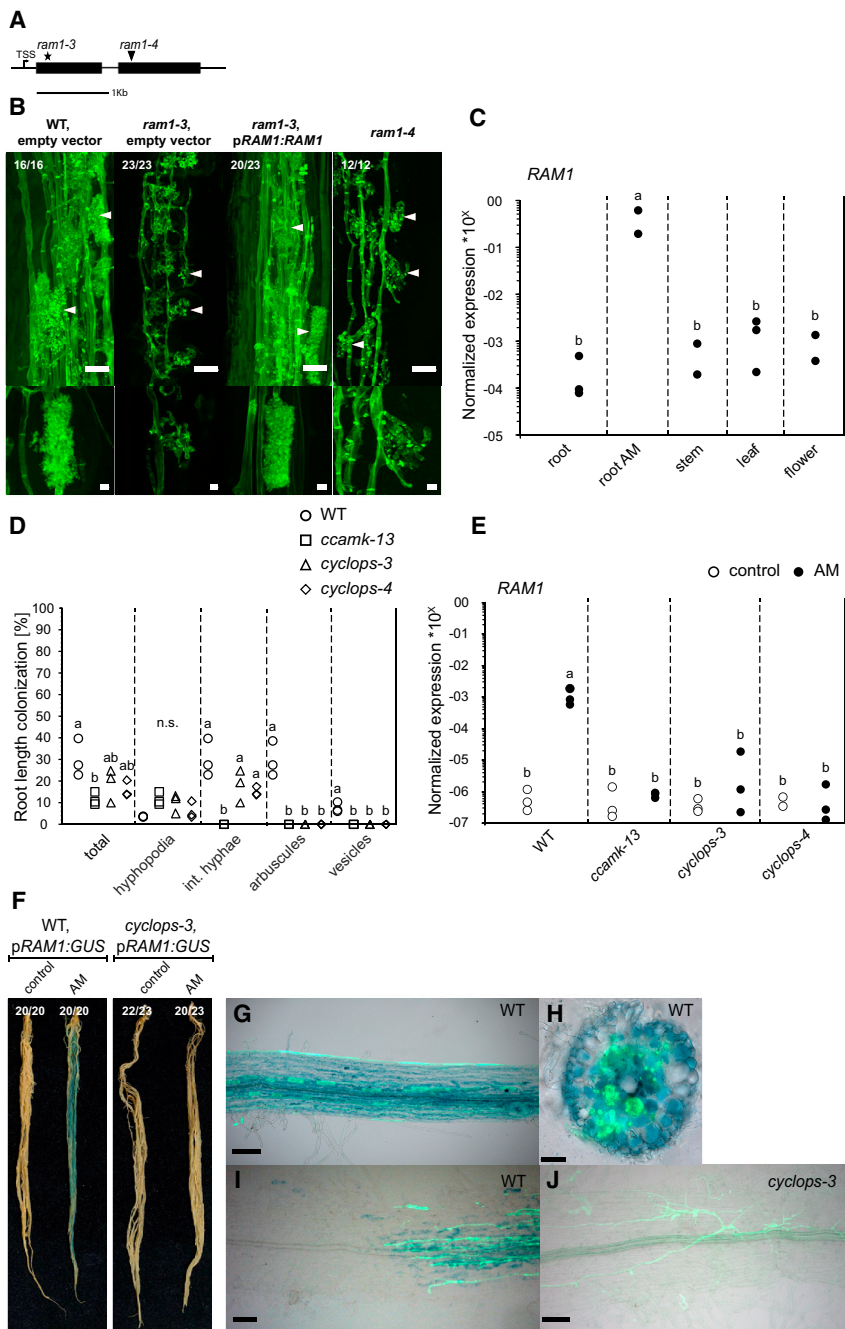


**Figure 1. Identification and Expression Pattern of *L. japonicus* RAM1**

(A) Gene structure of *L. japonicus* *RAM1* with locations of the identified stop codon mutation (star, *ram1-3*) and the LORE1 insertion (triangle, *ram1-4*). Black boxes indicate exons separated by introns (thin lines).

(B) Laser scanning confocal images of *L. japonicus* hairy roots colonized by *R. irregularis*. Wild-type and *ram1-3* mutant transformed with an empty vector control, *ram1-3* transformed with a genomic fragment containing the wild-type *RAM1* gene, and a 1,861-bp *RAM1* promoter fragment upstream of the transcriptional start site and of *ram1-4* mutant roots at 5 weeks post-inoculation (wpi) are shown; scale bar, 25  $\mu$ m. Close up of arbuscules; scale bar, 5  $\mu$ m. The fungus is stained with WGA-Alexa-Fluor488. Numbers indicate root systems with the displayed phenotype per total number of analyzed transgenic root systems. White arrowheads indicate arbuscules.

(C) *RAM1* expression in different plant organs and in roots colonized by *R. irregularis* (roots AM) at 5 wpi as determined by qRT-PCR. Expression of the housekeeping gene *EF1alpha* was used for normalization. Different letters indicate different statistical groups (ANOVA; post hoc Tukey;  $n = 15$ ;  $F_{4,8} = 27.08$ ;  $p \leq 0.001$ ).

(D) Percent root length colonization of wild-type, *ccamk-13*, *cyclops-3*, and *cyclops-4* roots by *R. irregularis* at 3.5 wpi as determined by gridline intersect method. Different letters indicate different statistical groups (ANOVA; post hoc Tukey;  $n = 12$ ;  $F_{(total)3,8} = 4.71$ ;  $F_{(hypophodia)3,8} = 4.21$ ;  $F_{(int. hyphae)3,8} = 37.12$ ;  $F_{(arbuscules)3,8} = 127.9$ ;  $F_{(vesicles)3,8} = 127.9$ ;  $p_{(total, hypophodia)} \leq 0.05$ ;  $p_{(int. hyphae, arbuscules, vesicles)} \leq 0.001$ ).

(E) *RAM1* expression in roots colonized by *R. irregularis* as determined by qRT-PCR. Expression of the housekeeping gene *Ubiquitin10* was used for normalization. Root samples from the same pots as in (D) were used. Different letters indicate different statistical groups (ANOVA; post hoc Tukey;  $n = 24$ ;  $F_{7,15} = 17.24$ ;  $p \leq 0.001$ ).

(F–J) *RAM1* promoter activity in *L. japonicus* roots colonized with *R. irregularis* at 5 wpi. *RAM1* promoter activity is indicated by blue GUS staining.

(F) GUS staining of entire root systems.

(G–J) Colonization in longitudinal root sections (G, I, and J) and a cross-section (H) is visualized by green fluorescent WGA-AlexaFluor488 staining.

See also [Figures S1](#) and [S2](#) and [Tables S1](#) and [S2](#).

Colonization of *cyclops-3* roots that expressed *pUbi:RAM1* led to transcript accumulation of the AM marker genes *SbtM1*, *BCP1*, *Vapyrin B*, *PT4*, *AMT2.2*, *RAM2*, and *STR* to similar levels as in colonized wild-type transformed with an empty vector. Most importantly, overexpression of *RAM1* activated all tested marker genes with the exception of *Vapyrin A*, *Vapyrin B*, and *BCP1* in wild-type [23] and *cyclops-3* in the absence of the fungus (Figure 3B). Fungus-independent expression of symbiosis-regulated genes was also observed in *ccamk-13* transformed with *pUbi:RAM1*. This is particularly interesting because the same construct did not restore colonization and arbuscule for-

mation in the inoculated *ccamk-13* mutant (Figures 3A, 3B, and S3). These data establish that *RAM1* overexpression can bypass the lack of *CCaMK* or *CYCLOPS* because it is sufficient to induce AM-associated marker genes. Thus, *RAM1* acts as a transcriptional activator downstream of *CCaMK* and *CYCLOPS*.

#### **RAM1 Overexpression Restores Arbuscule Formation in the Presence of GA**

In *M. truncatula*, arbuscule formation is inhibited by GA treatment [20]. Inhibition can be prevented by a GA-resistant version of DELLA (*p35S:DELLA1<sup>215</sup>*) [20]. Ectopic expression

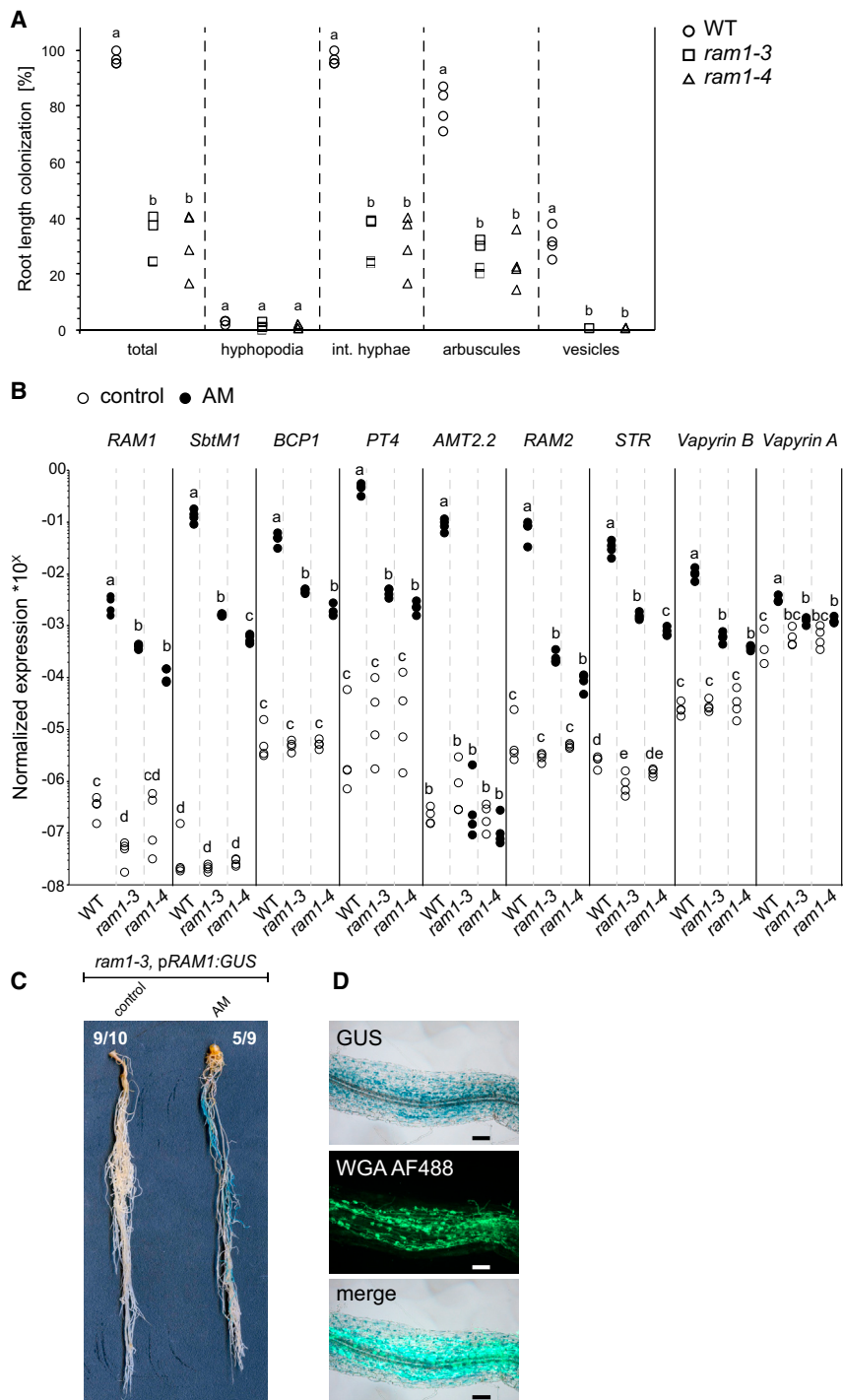


**Figure 2. AM Marker Gene Expression in *L. japonicus ram1* Mutants**

(A) Percent root length colonization at 5 wpi with *R. irregularis* of wild-type, *ram1-3*, and *ram1-4* mutant as determined by gridline intersect method. Different letters indicate statistically different groups (ANOVA; post hoc Tukey;  $n = 12$ ;  $F(\text{total})_{2,9} = 76.08$ ;  $F(\text{hyphopodia})_{2,9} = 2.79$ ;  $F(\text{int. hyphae})_{2,9} = 80.11$ ;  $F(\text{arbuscules})_{2,9} = 58.16$ ;  $F(\text{vesicles})_{2,9} = 308.6$ ;  $p \leq 0.001$  int. hyphae, intraradical hyphae).

(B) Transcript accumulation of *RAM1* and AM marker genes in root material from the experiment shown in (A) upon colonization by *R. irregularis*. Transcript accumulation was determined by qRT-PCR, and the housekeeping gene *Ubiquitin10* was used for normalization. Different letters indicate different statistical groups (ANOVA; post hoc Tukey;  $n = 24$ ;  $F(\text{RAM1})_{5,18} = 186.1$ ;  $F(\text{SbtM1})_{5,18} = 959.7$ ;  $F(\text{BCP1})_{5,18} = 506.6$ ;  $F(\text{PT4})_{5,18} = 45.44$ ;  $F(\text{AMT2.2})_{5,18} = 158.9$ ;  $F(\text{RAM2})_{5,18} = 226.9$ ;  $F(\text{STR})_{5,18} = 913.1$ ;  $p \leq 0.001$ ).

(C and D) p*RAM1*:GUS expression in the *ram1-3* mutant at 5 wpi with *R. irregularis*. Blue GUS staining is visible in whole roots (C) and correlates with colonized areas indicated by green fluorescent WGA-AlexaFluor488 staining (D). Numbers indicate root systems with the displayed phenotype per total number of analyzed transgenic root systems. See also [Tables S1](#) and [S2](#).

GA treatment inhibited arbuscule formation and accordingly AM-related marker gene expression in roots transformed with an empty vector. Roots transformed with p35S:*DELLA1*<sup>417</sup> or p*Ubi*:*RAM1* restored arbuscule formation and marker gene expression ([Figures 4A](#) and [4B](#)) although the plants had responded to GA with increased shoot elongation ([Figure S4](#)). This indicates that *RAM1* can either replace *DELLA* (because the two proteins are highly related; [Figure S2](#)) or is required at a lower hierarchy level than *DELLA*. However, 35S promoter-driven expression of *DELLA1*<sup>417</sup> in the *ram1-3* mutant did not restore fine branching of arbuscules ([Figure 5A](#)), although in the wild-type, it was sufficient to support formation of fully developed arbuscules in the presence of GA ([Figure 4](#)). Similarly, root treatment with the GA biosynthesis

inhibitor paclobutrazol (PAC), which promotes accumulation of *DELLA* proteins [30], did not restore fine branching nor quantitative colonization ([Figures 5B](#), [S5A](#), and [S5B](#)), although it was sufficient to restore formation of fully branched arbuscules in *cyclops* mutants ([Figures 5B](#) and [S5A](#)), similar to p35S:*DELLA1*<sup>417</sup> expression [20]. Taken together, these data indicate that *DELLA* cannot replace *RAM1*. Moreover, also in *Lotus*, ectopic *DELLA1*<sup>417</sup> expression and PAC treatment activated *RAM1* transcription in the absence of the fungus ([Figures 5C–5E](#)) [23],

of *M. truncatula* *DELLA1*<sup>418</sup> can also restore arbuscule formation in *cyclops-3* mutants similar to ectopic expression of *RAM1* [20], and it can induce *RAM1* expression in the absence of fungus [23]. This suggests that *DELLA* and *RAM1* may act sequentially. To address this, we examined whether p*Ubi*:*RAM1* restores arbuscule formation in *Lotus* roots in the presence of GA. As a positive control, we included hairy roots expressing a GA-resistant *DELLA1* version of *L. japonicus* (p35S:*DELLA1*<sup>417</sup>), similar to the published construct containing *Medicago* *DELLA1*<sup>418</sup> [20].

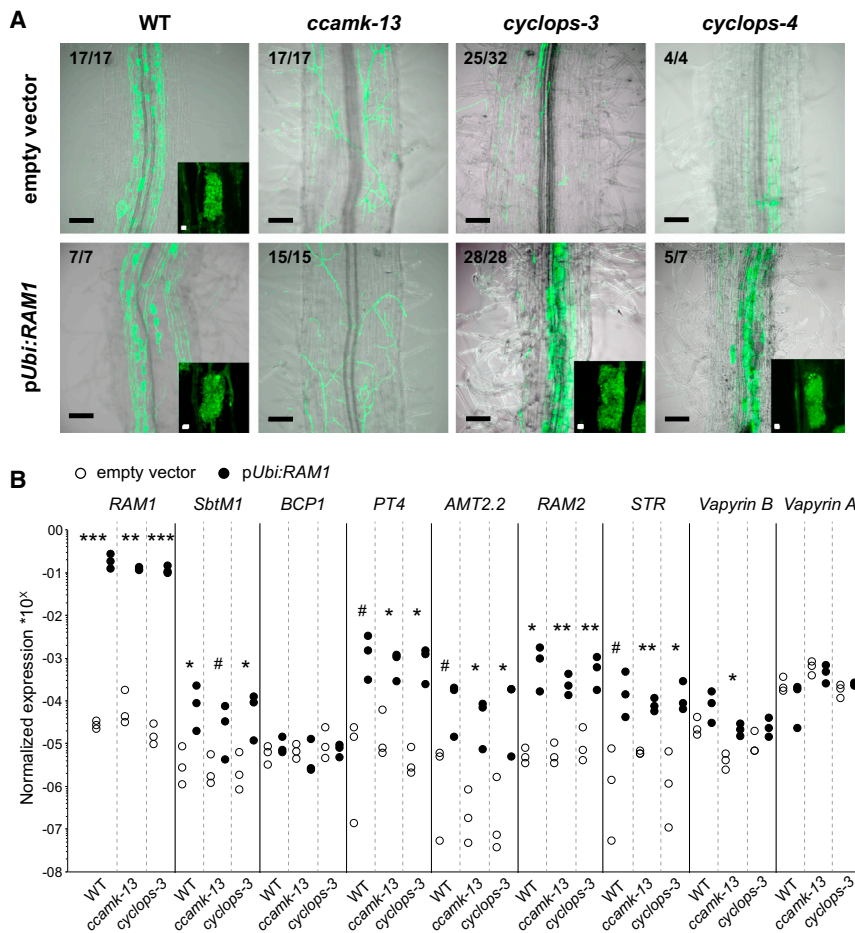


**Figure 3. *RAM1* Overexpression Restores Symbiotic Signaling in *ccamk* and *cyclops* Mutants**

(A) Laser scanning confocal images of hairy roots of *L. japonicus* wild-type, *ccamk-13*, *cyclops-3*, and *cyclops-4* mutants transformed with an empty vector control (upper panel) and with pUbi:RAM1 (lower panel) and colonized by *R. irregularis* at 5 wpi; scale bar, 100  $\mu$ m. Insets show close up of arbuscules; scale bar, 5  $\mu$ m. The fungus is stained with WGA-AlexaFluor488. Numbers indicate root systems with the displayed phenotype per total number of analyzed transgenic root systems.

(B) Transcript accumulation of AM marker genes in non-colonized hairy roots of wild-type, *ccamk-13*, and *cyclops-3* transformed with an empty vector or with pUbi:RAM1 at 6 wpi. Transcript accumulation was assessed by qRT-PCR, and expression of the housekeeping gene *Ubiquitin10* was used for normalization. Statistical analysis used a Welch t test ( $n = 6$ ; # $p \leq 0.1$ ; \* $p \leq 0.05$ ; \*\* $p \leq 0.01$ ; \*\*\* $p \leq 0.001$ ).

See also Figure S3 and Tables S1 and S2.

because the related GRAS protein RAM1 did not enhance the effect of CCaMK<sup>314</sup> and CYCLOPS on reporter expression (Figure 6A). This suggests that CCaMK<sup>314</sup>, CYCLOPS, and DELLA together activate the RAM1 promoter.

Congruently, we observed that the previously reported fungus-independent induction of RAM1 by CCaMK<sup>314</sup> in *L. japonicus* hairy roots [14] was abolished in a *cyclops-3* mutant and also by GA

indicating that DELLA is involved in RAM1's transcriptional regulation.

### The RAM1 Promoter Is Activated by a Complex of CCaMK<sup>314</sup>, CYCLOPS, and DELLA

A gain-of-function version of CCaMK (CCaMK<sup>314</sup>) consisting of the first 314 amino acids that constitute only the kinase domain but lack the autoinhibitory domain can activate RAM1 transcript accumulation in the absence of AM fungi [14]. These data together with our findings that RAM1 acts downstream of the CCaMK phosphorylation target CYCLOPS in arbuscule development and can be activated by DELLA1<sup>Δ177</sup> (Figures 3, 4, and 5) [23] suggested that RAM1 transcription could be directly regulated by CYCLOPS and/or DELLA. To test this in transactivation assays, pRAM1:GUS was co-expressed with NLS-CCaMK<sup>314</sup>-dsRed, 3xHA-CYCLOPS, and DELLA1<sup>Δ177</sup> in *Nicotiana benthamiana* leaves (Figure 6A). The reporter was expressed when both CYCLOPS and the autoactive CCaMK<sup>314</sup> were co-transformed with pRAM1:GUS, indicating that CYCLOPS is sufficient to induce the RAM1 promoter in *N. benthamiana* leaves in the presence of CCaMK<sup>314</sup>. When DELLA1<sup>Δ177</sup> was combined with CCaMK<sup>314</sup> and CYCLOPS, reporter expression level was higher than that induced by the combination of CCaMK<sup>314</sup> and CYCLOPS (Figure 6A). The amplification of pRAM1 activation was specific for DELLA

treatment in the wild-type (Figure 6B), showing that RAM1 expression depends on CYCLOPS as well as DELLA. DELLA proteins typically regulate promoter activation by interacting with DNA-binding transcription factors [31, 32]. Therefore, we asked whether DELLA would also physically interact with the DNA-binding transcription factor CYCLOPS [10] during RAM1 promoter activation. To test physical interaction, we performed Y2H assays (Figure 6C). Both CYCLOPS and DELLA show strong autoactivation in yeast when coupled with the DNA-binding domain of the yeast GAL4 protein [10, 33]. Therefore, we coupled full-length CYCLOPS to the GAL4 activation domain (AD) and fused truncated versions of DELLA1 (F1 and M5; Figure 6C) that were previously reported not to show autoactivation in yeast [33], to the GAL4 binding domain (BD). The combination of DELLA M5 and CYCLOPS promoted yeast growth without autoactivation, indicating that DELLA1 and CYCLOPS can interact in yeast and that the interaction site of DELLA1 is likely positioned between amino acids 381 and 408 (Figure 6C). However, in yeast, DELLA1 did not directly interact with full-length CCaMK or CCaMK<sup>314</sup> (Figure S6A). Interaction of CYCLOPS with DELLA1<sup>Δ177</sup> or full-length DELLA1 was also indicated by bimolecular fluorescence complementation (BiFC) (Figure 6D) and by co-immunoprecipitation (coIP) (Figure 6E). Both versions of DELLA also interacted with CYCLOPS when CCaMK<sup>314</sup> was co-expressed in *N. benthamiana* leaf cells and with CCaMK in

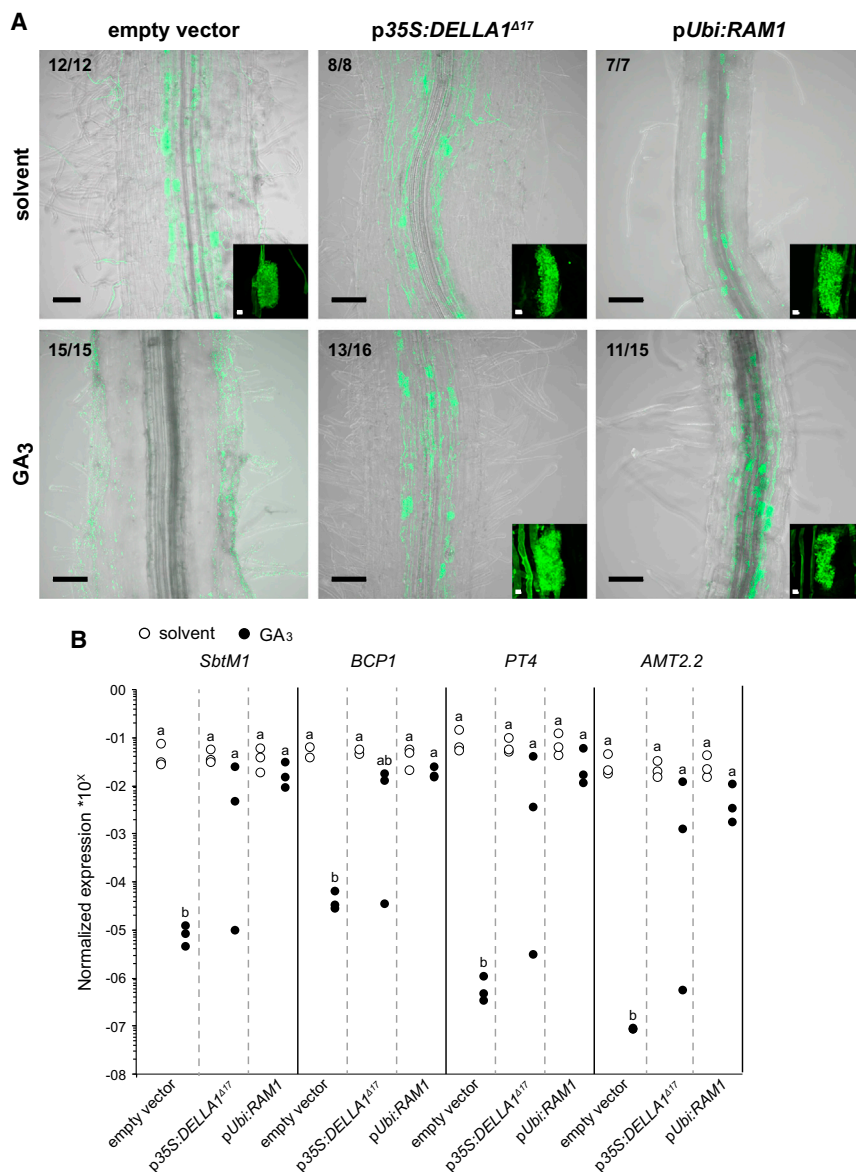


**Figure 4. *RAM1* Overexpression Restores Arbuscule Formation in the Presence of GA**

(A) Laser scanning confocal images of wild-type roots of *L. japonicus* transformed with an empty vector (left), p35S:DELLA1<sup>Δ17</sup> (middle), and pUbi:RAM1 (right) and colonized by *R. irregularis*. The roots were watered with solvent (0.002% ethanol) or 1 μM gibberellic acid3 (GA<sub>3</sub>) at 5 wpi. Treatment started at 1 wpi; scale bar, 100 μm. Insets show close ups of arbuscules; scale bar, 5 μm. The fungus is stained with WGA-AlexaFluor488. Numbers indicate root systems with the displayed phenotype per total number of analyzed transgenic root systems.

(B) Transcript accumulation of AM marker genes as assessed by qRT-PCR in *R. irregularis*-colonized hairy roots of wild-type, transformed with an empty vector, with p35S:DELLA1<sup>Δ17</sup> or with pUbi:RAM1. Expression of the housekeeping gene *Ubiquitin10* was used for normalization. Root samples from the same pots as in (A) were used. Different letters indicate different statistical groups (ANOVA; post hoc Tukey; n = 18; F(*SbtM1*)<sub>5,12</sub> = 11.23; F(*BCP1*)<sub>5,12</sub> = 10.96; F(*PT4*)<sub>5,12</sub> = 15.21; F(*AMT2.2*)<sub>5,12</sub> = 15.20; p ≤ 0.001).

See also Figure S4 and Tables S1 and S2.

site (Figures 7A and 7B) was identified as essential for activation by the CCaMK<sup>314</sup>/CYCLOPS complex. In electrophoretic mobility shift assays (EMSA), CYCLOPS-min, containing the binding and activation domain of CYCLOPS [10], bound the *AMCYC-RE* probe. This interaction was sequence specific because competition for binding to the labeled probe was successful with unlabeled wild-type *AMCYC-RE*, but unsuccessful with mutated *AMCYC-RE* (*mAMCYC-RE*) (Figure 7C). Taken together, this indicates that CYCLOPS activates the *RAM1* promoter through direct binding to the *AMCYC-RE*. In order to test the relevance

of this element in AM symbiosis, we analyzed a promoter deletion series in *Lotus* roots colonized by *R. irregularis* and found that the -325-bp promoter fragment containing this element was sufficient to drive GUS expression in colonized roots (Figure S7).

the presence of CYCLOPS, indicating that all three proteins form a complex (Figures 6D and 6E). Furthermore, we observed by coIP that also the CYCLOPS ortholog of *M. truncatula* called INTERACTING PROTEIN of DMI3 (IPD3) interacts with DELLA2 of *M. truncatula* (Figure S6B). Thus, CYCLOPS interaction with DELLA is conserved within the legumes and among different DELLA isoforms.

### CYCLOPS Transactivates the *RAM1* Promoter via Direct Binding to a *cis* Element

In order to identify the *cis* element responsible for CYCLOPS-mediated *RAM1* activation, we performed promoter deletion studies in *N. benthamiana* leaves. p*RAM1* deletion constructs were co-transformed with NLS-CCaMK<sup>314</sup>-*dsRed* and 3xHA-CYCLOPS, because these two proteins are sufficient for p*RAM1* activation (Figure 6A). A 30-bp response element “*AMCYC-RE*” 280 bp upstream of the transcriptional start

of this element in AM symbiosis, we analyzed a promoter deletion series in *Lotus* roots colonized by *R. irregularis* and found that the -325-bp promoter fragment containing this element was sufficient to drive GUS expression in colonized roots (Figure S7).

## DISCUSSION

Arbuscule development is accompanied by profound structural rearrangements of the host cortex cell. Genetic evidence demonstrates that the host cell plays a major role in determining the size, shape, and branching pattern of arbuscules [3, 34]. Many transcription-factor-encoding genes are activated during arbuscule formation [24, 35, 36]. This might reflect complex regulatory networks mediating host cell reorganization and arbuscule development. However, the genetic relevance, mechanistic role, and connectivity among these transcription factors are largely unknown.

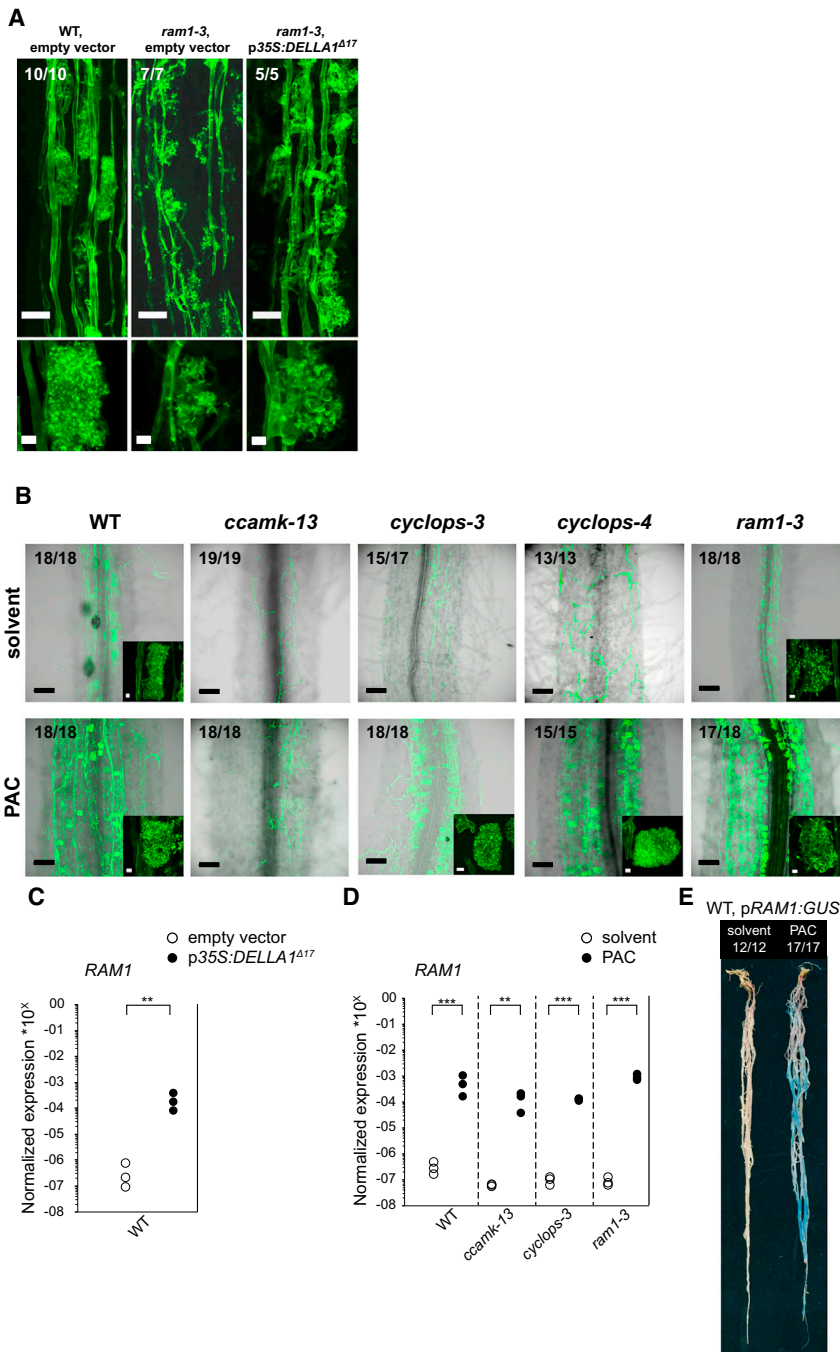


### Figure 5. Stabilized DELLA Induces Fungus-Independent *RAM1* Transcription

(A) Laser scanning confocal images of hairy roots of *L. japonicus* wild-type and *ram1-3* mutant transformed with an empty vector control and *ram1-3* transformed with p35S:DELLA<sup>Δ17</sup> colonized by *R. irregularis* at 5 wpi. The scale bars represent 25 μm. Insets show close ups of arbuscules; scale bars, 5 μm. Numbers indicate root systems with the displayed phenotype per total number of analyzed transgenic root systems. In (A) and (B), the fungus was stained with WGA-AlexaFluor488. Numbers indicate root systems with the displayed phenotype per total number of analyzed root systems.

(B) Laser scanning confocal images of *L. japonicus* wild-type, *ccamk-13*, *cyclops-3*, *cyclops-4*, and *ram1-3* roots colonized by *R. irregularis* at 5 wpi treated with solvent (0.01% ethanol) or 1 μM paclobutrazol (PAC). Treatment started at 1 wpi.

(C) Transcript accumulation of *RAM1* in non-colonized wild-type hairy roots transformed with an empty vector or with p35S:DELLA<sup>Δ17</sup> as assessed by qRT-PCR. In (C) and (D), expression of the housekeeping gene *Ubiquitin10* was used for normalization. Statistical comparisons were performed for each genotype separately (t test; \*\*p ≤ 0.01; \*\*\*p ≤ 0.001).

(D) Transcript accumulation of *RAM1* in non-colonized wild-type, *ccamk-13*, *cyclops-3*, and *cyclops-4* roots treated with solvent (0.01% ethanol) or 1 μM PAC at 5 weeks post-planting as assessed by qRT-PCR. Treatment started at 1 week post-planting (wpp).

(E) Promoter activity visualized by blue GUS staining in *L. japonicus* wild-type hairy root systems in response to solvent (0.01% ethanol) and 1 μM PAC at 5 weeks post-planting. Treatment started at 1 wpp. Treatments were performed in absence of the fungus.

See also Figure S5 and Tables S1 and S2.

Here, we describe a central regulatory cascade in which the GRAS protein *RAM1* is an essential regulator of arbuscule formation because, as also reported previously, (1) *ram1* mutants are perturbed in arbuscule branching (Figure 1A) and (2) ectopic *RAM1* expression is sufficient to induce genes with established functions in arbuscule development (Figure 2B) such as *STR* and *RAM2* [23–25, 27–29]. The transcriptional activation of target genes by ectopic *RAM1* expression in the absence of the fungus strongly suggests that *RAM1* acts as a transcription factor. Nevertheless, most examined marker genes were induced upon colonization in roots of two allelic *ram1* mutants

*ram1* mutants dissect *AMT2.2* from *PT4* expression (Figure 2B), indicating different players inducing peri-arbuscular membrane localized transporter-encoding genes (Figure 7D). Marker gene induction in *L. japonicus ram1* contrasts with *RAM1* dependence of arbuscule-related marker genes including *PT4*, *RAM2*, and *STR* in *Petunia* and *Medicago* [15, 23–25]. This partial redundancy at the level of *RAM1* appears therefore specific to *L. japonicus*. Nevertheless, the redundant factor in *L. japonicus* is insufficient to support arbuscule branching, suggesting that *RAM1* target genes co-regulated with *AMT2.2* are responsible for the *ram1* phenotype (Figure 7D). Several GRAS protein

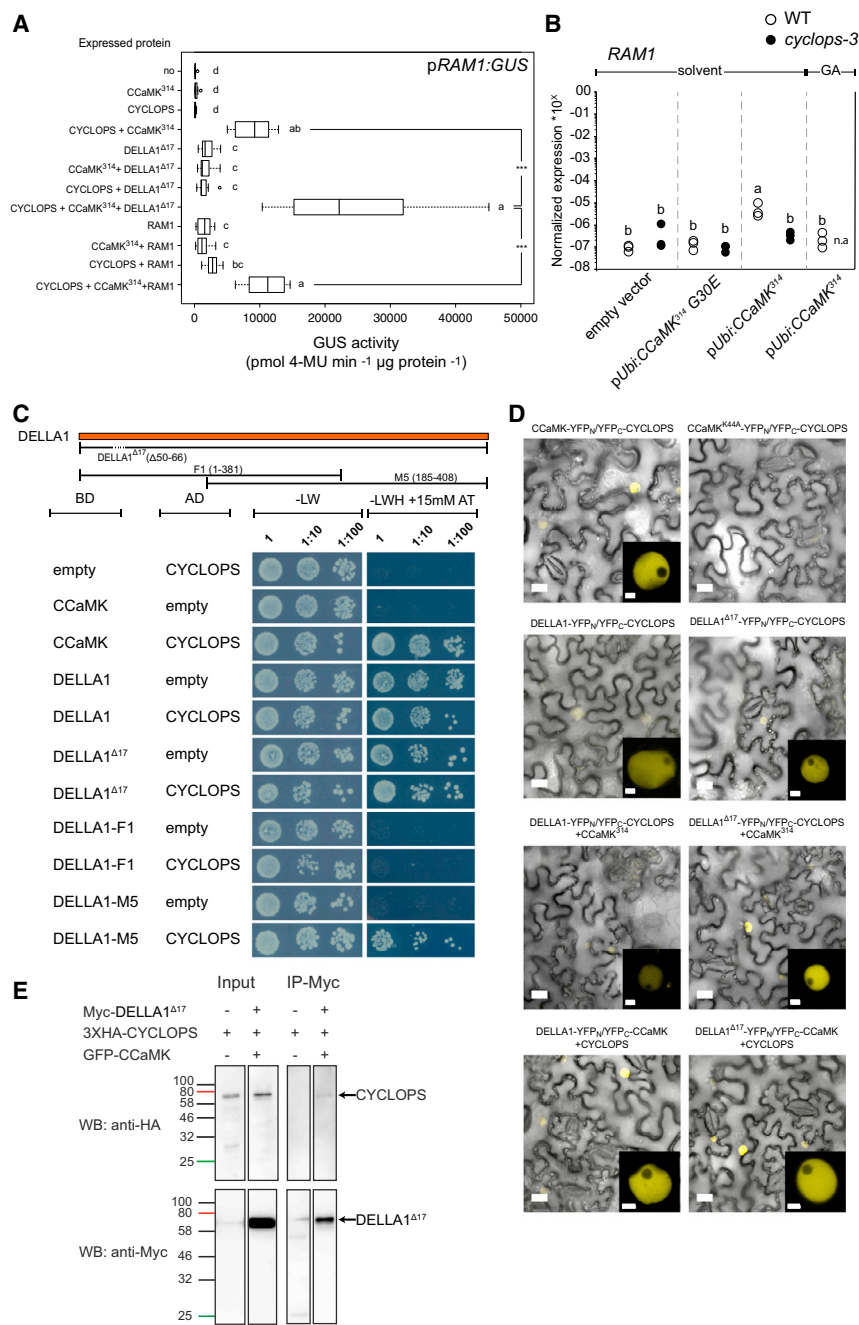


**Figure 6. A Complex of CCaMK<sup>314</sup>, CYCLOPS, and DELLA Activates the RAM1 Promoter**

(A) Transactivation assay in *Nicotiana benthamiana* leaves showing that the *RAM1* promoter is induced by a combination of CYCLOPS and CCaMK<sup>314</sup> and more strongly induced with additional co-expression of DELLA1<sup>Δ17</sup>. The pRAM1:GUS reporter plasmid was co-transformed with plasmids containing the genomic sequence of the proteins indicated at the y axis driven by constitutive promoters. Boxplots represent GUS activity from 6–12 replicate leaf disks. Bold black line, median; box, interquartile range; whiskers highest and lowest data point within 1.5 interquartile range; dots, outliers outside the 1.5 interquartile range. Different letters indicate different statistical groups (ANOVA; post hoc Tukey;  $F_{11,116} = 68.91$ ;  $p \leq 0.001$ ). Asterisks indicate statistical significant differences ( $**p \leq 0.001$ ) in pairwise comparisons by t test.

(B) *RAM1* transcript accumulation in wild-type (WT) and *cyclops-3* hairy roots transformed with an empty vector, with a kinase-dead version of CCaMK<sup>314</sup> (pUbi:CCaMK<sup>314</sup> G30E-NLS), or with pUbi:CCaMK<sup>314</sup>-NLS at 5 wpp in absence of AM fungi. Roots were treated with solvent (0.002% ethanol) or 1 μM GA. Treatment started at 1 wpp. *RAM1* transcript accumulation was assessed by qRT-PCR and normalized with the expression value of *Ubiquitin10*. Different letters indicate different statistical groups (ANOVA; post hoc Tukey;  $n = 21$ ;  $F_{6,14} = 11.31$ ;  $p \leq 0.001$ ). n.a., not analyzed.

(C) GAL4-based yeast two-hybrid assay for interaction of CYCLOPS as prey (AD) and different DELLA1 versions as bait (BD). The well-established interaction between CCaMK and CYCLOPS was used as a positive control and all coding-sequence-containing plasmids in combination with the complementary empty vector as negative controls. Transformed yeast strains were dropped at optical density 600 ( $OD_{600}$ ) = 0.6, 0.06 (1:10), and 0.006 (1:100) on synthetic medium lacking Leu and Trp (–LW) or lacking Leu, Trp, and His (–LWH) and containing 15 mM 3-AT to suppress autoactivation.

(D) Analysis for interaction of CYCLOPS and DELLA using bimolecular fluorescence complementation in *N. benthamiana* leaf epidermal cells. Leaves were transiently transformed with T-DNAs containing the indicated genes, and images were taken 72 hr after infiltration. YFP<sub>N</sub>, N-terminal half of YFP; YFP<sub>C</sub>, C-terminal half of YFP. Yellow fluorescence indicates interaction. Overlays of confocal and bright field images are shown. The size bars represent 100 μm. Insets are high-magnification micrographs

of yellow fluorescing nuclei. The size bars represent 5 μm. The interaction of CYCLOPS with CCaMK was used as a positive control and with the kinase-dead version CCaMK<sup>K44A</sup> as a negative control [10].

(E) Co-immunoprecipitation assay showing interaction of CYCLOPS and DELLA1<sup>Δ17</sup> in presence of CCaMK in *N. benthamiana* leaves. For the input blots, 0.3% input extract was loaded to detect 3xHA-CYCLOPS and MYC-DELLA1<sup>Δ17</sup>. After co-immunoprecipitation, 30% of the eluate was loaded, detecting both 3xHA-CYCLOPS and MYC-DELLA1<sup>Δ17</sup>.

See also Figure S6 and Tables S1 and S2.

encoding genes such as the closely related *REQUIRED FOR ARBUSCULE DEVELOPMENT* (*RAD1*) or *TF124* are induced upon AM [23, 24] and could act redundantly with *RAM1*.

Our data reveal *RAM1* as an entry point into AM-specific transcriptional regulation downstream of CYCLOPS, because the *RAM1* promoter is induced by CYCLOPS and autoactive

CCaMK and overexpression of *RAM1* restores arbuscule formation in *cyclops* mutants (Figure 3). We identified a *cis* element (*AMCYC-RE*) that is bound by CYCLOPS and required for *RAM1* promoter activation. It contains a palindrome that has computationally been identified in promoters of several AM-induced genes [40]. It is possible that the CCaMK-CYCLOPS

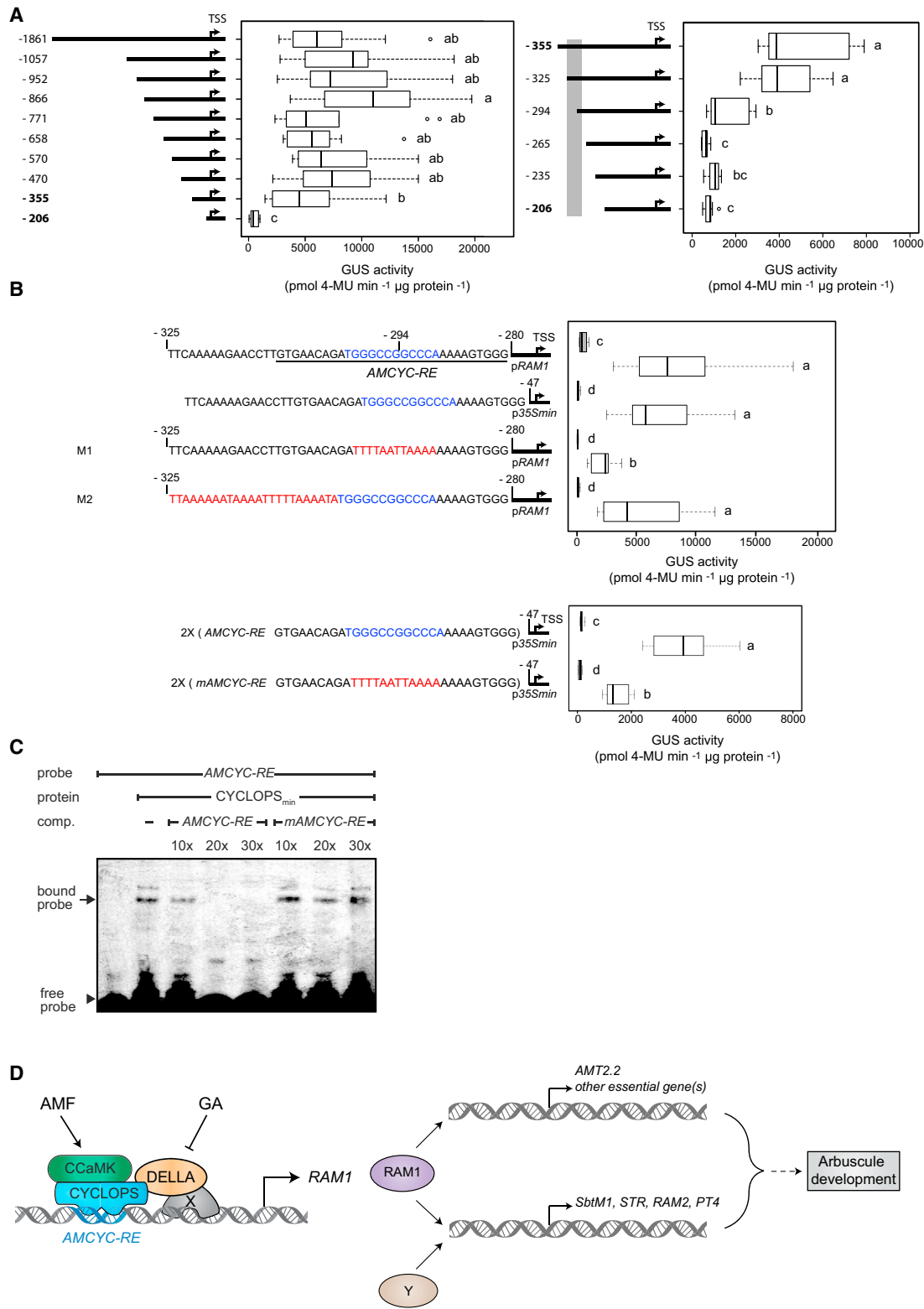


**Figure 7. The CCaMK<sup>314</sup>-CYCLOPS Complex Transactivates the *RAM1* Promoter through Binding to the Palindrome-Containing Response Element *AMCYC-RE***

(A and B) Identification of a CYCLOPS responsive *cis* element in the *RAM1* promoter. Indicated promoter fragments were fused to the *uidA* gene, and these constructs were transformed (gray) or co-transformed with p35S:*CYCLOPS* and p35S:*CCaMK*<sup>314</sup> (white) into *N. benthamiana* leaf cells. Boxplots represent GUS activity (legend continued on next page)

complex governs this regulon. *AMCYC-RE* differs from the previously identified *CYC-RE* in the *NIN* promoter [10]. Thus, *cis* element binding specificity by transcription factor complexes might be involved in the decision between AM and root nodule symbiosis downstream of common symbiosis signaling.

The failure to restore colonization of *ccamk-13* mutants is probably due to absence of cortical colonization of *ccamk-13* mutant roots with fungal hyphae, which is the prerequisite for arbuscule formation. It likely requires phosphorylation of additional CCaMK targets [41]. Still, *ccamk* mutants are able to trigger at least parts of the cortical program as evidenced by induction of arbuscule-related marker genes by *pUbi:RAM1* expression. Fungus-independent induction of arbuscule-development-related genes by *pUbi:RAM1* (Figure 3B) recapitulates the previously described induction of *RAM1*, *SbtM1*, and *RAM2* by p35S-driven expression of *CCaMK<sup>314</sup>* [14]. Thus, we reveal a key transcriptional regulatory cascade coordinating arbuscule development in which an activated CCaMK-CYCLOPS complex induces *RAM1* expression, and *RAM1* subsequently activates *SbtM1*, *RAM2*, *STR*, and other genes required for arbuscule development (Figure 7D).

Our analyses also resolve a role of DELLA proteins in arbuscule formation. Although our experiments involve only the GA-resistant DELLA1, results from GA and PAC treatments and the notion that DELLAs are replaceable and act redundantly [20, 42] suggest an involvement of DELLA proteins in general. They act upstream of *RAM1* (Figures 4 and 5) and participate in the complex with CCaMK and CYCLOPS that induces *RAM1* expression and therefore in the transcriptional cascade that starts AM-specific transcriptional regulation downstream of CYCLOPS (Figures 6 and 7). DELLAs themselves are likely not AM-specific factors as GA not only inhibits AM symbiosis but also nodulation [43]. Given that both CYCLOPS and DELLA are required for CCaMK<sup>314</sup>-mediated *RAM1* induction, it is somewhat surprising that *DELLA1<sup>d178</sup>* [20] and PAC treatment (Figure 5B) can restore arbuscule formation in *cyclops* mutants and spontaneously induce *RAM1*. This conundrum might point to a role of CYCLOPS in stabilizing DELLA to facil-

itate DELLA association with yet additional unknown transcriptional regulators that participate in activating the *RAM1* promoter and become sufficient in the presence of stabilized DELLA (Figure 7D).

Arbuscule formation is tightly controlled by the plant and needs to be synchronized with its nutritional and physiological needs. For example, colonization is inhibited by far-red light and arbuscule development is inhibited at high P-levels [44, 45]. This likely involves plant hormone signaling [45], which integrates plant physiology with development [41]. The *RAM1* promoter emerges as a central integration node of symbiotic (CCaMK/CYCLOPS) and hormonal (DELLA/GA) signaling and may be an important target during adaptation of AM development to the plant physiological status.

#### ACCESSION NUMBERS

The accession number for the *L. japonicus RAM1* sequence information reported in this paper is NCBI: KU557503.

#### SUPPLEMENTAL INFORMATION

Supplemental Information includes seven figures, Supplemental Experimental Procedures, and two tables and can be found with this article online at <http://dx.doi.org/10.1016/j.cub.2016.01.069>.

#### AUTHOR CONTRIBUTIONS

P.P. performed most experiments, designed experiments, prepared the figures, and contributed to conception of the study. S.C. contributed Figures 3B, S2, and S3 and performed all statistical analyses. M. Paries contributed Figures 2D, 5E, most of 7A, and S7. K.K. contributed Figure 7C. V.K. contributed yeast transformation and drop test for Figures 6C and S6A and supported some of the other experiments with cloning, cDNA preparation, and hairy root transformation. M.J.B. contributed transgenic roots and promoter deletion plasmids plus one biological replicate for the left graph of Figure 7A. L.K. generated preliminary data for Figure 6A. D.S.F. and M.J.H. contributed Figure S6B. M. Parniske contributed materials and contributed to conception of the study and editing the manuscript. C.G. identified the *ram1-3* mutation in NGS data, conceived the study, designed experiments, supervised the study, and wrote the manuscript.

activity in 8–13 (A) or 12–16 (B) replicate leaf disks from independent plants collected in three temporally independent experiments. Bold black line, median; box, interquartile range; whiskers highest and lowest data point within 1.5 interquartile range; dots, outliers outside the 1.5 interquartile range.

(A) Approximately 100 bp (left) and ~30 bp (right) deletion series of the *RAM1* promoter placed the CYCLOPS response element (*AMCYC-RE*) between –325 bp and –265 bp upstream of the transcriptional start site (TSS). Gray bar indicates the position of the *AMCYC-RE* shown in (B). Different letters indicate different statistical groups (ANOVA; post hoc Tukey;  $p \leq 0.001$ ; F(left)<sub>9,101</sub> = 23.28; F(right)<sub>5,51</sub> = 50.11).

(B) Upper graph: the promoter region between –331 and –280 contains a GC-rich palindromic sequence (blue) required for *RAM1* promoter activation. Mutation (red) of the palindrome (fragment M1) reduces transactivation whereas mutation of a random upstream sequence (fragment M2) does not change transactivation level. Lower graph: fusion of a 2× tandem repeat of the *AMCYC-RE* to the 35S minimal promoter is sufficient for transactivation by the CCaMK314-CYCLOPS complex. Different letters indicate different statistical groups (ANOVA; post hoc Tukey;  $p \leq 0.001$ ; F(upper graph)<sub>7,105</sub> = 138.4; F(lower graph)<sub>3,49</sub> = 250.9).

(C) CYCLOPS specifically binds the *RAM1* promoter. EMSA was performed using 6xHis-CYCLOPS<sub>min</sub> (100 pmol) and CY5-labeled *AMCYC-RE* (100 fmol) as probe. For specificity, unlabeled competitor DNA carrying either the wild-type (*AMCYC-RE*) or mutated palindrome (*mAMCYC-RE*) were added in 10-, 20-, or 30-fold molar excess. The arrow and arrowhead indicate the position of the specifically bound and the free probe, respectively. Samples were resolved on a 6% polyacrylamide gel.

(D) Proposed transcriptional cascade regulating arbuscule development. CYCLOPS and DELLA form a complex with CCaMK that is activated by signaling from arbuscular mycorrhiza fungi (AMF). This complex activates transcription of *RAM1* through direct binding of CYCLOPS to the *AMCYC* response element in the *RAM1* promoter. Restoration of arbuscule formation in *cyclops* mutants by stabilization of DELLA [20] (this work) suggests that DELLA might also interact with another transcription factor (X) that binds the *RAM1* promoter and becomes sufficient for induction when DELLA is stabilized. Gibberellin (GA) causes degradation of DELLA and therefore inhibits *RAM1* expression and arbuscule formation. In concert with a partially redundant factor (Y), *RAM1* directly or indirectly activates downstream genes required for arbuscule initiation, branching, and function such as *SbtM1*, *STR*, *RAM2*, and *PT4*. Transcriptional activation of *AMT2.2* and likely other genes essential for arbuscule branching fully depends on *RAM1*.

See also Figure S7 and Tables S1 and S2.

## ACKNOWLEDGMENTS

We thank Makoto Hayashi (RIKEN, Yokohama, Japan) for the *RFP-CCaMK<sup>314</sup>-NLS* plasmid. This work was supported by the Collaborative Research Center (SFB924) "Molecular mechanisms regulating yield and yield stability in plants" of the German Research Foundation (DFG). C.G. was supported by the Emmy Noether program (GU1423/1-1) of the DFG during part of the study.

Received: September 25, 2015

Revised: December 15, 2015

Accepted: January 28, 2016

Published: March 24, 2016

## REFERENCES

- Smith, S.E., and Smith, F.A. (2011). Roles of arbuscular mycorrhizas in plant nutrition and growth: new paradigms from cellular to ecosystem scales. *Annu. Rev. Plant Biol.* **62**, 227–250.
- Javot, H., Penmetsa, R.V., Terzaghi, N., Cook, D.R., and Harrison, M.J. (2007). A *Medicago truncatula* phosphate transporter indispensable for the arbuscular mycorrhizal symbiosis. *Proc. Natl. Acad. Sci. USA* **104**, 1720–1725.
- Gutjahr, C., and Parniske, M. (2013). Cell and developmental biology of arbuscular mycorrhiza symbiosis. *Annu. Rev. Cell Dev. Biol.* **29**, 593–617.
- Parniske, M. (2008). Arbuscular mycorrhiza: the mother of plant root endosymbioses. *Nat. Rev. Microbiol.* **6**, 763–775.
- Oldroyd, G.E. (2013). Speak, friend, and enter: signalling systems that promote beneficial symbiotic associations in plants. *Nat. Rev. Microbiol.* **11**, 252–263.
- Antolín-Llovera, M., Ried, M.K., Binder, A., and Parniske, M. (2012). Receptor kinase signaling pathways in plant-microbe interactions. *Annu. Rev. Phytopathol.* **50**, 451–473.
- Sun, J., Miller, J.B., Granqvist, E., Wiley-Kalil, A., Gobbato, E., Maillet, F., Cottaz, S., Samain, E., Venkateshwaran, M., Fort, S., et al. (2015). Activation of symbiosis signaling by arbuscular mycorrhizal fungi in legumes and rice. *Plant Cell* **27**, 823–838.
- Miller, J.B., Pratap, A., Miyahara, A., Zhou, L., Bornemann, S., Morris, R.J., and Oldroyd, G.E.D. (2013). Calcium/Calmodulin-dependent protein kinase is negatively and positively regulated by calcium, providing a mechanism for decoding calcium responses during symbiosis signaling. *Plant Cell* **25**, 5053–5066.
- Yano, K., Yoshida, S., Müller, J., Singh, S., Banba, M., Vickers, K., Markmann, K., White, C., Schuller, B., Sato, S., et al. (2008). *CYCLOPS*, a mediator of symbiotic intracellular accommodation. *Proc. Natl. Acad. Sci. USA* **105**, 20540–20545.
- Singh, S., Katzer, K., Lambert, J., Cerri, M., and Parniske, M. (2014). *CYCLOPS*, a DNA-binding transcriptional activator, orchestrates symbiotic root nodule development. *Cell Host Microbe* **15**, 139–152.
- Kistner, C., Winzer, T., Pitzschke, A., Mulder, L., Sato, S., Kaneko, T., Tabata, S., Sandal, N., Stougaard, J., Webb, K.J., et al. (2005). Seven *Lotus japonicus* genes required for transcriptional reprogramming of the root during fungal and bacterial symbiosis. *Plant Cell* **17**, 2217–2229.
- Takeda, N., Haage, K., Sato, S., Tabata, S., and Parniske, M. (2011). Activation of a *Lotus japonicus* subtilase gene during arbuscular mycorrhiza is dependent on the common symbiosis genes and two cis-active promoter regions. *Mol. Plant Microbe Interact.* **24**, 662–670.
- Gutjahr, C., Banba, M., Croset, V., An, K., Miyao, A., An, G., Hirochika, H., Imaizumi-Anraku, H., and Paszkowski, U. (2008). Arbuscular mycorrhiza-specific signaling in rice transcends the common symbiosis signaling pathway. *Plant Cell* **20**, 2989–3005.
- Takeda, N., Handa, Y., Tsuzuki, S., Kojima, M., Sakakibara, H., and Kawaguchi, M. (2015). Gibberellins interfere with symbiosis signaling and gene expression and alter colonization by arbuscular mycorrhizal fungi in *Lotus japonicus*. *Plant Physiol.* **167**, 545–557.
- Gobbato, E., Marsh, J.F., Vernié, T., Wang, E., Maillet, F., Kim, J., Miller, J.B., Sun, J., Bano, S.A., Ratet, P., et al. (2012). A GRAS-type transcription factor with a specific function in mycorrhizal signaling. *Curr. Biol.* **22**, 2236–2241.
- Murray, J.D., Muni, R.R.D., Torres-Jerez, I., Tang, Y., Allen, S., Andriankaja, M., Li, G., Laxmi, A., Cheng, X., Wen, J., et al. (2011). *Vapyrin*, a gene essential for intracellular progression of arbuscular mycorrhizal symbiosis, is also essential for infection by rhizobia in the nodule symbiosis of *Medicago truncatula*. *Plant J.* **65**, 244–252.
- El Ghachtouli, N., Martin-Tanguy, J., Paynot, M., and Gianinazzi, S. (1996). First report of the inhibition of arbuscular mycorrhizal infection of *Pisum sativum* by specific and irreversible inhibition of polyamine biosynthesis or by gibberellic acid treatment. *FEBS Lett.* **385**, 189–192.
- Foo, E., Ross, J.J., Jones, W.T., and Reid, J.B. (2013). Plant hormones in arbuscular mycorrhizal symbioses: an emerging role for gibberellins. *Ann. Bot. (Lond.)* **111**, 769–779.
- Yu, N., Luo, D., Zhang, X., Liu, J., Wang, W., Jin, Y., Dong, W., Liu, J., Liu, H., Yang, W., et al. (2014). A DELLA protein complex controls the arbuscular mycorrhizal symbiosis in plants. *Cell Res.* **24**, 130–133.
- Floss, D.S., Levy, J.G., Lévesque-Tremblay, V., Pumphin, N., and Harrison, M.J. (2013). DELLA proteins regulate arbuscule formation in arbuscular mycorrhizal symbiosis. *Proc. Natl. Acad. Sci. USA* **110**, E5025–E5034.
- Davière, J.-M., and Achard, P. (2013). Gibberellin signaling in plants. *Development* **140**, 1147–1151.
- Willige, B.C., Ghosh, S., Nill, C., Zourelidou, M., Dohmann, E.M.N., Maier, A., and Schwechheimer, C. (2007). The DELLA domain of GA INSENSITIVE mediates the interaction with the GA INSENSITIVE DWARF1A gibberellin receptor of *Arabidopsis*. *Plant Cell* **19**, 1209–1220.
- Park, H.J., Floss, D.S., Lévesque-Tremblay, V., Bravo, A., and Harrison, M.J. (2015). Hyphal branching during arbuscule development requires *Reduced Arbuscular Mycorrhiza1*. *Plant Physiol.* **169**, 2774–2788.
- Xue, L., Cui, H., Buer, B., Vijayakumar, V., Delaux, P.-M., Junkermann, S., and Bucher, M. (2015). Network of GRAS transcription factors involved in the control of arbuscule development in *Lotus japonicus*. *Plant Physiol.* **167**, 854–871.
- Rich, M.K., Schorderet, M., Bapaume, L., Falquet, L., Morel, P., Vandenbussche, M., and Reinhardt, D. (2015). The *Petunia* GRAS transcription factor *ATA/RAM1* regulates symbiotic gene expression and fungal morphogenesis in arbuscular mycorrhiza. *Plant Physiol.* **168**, 788–797.
- Groth, M., Kosuta, S., Gutjahr, C., Haage, K., Hardel, S.L., Schaub, M., Brachmann, A., Sato, S., Tabata, S., Findlay, K., et al. (2013). Two *Lotus japonicus* symbiosis mutants impaired at distinct steps of arbuscule development. *Plant J.* **75**, 117–129.
- Zhang, Q., Blaylock, L.A., and Harrison, M.J. (2010). Two *Medicago truncatula* half-ABC transporters are essential for arbuscule development in arbuscular mycorrhizal symbiosis. *Plant Cell* **22**, 1483–1497.
- Wang, E., Schornack, S., Marsh, J.F., Gobbato, E., Schwessinger, B., Eastmond, P., Schultze, M., Kamoun, S., and Oldroyd, G.E. (2012). A common signaling process that promotes mycorrhizal and oomycete colonization of plants. *Curr. Biol.* **22**, 2242–2246.
- Gutjahr, C., Radovanovic, D., Geoffroy, J., Zhang, Q., Siegler, H., Chiappello, M., Casieri, L., An, K., An, G., Guiderdoni, E., et al. (2012). The half-size ABC transporters STR1 and STR2 are indispensable for mycorrhizal arbuscule formation in rice. *Plant J.* **69**, 906–920.
- Feng, S., Martinez, C., Gusmaroli, G., Wang, Y., Zhou, J., Wang, F., Chen, L., Yu, L., Iglesias-Pedraz, J.M., Kircher, S., et al. (2008). Coordinated regulation of *Arabidopsis thaliana* development by light and gibberellins. *Nature* **451**, 475–479.
- Yoshida, H., Hirano, K., Sato, T., Mitsuda, N., Nomoto, M., Maeo, K., Koketsu, E., Mitani, R., Kawamura, M., Ishiguro, S., et al. (2014). DELLA protein functions as a transcriptional activator through the DNA binding of the indeterminate domain family proteins. *Proc. Natl. Acad. Sci. USA* **111**, 7861–7866.

32. Fukazawa, J., Teramura, H., Murakoshi, S., Nasuno, K., Nishida, N., Ito, T., Yoshida, M., Kamiya, Y., Yamaguchi, S., and Takahashi, Y. (2014). DELLAs function as coactivators of GAI-ASSOCIATED FACTOR1 in regulation of gibberellin homeostasis and signaling in *Arabidopsis*. *Plant Cell* *26*, 2920–2938.
33. de Lucas, M., Davière, J.-M., Rodríguez-Falcón, M., Pontin, M., Iglesias-Pedraz, J.M., Lorrain, S., Fankhauser, C., Blázquez, M.A., Titarenko, E., and Prat, S. (2008). A molecular framework for light and gibberellin control of cell elongation. *Nature* *457*, 480–484.
34. Harrison, M.J. (2012). Cellular programs for arbuscular mycorrhizal symbiosis. *Curr. Opin. Plant Biol.* *15*, 691–698.
35. Hogekamp, C., Arndt, D., Pereira, P.A., Becker, J.D., Hohnjec, N., and Küster, H. (2011). Laser microdissection unravels cell-type-specific transcription in arbuscular mycorrhizal roots, including CAAT-box transcription factor gene expression correlating with fungal contact and spread. *Plant Physiol.* *157*, 2023–2043.
36. Gaude, N., Bortfeld, S., Duensing, N., Lohse, M., and Krajinski, F. (2012). Arbuscule-containing and non-colonized cortical cells of mycorrhizal roots undergo extensive and specific reprogramming during arbuscular mycorrhizal development. *Plant J.* *69*, 510–528.
37. Harrison, M.J., Dewbre, G.R., and Liu, J. (2002). A phosphate transporter from *Medicago truncatula* involved in the acquisition of phosphate released by arbuscular mycorrhizal fungi. *Plant Cell* *14*, 2413–2429.
38. Kobae, Y., Tamura, Y., Takai, S., Banba, M., and Hata, S. (2010). Localized expression of arbuscular mycorrhiza-inducible ammonium transporters in soybean. *Plant Cell Physiol.* *51*, 1411–1415.
39. Pumplin, N., Zhang, X., Noar, R.D., and Harrison, M.J. (2012). Polar localization of a symbiosis-specific phosphate transporter is mediated by a transient reorientation of secretion. *Proc. Natl. Acad. Sci. USA* *109*, E665–E672.
40. Favre, P., Bapaume, L., Bossolini, E., Delorenzi, M., Falquet, L., and Reinhardt, D. (2014). A novel bioinformatics pipeline to discover genes related to arbuscular mycorrhizal symbiosis based on their evolutionary conservation pattern among higher plants. *BMC Plant Biol.* *14*, 333.
41. Gutjahr, C. (2014). Phytohormone signaling in arbuscular mycorrhiza development. *Curr. Opin. Plant Biol.* *20*, 26–34.
42. Gallego-Bartolomé, J., Minguet, E.G., Marín, J.A., Prat, S., Blázquez, M.A., and Alabadí, D. (2010). Transcriptional diversification and functional conservation between DELLA proteins in *Arabidopsis*. *Mol. Biol. Evol.* *27*, 1247–1256.
43. Maekawa, T., Maekawa-Yoshikawa, M., Takeda, N., Imaizumi-Anraku, H., Murooka, Y., and Hayashi, M. (2009). Gibberellin controls the nodulation signaling pathway in *Lotus japonicus*. *Plant J.* *58*, 183–194.
44. Breuillin, F., Schramm, J., Hajirezaei, M., Ahkami, A., Favre, P., Druege, U., Hause, B., Bucher, M., Kretschmar, T., Bossolini, E., et al. (2010). Phosphate systemically inhibits development of arbuscular mycorrhiza in *Petunia hybrida* and represses genes involved in mycorrhizal functioning. *Plant J.* *64*, 1002–1017.
45. Nagata, M., Yamamoto, N., Shigeyama, T., Terasawa, Y., Anai, T., Sakai, T., Inada, S., Arima, S., Hashiguchi, M., Akashi, R., et al. (2015). Red/far red light controls arbuscular mycorrhizal colonization via jasmonic acid and strigolactone signaling. *Plant Cell Physiol.* *56*, 2100–2109.

Current Biology, Volume 26

**Supplemental Information**

**A CCaMK-CYCLOPS-DELLA Complex**

**Activates Transcription of *RAM1***

**to Regulate Arbuscule Branching**

**Priya Pimprikar, Samy Carbonnel, Michael Paries, Katja Katzer, Verena Klingl, Monica J. Bohmer, Leonhard Karl, Daniela S. Floss, Maria J. Harrison, Martin Parniske, and Caroline Gutjahr**

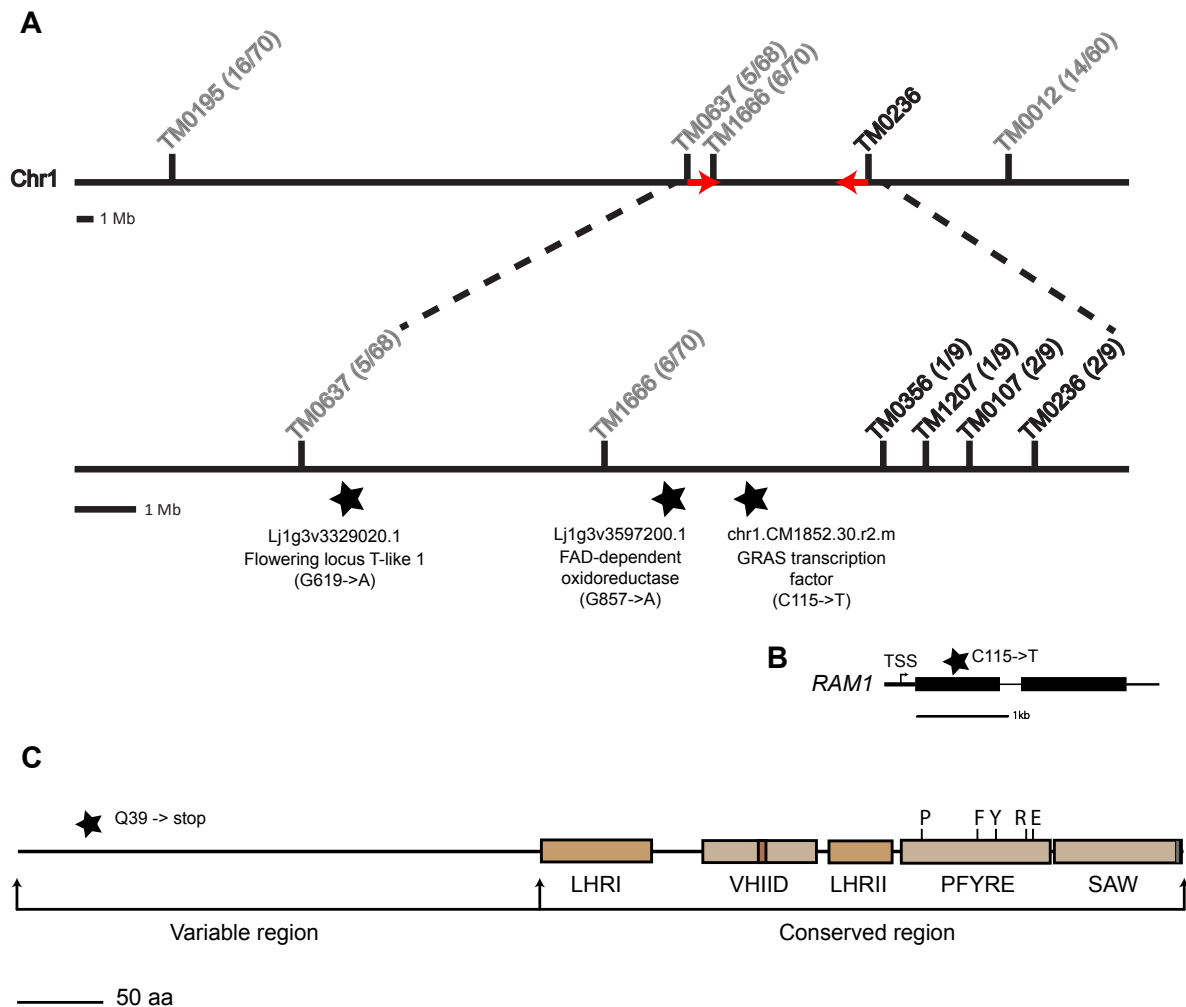
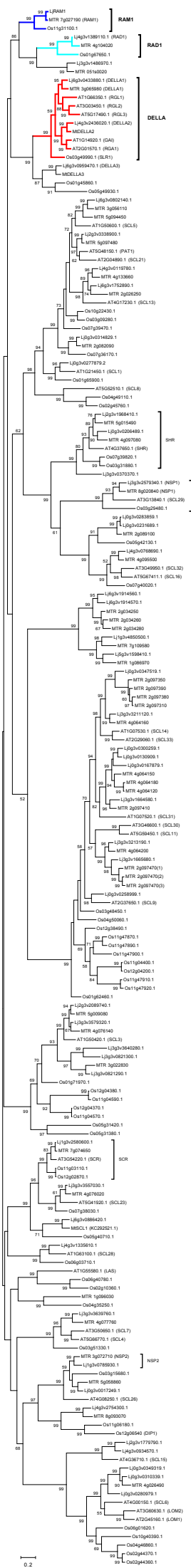
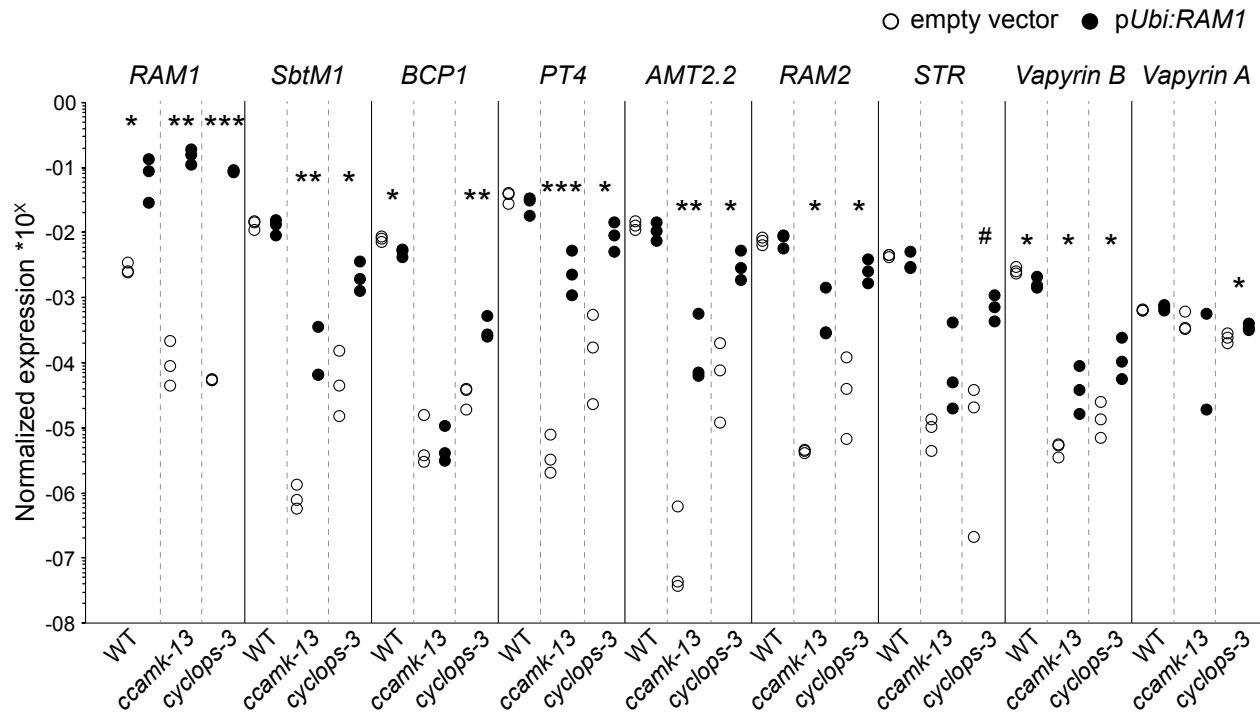


**Fig. S1 related to Fig. 1. Identification of the *ram1-3* mutation.** (A) Genetic map of the *red* locus on chromosome 1. Numbers next to marker positions refer to the proportion of recombinant individuals among the number of analyzed F2 mutant plants. Previous rough mapping (markers in grey) had positioned the mutation on the long arm of chromosome 1 close to the marker TM1666 [S1]. Further fine mapping (markers in black) placed the causative mutation north of TM1666 and narrowed down an interval between TM1666 and TM0356. By re-sequencing the mutant genome using next generation sequencing two nonsense mutations (black stars) were found in open reading frames of Lj1g3v3597200.1 (*FAD Oxidoreductase*) and chr1.CM1852.30.r2.m (*GRAS* protein encoding *RAM1*) within this interval. A third mutation causing a glycine to alanine replacement in Lj1g3v3329020.1 (flowering locus T like) was detected close to the interval. Red arrows indicate the genomic interval that was searched for mutations using NGS data. (B) The *RAM1* gene is composed of two exons (black boxes). The untranslated regions (UTRs) comprise 143 bp (5' UTR) and 432 bp (3' UTR). (C) *RAM1* contains the domains of a canonical *GRAS* protein with a variable N-terminal region and a conserved C-terminal region that contains two leucine heptad repeats (LHRI and II), a VHIID domain, a PFYRE domain and a SAW domain [S2].



0.2

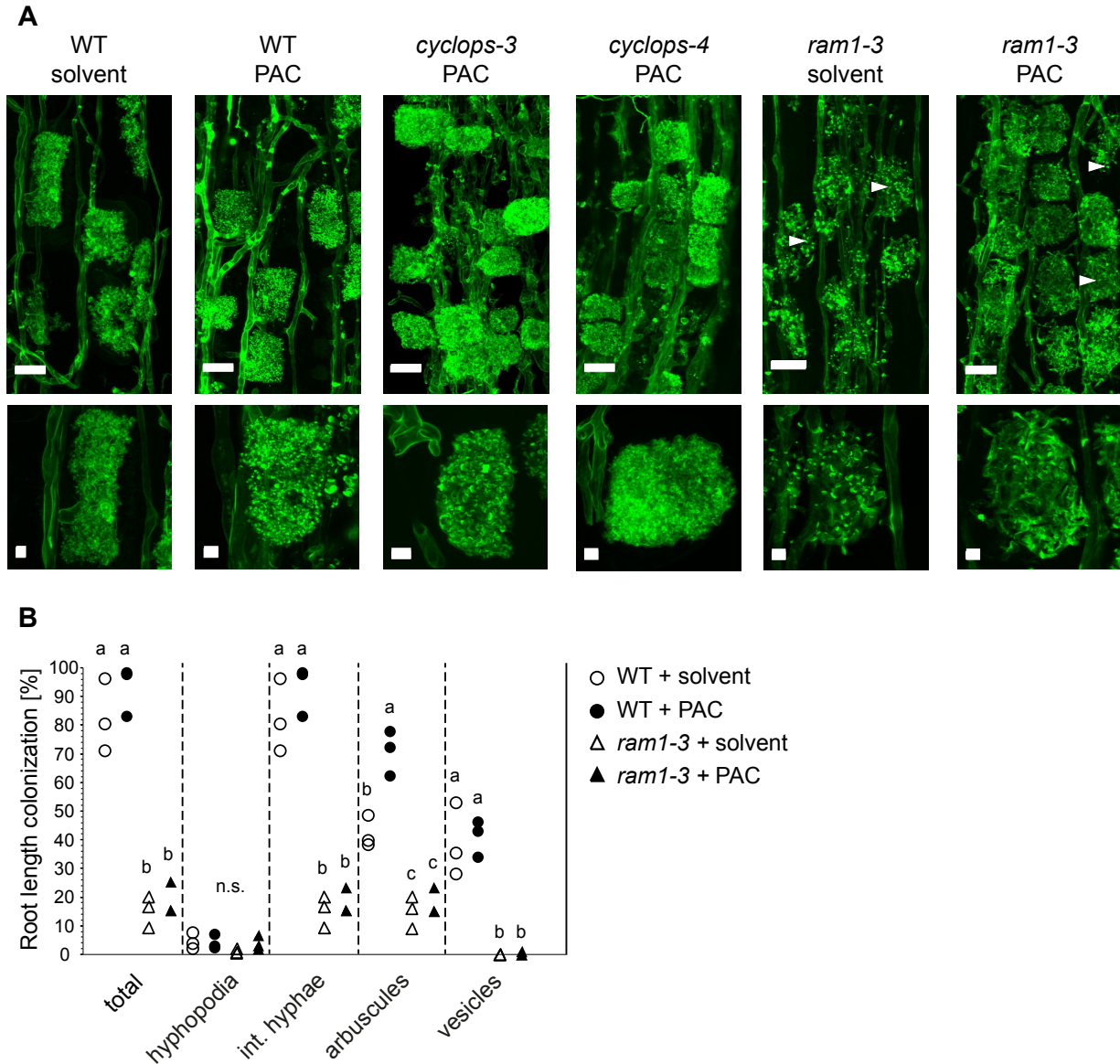
**Fig. S2 related to Fig. 1. Phylogenetic tree of GRAS proteins in *L. japonicus*.** Proteins from *Lotus japonicus* (n=50), *Medicago truncatula* (n=47), *Arabidopsis thaliana* (n=33), and *Oryza sativa* (n=49) were included into the tree. Protein sequences were aligned using MAFFT. MEGA5 was used to generate a Maximum-likelihood tree. Bootstrap values from 1000 replicates are indicated at each node. Bootstrap values below 50 were omitted from the tree. Brackets indicate clades containing characterized proteins.



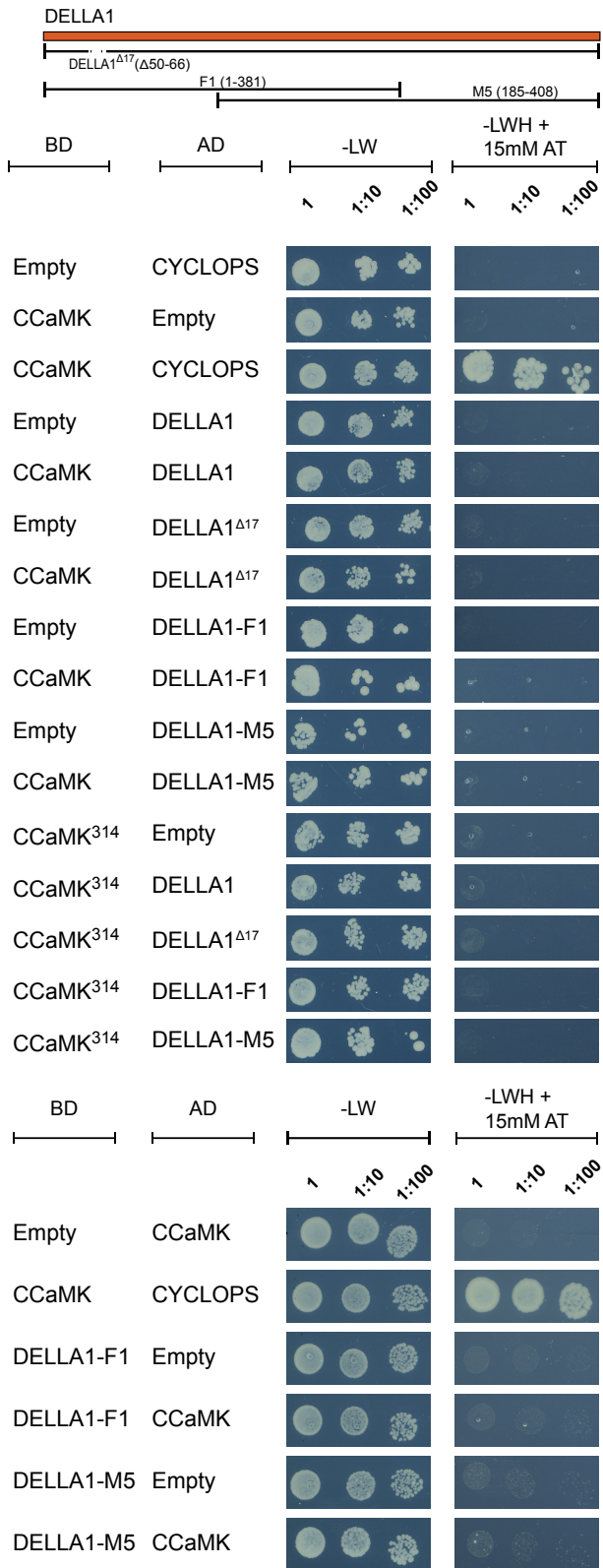
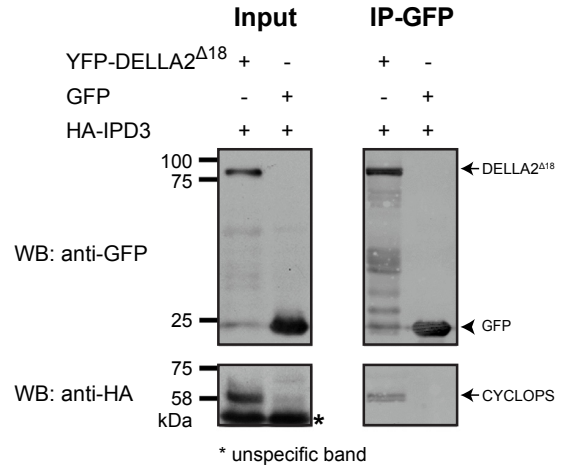
**Fig. S3 related to Fig. 3. RAM1 overexpression restores marker gene expression in inoculated ccamk and cyclops mutants.** Transcript accumulation at 6 wpi of AM marker genes in hairy roots of wild type, ccamk-13 and cyclops-3 transformed with an empty vector or with pUbi:RAM1 and colonized by *R. irregularis*. Inoculated plants were grown in parallel with those used for Fig. 2b. Transcript accumulation was assessed by qRT-PCR and expression of the housekeeping gene *Ubiquitin10* was used for normalization. Statistical analysis used a Welch t-test (n = 6, # p ≤ 0.1, \* p ≤ 0.05, \*\* p ≤ 0.01, \*\*\* p ≤ 0.001).



**Fig. S4 related to Fig. 4. Developmental phenotype after GA treatment.** Chimeric plants with WT shoots and transgenic hairy roots show clear shoot-elongation responses to 1  $\mu$ M GA 4 weeks after treatment.



**Fig. S5 related to Fig. 5. Arbuscule phenotypes after PAC treatment.** (A) Laser scanning confocal images of roots of *L. japonicus* wild-type, *ccamk-13*, *cyclops-3*, *cyclops-4* and *ram1-3* colonized by *R. irregularis* at 5 wpi treated with solvent (0.01 % ethanol) or 1  $\mu$ M paclobutrazol (PAC). Treatment was started at 1 wpi. The fungus was stained with WGA-AlexaFluor488. The close-up images of the experiment displayed in Fig. 5b clearly show that arbuscule formation and branching is fully restored by PAC treatment in *cyclops* mutants, while arbuscule branches in the *ram1* mutant still appear crude, branching remains underdeveloped and multiple septa are visible (white arrow heads). (B) Percent root length colonization at 5 wpi with *R. irregularis* of wild type and *ram1-3* treated with solvent (0.01 % ethanol) or 1  $\mu$ M paclobutrazol (PAC) as determined by the gridline intersect method. Different letters indicate statistically different groups (ANOVA; posthoc Tukey; n = 12;  $F(\text{total})_{3,8} = 37.02$ ,  $F(\text{hyphopodia})_{3,8} = 2.32$ ,  $F(\text{int. hyphae})_{3,8} = 38.23$ ,  $F(\text{arbuscules})_{3,8} = 45.86$ ,  $F(\text{vesicles})_{3,8} = 70.92$ ;  $p \leq 0.001$ ). int. hyphae, intraradical hyphae.

**A****B**

**Fig. S6 related to Fig. 6. Interaction of DELLA with the CCaMK-CYCLOPS complex.** (A) *L. japonicus* DELLA1 does not interact with CCaMK or CCaMK<sup>314</sup> in a binary interaction examined by yeast two-hybrid assay. (B) *M. truncatula* IPD3 (Medtr5g026850) interacts with DELLA2. Co-immunoprecipitation assay showing the physical interaction between *M. truncatula* IPD3 and DELLA2 in leaves of *N. benthamiana*. To increase sensitivity a GA-insensitive mutant protein of DELLA2 (DELLA2<sup>Δ18</sup>) was used. For the input blots, 2.5% input extract was loaded to detect HA-IPD3, 0.5% input extract to detect YFP-DELLA2<sup>Δ18</sup>, and 0.1% input extract to detect GFP. Asterisk indicates unspecific band.

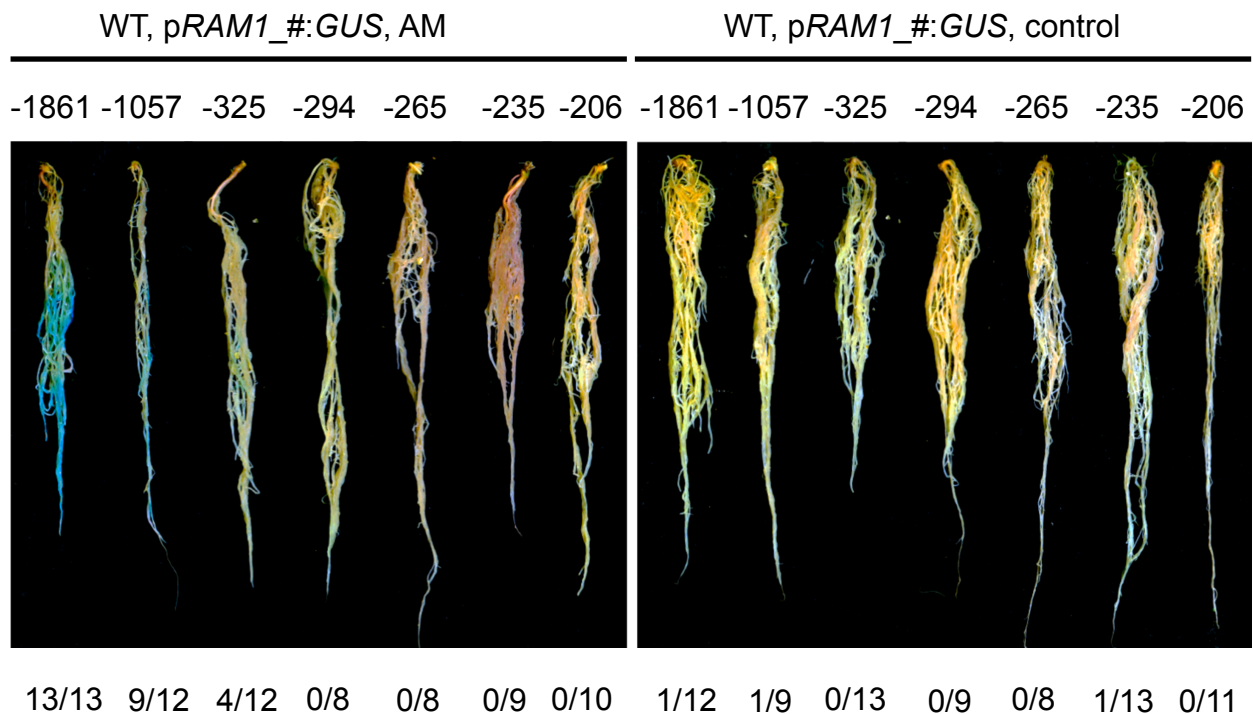


**Fig. S7 related to Fig. 7. A 325 bp RAM1 promoter fragment is sufficient to drive GUS-expression in colonized *L. japonicus* roots.** Activity of *RAM1* promoter fragments in wild-type *L. japonicus* roots colonized with *R. irregularis* at 6 wpi. Promoter-fragment activity is indicated by blue GUS-staining. Numbers above the roots indicated the length of the promoter fragment upstream of the transcriptional start site. Numbers below the roots indicate transgenic root systems with blue GUS-staining as compared to the total number of analyzed transgenic root systems.

## Supplemental experimental procedures

**Plant material, growth conditions and inoculation with AM fungi.** For all experiments *L. japonicus* ecotype Gifu wild type and mutants were used. The mutants *ccamk-13*, *cyclops-3* and *cyclops-4* have been previously described [S3, S4]. The *ram1-3* mutant was derived from the line SL0181-N [S1] (see identification of *RAM1*). The *ram1-4* mutant corresponds to the LORE1 insertion line 30054130 [S5] and carries a LORE1 insertion after 1284 bp from ATG in the genomic sequence of *RAM1*. Seeds were scarified with sand paper and surface sterilized with 1% NaClO. Imbibed seeds were germinated on 0.8% Bacto Agar (Difco) at 24°C for 10 - 14 days. Plantlets were then transferred to pots (6-9 per pot) containing a sand-vermiculite mix (2:1) and grown at 24 °C constant temperature, 60% air humidity and 16-h-light/8-h-dark cycles. Each pot was fertilized once a week with 30 ml of modified half-strength B&D medium [S6] containing 5 µM phosphate and twice a week with a 1:1 mix of tap water and deionized water. For arbuscular mycorrhiza colonization plants were inoculated with 500 spores per plant of *R. irregularis* DAOM197198 (SYMPLANTA, Munich Germany or Agronutrition, Toulouse France). For treatment with gibberellin3 (GA<sub>3</sub>) or pacloputrazol (PAC) 50 mM and 10 mM stock solution of GA<sub>3</sub> (Sigma, G7645) and PAC (Fluka, 46046) respectively were prepared in absolute ethanol. Plants were watered three times a week with 30 ml of 1 µM GA<sub>3</sub> or PAC solution per pot containing 6-9 plants. The control plants received 30 ml of control solution containing an equivalent volume of absolute ethanol. The treatment was started 1 week post inoculation with *R. irregularis* or post planting.

**Visualization and quantification of root colonization.** *R. irregularis* in colonized *L. japonicus* roots was stained with acid ink [S7]. Root length colonization was quantified using a modified gridline intersect method [S8] and 10X magnification at a light microscope (Leica, type 020-518500 DM/LS). For confocal laser scanning microscopy using a Leica SP5 fungal structures were stained with 1 µg WGA Alexa Fluor 488 (Molecular Probes, <http://www.lifetechnologies.com/>) [S9].

**Identification of *RAM1* by map-based cloning and next generation sequencing.** The *L. japonicus* mutant *reduced and degenerate arbuscules* (*red*, line SL0181-N [S1]) resulting from an EMS mutagenesis program [S4, S10] was outcrossed to the ecotype MG20 and previously found to segregate for two mutations, one on chromosome 1 linked to marker TM1666 and one on chromosome 6 [S1]. To identify SL0181-N-specific mutations linked to the *red* locus, we employed a genome re-sequencing strategy using DNA from an M6 mutant family (seedbag 88820). Nuclear DNA [S11] of Gifu wild-type and the SL0181-N mutant was subjected to paired end sequencing (2x100bp) of a 300-500 bp insert library, on an Illumina Hi-Seq 2000 instrument resulting in between 16.7 and 19.5 Gigabases per sample, equivalent to roughly 35-41 fold coverage assuming a genome size of 470 Megabases. Reads were mapped to the reference genome of MG20 v2.5 [S12] and single nucleotide polymorphisms identified using CLC Genomics Workbench (CLC bio, Aarhus, Denmark). SL0181-N-specific SNPs were identified by subtracting Gifu/MG-20 from SL0181-N/MG-20 polymorphisms. In parallel we produced a new SL0181-N outcross to MG20 using a plant from the same M6 family (seedbag 88820) that had been used for re-sequencing the mutant genome. The F2 generation of

this outcross segregated for only one mutation as 9 out of 60 individuals exhibited the mutant phenotype ( $\chi^2$ : P(3:1)=0.83). Fine mapping using additional markers South of TM0166 revealed that the new F2 population only contained the mutant locus on chromosome 1. Inspection of the polymorphisms in the candidate interval (Figure S1) identified three SNPs. One caused a stop codon mutation in chr1.CM1852.30.r2.m, which encodes the GRAS protein REDUCED ARBUSCULAR MYCORRHIZA1 (RAM1). The other two were in open reading frames of Lj1g3v3329020.1 (*flowering locus T like*) and Lj1g3v3597200.1 (*FAD Oxidoreductase*). Co-segregation analysis using KASP assay (<http://www.lgcgroup.com>), transgenic complementation and phenotyping of an independent *ram1* mutant (*ram1-4*) generated by LORE1 insertion [S5] confirmed that the mutation in *RAM1* caused the stunted arbuscule phenotype. Untranslated regions of *RAM1* were determined using the Ambion FirstChoice® RLM RACE kit according to manufacturers instructions (<http://www.ambion.de/>). *L. japonicus* *RAM1* sequence information can be found under the NCBI accession number KU557503.

**Gene expression analysis.** For analysis of transcript levels by qRT-PCR, plant tissue was rapidly shock frozen in liquid nitrogen. RNA was extracted using the Spectrum Plant Total RNA Kit ([www.sigmaaldrich.com](http://www.sigmaaldrich.com)). The RNA was treated with Invitrogen DNase I amp. grade ([www.invitrogen.com](http://www.invitrogen.com)) and tested for purity by PCR. cDNA synthesis was performed with 1 µg RNA using the Superscript III kit ([www.invitrogen.com](http://www.invitrogen.com)). Real time RT-PCR was performed with GoTaq G2 DNA polymerase (Promega), 5 x colorless GoTaq Buffer (Promega) and SYBR Green I (Invitrogen S7563, 10,000x concentrated, 500 µl) - diluted 100-fold in DMSO for storage and subsequently diluted another 50-times in 10mM Tris, pH 8.0 as working solution. Primers were designed with primer3 [S13] and are shown in Table S1. The qPCR reaction was run on an iCycler (Biorad, [www.bio-rad.com/](http://www.bio-rad.com/)) according to manufacturers instructions. Thermal cycler conditions were: 95°C 2 min, 45 cycles of 95°C 30 sec, 58°/60°C/62°C 30sec and 72°C 20 sec followed by dissociation curve analysis. Expression levels were calculated according to the  $\Delta\Delta C_t$  method [S14]. For each genotype and treatment three to four biological replicates were monitored and each sample was represented by two to three technical replicates.

**Plasmid generation.** Genes and promoter regions were amplified using Phusion PCR according to standard protocols and using primers indicated in Table S1. Plasmids were constructed by gateway cloning using pENTR-D/TOPO (Invitrogen) as entry vector and LR clonase (Invitrogen) for recombination into the destination vector or by golden gate cloning [S15] as indicated in Table S2.

**Plant transformation.** For induction of transgenic hairy roots *L. japonicus* hypocotyls were transformed with plasmids shown in Table S3 using transgenic *A. rhizogenes* AR1193 as described [S16]. Transformed roots were screened by stereomicroscope (Leica MZ16 FA) using a mCherry fluorescent transformation marker. *Nicotiana benthamiana* leaves were transiently transformed by infiltration of transgenic *A. tumefaciens* strain AGL1 as described [S3].

**Promoter GUS analysis and transactivation assay.** *L. japonicus* hairy roots transformed with plasmids containing p*RAM1*:*GUS* constructs (Table S2) were

subjected to GUS staining as described [S16]. Transactivation assays in *N. benthamiana* leaves were performed as described [S17].

**Yeast-two-hybrid and BiFC assay.** Coding sequences of *DELLA* and deletion versions thereof were cloned into a Gateway modified yeast vectors pBDGAL4-GW (Stratagene). pBDGAL4-GW and pADGAL4-GW containing CCaMK and CYCLOPS sequences were obtained from [S3]. Constructs are listed in Table S2. Transformation of the yeast reporter strain HF7c and drop test were performed according to standard protocols (Stratagene product manual). BiFC analyses using plasmids listed in Table S2 were performed as described previously [S3]. For each interaction a mix of three transformed *A. tumefaciens* strains was infiltrated into *N. benthamiana* leaves: Two contained one of the split-YFP plasmids and the third one contained either a plasmid expressing free RFP (pK9) or RFP-CCaMK<sup>314</sup>.

**Co-immunoprecipitation assay and Western blot for *L. japonicus* proteins.** For co-immunoprecipitation assays, appropriate plasmids were transiently expressed in four weeks old *N. benthamiana* leaves. For that purpose, an equal volume of mixture of *A. tumefaciens* (strain AGL1) cultures containing desired plasmids was adjusted to a final OD<sub>600</sub> of 0.25 with infiltration buffer (10 mM MgCl<sub>2</sub>, 10 mM MES, 150 μM acetosyringone, pH 5.6). Per assay, one entire leaf from three plants was infiltrated with the *A. tumefaciens* mixture using a needle-less syringe. Two days after infiltration, leaves were collected and frozen in liquid nitrogen. Leaves were ground in liquid nitrogen and homogenized in 5 mL cold buffer lysis buffer (Miltenyl Protein Isolation kit) containing protease inhibitors (Sigma-Aldrich). Samples were incubated at 4°C on a rotating wheel for 10 min and centrifuged at 10,000 rpm for 15 min at 4°C. The supernatant was passed through a 0.45 μm sterile syringe filter, and filtrated extract was added to 50 μL μMACS c-myc tagged magnetic beads (μMACS c-myc tagged Protein Isolation Kit, Miltenyl, 130-091-123). Filtrate extract containing the c-myc tagged magnetic beads were incubated on a rotating wheel for 2 hours at 4°C. Subsequent steps were performed according to the manufacturers instruction (μMACS c-myc tagged Protein Isolation Kit, Miltenyl, 130-091-123). The resulting 60 μL supernatants were subjected to Western blot analysis, where 10 μL i.e, 0.2% (anti-Myc) and 25 μL i.e, 0.5% (anti-HA) aliquots were loaded onto an SDS gel.

For Western blot analysis, proteins were separated on 10% (w/v) SDS gels and transferred to 0.45 μm Immobilon®FL PVDF membranes (Millipore) using the BioRad minigel and blotting system. Membranes were blocked in 5% instant nonfat dry milk (w/v, milk powder) in PBS-T (PBS, 0.05% Tween-20) and probed with the primary antibody (anti-Myc, Roche or anti-HA-peroxidase conjugated, Roche) in 5% instant nonfat dry milk (w/v) in PBS-T overnight at 4°C. Membranes were washed and either processed for detection or incubated with peroxidase-conjugated anti-mouse secondary antibody (Biomol) for 3 hours at 4°C. Bound antibodies were detected using the Super Signal West Femto Maximum sensitivity substrate (34096) for Anti-HA and Pierce ECL western blotting substrate (32106) for Anti-Myc.

**Co-immunoprecipitation assay and Western blot for *M. truncatula* proteins.** Transient expression of proteins in *N. benthamiana* leaves and protein extraction was performed as for *L. japonicus* proteins except that the *A. tumefaciens* strain GV2260 and

5 ml cold extraction buffer (150 mM Tris-HCl, pH 7.5, 150 mM NaCl, 10% glycerol, 10 mM EDTA, 20 mM NaF, 10 mM DTT, 0.5% (w/v) polyvinylpyrrolidone, 0.1% Tween-20, protease inhibitors (Sigma-Aldrich)) per 2 g powdered tissue were used. Samples were incubated on ice until entirely thawed and centrifuged at 3,200 g for 15 min at 4°C. The supernatant was passed through a 0.45 µm sterile syringe filter (Corning®), and 1.5 mL filtrated extract was added to 20 µL equilibrated GFP-binding affinity resin (GFP-Trap®\_A beads, ChromoTek). Samples were incubated on a rotating wheel overnight at 4°C. GFP-Trap®\_A beads were collected by centrifugation at 2,000 g for 2 min at 4°C and washed three times with 1 mL wash buffer (10 mM Tris-HCl, pH 7.5, 150 mM NaCl, 0.5 mM EDTA, 0.1% Tween-20). Proteins were eluted by adding 40 µL 2x SDS-sample buffer followed by incubation for 10 min at 95°C. The resulting supernatants were subjected to Western blot analysis, where 3 µL (anti-GFP) and 25 µL (anti-HA) aliquots were loaded onto an SDS-PAA gel.

For Western blot analysis, proteins were separated on 10% (w/v) SDS-PAA gels and transferred to 0.45 µm Immobilon®FL PVDF membranes (Millipore) using the BioRad minigel and blotting system. Membranes were blocked in 5% instant nonfat dry milk (w/v, Carnation milk, Nestlé) in PBS-T (PBS, 0.05% Tween-20) and probed with the primary antibody (anti-GFP, Roche or anti-HA, Sigma-Aldrich) in 5% instant nonfat dry milk (w/v) in PBS-T overnight at 4°C. Membranes were washed and incubated with either peroxidase-conjugated anti-mouse secondary antibody (Promega) (input blots) or Infrared IRDye®-labeled secondary antibodies (LI-COR® Biosciences) (IP blots) for 2 hours at room temperature. Bound antibodies were detected using the Immobilon™ Western Chemiluminescent HRP Substrate (Millipore) or the Odyssey® Infrared Imaging System (LI-COR® Biosciences).

**Electrophoretic Mobility Shift Assay (EMSA).** Recombinantly expressed 6xHis-CYCLOPS<sub>min</sub> (100 pmol) was equilibrated in binding buffer (10 mM Tris-HCl pH 6.8, 200 mM KCl, 0.5 mM DTT, 2.5% (vol/vol) glycerol, 5 mM MgCl<sub>2</sub>, 10 ng/µl poly (dl-dC) and 0.2 mM EDTA) and 100 fmol of a random DNA sequence (5'-TTCTGGTTTATATAGAAACTCAAGTGAAGA-3') to reduce unspecific binding. The mixture was incubated with 10-, 20- and 30-fold molar excess of competitor DNA on ice for 10 min. 100 fmol 5' CY5-labeled *AMCYC-RE* probe was added and binding reaction was performed for 15 min at room temperature. Samples were resolved on 6 % native, pre-run polyacrylamide gels in 0.5x TBE pH 8.3. Electrophoresis was conducted for 10 min at 150 V until samples entered the gel and then reduced to 100 V for 60 min. CY5-labeled DNA was visualized with the Typhoon TriO phosphoimager (Amersham Biosciences). Complementary pairs of CY5-labeled and unlabeled oligonucleotide probes correspond to (lines indicate the mutated palindrome):

*AMCYC-RE\_Fwd* GTGAACAGATGGGCCGGCCCAAAAAGTGGG  
*CY5-AMCYC-RE\_Rev* CY5-CCCACTTTTTGGGCCGGCCCATCTGTTCAC  
*mAMCYC-RE\_Fwd* GTGAACAGATTTTTAATTAAAAAAAGTGGG  
*mAMCYC-RE\_Rev* CCCACTTTTTTTAATTAAAATCTGTTCAC

**Phylogenetic analysis.** GRAS protein sequences from *A. thaliana* and *O. sativa* were retrieved from the Plant Transcription Factor Database (Perez-Rodriguez, et al., 2009). The sequences of DELLA1, 2 and 3 from *M. truncatula* were taken from [S18]. The other GRAS proteins from *M. truncatula* and *L. japonicus* were identified using tBLASTn against the NCBI database and the Lotus genome V2.5 (<http://www.kazusa.or.jp/lotus/>) respectively. GRAS proteins from *L. japonicus* that were not available in the *Lotus* genome sequence V2.5 were identified by tBLASTn in an in-house genome generated by next generation sequencing using CLC Main Workbench. All of them (except RAM1) were afterwards found in the new release of the *Lotus* genome V3.0 and renamed accordingly. The MAFFT alignment of the protein sequences was used to generate a Maximum-likelihood tree with 1000 bootstrap replicates in MEGA5 [S19].

**Statistical analysis.** All statistical analyses were performed in R-studio ([www.r-project.org](http://www.r-project.org)). To ensure equal variance gene expression data and GUS-activity data (transactivation assay) were log<sub>10</sub> transformed and % colonization was arcsin transformed before analysis.

## References

- S1. Groth, M., Kosuta, S., Gutjahr, C., Haage, K., Hardel, S.L., Schaub, M., Brachmann, A., Sato, S., Tabata, S., Findlay, K., et al. (2013). Two *Lotus japonicus* symbiosis mutants impaired at distinct steps of arbuscule development. *Plant J.* 75, 117-129.
- S2. Bolle, C. (2004). The role of GRAS proteins in plant signal transduction and development. *Planta* 218, 683-692.
- S3. Yano, K., Yoshida, S., Müller, J., Singh, S., Banba, M., Vickers, K., Markmann, K., White, C., Schuller, B., Sato, S., et al. (2008). CYCLOPS, a mediator of symbiotic intracellular accommodation. *Proc. Natl. Acad. Sci. USA* 105, 20540-20545.
- S4. Perry, J., Brachmann, A., Welham, T., Binder, A., Charpentier, M., Groth, M., Haage, K., Markmann, K., Wang, T.L., and Parniske, M. (2009). TILLING in *Lotus japonicus* identified large allelic series for symbiosis genes and revealed a bias in functionally defective ethyl methanesulfonate alleles toward glycine replacements. *Plant Physiol.* 151, 1281-1291.
- S5. Urbański, D.F., Małolepszy, A., Stougaard, J., and Andersen, S.U. (2012). Genome-wide LORE1 retrotransposon mutagenesis and high-throughput insertion detection in *Lotus japonicus*. *Plant J.* 69, 731-741.
- S6. Broughton, W.J., and Dilworth, M.J. (1971). Control of leghaemoglobin synthesis in snake beans. *Biochem. J.* 125, 1075-1080.
- S7. Vierheilig, H., Coughlan, A.P., Wyss, U., and Piché, Y. (1998). Ink and vinegar, a simple staining technique for arbuscular-mycorrhizal fungi. *Appl. Environ. Microbiol.* 64, 5004-5007.
- S8. McGonigle, T., Miller, M., Evans, D., Fairchild, G., and Swan, J. (1990). A new method which gives an objective measure of colonization of roots by vesicular-arbuscular mycorrhizal fungi. *New Phytol.* 115, 495-501.
- S9. Panchuk-Voloshina, N., Haugland, R.P., Bishop-Stewart, J., Bhargat, M.K., Millard, P.J., Mao, F., Leung, W.-Y., and Haugland, R.P. (1999). Alexa dyes, a series of new fluorescent dyes that yield exceptionally bright, photostable conjugates. *J. Histochem. Cytochem.* 47, 1179-1188.

- S10. Perry, J.A., Wang, T.L., Welham, T.J., Gardner, S., Pike, J.M., Yoshida, S., and Parniske, M. (2003). A TILLING reverse genetics tool and a web-accessible collection of mutants of the legume *Lotus japonicus*. *Plant Physiol.* *131*, 866-871.
- S11. Gendrel, A.-V., Lippman, Z., Martienssen, R., and Colot, V. (2005). Profiling histone modification patterns in plants using genomic tiling microarrays. *Nat. Meth.* *2*, 213-218.
- S12. Sato, S., Nakamura, Y., Kaneko, T., Asamizu, E., Kato, T., Nakao, M., Sasamoto, S., Watanabe, A., Ono, A., Kawashima, K., et al. (2008). Genome structure of the legume, *Lotus japonicus*. *DNA Res.* *15*, 227-239.
- S13. Rozen, S., and Skaletsky, H. (2000). Primer3 on the WWW for general users and for biologist programmers. . In *Bioinformatics Methods and Protocols: Methods in Molecular Biology.* , S. Krawets and S. Misener, eds. (Totwana, NJ, USA: Humana Press), pp. 365-386.
- S14. Czechowski, T., Bari, R.P., Stitt, M., Scheible, W.-R., and Udvardi, M.K. (2004). Real-time RT-PCR profiling of over 1400 Arabidopsis transcription factors: unprecedented sensitivity reveals novel root- and shoot-specific genes. *Plant J.* *38*, 366-379.
- S15. Binder, A., Lambert, J., Morbitzer, R., Popp, C., Ott, T., Lahaye, T., and Parniske, M. (2014). A modular plasmid assembly kit for multigene expression, gene silencing and silencing rescue in plants. *PLoS ONE* *9*, e88218.
- S16. Takeda, N., Sato, S., Asamizu, E., Tabata, S., and Parniske, M. (2009). Apoplastic plant subtilases support arbuscular mycorrhiza development in *Lotus japonicus*. *Plant J.* *58*, 766-777.
- S17. Singh, S., Katzer, K., Lambert, J., Cerri, M., and Parniske, M. (2014). CYCLOPS, a DNA-binding transcriptional activator, orchestrates symbiotic root nodule development. *Cell Host Microbe* *15*, 139-152.
- S18. Floss, D.S., Levy, J.G., Lévesque-Tremblay, V., Pumplin, N., and Harrison, M.J. (2013). DELLA proteins regulate arbuscule formation in arbuscular mycorrhizal symbiosis. *Proc. Natl. Acad. Sci. USA* *110*, E5025-E5034.
- S19. Tamura, K., Peterson, D., Peterson, N., Stecher, G., Nei, M., and Kumar, S. (2011). MEGA5: molecular evolutionary genetics analysis using maximum likelihood, evolutionary distance, and maximum parsimony methods. *Mol. Biol. Evol.* *28*, 2731-2739.
- S20. Takeda, N., Handa, Y., Tsuzuki, S., Kojima, M., Sakakibara, H., and Kawaguchi, M. (2015). Gibberellins interfere with symbiosis signaling and gene expression and alter colonization by arbuscular mycorrhizal fungi in *Lotus japonicus*. *Plant Physiol.* *167*, 545-557.
- S21. Kojima, T., Saito, K., Oba, H., Yoshida, Y., Terasawa, J., Umehara, Y., Suganuma, N., Kawaguchi, M., and Ohtomo, R. (2014). Isolation and phenotypic characterization of *Lotus japonicus* mutants specifically defective in arbuscular mycorrhizal formation. *Plant Cell Physiol.* *55*, 928-941.
- S22. Giovannetti, M., Mari, A., Novero, M., and Bonfante, P. (2015). Early *Lotus japonicus* root transcriptomic responses to symbiotic and pathogenic fungal exudates. *Front. Plant Sci.* *6*.
- S23. Karimi, M., Inzé, D., and Depicker, A. (2002). GATEWAY™ vectors for *Agrobacterium*-mediated plant transformation. *Trends Plant Sci.* *7*, 193-195.
- S24. Takeda, N., Maekawa, T., and Hayashi, M. (2012). Nuclear-localized and deregulated calcium- and calmodulin-dependent protein kinase activates rhizobial and mycorrhizal responses in *Lotus japonicus*. *Plant Cell* *24*, 810-822.
- S25. Earley KW, Haag JR, Pontes O, Opper K, Juehne T, Song K, and CS, P. (2006). Gateway-compatible vectors for plant functional genomics and proteomics. *Plant J.* *45*, 616-629.

**Table S1. Primers Used in This Study, Related to Figures 1-7**

Use	Name	Sequence
pRAM1 fragment 1 cloning for pRAM1:RAM1 and pRAM1:GUS	PP2	ATGAAGACTTTACGGGTCTCAGCGGGTAAGAGATA ATGCGCGTTTGG
	PP132	TAGAAGACAAGATCAAATATCATTGTAATGCCTAC ATC
pRAM1 fragment 2 cloning for pRAM1:RAM1 and pRAM1:GUS	PP133	ATGAAGACTTGATCTGTATTCAAATTATGAATAAA TTAC
	PP3	ATGAAGACTTCAGAGGTCTCACAGAGTTTTGTCTTTT TGGTAGAACAGAAA
GUS cloning for pRAM1:GUS to localize promoter activity	PP97	ATGGTCTCATCTGAACAATGTTACGTCCTGTAGAAA CCCCAAC
	PP98	TAGGTCTCAGATTCATTGTTTGCCTCCCTGCTG
CCaMK <sup>314</sup> fragment 1 cloning for overexpression of CCaMK <sup>314</sup>	PP82	ATGAAGACTTTACGGGTCTCACACCATGGGATATGA TCAAACCAGAAAG
	PP83	TAGAAGACAATGACCACATGTCACCTTGGCAG
CCaMK <sup>314</sup> fragment 2 cloning for overexpression of CCaMK <sup>314</sup>	PP84	ATGAAGACTTGTCACCTGGGAGTGATTCTATATATC
	PP85	TAGAAGACAATTTCTCATAGAACTGAAATTCCCA
CCaMK <sup>314</sup> fragment 3 cloning for overexpression of CCaMK <sup>314</sup>	PP86	TAGAAGACAAGAAAACCTTGAAGGGCATTAC
	PP87	ATGAAGACTTCAGAGGTCTCACCTTAATCTCAGGGT CCATTTGCTC
RAM1 fragment A cloning for pRAM1:RAM1 and pUbi:RAM1	PP5	ATGAAGACTTTACGGGTCTCACACCATGATCAATTC AATGTGTGGAAG
	PP6	TAGAAGACAAAACCTTGTTTGATGAATTTGAATACC
RAM1 fragment B cloning for pRAM1:RAM1 and pUbi:RAM1	PP7	ATGAAGACTTGTTTTCTTCTGATATTGGAAGCTC
	PP8	TAGAAGACAATCCCTGCTTAAGCTATGCAA
RAM1 fragment C cloning for pRAM1:RAM1 and pUbi:RAM1	PP9	ATGAAGACTTGGGACTCTGGTTGATCCTACC
	PP10	TAGAAGACAACCTTATCATGGACAACAAATTCC
RAM1 fragment D cloning for pRAM1:RAM1 and pUbi:RAM1	PP11	TAGAAGACAAAAGGGACCAAGCACCTAACA
	PP12	ATGAAGACTTCAGAGGTCTCACCTTGCATCTCCATG CAGAGGC
DELLA1 <sup>Δ17</sup> fragment A cloning for p35S:DELLA1 <sup>Δ17</sup> and pUbi:Myc DELLA1 <sup>Δ17</sup>	PP60	ATGAAGACTTTACGGGTCTCACACCATGAAGAGAG ATCACCAAGATAGCTG
	PP61	TAGAAGACAATCAACTCCGGCGGCGCC
DELLA1 <sup>Δ17</sup> fragment B cloning for p35S:DELLA1 <sup>Δ17</sup> and pUbi:Myc DELLA1 <sup>Δ17</sup>	PP62	ATGAAGACTTTGATGTTGCCAGAAAGATGGAACA
	PP63	TAGAAGACAAAACCCTTGAAGCGTTGTTGTTGAG
DELLA1 fragment B cloning for ENTR-DELLA1	PP134	ATGAAGACTTTGATGAGCTTCTGGCGGCTTTAGG
	PP135	TAGAAGACAAAACCCTTGAAGCGTTGTTGTTGAG
DELLA1 <sup>Δ17</sup> fragment C cloning for	PP65	ATGAAGACTTGGTTTTCAACGATGATTCTGAATAC
	PP66	TAGAAGACAATTTCAATCGCTTGGGTTTCG

p35S:DELLA1 <sup>Δ17</sup> and pUbi:Myc DELLA1 <sup>Δ17</sup>		
DELLA1 <sup>Δ17</sup> fragment cloning for p35S:DELLA1 <sup>Δ17</sup> and pUbi:Myc DELLA1 <sup>Δ17</sup>	PP67	ATGAAGACTTGAAAACATGGTCAATCAAATC
	PP68	TAGAAGACAAAACCTGAGTTGACAGCGAC
DELLA1 <sup>Δ17</sup> fragment cloning for p35S:DELLA1 <sup>Δ17</sup> and pUbi:Myc DELLA1 <sup>Δ17</sup>	PP69	ATGAAGACTTAGTTTTTCGAGCTCCACCGCATGTTAG
	PP70	TAGAAGACAATTCGTGCCGCTCGACCCG
DELLA1 <sup>Δ17</sup> fragment cloning for p35S:DELLA1 <sup>Δ17</sup> and pUbi:Myc DELLA1 <sup>Δ17</sup>	PP71	TAGAAGACAACGAAACCCTGGTCCAATGGAGGAC
	PP72	ATGAAGACTTCAGAGGTCTCACCTTCGACTCACTGGTGTGGAAGCTTC
DELLA1 fragment cloning for ENTR-DELLA1	PP136	TTTGGTCTCTCACCATGAAGAGAGATCACCAAGATAGCTG
	PP137	AAAGGTCTCACCTTCGACTCACTGGGTTGTGGAAG
DELLA1 <sup>Δ17</sup> fragment cloning for ENTR-DELLA1 <sup>Δ17</sup>	PP138	TTTGGTCTCTCACCATGAAGAGAGATCACCAAGATAGCTG
	PP139	AAAGGTCTCACCTTCGACTCACTGGGTTGTGGAAG
DELLA1-F1 fragment cloning for ENTR-DELLA1-F1	PP140	TTTGGTCTCTCACCATGAAGAGAGATCACCAAGATAGCTG
	PP141	AAAGGTCTCACCTTTTGAGCAAGCTGAGCGAGC
DELLA1-M5 fragment cloning for ENTR-DELLA1-M5	PP142	TTTGGTCTCTCACCATGAAGCGATTGAAGACATGGTC
	PP143	AAAGGTCTCACCTTCGACTCACTGGGTTGTGGAAG
pRAM1 fragment for LIIIβ F A-B pRAM1_1057:GUS	MB2	ATGGTCTCAGCGGATAATTGTTACGGTGAAAATAG AAG
	MB1	TAGGTCTCACAGAGTTTTGTCTTTTTGGTAGAACAGAA
pRAM1 fragment for LIIIβ F A-B pRAM1_355:GUS	MB3	ATGGTCTCAGCGGATGCCCATGATTGCAA AAG
	MB1	TAGGTCTCACAGAGTTTTGTCTTTTTGGTAGAACAGAA
pRAM1 fragment for LIIIβ fin 1-2 pRAM1_962:GUS	MB4	TTTCGTCTCAGCGGGATCTGTATTCAA AATTATGAAT AAA
	PP96	TTTCGTCTCACAGAGTTTTGTCTTTTTGGTAGAACAG
pRAM1 fragment for LIIIβ fin 1-2 pRAM1_866:GUS	MB5	TTTCGTCTCAGCGCAAGTGCATATAAAATTCATTTTT TCA
	PP96	TTTCGTCTCACAGAGTTTTGTCTTTTTGGTAGAACAG
pRAM1 fragment for LIIIβ fin 1-2 pRAM1_771:GUS	MB6	TTTCGTCTCAGCGGCTTGAAATAAGAAA AATTATAG TGAA
	PP96	TTTCGTCTCACAGAGTTTTGTCTTTTTGGTAGAACAG
pRAM1 fragment for LIIIβ fin 1-2 pRAM1_658:GUS	MB7	TTTCGTCTCAGCGGTCACATTCACATTGACTTTTTCT
	PP96	TTTCGTCTCACAGAGTTTTGTCTTTTTGGTAGAACAG
pRAM1 fragment for LIIIβ fin 1-2 pRAM1_570:GUS	MB8	TTTCGTCTCAGCGGTTACATATTTCA TTTCTCTCACTC CT
	PP96	TTTCGTCTCACAGAGTTTTGTCTTTTTGGTAGAACAG
pRAM1 fragment for LIIIβ fin 1-2 pRAM1_470:GUS	MB9	TTTCGTCTCAGCGGATTTTGGTCCACA AATTATTTAT TAT

	PP96	TTTCGTCTCACAGAGTTTTGTCTTTTTGGTAGAACAG
pRAM1 fragment for LIIIβ fin 1-2 pRAM1_206:GUS	MB10	TTTCGTCTCAGCGGAGTTAAACAGGTAATCCTAAC TG
	PP96	TTTCGTCTCACAGAGTTTTGTCTTTTTGGTAGAACAG
pRAM1 fragment for LIIIβ fin 1-2 pRAM1_325:GUS	MP1	TTTCGTCTCAGCGGTCAAAAAGAACCTTGTGAAC
	PP96	TTTCGTCTCACAGAGTTTTGTCTTTTTGGTAGAACAG
pRAM1 fragment for LIIIβ fin 1-2 pRAM1_294:GUS	MP2	TTTCGTCTCAGCGGGCCCAAAAAGTGGGGTC
	PP96	TTTCGTCTCACAGAGTTTTGTCTTTTTGGTAGAACAG
pRAM1 fragment for LIIIβ fin 1-2 pRAM1_265:GUS	MP3	TTTCGTCTCAGCGGTGTCCTCATTAAACAAGCACAAG
	PP96	TTTCGTCTCACAGAGTTTTGTCTTTTTGGTAGAACAG
pRAM1 fragment for LIIIβ fin 1-2 pRAM1_235:GUS	MP4	TTTCGTCTCAGCGGAGCCTTCTGAAAGCACAAG
	PP96	TTTCGTCTCACAGAGTTTTGTCTTTTTGGTAGAACAG
pRAM1 fragment for LIIIβ fin 3-4 pRAM1_325_M1:GUS	KK1	TTTCGTCTCAGCGGTCAAAAAGAACCTTGTGAACA GATTTTAATTAATAAAAAAAGTGGGGTCCACCAA ACT ATTTGTCCTCAT
	PP96	TTTCGTCTCACAGAGTTTTGTCTTTTTGGTAGAACAG
pRAM1 fragment for LIIIβ fin 3-4 pRAM1_325_M2:GUS	KK2	TTTCGTCTCAGCGGTAAAAAATAAAATTTTAAAA TATGGGCCCGCCCAAAAAGTGGGGTCCACCAA ACT ATTTGTCCTCAT
	PP96	TTTCGTCTCACAGAGTTTTGTCTTTTTGGTAGAACAG
pRAM1 fragment for LIIIβ fin 3-4 AMCYC-RE_ p35Smin:GUS	PP161	TTTCGTCTCAGCGGAGTGATTTCAAAAAGAACCTTG TGAACAGATGGGCCCGCCCAAAAAGTGGGCGCAAG ACCCTTCCTCTATATAAG
	PP160	TTTCGTCTCACAGACGATCCCCTGTAATTGTAATTG
pRAM1 fragment for LIIIβ fin 3-4 2XAMCYC-RE_ p35Smin:GUS	PP162	TTTCGTCTCAGCGGGTGAACAGATGGGCCCGCCCAA AAAGTGGGGTGAACAGATGGGCCCGCCCAAAAAGT GGGCGCAAGACCCTTCCTCTATATAAG
	PP160	TTTCGTCTCACAGACGATCCCCTGTAATTGTAATTG
pRAM1 fragment for LIIIβ fin 3-4 2XmAMCYC-RE_ p35Smin:GUS	PP163	TTTCGTCTCAGCGGGTGAACAGATTTTAATTAATAAAA AAAGTGGGGTGAACAGATTTTAATTAATAAAAAAAGT GGGCGCAAGACCCTTCCTCTATATAAG
Overexpression of <i>DELLA2<sup>Δ18</sup></i> for	DELL A2 <sup>Δ18</sup> 1	GTGAAAGATGAAGAGAGAGCATAAGCTTGAACATG AAG
	DELL A2 <sup>Δ18</sup> 2	GAGCAACTTCACCACCACCGTCGTCCTCCCAACAAA C
Overexpression of <i>DELLA2<sup>Δ18</sup></i>	DELL A2 <sup>Δ18</sup> 3	AGTTGAATCAGTGCGAAACCACCACTGAGTTAG
	DELL A2 <sup>Δ18</sup> 4	CGGTGGTGGTGAAGTTGCTCAAAAAGTGAACA ACT TG
Overexpression of <i>DELLA2<sup>Δ18</sup></i>	DELL A2 <sup>Δ18</sup> 5	GGGGACAAGTTTGTACAAAAAGCAGGCTTCATGA AGAGAGAGCATAAGCTTG
	DELL A2 <sup>Δ18</sup> 6	GGGGACCACTTTGTACAAGAAAGCTGGGTTTCAGTG CGAAACCACCACTGAG

Overexpression of IPD3	IPD3_1	GGGGACAAGTTTGTACAAAAAAGCAGGCTTCATGG AAGGGAGAGGATTTTCTGG
	IPD3_2	GGGGACCACTTTGTACAAGAAAGCTGGGTTTCAAAT CTTCCAGTTTCTGATAG
qPCR <i>Ubiquitin</i> [S16]	Ubi F	ATGCAGATCTTCGTCAAGACCTTG
	Ubi R	ACCTCCCCTCAGACGAAG
qPCR <i>EF1alpha</i> [S16]	EF1alpha F	GCAGGTCTTTGTGTCAAGTCTT
	EF1alpha R	CGATCCAGAACCCAGTTCT
qPCR 3'UTR <i>RAM1</i>	PP99	TGCATTGAATCATGCTACGTT
	PP100	CCTTGTGGAGACCATCCATT
qPCR <i>SbtM1</i> [S1]	SbtM1 F	CACGTTGTTAGGACCCCAAT
	SbtM1 R	TTGAGCAGCACCCCTCTCTATC
qPCR <i>BCP1</i> [S1]	BCP1 F	TCATCTGTCCTTGGGGTCAT
	BCP1 R	CAGCTGCAGAAGTTGCATTT
qPCR <i>PT4</i> [S1]	PT4 F	GAATAAAGGGGCCAAAATCG
	PT4 R	GCTGTATCCTATCCCCATGC
qPCR <i>AMT2.2</i> [S1]	AMT2.2 F	TGGTTCAACTTTTCGTTCCA
	AMT2.2 R	CTTATCACCCCTGACCCCAAGA
qPCR <i>RAM2</i> [S20]	RAM2 F	ATCCTATGAGTGCCTAGCTTTACTAGAAG
	RAM2 R	AACGAGCAAATTA AAACTGAAAGAGAGTAC
qPCR <i>STR</i> [S21]	STR F	CTATATTGGTGACGAGGGAAGG
	STR R	GTCCTGAGGTAGGTTTCATCCAG
qPCR <i>Vapyrin A</i> [S22]	Vapyrin A F	GCTATCTCACAGAAGAGACC
	Vapyrin A R	AACAGAGTCACCAGAACC
qPCR <i>Vapyrin B</i>	Vapyrin B F	CCATCAATGGAAGGGATCAG
	Vapyrin B R	TCGATCCCTTTCTCCACAAG
qPCR CDS <i>RAM1</i>	SC307	TGGAGGAAGATCATGGAAGG
	SC308	AGCAACAAGCACCCCTTTGTC

**Table S2. Plasmid used in this study, Related to Figure 1-7**

Purpose	Name	Description

Golden gate level III plasmids		
<i>ram1-3</i> transgenic complementation (Fig 1B)	LIIIβ F A-B p <i>RAM1:RAM1</i>	Assembled by BpiI cut ligation from: LIIc F 1-2 p <i>RAM1:RAM1</i> + LII 2-3 ins (BB43) + LIIc R 3-4 p <i>Ubi:mCherry</i> + LII 4-6 dy (BB41) + LIIIβ F A-B (BB53)
Localization of <i>RAM1</i> promoter activity and transactivation assay (Fig 1F-J, 2C-D, 5E, 6A, 7A)	LIIIβ F A-B p <i>RAM1:GUS</i>	Assembled by BpiI cut ligation from: LIIc F 1-2 p <i>RAM1:GUS</i> + LII 2-3 ins (BB43) + LIIc R 3-4 p <i>Ubi:mCherry</i> + LII 4-6 dy (BB41) + LIIIβ F A-B (BB53)
Overexpression of <i>RAM1</i> (Fig 3A-B, 4A-B S3 and S4)	LIIIβ F A-B p <i>Ubi:RAM1</i>	Assembled by BpiI cut ligation from: LIIc F 1-2 p <i>Ubi:RAM1</i> + LII 2-3 ins (BB43) + LIIc R 3-4 p35S: <i>mCherry</i> + LII 4-6 dy (BB41) + LIIIβ F A-B (BB53)
Overexpression of <i>DELLA1<sup>Δ17</sup></i> (Fig 4A-B, 5A, C and S4)	LIIIβ F A-B p35S: <i>DELLA1<sup>Δ17</sup></i>	Assembled by BpiI cut ligation from: LIIc F 1-2 p35S: <i>DELLA1<sup>Δ17</sup></i> + LII 2-3 ins (BB43) + LIIc R 3-4 p <i>Ubi:mCherry</i> + LII 4-6 dy (BB41) + LIIIβ F A-B (BB53)
Overexpression of <i>CCaMK<sup>314</sup></i> (Fig 6B)	LIIIβ F A-B p <i>Ubi:CCaMK<sup>314</sup></i>	Assembled by BpiI cut ligation from: LII 1-3 dy (BB38) + LIIc R 3-4 p35S: <i>mCherry</i> + LII 4-5 dy (BB40) + LIIc R 5-6 p <i>Ubi:CCaMK<sup>314</sup></i> + LIIIβ F A-B (BB53)
Overexpression of <i>CCaMK<sup>314</sup>G30E</i> (Fig 6B)	LIIIβ F A-B p <i>Ubi:CCaMK<sup>314</sup>G30E</i>	Assembled by BpiI cut ligation from: LII 1-3 dy (BB38) + LIIc R 3-4 p35S: <i>mCherry</i> + LII 4-5 dy (BB40) + LIIc R 5-6 p <i>Ubi:CCaMK<sup>314</sup>G30E</i> + LIIIβ F A-B (BB53)
Empty vector	EV	Assembled by BpiI cut ligation from: LII 1-3 dy (BB38) + LIIc R 3-4 p35S: <i>mCherry</i> + LII 4-6 dy (BB41) + LIIIβ F A-B (BB53)
Overexpression of <i>DELLA1<sup>Δ17</sup></i> (Fig 6E)	LIIIβ F A-B p <i>Ubi:Myc:DELLA1<sup>Δ17</sup></i>	Assembled by BpiI cut ligation from: LIIc F 1-2 p <i>Ubi:Myc:DELLA1<sup>Δ17</sup></i> + LII 2-3 ins (BB43) + LIIc R 3-4 p35S: <i>mCherry</i> + LII 4-6 dy (BB41) + LIIIβ F A-B (BB53)
Overexpression of <i>CCaMK</i> (Fig 6E)	p35S: <i>GFP:CCaMK</i>	LR reaction with <i>CCaMK</i> cDNA entry clone [S3] and pK7FWG0 [S23]
Transactivation of promoters and localization of promoter activity	LIIIβ fin 1-2 p <i>OI:GUS</i>	Assembled by BpiI cut ligation from: LIIc F 1-2 p <i>OI:GUS</i> + LII 2-3 ins (BB43) + LIIc R 3-4 p <i>Ubi:mCherry</i> + LII 4-6 dy (BB41) + LIIIβ fin (BB52)

Transactivation and localization of pRAM1_1057:GUS (Fig. 7A, S7)	LIIIβ F A-B pRAM1_1057:GUS	Assembled by BpiI cut ligation from: LIIc F 1-2 pRAM1_1057:GUS + LII 2-3 ins (BB43) + LIIc R 3-4 pUbi:mCherry + LII 4-6 dy (BB41) + LIIIβ F A-B (BB53)
Transactivation and localization of pRAM1_962:GUS (Fig. 7A)	LIIIβ fin1-2 pRAM1_962:GUS	Assembled by Esp3I cut ligation from: LIIIβ fin 1-2 pOI:GUS + Fragment: MB4 + PP96
Transactivation and localization of pRAM1_866:GUS (Fig. 7A)	LIIIβ fin1-2 pRAM1_866:GUS	Assembled by Esp3I cut ligation from: LIIIβ fin 1-2 pOI:GUS + Fragment: MB5 + PP96
Transactivation and localization of pRAM1_771:GUS (Fig. 7A)	LIIIβ fin1-2 pRAM1_771:GUS	Assembled by Esp3I cut ligation from: LIIIβ fin 1-2 pOI:GUS + Fragment: MB6 + PP96
Transactivation and localization of pRAM1_658:GUS (Fig. 7A)	LIIIβ fin1-2 pRAM1_658:GUS	Assembled by Esp3I cut ligation from: LIIIβ fin 1-2 pOI:GUS + Fragment: MB7 + PP96
Transactivation and localization of pRAM1_570:GUS (Fig. 7A)	LIIIβ fin1-2 pRAM1_570:GUS	Assembled by Esp3I cut ligation from: LIIIβ fin 1-2 pOI:GUS + Fragment: MB8 + PP96
Transactivation and localization of pRAM1_470:GUS (Fig. 7A)	LIIIβ fin1-2 pRAM1_470:GUS	Assembled by Esp3I cut ligation from: LIIIβ fin 1-2 pOI:GUS + Fragment: MB9 + PP96
Transactivation and localization of pRAM1_355:GUS (Fig. 7A)	LIIIβ F A-B pRAM1_355:GUS	Assembled by BpiI cut ligation from: LIIc F 1-2 pRAM1_355:GUS + LII 2-3 ins (BB43) + LIIc R 3-4 pUbi:mCherry + LII 4-6 dy (BB41) + LIIIβ F A-B (BB53)
Transactivation and localization of pRAM1_206:GUS (Fig. 7a, S7)	LIIIβ fin1-2 pRAM1_206:GUS	Assembled by Esp3I cut ligation from: LIIIβ fin 1-2 pOI:GUS + Fragment: MB10 + PP96
Transactivation and localization of pRAM1_325:GUS (Fig. 7A, S7)	LIIIβ fin1-2 pRAM1_325:GUS	Assembled by Esp3I cut ligation from: LIIIβ fin 1-2 pOI:GUS + Fragment: MP1 + PP96
Transactivation and localization of pRAM1_294:GUS (Fig. 7A, S7)	LIIIβ fin1-2 pRAM1_294:GUS	Assembled by Esp3I cut ligation from: LIIIβ fin 1-2 pOI:GUS + Fragment: MP2 + PP96
Transactivation and localization of pRAM1_265:GUS (Fig. 7A, S7)	LIIIβ fin1-2 pRAM1_265:GUS	Assembled by Esp3I cut ligation from: LIIIβ fin 1-2 pOI:GUS + Fragment: MP3 + P96
Transactivation and localization of pRAM1_235:GUS (Fig. 7A, S7)	LIIIβ fin1-2 pRAM1_235:GUS	Assembled by Esp3I cut ligation from: LIIIβ fin 1-2 pOI:GUS + Fragment: MP4 + PP96
Transactivation of promoter	LIIIβ fin 3-4 pOI :GUS	Assembled by BpiI cut ligation from: LIIc 1-2 pUbi:mCherry + LII 2-3 ins (BB43) + LIIc F 3-4

		<i>pOI:GUS</i> + LII 4-6 dy (BB41) + LIIIβ fin (BB52)
Transactivation of <i>pRAM1_325_M1:GUS</i> (Fig. 7a)	LIIIβ fin 3-4 <i>pRAM1_325_M1:GUS</i>	Assembled by Esp3I cut ligation from: LIIIβ fin 3-4 <i>pOI:GUS</i> + Fragment: KK1+ P96
Transactivation of <i>pRAM1_325_M2:GUS</i> (Fig. 7B)	LIIIβ fin 3-4 <i>pRAM1_325_M2:GUS</i>	Assembled by Esp3I cut ligation from: LIIIβ fin 3-4 <i>pOI:GUS</i> + Fragment: KK2+ P96
Transactivation of <i>AMCYC-RE_p35Smin:GUS</i> (Fig. 7B)	LIIIβ fin 3-4 <i>p35Smin_AMCYC-RE:GUS</i>	Assembled by Esp3I cut ligation from: LIIIβ fin 3-4 <i>pOI:GUS</i> + Fragment: PP161+PP160
Transactivation of <i>2XAMCYC-RE_p35Smin:GUS</i> (Fig. 7B)	LIIIβ fin 3-4 <i>p35Smin_2XAMCYC-RE:GUS</i>	Assembled by Esp3I cut ligation from: LIIIβ fin 3-4 <i>pOI:GUS</i> + Fragment: PP162+PP160
Transactivation of <i>2XmAMCYC-RE_p35Smin:GUS</i> (Fig. 7B)	LIIIβ fin 3-4 <i>p35Smin_2XmAMCYC-RE:GUS</i>	Assembled by Esp3I cut ligation from: LIIIβ fin 3-4 <i>pOI:GUS</i> + Fragment: PP163+PP160
Golden gate level II plasmids		
	LIIc F 1-2 <i>pRAM1:RAM1</i>	Assembled by BsaI cut ligation from: LI A-B <i>pRAM1</i> + LI B-C dy (BB06) + LI C-D <i>RAM1</i> + LI D-E dy (BB08) + LI E-F nos-T (G006) + LI F-G dy (BB09) + LIIc F 1-2 (BB30)
	LIIc F 1-2 <i>pRAM1:GUS</i>	Assembled by BsaI cut ligation from: LI A-B <i>pRAM1</i> + LI B-C dy (BB06) + LI C-D <i>GUS</i> + LI D-E dy (BB08) + LI E-F nos-T (G006) + LI F-G dy (BB09) + LIIc F 1-2 (BB30)
	LIIc F 1-2 <i>pUbi:RAM1</i>	Assembled by BsaI cut ligation from: LI A-B <i>pUbi</i> (G007) + LI B-C dy (BB06) + LI C-D <i>RAM1</i> + LI D-E dy (BB08) + LI E-F nos-T (G006) + LI F-G dy (BB09) + LIIc F 1-2 (BB30)
	LIIc F 1-2 <i>p35S:DELLA1<sup>Δ17</sup></i>	Assembled by BsaI cut ligation from: LI A-B <i>p35S</i> (G005) + LI B-C (BB06) dy + LI C-D <i>DELLA1<sup>Δ17</sup></i> + LI D-E dy (BB08) + LI E-F nos-T (G006) + LI F-G dy (BB09) + LIIc F 1-2 (BB30)
	LIIc F 1-2 <i>pUbi:Myc:DELLA1<sup>Δ17</sup></i>	Assembled by BsaI cut ligation from: LI A-B <i>pUbi</i> (G007) + LI B-C <i>Myc</i> (G069) dy + LI C-D <i>DELLA1<sup>Δ17</sup></i> + LI D-E dy (BB08) + LI E-F nos-T (G006) + LI F-G dy (BB09) + LIIc F 1-2 (BB30)
	LIIc R 3-4 <i>pUbi:mCherry</i>	Assembled by BsaI cut ligation from: LI A-B <i>pUbi</i> (G007) + LI B-C (BB06) dy + LI C-D <i>mCherry</i>

		(G023) + LI D-E (BB08) dy + LI E-F 35S-T (G059) + LI F-G dy (BB09) + LIc R 3-4 (BB34)
	LIc R 3-4 p35S:mCherry	Assembled by BsaI cut ligation from: LI A-B p35S (G005) + LI B-C dy (BB06) + LI C-D mCherry (G023) + LI D-E (BB08) dy + LI E-F 35S-T (G059) + LI F-G dy (BB09) + LIc R 3-4 (BB34)
	LIc R 5-6 pUbi:CCaMK <sup>314</sup>	Assembled by BsaI cut ligation from: LI A-B pUbi (G007) + LI B-C dy (BB06) + LI C-D CCaMK <sup>314</sup> + LI D-E dy (BB08) + LI E-F HSP-T (G045) + LI F-G dy (BB09) + LIc R 5-6 (BB37)
	LIc R 5-6 pUbi:CCaMK <sup>314</sup> G30E	Assembled by BsaI cut ligation from: LI A-B pUbi (G007) + LI B-C dy (BB06) + LI C-D CCaMK <sup>314</sup> G30E+ LI D-E dy (BB08) + LI E-F HSP-T (G045) + LI F-G dy (BB09) + LIc R 5-6 (BB37)
	LIc F 1-2 pRAM1_1057:GUS	Assembled by BsaI cut ligation from: LI A-B pRAM1_1057 + LI B-C dy (BB06) + LI C-D GUS + LI D-E dy (BB08) + LI nos-T (G006) + LI F-G dy (BB09) + LIc F 1-2 (BB30)
	LIc F 1-2 pRAM1_355:GUS	Assembled by BsaI cut ligation from: LI A-B pRAM1_355 + LI B-C dy (BB06) + LI C-D GUS + LI D-E dy (BB08) + LI nos-T (G006) + LI F-G dy (BB09) + LIc F 1-2 (BB30)
	LIc F 1-2 pOI:GUS	Assembled by BsaI cut ligation from: LI A-B Esp3I-lacZ dy (G082) + LI B-C dy (BB06) + LI C-D GUS + LI D-E dy (BB08) + LI nos-T (G006) + LI F-G dy (BB09) + LIc F 1-2 (BB30)
	LIc F 3-4 pOI:GUS	Assembled by BsaI cut ligation from: LI A-B Esp3I-lacZ dy (G082) + LI B-C dy (BB06) + LI C-D GUS + LI D-E dy (BB08) + LI nos-T (G006) + LI F-G dy (BB09) + LIc F 3-4 (BB33)
	LIc F 1-2 pUbi:mCherry	Assembled by BsaI cut ligation from: LI A-B pUbi (G007) + LI B-C (BB06) dy + LI C-D mCherry (G023) + LI D-E (BB08) dy + LI E-F 35S-T (G059) + LI F-G dy (BB09) + LIc F 1-2 (BB30)

Golden gate level I plasmids		
	LI A-B pRAM1	Assembled from two PCR amplified fragment from <i>L. japonicus</i> Gifu genomic DNA with primers. Assembly by BpiI cut ligation into LI-BpiI (BB03). Fragment 1: PP2+PP132 Fragment 2: PP133+PP3
	LI C-D RAM1	Assembled by BpiI cut ligation from: L0 RAM1A + L0 RAM1B + L0 RAM1C + L0 RAM1D + LI-BpiI (BB03)
	LI C-D GUS	PCR amplification of 1.838 kb fragment from LI-GUS (Singh, <i>et al.</i> 2014) with primers PP97 + PP98. Assembly by SmaI cut ligation into LI-pUC57 (BB02)
	LI C-D DELLA1 <sup>Δ17</sup>	Assembled by BpiI cut ligation from: L0 DELLA1 <sup>Δ17</sup> A + L0 DELLA1 <sup>Δ17</sup> B + L0 DELLA1 <sup>Δ17</sup> C + L0 DELLA1 <sup>Δ17</sup> D + L0 DELLA1 <sup>Δ17</sup> E + L0 DELLA1 <sup>Δ17</sup> F + LI-BpiI (BB03)
	LI C-D DELLA1	Assembled by BpiI cut ligation from: L0 DELLA1 <sup>Δ17</sup> A + L0 DELLA1B + L0 DELLA1 <sup>Δ17</sup> C + L0 DELLA1 <sup>Δ17</sup> D + L0 DELLA1 <sup>Δ17</sup> E + L0 DELLA1 <sup>Δ17</sup> F + LI-BpiI (BB03)
	LI C-D CCaMK <sup>314</sup>	Assembled from three PCR amplified fragment from RFP-Kinase (CCaMK <sup>314</sup> )+NLS (pK7WGR2) [S24] with primers. Assembly by BpiI cut ligation into LI-BpiI (BB03). Fragment 1: PP82+PP83 Fragment 2: PP84+PP85 Fragment 3: PP86+PP87
	LI C-D CCaMK <sup>314</sup> G30E	Assembled from three PCR amplified fragment from RFP-Kinase G30E (CCaMK <sup>314</sup> )+NLS (pK7WGR2) [S3] with primers. Assembly by BpiI cut ligation into LI-BpiI (BB03). Fragment 1: PP82+PP83 Fragment 2: PP84+PP85 Fragment 3: PP86+PP87
	LI A-B pRAM1_1057	Assembled by SmaI blunt end cut ligation: pUC57 (BB02) + Fragment: MB2 + MB1

	LI A-B pRAM1_355	Assembled by SmaI blunt end cut ligation: pUC57 (BB02) + Fragment: MB3 + MB1
Golden gate level 0 plasmids		
	L0 RAM1A	PCR amplification of 638 bp fragment <i>L. japonicus</i> Gifu genomic DNA with primers PP5 + PP6. Assembly by SmaI cut ligation into LI-Amp (BB01)
	L0 RAM1B	PCR amplification of 486 bp fragment <i>L. japonicus</i> Gifu genomic DNA with primers PP7 + PP8. Assembly by SmaI cut ligation into LI-Amp (BB01)
	L0 RAM1C	PCR amplification of 850 bp fragment <i>L. japonicus</i> Gifu genomic DNA with primers PP9 + PP10. Assembly by StuI cut ligation into LI-Amp (BB01)
	L0 RAM1D	PCR amplification of 468 bp fragment <i>L. japonicus</i> Gifu genomic DNA with primers PP11 + PP12. Assembly by SmaI cut ligation into LI-Amp (BB01)
	L0 DELLA1 <sup>Δ17A</sup>	PCR amplification of 185 bp fragment <i>L. japonicus</i> Gifu genomic DNA with primers PP60 + PP61. Assembly by SmaI cut ligation into LI-Amp (BB01)
	L0 DELLA1 <sup>Δ17B</sup>	PCR amplification of 282 bp fragment <i>L. japonicus</i> Gifu genomic DNA with primers PP62 + PP63. Assembly by SmaI cut ligation into LI-Amp (BB01)
	L0 DELLA1B	PCR amplification of 333 bp fragment <i>L. japonicus</i> Gifu genomic DNA with primers PP134 + PP135. Assembly by SmaI cut ligation into LI-Amp (BB01)
	L0 DELLA1 <sup>Δ17C</sup>	PCR amplification of 129 bp fragment <i>L. japonicus</i> Gifu genomic DNA with primers PP65 + PP66. Assembly by SmaI cut ligation into LI-Amp (BB01)
	L0 DELLA1 <sup>Δ17D</sup>	PCR amplification of 714 bp fragment <i>L. japonicus</i> Gifu genomic DNA with primers PP67 + PP68. Assembly by StuI cut ligation into LI-Amp (BB01)

	L0 <i>DELLA1</i> <sup>Δ17E</sup>	PCR amplification of 330 bp fragment <i>L. japonicus</i> Gifu genomic DNA with primers PP69 + PP70. Assembly by SmaI cut ligation into LI-Amp (BB01)
	L0 <i>DELLA1</i> <sup>Δ17F</sup>	PCR amplification of 255 bp fragment <i>L. japonicus</i> Gifu genomic DNA with primers PP71 + PP72. Assembly by SmaI cut ligation into LI-Amp (BB01)
Gateway expression plasmids		
Transactivation assay (Fig. 6A, 7A-B)	pAMPATp35S:3xHA-CYCLOPS	[S17]
Transactivation assay (Fig. 6A, 7A-B)	<i>Kinase-RFP (CCaMK<sup>314</sup>)+NLS (pK7WGR2)</i>	[S24]
Y2H assay (Fig. 6C, S6A)	pAD- <i>DELLA1-F1</i>	LR clonase (Invitrogen) recombination of ENTR- <i>DELLA1-F1</i> with pAD- <i>GAL4</i>
Y2H assay (Fig. 6C, S6A)	pAD- <i>DELLA1-M5</i>	LR clonase (Invitrogen) recombination of ENTR- <i>DELLA1-M5</i> with pAD- <i>GAL4</i>
Y2H assay (Fig. 6C, S6A)	pBD- <i>CCaMK</i>	[S3]
Y2H assay (Fig. S6A)	pAD- <i>CCaMK</i>	assembled as described [S3]
Y2H assay (Fig. S6A)	pBD- <i>CCaMK<sup>314</sup></i>	[S3]
Y2H assay (Fig. 6C)	pBD- <i>DELLA1</i>	LR clonase (Invitrogen) recombination of ENTR- <i>DELLA1</i> with pBD- <i>GAL4</i>
Y2H assay (Fig. 6C)	pBD- <i>DELLA1</i> <sup>Δ17</sup>	LR clonase (Invitrogen) recombination of ENTR- <i>DELLA1</i> <sup>Δ17</sup> with pBD- <i>GAL4</i>
Y2H assay (Fig. 6C, S6A)	pBD- <i>DELLA1-F1</i>	LR clonase (Invitrogen) recombination of ENTR- <i>DELLA1-F1</i> with pBD- <i>GAL4</i>
Y2H assay (Fig. 6C, S6A)	pBD- <i>DELLA1-M5</i>	LR clonase (Invitrogen) recombination of ENTR- <i>DELLA1-M5</i> with pBD- <i>GAL4</i>
Y2H assay (Fig. 6C)	pAD-CYCLOPS	[S3]
BiFC assay (Fig. 6D)	<i>DELLA1-YFP<sub>N</sub></i>	LR clonase (Invitrogen) recombination of ENTR- <i>DELLA1</i> PvuI/NruI digested product with pSPYNE
BiFC assay (Fig. 6D)	<i>DELLA1</i> <sup>Δ17</sup> - <i>YFP<sub>N</sub></i>	LR clonase (Invitrogen) recombination of ENTR- <i>DELLA1</i> <sup>Δ17</sup> PvuI/NruI digested product with pSPYNE
BiFC assay (Fig. 6D)	<i>YFP<sub>c</sub>-CCaMK</i>	assembled as described [S3]
BiFC assay (Fig. 6D)	<i>CCaMK-YFP<sub>N</sub></i>	[S3]
BiFC assay (Fig. 6D)	<i>CCaMK</i> <sup>K44A</sup> - <i>YFP<sub>N</sub></i>	[S3]

BiFC assay (Fig. 6D)	<i>YFP<sub>c</sub>-CYCLOPS</i>	[S3]
CoIP from Medicago (Fig S6B)	<i>YFP- DELLA2<sup>Δ18</sup></i>	LR clonase (Invitrogen) recombination of ENTR- <i>DELLA2<sup>Δ18</sup></i> with pEarleyGate104 [S25]
CoIP from Medicago (Fig S6B)	<i>HA-IPD3</i>	LR clonase (Invitrogen) recombination of ENTR- <i>IPD3</i> with pEarleyGate201 [S25]
Gateway entry plasmids		
	<i>ENTR-DELLA1</i>	PCR amplification of 1804 bp fragment from LI <i>DELLA1</i> with primers PP136+ PP137. Assembly by BsaI cut ligation into p <i>ENTR-BsaI</i>
	<i>ENTR-DELLA1<sup>Δ17</sup></i>	PCR amplification of 1753 bp fragment from LI <i>DELLA1<sup>Δ17</sup></i> with primers PP138 + PP139. Assembly by BsaI cut ligation into p <i>ENTR-BsaI</i>
	<i>ENTR-DELLA1-F1</i>	PCR amplification of 1171 bp fragment from LI <i>DELLA1</i> with primers PP140 + PP141. Assembly by BsaI cut ligation into p <i>ENTR-BsaI</i>
	<i>ENTR-DELLA1-M5</i>	PCR amplification of 1255 bp fragment from LI <i>DELLA1</i> with primers PP142 + PP143. Assembly by BsaI cut ligation into p <i>ENTR-BsaI</i>
	<i>DELLA2<sup>Δ18</sup></i>	Fusion PCR as in [S12] of fragment 1 amplified using primers <i>DELLA2<sup>Δ18</sup></i> 1+ <i>DELLA2<sup>Δ18</sup></i> 2 and fragment 2 amplified using primers <i>DELLA2<sup>Δ18</sup></i> 3+ <i>DELLA2<sup>Δ18</sup></i> 4
	<i>ENTR- DELLA2<sup>Δ18</sup></i>	BP clonase reaction: PCR fragment amplified using primers <i>DELLA2<sup>Δ18</sup></i> 5+ <i>DELLA2<sup>Δ18</sup></i> 6 and pDONR207 (Invitrogen)
	<i>ENTR-IPD3</i>	BP clonase reaction: PCR fragment amplified using primers <i>IPD3_1+</i> <i>IPD3_2</i> and pDONR207 (Invitrogen)

**Paper II:** Lipid transfer from plants to arbuscular mycorrhiza fungi

Reference: Keymer A#, **Pimprikar P#**, Wewer V, Huber C, Brands M, Bucerius SL, Delaux PM, Klingl V, von Roepenack-Lahaye E, Wang TL, Eisenreich W, Dörmann P, Parniske M, Gutjahr C (2017). Lipid transfer from plants to arbuscular mycorrhiza fungi. *eLife* 6. pii: e29107.

# These authors contributed equally to the work

# Lipid transfer from plants to arbuscular mycorrhiza fungi

Andreas Keymer<sup>1†</sup>, Priya Pimprakar<sup>1†</sup>, Vera Wewer<sup>2‡</sup>, Claudia Huber<sup>3</sup>, Mathias Brands<sup>2</sup>, Simone L Bucerius<sup>1</sup>, Pierre-Marc Delaux<sup>4</sup>, Verena Klingl<sup>1</sup>, Edda von Röpenack-Lahaye<sup>5§</sup>, Trevor L Wang<sup>6</sup>, Wolfgang Eisenreich<sup>3</sup>, Peter Dörmann<sup>2</sup>, Martin Parniske<sup>1</sup>, Caroline Gutjahr<sup>1\*</sup>

<sup>1</sup>Faculty of Biology, Genetics, LMU Munich, Biocenter Martinsried, Munich, Germany; <sup>2</sup>Institute of Molecular Physiology and Biotechnology of Plants, University of Bonn, Bonn, Germany; <sup>3</sup>Biochemistry, Technical University Munich, Garching, Germany; <sup>4</sup>Laboratoire de Recherche en Sciences Végétale, Centre National de la Recherche Scientifique, Toulouse, France; <sup>5</sup>Faculty of Biology, Plant Sciences, LMU Munich, Biocenter Martinsried, Munich, Germany; <sup>6</sup>John Innes Centre, Norwich Research Park, Norwich, United Kingdom

\*For correspondence: caroline.gutjahr@lmu.de

†These authors contributed equally to this work

Present address: ‡Mass Spectrometry Metabolomics Facility, Cluster of Excellence on Plant Sciences, University of Cologne Biocenter, Cologne, Germany; §Analytics Facility, Center for Plant Molecular Biology, University of Tübingen, Tübingen, Germany

Competing interests: The authors declare that no competing interests exist.

Funding: See page 28

Received: 31 May 2017

Accepted: 13 July 2017

Published: 20 July 2017

Reviewing editor: Gary Stacey, University of Missouri, United States

© Copyright Keymer et al. This article is distributed under the terms of the [Creative Commons Attribution License](#), which permits unrestricted use and redistribution provided that the original author and source are credited.

**Abstract** Arbuscular mycorrhiza (AM) symbioses contribute to global carbon cycles as plant hosts divert up to 20% of photosynthate to the obligate biotrophic fungi. Previous studies suggested carbohydrates as the only form of carbon transferred to the fungi. However, *de novo* fatty acid (FA) synthesis has not been observed in AM fungi in absence of the plant. In a forward genetic approach, we identified two *Lotus japonicus* mutants defective in AM-specific paralogs of lipid biosynthesis genes (*KASI* and *GPAT6*). These mutants perturb fungal development and accumulation of emblematic fungal 16:1 $\omega$ 5 FAs. Using isotopolog profiling we demonstrate that <sup>13</sup>C patterns of fungal FAs recapitulate those of wild-type hosts, indicating cross-kingdom lipid transfer from plants to fungi. This transfer of labelled FAs was not observed for the AM-specific lipid biosynthesis mutants. Thus, growth and development of beneficial AM fungi is not only fueled by sugars but depends on lipid transfer from plant hosts.

DOI: [10.7554/eLife.29107.001](https://doi.org/10.7554/eLife.29107.001)

## Introduction

Arbuscular mycorrhiza (AM) is a widespread symbiosis between most land plants and fungi of the Glomeromycota ([Smith and Read, 2008](#)). The fungi provide mineral nutrients to the plant. These nutrients are taken up from the soil and released inside root cortex cells at highly branched hyphal structures, the arbuscules ([Javot et al., 2007](#)). For efficient soil exploration, arbuscular mycorrhiza fungi (AMF) develop extended extraradical hyphal networks. Their growth requires a large amount of energy and carbon building blocks, which are transported mostly as lipid droplets and glycogen to the growing hyphal tips ([Bago et al., 2002, 2003](#)). AMF are obligate biotrophs, as they depend on carbon supply by their host ([Smith and Read, 2008](#)). In the past, detailed <sup>13</sup>C-labeled tracer-based NMR studies demonstrated that hexose sugars are a major vehicle for carbon transfer from plants to fungi ([Shachar-Hill et al., 1995](#)). In addition, a fungal hexose transporter, with high transport activity for glucose is required for arbuscule development and quantitative root colonization as shown by host induced gene silencing ([Helber et al., 2011](#)), indicating the importance of hexose transfer for intra-radical fungal development.

AMF store carbon mainly in the form of lipids ([Trépanier et al., 2005](#)). The predominant storage form is triacylglycerol (TAG) and the major proportion of FAs found in AMF is composed of 16:0 (palmitic acid), and of 16:1 $\omega$ 5 (palmitavaccenic acid). The latter is specific to AM fungi and certain

**eLife digest** Most land plants are able to form partnerships with certain fungi – known as arbuscular mycorrhiza fungi – that live in the soil. These fungi supply the plant with mineral nutrients, especially phosphate and nitrogen, in return for receiving carbon-based food from the plant. To exchange nutrients, the fungi grow into the roots of the plant and form highly branched structures known as arbuscules inside plant cells.

Due to the difficulties of studying this partnership, it has long been believed that plants only provide sugars to the fungus. However, it has recently been discovered that these fungi lack important genes required to make molecules known as fatty acids. Fatty acids are needed to make larger fat molecules that, among other things, store energy for the organism and form the membranes that surround each of its cells. Therefore, these results raise the possibility that the plant may provide the fungus with some of the fatty acids the fungus needs to grow.

Keymer, Pimprikar et al. studied how arbuscules form in a plant known as *Lotus japonicus*, a close relative of peas and beans. The experiments identified a set of mutant *L. japonicus* plants that had problems forming arbuscules. These plants had mutations in several genes involved in fat production that are only active in plant cells containing arbuscules.

Further experiments revealed that certain fat molecules that are found in fungi, but not plants, were present at much lower levels in samples from mutant plants colonized with the fungus, compared to samples from normal plants colonized with the fungus. This suggests that the fungi colonizing the mutant plants may be starved of fat molecules. Using a technique called stable isotope labelling it was possible to show that fatty acids made in normal plants can move into the colonizing fungus.

The findings of Keymer, Pimprikar et al. provide evidence that the plant feeds the fungus not only with sugars but also with fat molecules. The next challenge will be to find out exactly how the fat molecules are transferred from the plant cell to the fungus. Many crop plants are able to form partnerships with arbuscular mycorrhizal fungi. Therefore, a better understanding of the role of fat molecules in these relationships may help to breed crop plants that, by providing more support to their fungal partner, may grow better in the field.

DOI: [10.7554/eLife.29107.002](https://doi.org/10.7554/eLife.29107.002)

bacteria and is frequently used as marker for the detection of AM fungi in soil (Graham et al., 1995; Bentivenga and Morton, 1996; Madan et al., 2002; Trépanier et al., 2005). Fungus-specific 16:1 $\omega$ 5 FAs are not exclusive to glycerolipids but also incorporated into membrane phospholipids (van Aarle and Olsson, 2003). Furthermore, 18:1 $\omega$ 7 and 20:1 $\omega$ 11 are considered specific for AMF but do not occur in all AMF species (Madan et al., 2002; Stumpe et al., 2005).

It has long been assumed that AMF use sugars as precursors for lipid biosynthesis (Pfeffer et al., 1999). However, *de novo* biosynthesis of fungal fatty acids (FAs) was only observed inside colonized roots and not in extraradical mycelia or spores (Pfeffer et al., 1999; Trépanier et al., 2005). The authors concluded that AM fungi can produce FAs only inside the host. The hypothesis that plants directly provide lipids to the fungus could not be supported at that time (Trépanier et al., 2005), due to experimental limitations and the lack of appropriate plant mutants. However, recently available whole genome sequences of AMF have revealed that genes encoding multi-domain cytosolic FA synthase subunits, typically responsible for most of the *de novo* 16:0 FA synthesis in animals and fungi, are absent from the genomes of the model fungi *Rhizophagus irregularis*, *Gigaspora margarita* and *Gigaspora rosea* (Wewer et al., 2014; Ropars et al., 2016; Salvioli et al., 2016; Tang et al., 2016). Hence, AMF appear to be unable to synthesize sufficient amounts of 16:0 FAs, but their genomes do encode the enzymatic machinery for 16:0 FA elongation to higher chain length and for FA desaturation (Trépanier et al., 2005; Wewer et al., 2014).

Development of fungal arbuscules is accompanied by activation of a cohort of lipid biosynthesis genes in arbuscocytes (arbuscule-containing plant cells) (Gaude et al., 2012a, 2012b). Furthermore, lipid producing plastids increase in numbers and together with other organelles such as the endoplasmic reticulum change their position and gather in the vicinity of the arbuscule (Lohse et al., 2005; Ivanov and Harrison, 2014), symptomatic of high metabolic activity to satisfy the high

demands of arbuscules for metabolites including lipids. The importance of plant lipid biosynthesis for arbuscule development has been demonstrated by *Medicago truncatula* mutants in AM-specific paralogs of two lipid biosynthesis genes *FatM* and *REDUCED ARBUSCULAR MYCORRHIZA2* (*RAM2*) (Wang et al., 2012; Bravo et al., 2017). *FatM* encodes an ACP-thioesterase, which terminates fatty acid chain elongation in the plastid by cleaving the ACP off the acyl group releasing free FAs and soluble ACP (Jones et al., 1995). *RAM2* encodes a glycerol 3-phosphate acyl transferase (GPAT) and is most similar to *Arabidopsis* GPAT6. In *Arabidopsis*, GPAT6 acetylates the *sn*-2 position of glycerol-3-phosphate with an FA and cleaves the phosphate from lysophosphatidic acid, thereby producing *sn*-2-monoacylglycerol ( $\beta$ MAG, Yang et al., 2010). Mutations in both *FatM* and *RAM2* impair arbuscule branching (Wang et al., 2012; Bravo et al., 2017). In addition, arbuscule branching requires a complex of two half ABC transporters *STR* and *STR2* (Zhang et al., 2010; Gutjahr et al., 2012). The substrate of *STR/STR2* is unknown but other members of the ABCG transporter family are implicated in lipid transport (Wittenburg and Carey, 2002; Wang et al., 2011; Fabre et al., 2016; Hwang et al., 2016; Lee et al., 2016). Therefore, and due to its localization in the peri-arbuscular membrane (Zhang et al., 2010) it was speculated that the *STR/STR2* complex may transport lipids towards arbuscules (Gutjahr et al., 2012; Bravo et al., 2017). Transcriptional activation of *RAM2* and *STR* is controlled by the GRAS transcription factor *REDUCED ARBUSCULAR MYCORRHIZA1* (*RAM1*) (Gobbato et al., 2012; Park et al., 2015; Pimprikar et al., 2016) and also in *ram1* mutants, arbuscule branching is impaired (Park et al., 2015; Xue et al., 2015; Pimprikar et al., 2016). Thus, *RAM1*, *FatM*, *RAM2* and *STR/STR2* appear to form an AM-specific operational unit for lipid biosynthesis and transport in arbuscules. Consistently, they were found to be absent from genomes of plants that have lost the ability to form AM (Delaux et al., 2014; Favre et al., 2014; Bravo et al., 2016).

Here, we analyzed two *Lotus japonicus* mutants identified in a forward genetic screen, which are impaired in arbuscule branching (Groth et al., 2013). Positional cloning combined with genome resequencing revealed mutations in a novel AM-specific  $\beta$ -keto-acyl ACP synthase I (*KASI*) gene and in the *L. japonicus* ortholog of *M. truncatula* *RAM2*. *KASI* likely acts upstream of *RAM2* in producing 16:0 FAs. The identity of the genes and the phenotypes led us to hypothesize that AMF may depend on delivery of 16:0 FAs from the plant host. Using a combination of microscopic mutant characterization, lipidomics and isotopolog profiling of 16:0 and 16:1 $\omega$ 5 FAs in roots and extraradical fungal mycelium, we provide strong evidence for requirement of both genes for AM-specific lipid biosynthesis and cross-kingdom lipid transfer from plants to AMF.

## Results

### Two *L. japonicus* arbuscule-branching mutants are defective in lipid-biosynthesis genes

We previously identified two *L. japonicus* mutants *disorganized arbuscules* (*dis-1*, SL0154-N) and SL0181-N (*red*) deficient in arbuscule branching (Groth et al., 2013) (Figure 1A–B). Both mutants also suffered from a reduction in root length colonization and blocked the formation of lipid-containing vesicles of the fungus *Rhizophagus irregularis* (Figure 1C–D). We identified the causative mutations with a combination of classical mapping and next generation sequencing (see Materials and methods). *DIS* encodes a  $\beta$ -keto-acyl ACP synthase I (*KASI*, Figure 1—figure supplements 1A–C and 2). *KASI* enzymes catalyze successive condensation reactions during fatty acyl chain elongation from C4:0-ACP to C16:0-ACP (Li-Beisson et al., 2010). SL0181-N carries one mutation (*ram2-1*) in the *L. japonicus* orthologue of the previously identified *Medicago truncatula* *REDUCED ARBUSCULAR MYCORRHIZA2* (*RAM2*, Figure 1—figure supplements 3 and 4). *Arabidopsis* GPAT6 has been shown to produce  $\beta$ -MAG with a preference for 16:0 FAs (Yang et al., 2012). Therefore, we hypothesized that *DIS* and *RAM2* act in the same biosynthetic pathway.

We identified additional allelic *dis* mutants by TILLING (Figure 1—figure supplement 1E, Supplementary file 1) (Perry et al., 2003) and a *ram2* mutant caused by a LORE1 insertion in the *RAM2* gene (Figure 1—figure supplement 3B) (Malolepszy et al., 2016). Among the allelic *dis* mutants we chose *dis-4* for further investigation because it suffers from a glycine replacement at the border of a conserved  $\beta$ -sheet (Figure 1—figure supplement 2), which likely affects protein folding (Perry et al., 2009). Both allelic mutants *dis-4* and *ram2-2* phenocopied *dis-1* and *ram2-1*,

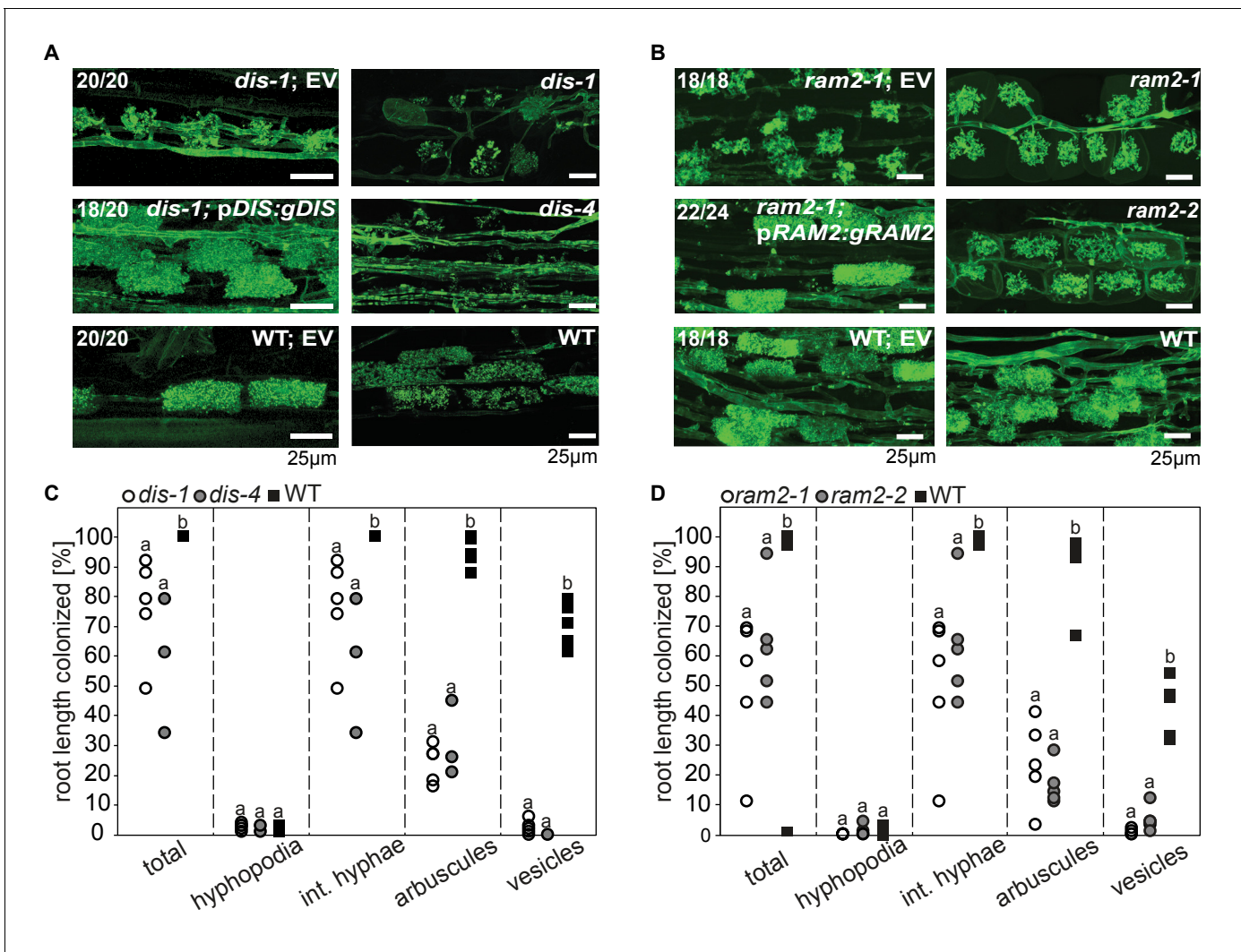


**Figure 1.** *DIS* and *RAM2* are required for arbuscule branching and vesicle formation. Arbuscule phenotype and complementation of *dis* (A) and *ram2* (B) mutants. The fungus was stained with wheat-germ agglutinin (WGA)-AlexaFluor488. (C-D) Percent root length colonization of *dis* (C) and *ram2* (D) mutants as compared to wild-type. Different letters indicate significant differences among treatments (ANOVA; posthoc Tukey). (C):  $n = 13$ ;  $p \leq 0.1$ ,  $F_{2,10} = 8.068$  (total & int. hyphae);  $p \leq 0.001$ ,  $F_{2,10} = 124.5$  (arbuscules);  $p \leq 0.001$ ,  $F_{2,10} = 299.1$  (vesicles) (D):  $n = 15$ ;  $p \leq 0.1$ ,  $F_{2,12} = 10.18$  (total & int. hyphae);  $p \leq 0.001$ ,  $F_{2,12} = 57.86$  (arbuscules);  $p \leq 0.001$ ,  $F_{2,12} = 72.37$  (vesicles). (A-D) Plants were inoculated with *R. irregularis* and harvested at 5 weeks post inoculation (wpi).

DOI: 10.7554/eLife.29107.003

The following figure supplements are available for figure 1:

**Figure supplement 1.** Identification of the *dis* mutation.

DOI: 10.7554/eLife.29107.004

**Figure supplement 2.** Protein sequence alignment of *L. japonicus* *DIS* with other KASI proteins.

DOI: 10.7554/eLife.29107.005

**Figure supplement 3.** Identification of mutation in the *RAM2* gene.

DOI: 10.7554/eLife.29107.006

**Figure supplement 4.** Protein sequence alignment of *L.*

DOI: 10.7554/eLife.29107.007

respectively. Furthermore, transgenic complementation of both *dis-1* and *ram2-1* with the wild-type versions of the mutated genes restored arbuscule-branching and wild-type-like levels of root length colonization and vesicle formation (Figure 1A-B). Taken together this confirmed identification of both causal mutations.

## ***DIS* and *RAM2* expression in arbusocytes is sufficient for arbuscule development**

Transcript levels of both *DIS* and *RAM2* increased in colonized roots (**Figure 3—figure supplement 1A**). To analyze the spatial activity pattern of the *DIS* and *RAM2* promoters during colonization we fused 1.5 kb for *DIS* and 2.275 kb for *RAM2* upstream of the translational start site to the *uidA* gene. Consistent with a role of both genes in arbuscule development GUS activity was predominantly detected in arbusocytes (arbuscule-containing cells) in both wild-type and the corresponding mutant roots (**Figure 2—figure supplement 1A–B**).

To correlate promoter activity with the precise stage of arbuscule development we used nuclear localized YFP as a reporter. To visualize the fungus, the promoter:reporter cassette was co-transformed with a second expression cassette containing secreted *mCherry* fused to the *SbtM1* promoter. This promoter drives expression in colonized cells, in cells neighboring apoplastically growing hyphae and in cells forming pre-penetration *apparatus* (PPAs, cytoplasmic aggregations that assemble in cortex cells prior to arbuscule development) (**Genre et al., 2008; Takeda et al., 2009, 2012**). When expressed under the control of the *SbtM1* promoter, secreted *mCherry* accumulates in the apoplast surrounding fungal structures and PPAs, thereby revealing the silhouette of these structures (**Figure 2A–B, Videos 1–2**). Nuclear localized YFP fluorescence indicated activity of both promoters in cells containing PPAs (c, **Videos 1–2**) and containing sparsely branched (d) or mature (e) arbuscules. Furthermore, we rarely detected YFP fluorescence in non-colonized cells in direct neighborhood of arbusocytes, which were possibly preparing for PPA formation (a). However, YFP signal was absent from cells containing collapsed arbuscules (f), indicating that the promoters were active during arbuscule development and growth but inactive during arbuscule degeneration (**Figure 2A–B**). *RAM2* promoter activity was strictly correlated with arbusocytes, while the *DIS* promoter showed additional activity in cortical cells of non-colonized root segments (**Figure 2A–B, Figure 2—figure supplement 1C–D, Videos 3–6**).

To examine, whether arbusocyte-specific expression of *DIS* and *RAM2* is sufficient for fungal development we complemented the *dis-1* and *ram2-1* mutants with the corresponding wild-type genes fused to the arbusocyte-specific *PT4* promoter (**Volpe et al., 2013**). This restored arbuscule-branching, vesicle formation as well as root length colonization in the mutants (**Figure 2C–F**), showing that arbusocyte-specific expression of *DIS* and *RAM2* suffices to support AM development. Thus, expression of lipid biosynthesis genes in arbusocytes is not only important for arbuscule branching but also for vesicle formation and quantitative colonization.

## **The *KASI* family comprises three members in *L. japonicus***

Growth and development of *dis* and *ram2* mutants are not visibly affected (**Figure 3—figure supplement 2**), although they carry defects in important lipid biosynthesis genes. *RAM2* is specific to AM-competent plants (**Wang et al., 2012; Delaux et al., 2014; Favre et al., 2014; Bravo et al., 2016**) and activated in an AM-dependent manner (**Figure 2, Figure 3—figure supplement 1A**) (**Gobbato et al., 2012, 2013**). Plants contain an additional *GPAT6* paralog, which likely fulfills the housekeeping function (**Figure 1—figure supplement 4, Yang et al., 2012; Delaux et al., 2015**). To understand whether the same applies to *DIS* we searched the *L. japonicus* genome for additional *KASI* genes. We detected three paralogs *KASI*, *DIS* and *DIS-LIKE* (**Figure 1—figure supplement 1D–E and Figure 1—figure supplement 2**), of which only *DIS* was transcriptionally activated in AM roots (**Figure 3—figure supplement 1A**). Phylogenetic analysis revealed a split of seed plant *KASI* proteins into two different clades, called *KASI* and *DIS* (**Figure 3**). Members of the *KASI* clade, are presumably involved in housekeeping functions as this clade contains the product of the *KASI* single copy gene in *Arabidopsis* (**Wu and Xue, 2010**). Members of the *DIS* clade are found specifically in AM-host dicotyledons and in a gymnosperm (**Figure 3**). As confirmed by synteny analysis (**Figure 3—figure supplement 3**), *DIS* is absent from all eight analyzed non-host dicotyledon genomes, a phylogenetic pattern similar to other symbiosis genes (**Delaux et al., 2014; Favre et al., 2014; Bravo et al., 2016**). The occurrence of *DIS* in *Lupinus* species, which lost AM competence but still form root nodule symbiosis, may be a relic from the AM competent ancestor. An apparently, *Lotus*-specific, and thus recent duplication of the *DIS* gene resulted in an 87% identical copy (*DIS-LIKE*) located directly adjacent to *DIS* in a tail-to-tail orientation (**Figure 1—figure supplements 1B–C, 2**). *DIS-LIKE* was expressed at very low levels and not induced upon AM (**Figure 3—figure**

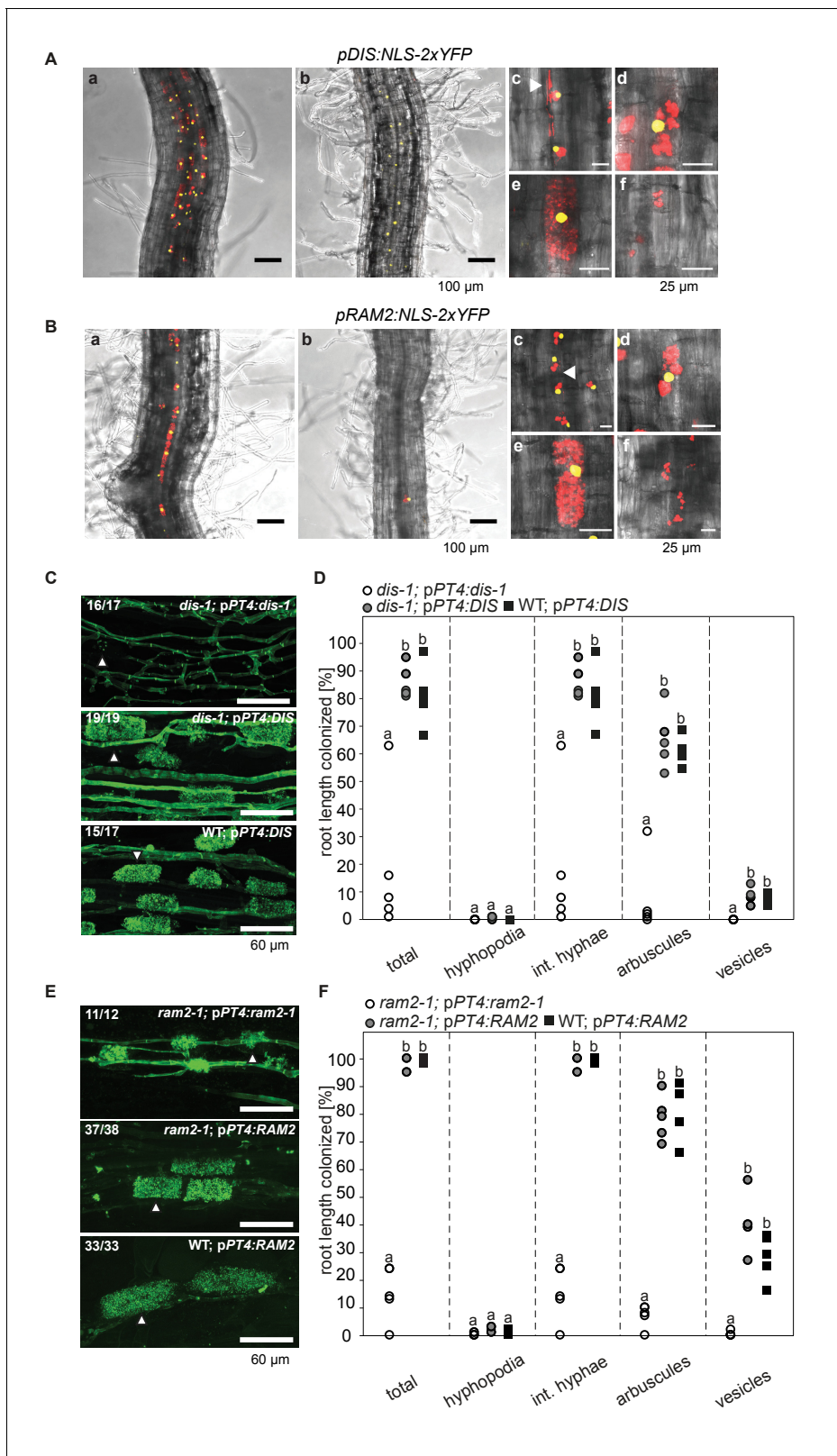


**Figure 2.** Arbuscocyte-specific expression of *DIS* and *RAM2* is sufficient for arbuscule branching. Promoter activity indicated by nuclear localized yellow fluorescence in colonized transgenic *L. japonicus* wild-type roots transformed with constructs containing a 1.5 kb promoter fragment of *DIS* (A) or a 2.275 kb promoter fragment of *RAM2* (B) fused to NLS-YFP. (A-B) Red fluorescence resulting from expression of *pSbtM1:SP-mCherry* labels the apoplastic space surrounding pre-penetration apparatus (PPAs) and fungal structures, thereby evidencing the silhouette of these structures. a Figure 2 continued on next page

Figure 2 continued

Colonized root, b non-colonized part of colonized root, c PPAs, (white arrow heads indicate the silhouette of fungal intraradical hyphae) d small arbuscules, e fully developed arbuscules f collapsed arbuscules. Merged confocal and bright field images of whole mount roots are shown. (C-D) Transgenic complementation of *dis-1* (C) and *ram2-1* (D) hairy roots with the respective wild-type gene driven by the *PT4* promoter. The mutant gene was used as negative control. White arrowheads indicate arbuscules. (E-F) Quantification of AM colonization in transgenic roots shown in (C-D). Different letters indicate significant differences (ANOVA; posthoc Tukey; n = 15;  $p \leq 0.001$ ) among genotypes for each fungal structure separately. Int. hyphae, intraradical hyphae. (E):  $F_{2,12} = 26.53$  (total),  $F_{2,12} = 46.97$  (arbuscules),  $F_{2,12} = 27.42$  (vesicles). (F)  $F_{2,12} = 341.5$  (total),  $F_{2,12} = 146.3$  (arbuscules),  $F_{2,12} = 35.86$  (vesicles).

DOI: [10.7554/eLife.29107.008](https://doi.org/10.7554/eLife.29107.008)

The following figure supplement is available for figure 2:

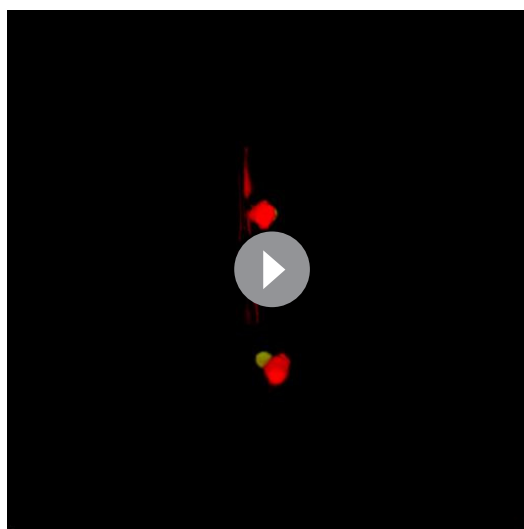
**Figure supplement 1.** *DIS* and *RAM2* promoter activity in wild type and *dis* and *ram2* mutants.

DOI: [10.7554/eLife.29107.009](https://doi.org/10.7554/eLife.29107.009)

**supplement 1A).** Nevertheless, because of its sequence similarity to *DIS*, we examined whether *DIS-LIKE* is also required for arbuscule formation using the *dis-like-5* mutant, which suffers from a glycine replacement at position 180 at the border of a highly conserved  $\beta$ -sheet that likely affects protein function (Perry et al., 2009) (Supplementary file 1, Figure 1—figure supplement 2). However, in roots of *dis-like-5* AM and arbuscule development was indistinguishable from wild type (Figure 3—figure supplement 1B). Therefore, *DIS-LIKE* might have lost its major role in arbuscule development after the duplication.

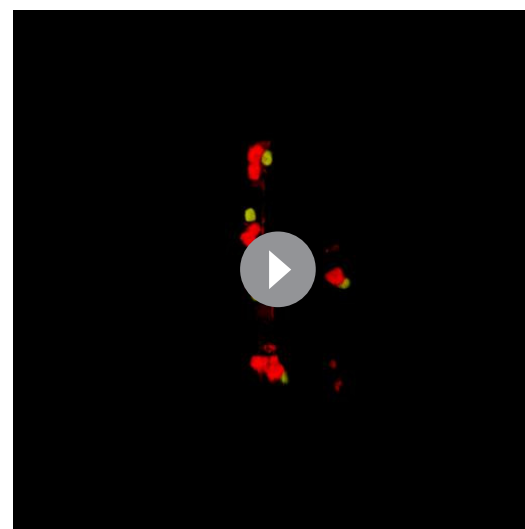
### DIS functions like a canonical KASI in planta

We examined whether *DIS* can substitute the phylogenetically related housekeeping *KASI*. To this end we transgenically complemented an *Arabidopsis kasl* mutant (Wu and Xue, 2010) with *Lotus DIS* driven by the *Arabidopsis KASI* promoter. *Arabidopsis kasl* exhibits an altered FA profile and reduced rosette growth (Wu and Xue, 2010). Complementation with *DIS* restored both wild-type-like rosette growth and FA accumulation. The *kasl* phenotypes persisted when the *dis-1* mutant allele was transformed as a negative control (Figure 4C–E). In the reverse cross-species complementation *AtKASI* driven by the *DIS* promoter restored colonization, arbuscule branching and vesicle



**Video 1.** 3D animation of Figure 2Ac illustrating that the silhouette of the fungal intraradical hyphae (red fluorescent vertical line) aligns with the silhouette of pre-penetration apparatus (red fluorescent bag-like structure). Yellow fluorescence in nuclei indicates activation of *pDIS:YFP*.

DOI: [10.7554/eLife.29107.010](https://doi.org/10.7554/eLife.29107.010)



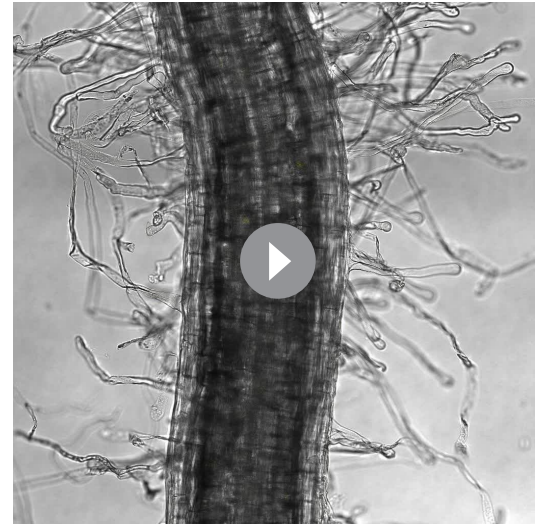
**Video 2.** 3D animation of Figure 2Bc illustrating that the silhouette of the fungal intraradical hyphae (red fluorescent vertical line) aligns with the silhouette of pre-penetration apparatus (red fluorescent bag-like structure). Yellow fluorescence in nuclei indicates activation of *pRAM2:YFP*.

DOI: [10.7554/eLife.29107.011](https://doi.org/10.7554/eLife.29107.011)



**Video 3.** Scan through confocal z-stack of **Figure 2Aa** illustrating correlation of *DIS* promoter activity with arbuscules.

DOI: [10.7554/eLife.29107.012](https://doi.org/10.7554/eLife.29107.012)



**Video 4.** Scan through confocal z-stack of **Figure 2Ab** illustrating *DIS* promoter activity exclusively in the cortex.

DOI: [10.7554/eLife.29107.013](https://doi.org/10.7554/eLife.29107.013)

formation in *dis-1* roots (**Figure 4A–B**). Furthermore, *DIS* contains a KASI-typical plastid transit peptide and - as predicted - localizes to plastids in *Nicotiana benthamiana* leaves and *L. japonicus* roots (**Figure 1—figure supplement 1F Figure 4F–G**). Thus, the enzymatic function of *DIS* is equivalent to the housekeeping KASI of *Arabidopsis* and the AM-specific function must result from its AM-dependent expression pattern.



**Video 5.** Scan through confocal z-stack of **Figure 2Ba** illustrating correlation of *RAM2* promoter activity with arbuscules.

DOI: [10.7554/eLife.29107.014](https://doi.org/10.7554/eLife.29107.014)



**Video 6.** Scan through confocal z-stack of **Figure 2Bb** illustrating absence of *RAM2* promoter activity from non-colonized cells.

DOI: [10.7554/eLife.29107.015](https://doi.org/10.7554/eLife.29107.015)

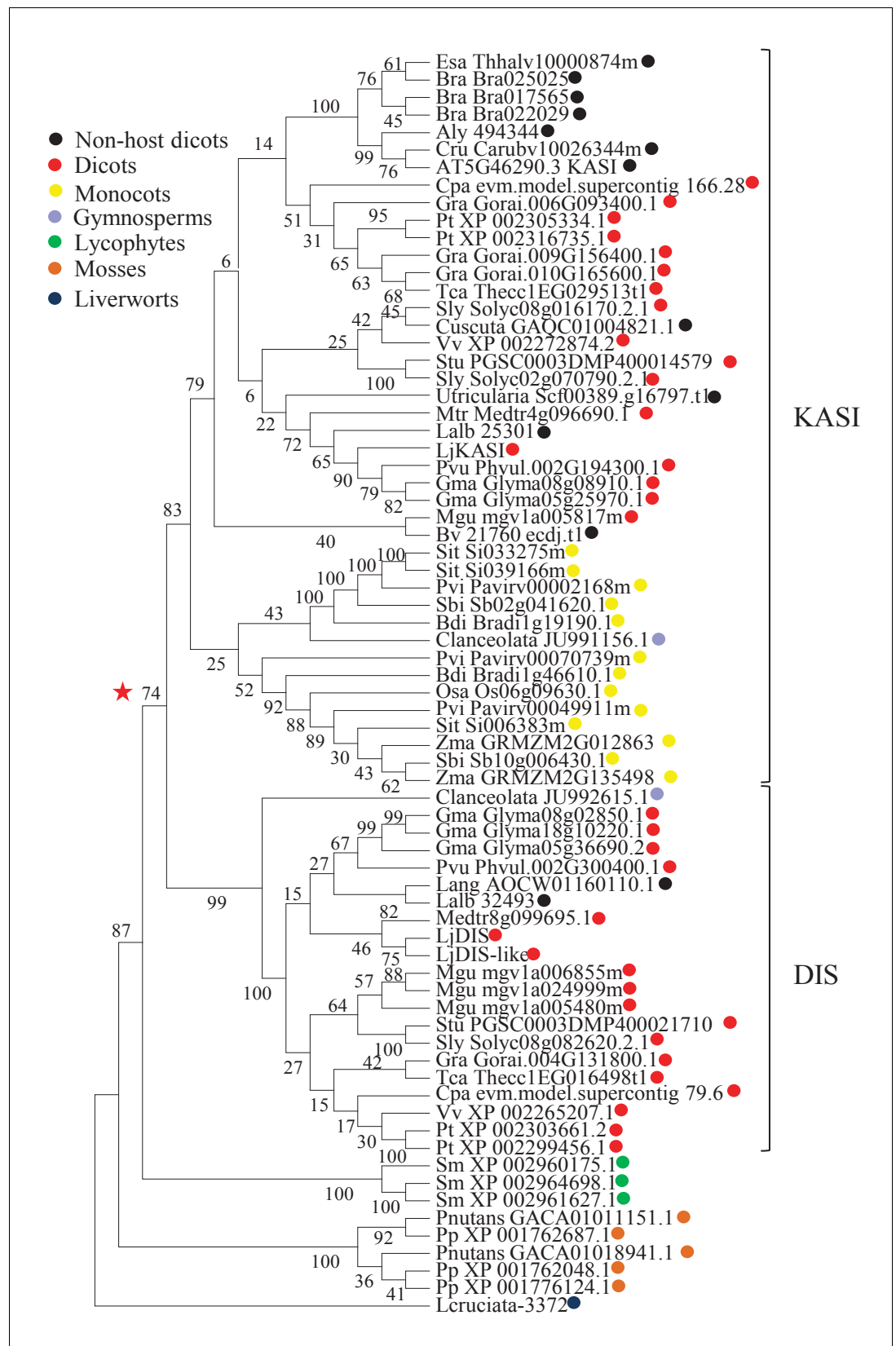


**Figure 3.** Phylogenetic tree of KASI proteins in land plants. Protein sequences were aligned using MAFFT. Phylogenetic trees were generated by neighbor-joining implemented in MEGA5 (Tamura et al., 2011). Partial gap Figure 3 continued on next page

Figure 3 continued

deletion (95%) was used together with the JTT substitution model. Bootstrap values were calculated using 500 replicates. DIS likely originated before the angiosperm divergence (red star).

DOI: [10.7554/eLife.29107.016](https://doi.org/10.7554/eLife.29107.016)

The following source data and figure supplements are available for figure 3:

**Source data 1.** Accession numbers for protein sequences used in the phylogenetic tree.

DOI: [10.7554/eLife.29107.017](https://doi.org/10.7554/eLife.29107.017)

**Figure supplement 1.** Transcript accumulation of *KASI* and *RAM2* genes.

DOI: [10.7554/eLife.29107.018](https://doi.org/10.7554/eLife.29107.018)

**Figure supplement 2.** Shoot phenotypes of *dis* and *ram2* mutants.

DOI: [10.7554/eLife.29107.019](https://doi.org/10.7554/eLife.29107.019)

**Figure supplement 3.** Genomic comparison of the *DIS* locus in host and non-host species.

DOI: [10.7554/eLife.29107.020](https://doi.org/10.7554/eLife.29107.020)

## The AM-specific increase in 16:0 and 16:1 $\omega$ 5 FA containing lipids is abolished in the *dis* mutant

To characterize the role of DIS in determining the lipid composition of non-colonized and colonized roots we quantified triacylglycerols (TAGs), diacylglycerols (DAGs), galactolipids and phospholipids in wild-type and *dis-1*. The lipid profile of colonized roots contains both plant and fungal lipids, however using the fungal marker FA 16:1 $\omega$ 5 and previous data on fungus-specific lipids (Wewer et al., 2014), many fungal lipids can be clearly distinguished from plant lipids. The lipid profile of non-colonized roots was not affected by the *dis-1* mutation. However, the strong and significant increase of 16:0 and 16:1 (most probably fungus-specific 16:1 $\omega$ 5) containing TAGs, which is characteristic for colonization of wild-type roots (Wewer et al., 2014) was abolished in *dis-1* (Figure 5A–D, Figure 5—figure supplement 1B). Also, AM- and fungus-specific DAG and phospholipid molecular species were enhanced in colonized wild-type roots but not in colonized *dis-1* roots (Figure 5—figure supplements 1A and 2). In contrast, galactolipids were not affected by root colonization or genotype (Figure 5—figure supplement 3). In summary, DIS affects the glycerolipid and phospholipid profile of colonized *L. japonicus* roots and does not interfere with lipid accumulation in the non-colonized state. Most lipids affected by the *DIS* mutation are fungus-specific and therefore reflect the amount of root colonization and of fungal lipid-containing vesicles. However, since the root lipid profile is hardly affected, absence of FA elongation by DIS was the cause of reduced lipid accumulation and root colonization.

## RAM1, DIS, RAM2 and STR are required for accumulation of AM signature lipids

Similar to *dis* and *ram2* *L. japonicus* mutants in the ABCG half-transporter STR and the GRAS protein RAM1 are affected in arbuscule branching (Kojima et al., 2014; Pimprikar et al., 2016; Xue et al., 2015), quantitative root colonization and formation of lipid-containing fungal vesicles (Figure 5—figure supplement 4). Moreover, the AM-dependent transcriptional activation of *DIS* and *KASIII*, the latter of which is a single copy gene in *L. japonicus* and produces precursors for DIS-activity by catalyzing FA chain elongation from C2 to C4, was absent from *ram1* mutants (Figure 6). In contrast, induction of the single copy gene *KASII*, which elongates fatty acyl chains from C16 to C18 was not hampered by *RAM1* deficiency. Thus, *RAM1* may play an important role in the regulation of lipid biosynthesis in arbuscocytes, since it also mediates expression of *RAM2* and *STR* (Gobbato et al., 2012; Park et al., 2015; Pimprikar et al., 2016; Luginbuehl et al., 2017).

We hypothesized that *RAM1*, *DIS*, *RAM2* and *STR* form a specific operational unit for lipid biosynthesis and transport in arbuscocytes. Therefore, we directly compared their impact on the AM-specific root lipid profile and measured galactolipids, phospholipids, TAGs and also total and free fatty acids in colonized roots of *ram1*, *dis*, *ram2*, *str* mutants and wild-type in parallel. Consistent with our previous observation in *dis-1*, galactolipid accumulation was similar in colonized roots of wild-type and all mutants (Figure 5—figure supplement 3C–D). In contrast, total 16:0 FAs (FAMES) as well as 16:1 and 18:1 (likely 18:1 $\omega$ 7 FA of fungal origin) FAs were strongly reduced in all colonized mutants compared to the corresponding wild-type. Free FAs showed a similar pattern except for 18:1 FAs

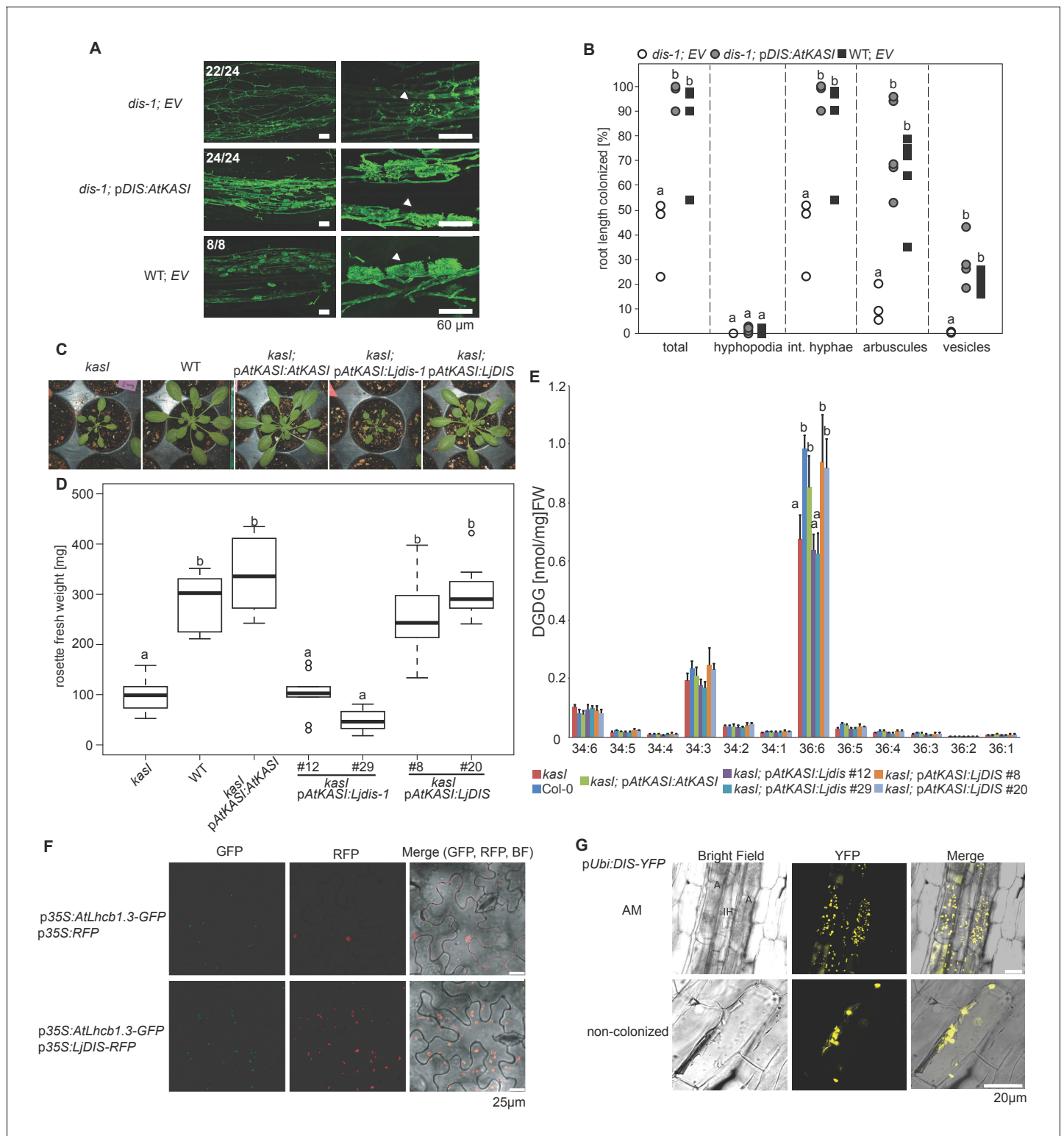


**Figure 4.** DIS function is equivalent to a canonical KASI. (A) Microscopic AM phenotype of transgenic *dis-1* mutant and wild-type hairy roots transformed with either an empty vector (EV) or the *Arabidopsis* KASI gene fused to the *L. japonicus* DIS promoter. White arrowheads indicate arbuscules. (B) Quantification of AM colonization in transgenic roots of *dis-1* transformed with EV (open circles), *dis-1* transformed with pDIS-AtKASI (grey circles) and wild-type transformed with EV (black squares). int. hyphae, intraradical hyphae. Different letters indicate significant differences (ANOVA; posthoc Tukey; n = 15; p ≤ 0.001) among genotypes for each fungal structure separately. F<sub>2,12</sub> = 0.809 (total and intraradical hyphae), F<sub>2,12</sub> = 43.65 (arbuscules), F<sub>2,12</sub> = 0.0568 (vesicles). (C) Rosettes of *Arabidopsis*, *kasl* mutant, Col-0 wild-type plants and *kasl* mutant plants transformed either with empty vector (EV) or the *Arabidopsis* KASI gene fused to the *L. japonicus* DIS promoter. (D) Rosette fresh weight of *Arabidopsis* plants. (E) DGDG levels in roots of *Arabidopsis* plants. (F) Localization of GFP and RFP in roots of *Arabidopsis* plants. (G) Localization of YFP in roots of *Arabidopsis* plants. Figure 4 continued on next page

Figure 4 continued

with the native *AtKASI* gene, the *dis-1* mutant or the *DIS* wild-type gene driven by the *Arabidopsis KASI* promoter at 31 days post planting. (D) Rosette fresh weight of *kasI* mutant, Col-0 wild-type plants, one transgenic *pAtKASI:AtKASI* complementation line (Wu and Xue, 2010) and two independent transgenic lines each of *kasI* mutant plants transformed either with the *dis-1* mutant or the *DIS* wild-type gene driven by the *Arabidopsis KASI* promoter at 31 days post planting. Different letters indicate significant differences (ANOVA; posthoc Tukey;  $n = 70$ ;  $p \leq 0.001$ ;  $F_{6,63} = 34.06$ ) among genotypes. (E) Q-TOF MS/MS analysis of absolute amount of digalactosyldiacylglycerols (DGDG) containing acyl chains of 16:x + 18:x(34:x DGDG) or di18:x(36:x DGDG) derived from total leaf lipids of the different *Arabidopsis* lines. Different letters indicate significant differences (ANOVA; posthoc Tukey;  $n = 32$ ; ( $p \leq 0.05$ ,  $F_{6,25} = 14.48$  (36:6)). (F) Subcellular localization of DIS in transiently transformed *Nicotiana benthamiana* leaves. Free RFP localizes to the nucleus and cytoplasm (upper panel). RFP fused to DIS co-localizes with the *Arabidopsis* light harvesting complex protein AtLHCB1.3-GFP in chloroplasts (lower panel). (G) Subcellular localization in plastids of DIS-YFP expressed under the control of the *L. japonicus Ubiquitin* promoter in *R. irregularis* colonized (upper panel) and non-colonized (lower panel) *L. japonicus* root cortex cells. BF, bright field; IH, intercellular hypha; A, arbuscule. DOI: 10.7554/eLife.29107.021

(Figure 5—figure supplement 5). Also for TAGs and phospholipids, AMF-specific molecular species and 16:0 FA containing molecular species were strongly reduced in all mutants (Figure 5E–H, Figure 5—figure supplements 6–11). However, the two allelic *ram2* mutants formed an exception. They specifically over-accumulated 16:0-16:0 FA-containing phospholipids in particular 32:0 PA and 32:0-PC but also to a smaller extent 32:0-PE and 32:0-PI (Figure 5—figure supplements 6–10). A similar pattern was observed for tri-16:0 TAGs (Figure 5F). This suggests that RAM2 acts downstream of DIS in a biosynthetic pathway and uses the 16:0 FAs synthesized by DIS in arbuscules as substrates. In the absence of functional RAM2 the FA products of DIS, are probably redirected into phospholipid biosynthesis and storage lipid biosynthesis via PA and PC (Li-Beisson et al., 2010) leading to the observed higher accumulation of 16:0 FA containing lipid species in *ram2* mutants. This higher accumulation of specific lipids did not correlate with colonization levels in *ram2* mutants (Figure 5—figure supplement 4) confirming that reduced colonization levels are not the primary cause for altered lipid profiles in the colonized mutant roots. Instead, defective AM-specific lipid biosynthesis in the mutants more likely impairs fungal development.

### The abundance of 16:0 $\beta$ -monoacyl-glycerol is reduced in all mutants

The first step in TAG and phospholipid production after FA biosynthesis is the esterification of FAs with glycerol by GPATs in the plastid or endoplasmic reticulum to produce  $\alpha$ -MAGs (sn1/3-MAGs, Li-Beisson et al., 2010). RAM2 is predicted to produce a different type of glycerolipid  $\beta$ -MAG (sn2-MAG) with a preference towards 16:0 and 18:1 FAs (Yang et al., 2010; Wang et al., 2012; Yang et al., 2012). To examine the role of RAM2 in MAG biosynthesis, we quantified  $\alpha$ -MAG and  $\beta$ -MAG species in colonized roots of wild-type and all mutants. The abundance of  $\beta$ -MAGs was generally lower than that of  $\alpha$ -MAGs (Figure 7). The amount of most  $\alpha$ -MAG species did not differ among the genotypes. Only the fungus-specific 16:1 and 18:1 $\omega$ 7  $\alpha$ -MAGs were reduced in all mutants reflecting the lower fungal biomass (Figure 7A). Fungus-specific  $\beta$ -MAGs with 16:1 and 18:1 $\omega$ 7 acyl groups were not detected and most  $\beta$ -MAG molecular species accumulated to similar levels in all genotypes. Exclusively the levels of 16:0  $\beta$ -MAGs were significantly lower in all mutants as compared to the corresponding wild-type roots (Figure 7B). This supports a role of RAM2 in 16:0  $\beta$ -MAG synthesis during AM and a role of DIS in providing 16:0 FA precursors for RAM2 activity. A low accumulation, of 16:0  $\beta$ -MAGs in *ram1* mutants is consistent with RAM1's role in regulating the FA and lipid biosynthesis genes (Figure 6) (Gobbato et al., 2012; Pimprikar et al., 2016). In *str* 16:0  $\beta$ -MAGs likely did not accumulate because of reduced RAM2 expression in *str* roots due to low root length colonization and/or a regulatory feedback loop (Bravo et al., 2017).

### DIS, RAM2 and STR are required for transfer of $^{13}\text{C}$ label from plant to fungus

In plants,  $\beta$ -MAGs serve as precursors for cutin polymers at the surface of aerial organs (Yang et al., 2012; Yeats et al., 2012). For their use in membrane or storage lipid biosynthesis they first need to be isomerized to  $\alpha$ -MAGs (Li-Beisson et al., 2010). The recruitment of a GPAT6 (RAM2) instead of a  $\alpha$ -MAG-producing GPAT for AM-specific lipid synthesis supports the idea that RAM2-products are destined for something else than membrane biosynthesis of the host cell. Since AM fungal genomes lack genes encoding cytosolic FA synthase subunits (Wewer et al., 2014; Ropars et al., 2016;

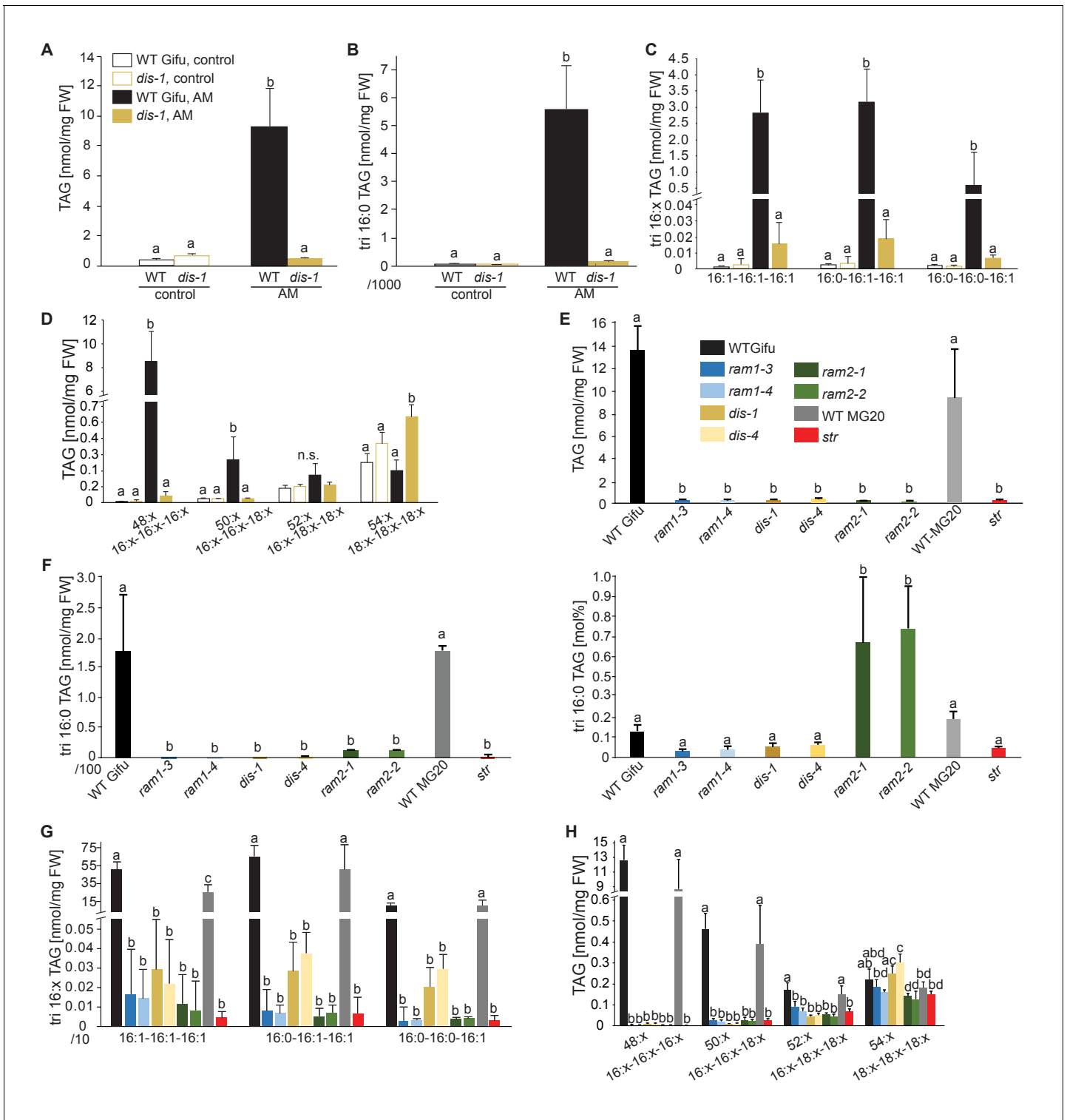


**Figure 5.** Lack of characteristic accumulation of triacylglycerols in AM-defective mutants. (A-D) Quantitative accumulation of (A) total triacylglycerols, (B) tri16:0-triacylglycerol (C) tri16:x-triacylglycerols and (D) of triacylglycerols harbouring 16:x and 18:x FA-chains in non-colonized and *R. irregularis* colonized wild-type and *dis-1* roots. Different letters indicate significant differences (ANOVA; posthoc Tukey) (A): n = 18; p<0.001; F<sub>3,14</sub> = 68.16. (B): n = 18; p<0.001; F<sub>3,14</sub> = 68.48. (C): n = 19; p<0.01, F<sub>3,15</sub> = 7.851 (16:1-16:1-16:1); p<0.001, F<sub>3,15</sub> = 14.52 (16:0-16:1-16:1); p<0.001, F<sub>3,15</sub> = 39.22 (16:0-16:0-16:1). (D): n = 19; p<0.001, F<sub>3,15</sub> = 12.15 (48:x), F<sub>3,15</sub> = 15.56 (50:x); p<0.01, F<sub>3,15</sub> = 22.93 (54:x). (E-G) Quantitative accumulation of (E) total triacylglycerols, (F) tri16:0-triacylglycerols, (G) tri16:x-triacylglycerols and (H) of triacylglycerols harbouring 16:x and 18:x FA-chains in colonized roots of *L. japonicus* wild-type Gifu, wild-type MG-20 and arbuscule-defective mutants. Different letters indicate significant differences (ANOVA; posthoc Tukey). Figure 5 continued on next page

Figure 5 continued

(E):  $n = 40$ ;  $p \leq 0.001$ ;  $F_{8,31} = 38.42$ . (F) Left: absolute tri16:0 TAG content:  $n = 40$ ;  $p \leq 0.001$ ;  $F_{8,31} = 19.05$ . Right: tri16:0 TAG proportion among all TAGs,  $n = 40$ ;  $p \leq 0.001$ ;  $F_{8,31} = 14.21$ . (G):  $p \leq 0.001$ ;  $n = 41$ ,  $F_{8,32} = 86.16$  (16:1-16:1-16:1);  $n = 39$ ,  $F_{8,30} = 24.16$  (16:0-16:1-16:1);  $n = 40$ ,  $F_{8,31} = 17.67$  (16:0-16:0-16:1). (H):  $n = 40$ ;  $p \leq 0.001$ ,  $F_{8,31} = 39.26$  (48:x),  $F_{8,31} = 28.93$  (50:x);  $p \leq 0.01$ ,  $F_{8,31} = 19.78$  (52:x);  $p \leq 0.05$ ,  $F_{8,31} = 13.77$  (54:x). (A-H) Bars represent means  $\pm$  standard deviation (SD) of 3–5 biological replicates.

DOI: [10.7554/eLife.29107.022](https://doi.org/10.7554/eLife.29107.022)

The following source data and figure supplements are available for figure 5:

**Source data 1.** Raw data for lipid profiles in **Figure 5** and **Figure 5—figure supplements 1–3** and **5–11**.

DOI: [10.7554/eLife.29107.023](https://doi.org/10.7554/eLife.29107.023)

**Figure supplement 1.** Diacylglycerol (DAG) and triacylglycerol (TAG) profiles of *L. japonicus* WT and *dis-1* control and AM roots.

DOI: [10.7554/eLife.29107.024](https://doi.org/10.7554/eLife.29107.024)

**Figure supplement 2.** Profiles of phospholipids in non-colonized and colonized *L. japonicus* WT Gifu and *dis-1* roots.

DOI: [10.7554/eLife.29107.025](https://doi.org/10.7554/eLife.29107.025)

**Figure supplement 3.** MGDG and DGDG profiles do not differ among *L. japonicus* wild-type and mutant roots.

DOI: [10.7554/eLife.29107.026](https://doi.org/10.7554/eLife.29107.026)

**Figure supplement 4.** All arbuscule-deficient mutants show reduced root length colonization.

DOI: [10.7554/eLife.29107.027](https://doi.org/10.7554/eLife.29107.027)

**Figure supplement 5.** Total fatty acid and free fatty acid profiles of colonized *L. japonicus* WT and AM-defective mutant roots.

DOI: [10.7554/eLife.29107.028](https://doi.org/10.7554/eLife.29107.028)

**Figure supplement 6.** Triacylglycerol (TAG) profiles of colonized *L. japonicus* WT and AM-defective mutant roots.

DOI: [10.7554/eLife.29107.029](https://doi.org/10.7554/eLife.29107.029)

**Figure supplement 7.** Phosphatidic acid (PA) profiles in *L. japonicus* WT and AM-defective mutants.

DOI: [10.7554/eLife.29107.030](https://doi.org/10.7554/eLife.29107.030)

**Figure supplement 8.** Profile of phosphatidylcholines (PC) in *L. japonicus* WT and AM-defective mutants.

DOI: [10.7554/eLife.29107.031](https://doi.org/10.7554/eLife.29107.031)

**Figure supplement 9.** Phosphatidylethanolamine (PE) profile in *L. japonicus* WT and AM-defective mutants.

DOI: [10.7554/eLife.29107.032](https://doi.org/10.7554/eLife.29107.032)

**Figure supplement 10.** Phosphatidylinositol (PI) profile in *L. japonicus* WT and AM-defective mutants.

DOI: [10.7554/eLife.29107.033](https://doi.org/10.7554/eLife.29107.033)

**Figure supplement 11.** Phosphatidylserine (PS) profile in *L. japonicus* WT and AM-defective mutants.

DOI: [10.7554/eLife.29107.034](https://doi.org/10.7554/eLife.29107.034)

*Tang et al., 2016*) we hypothesized that 16:0  $\beta$ -MAGs synthesized by DIS- and RAM2 are predominantly delivered to the fungus. To test this hypothesis, we examined lipid transfer by FA isotopolog profiling. Isotopologs are molecules that differ only in their isotopic composition. For isotopolog profiling an organism is fed with a heavy isotope labelled precursor metabolite. Subsequently the labelled isotopolog composition of metabolic products is analyzed. The resulting characteristic isotopolog pattern yields information about metabolic pathways and fluxes (*Ahmed et al., 2014*).

We could not detect fungus-specific 16:1 $\omega$ 5  $\beta$ -MAGs in colonized roots (**Figure 7B**). Therefore, we reasoned that either a downstream metabolite of  $\beta$ -MAG is transported to the fungus, or alternatively,  $\beta$ -MAG is rapidly metabolized in the fungus prior to desaturation of the 16:0 acyl residue. Since the transported FA groups can be used by the fungus for synthesizing a number of different lipids, we focused on total 16:0 FA methyl esters (FAMES, subsequently called FAs for simplicity) and 16:1 $\omega$ 1 FAMES as markers for lipid transfer. We fed *L. japonicus* wild-type, *dis-1*, *ram2-1* and *str* with [U- $^{13}\text{C}_6$ ]glucose and then measured the isotopolog composition of 16:0 FAs and 16:1 $\omega$ 5 FAs in *L. japonicus* roots and in associated extraradical fungal mycelium with spores. To generate sufficient hyphal material for our measurements the fungus was pre-grown on split Petri dishes in presence of a carrot hairy root system as nurse plant (**Figure 8—figure supplement 1**). Once the fungal mycelium had covered the plate, *L. japonicus* seedlings were added to the plate on the side opposing the carrot root. During the whole experiment, the fungus was simultaneously supported by the carrot hairy root and the *L. japonicus* seedling. Once the *L. japonicus* roots had been colonized, labelled glucose was added to the side containing *L. japonicus*. After an additional week, FAs were esterified and extracted from colonized *L. japonicus* roots and from the associated extraradical mycelium and the total amount of  $^{13}\text{C}$  labelled 16:0 and 16:1 $\omega$ 5 FAs as well as their isotopolog composition was determined. In *L. japonicus* wild-type  $^{13}\text{C}$ -labelled 16:0 and 16:1 $\omega$ 5 FAs were detected in colonized

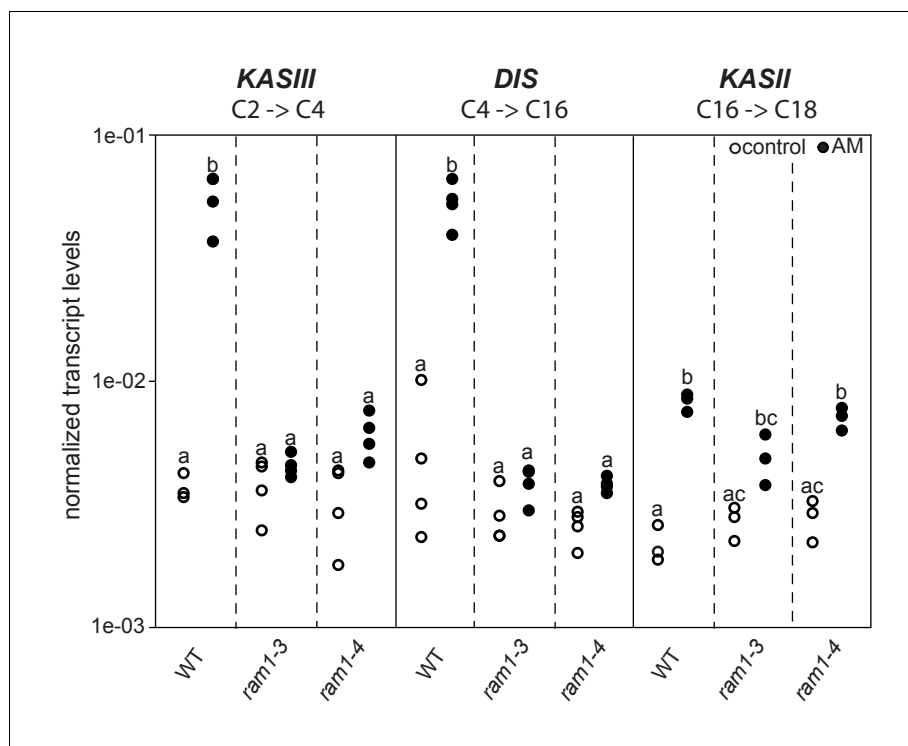


**Figure 6.** Loss of *RAM1* affects AM-dependent induction of *KASIII* and *DIS*. (A) *RAM1* effects on AM-dependent induction of *KASIII* and *DIS*, which catalyze 16:0 FA biosynthesis, and absence of effects on *KASII*. According to BLAST analysis via Kazusa (<http://www.kazusa.or.jp/lotus/>) and NCBI (<http://www.ncbi.nlm.nih.gov/>) *KASIII* and *KASII* are single copy genes in *L.japonicus*. Transcript accumulation of *KASIII*, *DIS* and *KASII* in non-colonized (open circles) and colonized (black circles) roots of Gifu WT, *ram1-3* and *ram1-4*. Different letters indicate different statistical groups (ANOVA; posthoc Tukey;  $p \leq 0.001$ ;  $n = 23$   $F_{5,12} = 65.04$ (*KASIII*);  $n = 24$   $F_{5,18} = 54.42$  (*DIS*);  $n = 18$   $F_{5,12} = 33.11$  (*KASII*)). Transcript accumulation was determined by qRT-PCR and the housekeeping gene *Ubiquitin10* was used for normalization. AM plants were inoculated with *R. irregularis* and harvested 5 wpi. DOI: 10.7554/eLife.29107.035

roots as well as in the extraradical fungal mycelium (Figure 8A–B, Figure 8—figure supplement 2A–B), indicating that  $^{13}\text{C}$ -labelled organic compounds were transferred from the root to the fungus. No labelled FAs were detected in the fungal mycelium when the fungus was supplied with  $[\text{U-}^{13}\text{C}_6]$  glucose in absence of a plant host (Figure 8A–B, Figure 8—figure supplements 2A–B,3), indicating that the fungus itself could not metabolize labelled glucose to synthesize FAs. The three mutants incorporated  $^{13}\text{C}$  into 16:0 FAs at similar amounts as the wild-type but hardly any  $^{13}\text{C}$  was transferred to the fungus (Figure 8A–B, Figure 8—figure supplement 2A–B).

### Host plants determine the isotopolog pattern of fungal FAs

Remarkably, the isotopolog profile of 16:0 FAs was close to identical between colonized *L. japonicus* roots and the connected extraradical mycelium, for 11 independent samples of wild-type Gifu (Figure 8C–D, Figure 8—figure supplement 4) and for 5 independent samples of wild-type MG20 (Figure 8—figure supplement 2C–D). Moreover, the isotopolog profile of fungus-specific 16:1 $\omega$ 5 FAs mirrored the profile of 16:0 FAs (Figure 8C, Figure 8—figure supplements 2,4). Pattern conservation between root and associated extraradical mycelium occurred independently of pattern variation among individual samples. Since the fungus does not incorporate  $^{13}\text{C}$  into the analyzed FAs in the absence of the plant (Figure 8A–B, Figure 8—figure supplement 2A–B) this conserved pattern demonstrates transfer of 16:0 FA-containing lipids from the host plant to the fungus because the plant determines the isotopolog pattern of fungal 16:0 and 16:1 $\omega$ 5 FAs. The 16:0 FA isotopolog pattern of colonized *dis-1*, *ram2* and *str* mutant roots resembled the wild-type profile, indicating intact uptake and metabolism of labelled glucose. However, the 16:0 FA isotopolog pattern of the

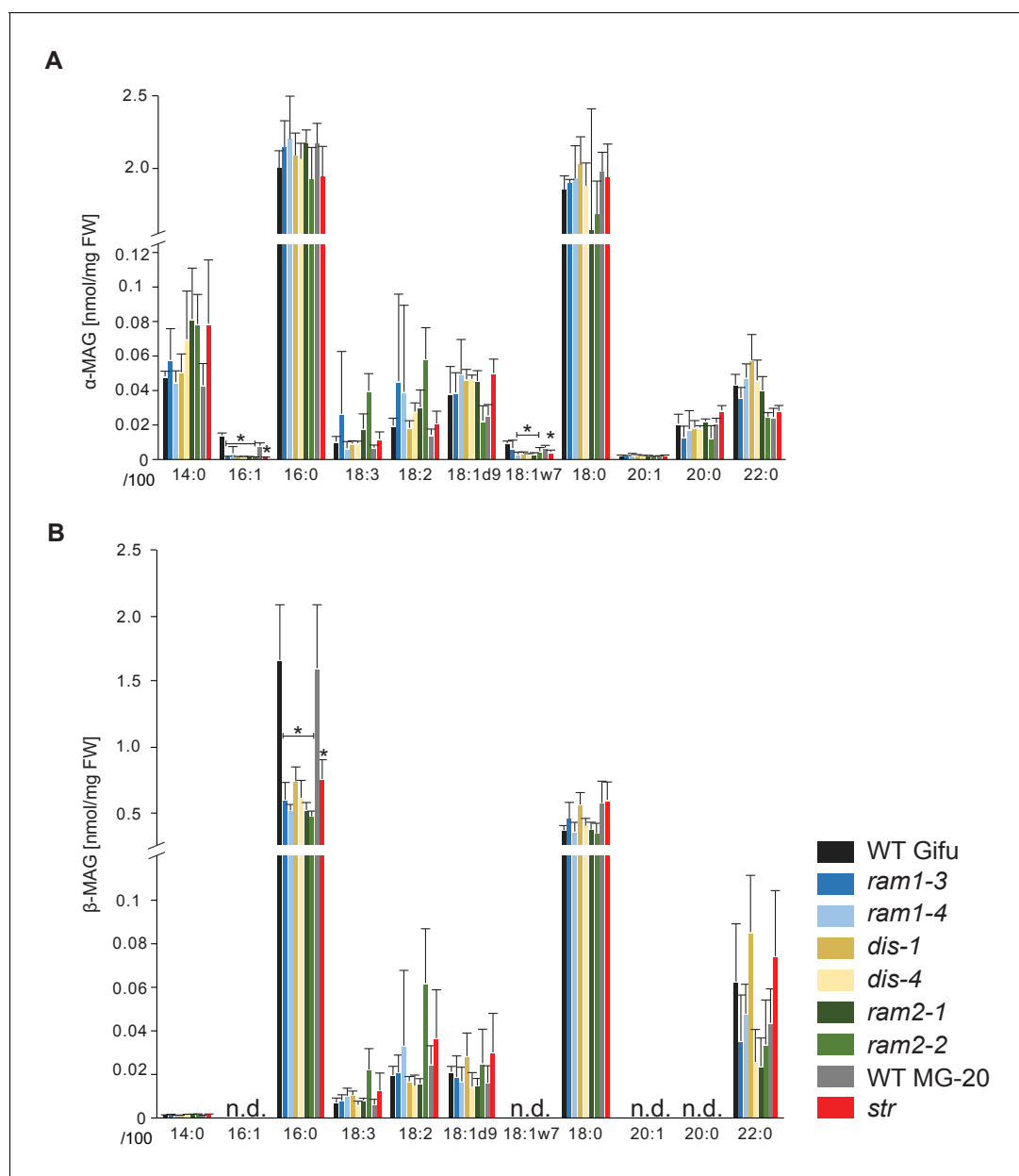


**Figure 7.** *sn-1* monoacylglycerol ( $\alpha$ -MAG) and *sn-2* monoacylglycerol ( $\beta$ -MAG) profiles of colonized *L. japonicus* wild-type and AM-defective mutant roots. (A) Total amounts of  $\alpha$ -MAG molecular species in the different genotypes. (B) Total amounts of  $\beta$ -MAG molecular species in the different genotypes. 16:0  $\beta$ -MAG levels are significantly reduced in all mutant lines compared to the respective wild-type. (A–B) Bars represent means  $\pm$  standard deviation (SD) of 3–5 biological replicates. Black asterisk indicates significant difference of mutants vs. wild-type according to Student's t-test,  $p < 0.05$ .

DOI: 10.7554/eLife.29107.036

extraradical mycelium associated with mutant roots and the fungal 16:1 $\omega$ 5 FA profile inside and outside the roots differed strongly from the 16:0 FA profile of the mutant host roots (Figure 8C, Figure 8—figure supplements 2C,4), consistent with very low FA transfer from the mutant plants to the fungus. The losses in isotopolog profile conservation between plant and fungal FAs in the mutants likely result from dilution of labelled FAs by unlabeled FAs from the carrot hairy root (Figure 8D, Figure 8—figure supplements 1 and 2D) and/or from biases due to quantification of FAs at the detection limit.

To confirm that the plant determines the fungal FA isotopolog pattern we switched plant system and profiled isotopologs after labelling carrot root organ culture (ROC) in the absence of *L.*

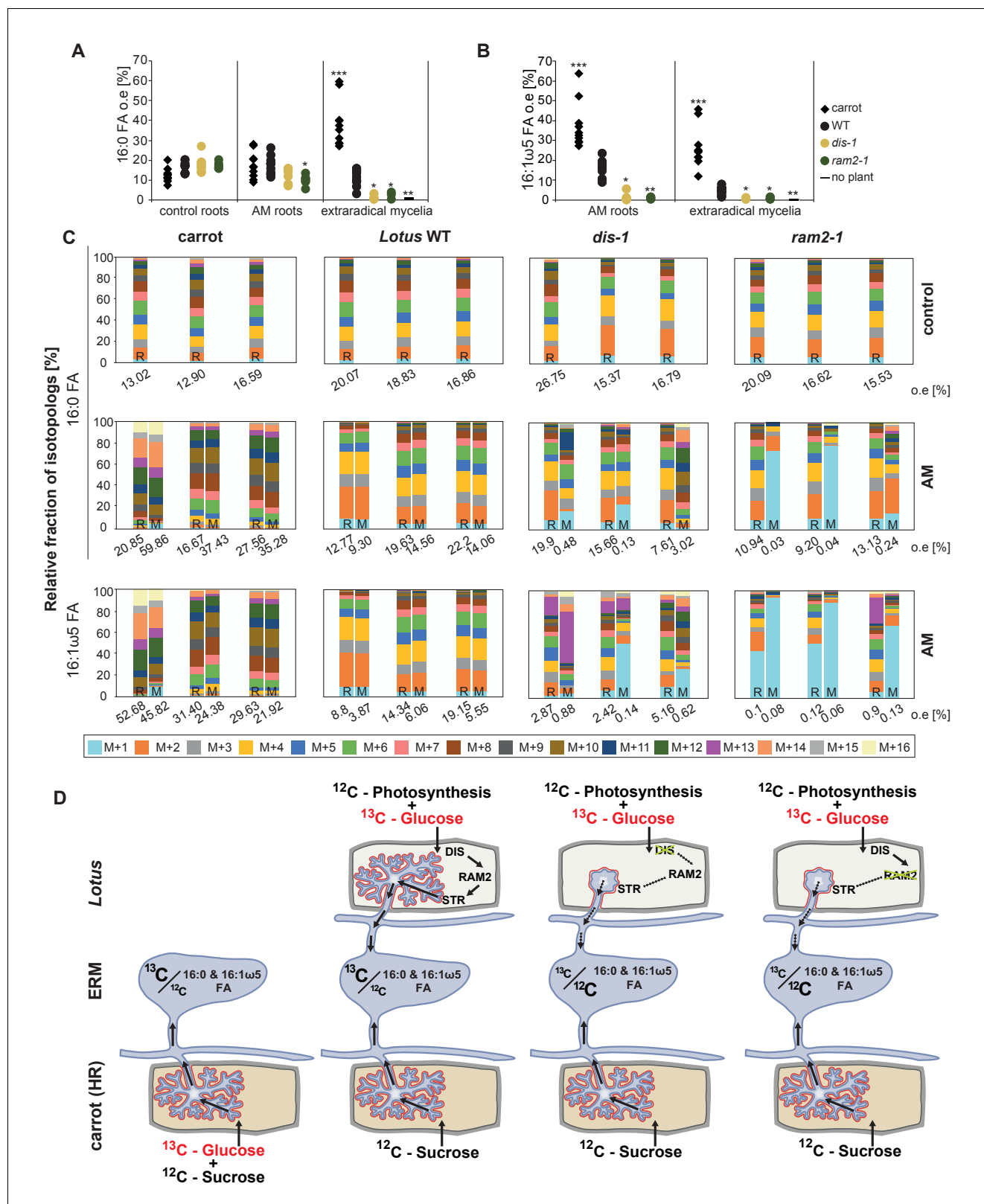


**Figure 8.** Isotopolog profiling indicates lipid transfer from plant to fungus. (A–B) Overall excess (o.e.) <sup>13</sup>C over air concentration in 16:0 FAs (A) and in 16:1ω5 FAs (B) detected in non-colonized (only 16:0 FAs) and colonized carrot, *L. japonicus* wild-type, *dis-1*, *ram2-1* roots and in the extraradical mycelium of *R. irregularis*. P values were generated by ANOVA using the Dunnett Test for multiple comparisons to *L. japonicus* wild-type (n = 29 (16:0 control roots); n = 33 (16:0 root AM); n = 39 (16:0 extraradical mycelium); n = 33 (16:1ω5 root AM); n = 39 (16:1ω5 extraradical mycelium), \*\*\*p<0.001, Figure 8 continued on next page

Figure 8 continued

\*\* $p < 0.01$ , \* $p < 0.05$ ). (C) Relative fraction of  $^{13}\text{C}$  isotopologs for 16:0 FAs of three replicates of carrot, *L. japonicus* WT Gifu, *dis-1*, *ram2-1* in control roots (upper panel) and AM roots and each of the associated *R. irregularis* extraradical mycelia with spores (middle panel) and 16:1 $\omega$ 5 FAs in AM roots and extraradical mycelia with spores (lower panel). Individual bars and double bars indicate individual samples. Values from roots are indicated by 'R' and from fungal extraradical mycelia with spores by 'M'. For carrot and *L. japonicus* WT the  $^{13}\text{C}$  labelling pattern of 16:0 and 16:1 $\omega$ 5 FAs in the plant is recapitulated in the fungal extraradical mycelium. Extraradical mycelium associated with *dis-1* and *ram2-1* does not mirror these patterns. Compare bars for AM roots and extraradical mycelium side by side. Black numbers indicate  $^{13}\text{C}$  o. e. for individual samples. Colors indicate  $^{13}\text{C}$ -isotopologs carrying one, two, three, etc.  $^{13}\text{C}$ -atoms (M + 1, M + 2, M + 3, etc.). (D) Schematic and simplified illustration of carbon flow and  $^{12}\text{C}$  vs.  $^{13}\text{C}$ -carbon contribution to plant lipid metabolism and transport to the fungus in the two-compartment cultivation setup used for isotope labelling. Carbohydrate metabolism and transport is omitted for simplicity. ERM, extraradical mycelium.

DOI: [10.7554/eLife.29107.037](https://doi.org/10.7554/eLife.29107.037)

The following source data and figure supplements are available for figure 8:

**Source data 1.** Raw data for isotopolog profiles in **Figure 8** and **Figure 8—figure supplements 2,4**.

DOI: [10.7554/eLife.29107.038](https://doi.org/10.7554/eLife.29107.038)

**Figure supplement 1.** Two-compartment cultivation setup used for labelling experiments.

DOI: [10.7554/eLife.29107.039](https://doi.org/10.7554/eLife.29107.039)

**Figure supplement 2.** Isotopolog profiles of wild-type MG20 and *str*.

DOI: [10.7554/eLife.29107.040](https://doi.org/10.7554/eLife.29107.040)

**Figure supplement 3.** Proportion of 16:0 and 16:1 $\omega$ 5 FA containing only non-labelled  $^{12}\text{C}$  in plant and fungal tissue.

DOI: [10.7554/eLife.29107.041](https://doi.org/10.7554/eLife.29107.041)

**Figure supplement 4.** Isotopolog profiles of additional samples.

DOI: [10.7554/eLife.29107.042](https://doi.org/10.7554/eLife.29107.042)

*japonicus* seedlings (**Figure 8D**, **Figure 8—figure supplement 1**). In these root organ cultures, sugar uptake from the medium does not compete with photosynthesis, as in whole seedlings. Additionally, the carrot roots explore a larger surface of the Petri dish, increasing access to substances in the nutrient medium. Consequently, and likely because of increased uptake of labelled glucose from the medium, the isotopolog pattern of carrot ROCs differed from *Lotus* and was shifted towards more highly labeled 16:0 FA isotopologs. This fingerprint was again recapitulated in the extraradical fungal mycelium as well as in fungus-specific 16:1 $\omega$ 5 FAs inside and outside the root for 10 independent samples (**Figure 8C**, **Figure 8—figure supplement 4**). These data provide strong support for direct transfer of a 16:0 FA containing lipid from plants to AMF (**Figure 9**).

## Discussion

Here we identified *DIS* and *RAM2*, two AM-specific paralogs of the lipid biosynthesis genes *KASI* and *GPAT6* using forward genetics in *Lotus japonicus*. The *dis* and *ram2* mutants enabled us to demonstrate lipid transfer from plants to AMF using isotopolog profiling.

During AM symbiosis, an array of lipid biosynthesis genes is induced in arbuscocytes (**Gaude et al., 2012a, 2012b**), indicating a large demand for lipids in these cells. Indeed, two genes encoding lipid biosynthesis enzymes, the thioesterase *FatM* and the *GPAT6* *RAM2*, have previously been shown to be required for arbuscule branching in *M. truncatula* (**Wang et al., 2012; Bravo et al., 2017; Jiang et al., 2017**). Both enzymes have a substrate preference for 16:0 FAs (**Salas and Ohlrogge, 2002; Yang et al., 2012; Bravo et al., 2017**) and, consistent with this, we and others observed that colonized *ram2* mutant roots over-accumulate 16:0 FA containing phospholipids and TAGs (**Figure 7**, [**Bravo et al., 2017**]), indicating re-channeling of superfluous 16:0 FAs in the absence of *RAM2* function and placing *RAM2* downstream of *FatM* (**Figure 9**).

Our discovery of *DIS*, a novel and AM-specific *KASI* gene, now provides evidence for the enzyme which synthesizes these 16:0 FAs in arbuscocytes. The arbuscule phenotype, as well as the lipid profile of colonized *dis* mutants is very similar to *fatm* and *ram2* mutants except for the accumulation of 16:0 FA-containing lipids in *ram2* (**Figure 1**, **Figure 5** and all figure supplements), consistent with the predicted function. Together, this strongly suggests that *DIS*, *FatM* and *RAM2* act in the same lipid biosynthesis pathway, which is specifically and cell-autonomously induced when a resting root cortex cell differentiates into an arbuscocyte (**Figure 2A–B**, **Figure 9**, [**Bravo et al., 2017**]). Interestingly, *DIS* was exclusively found in genomes of AM-competent dicotyledons and a gymnosperm (**Figure 3**). This implies that *DIS* has been lost at the split of the mono- from dicotyledons. Despite the

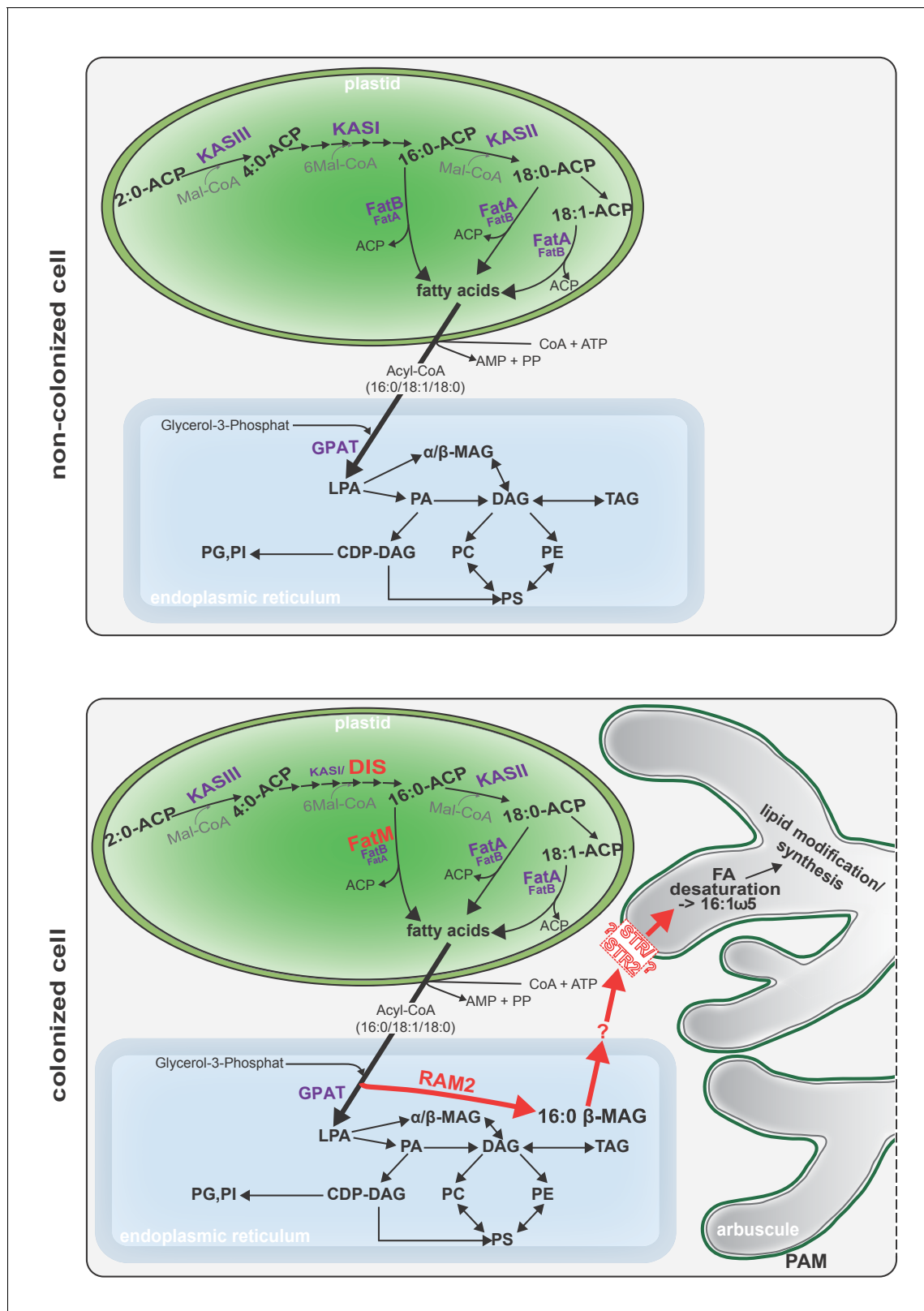


**Figure 9.** Schematic representation of plant fatty acid and lipid biosynthesis in a non-colonized root cell and a root cell colonized by an arbuscule. In non-colonized cells FAs are synthesized in the plastid, bound via esterification to glycerol to produce LPA in the ER, where further lipid synthesis and modification take place. Upon arbuscule formation AM-specific FA and lipid biosynthesis genes encoding DIS, FatM and RAM2 are activated to synthesize specifically high amounts of 16:0 FAs and 16:0-β-MAGs or further modified lipids (this work and **Bravo et al., 2017**). These are transported

Figure 9 continued on next page

Figure 9 continued

from the plant cell to the fungus. The PAM-localized ABCG transporter STR/STR2 is a hypothetical candidate for lipid transport across the PAM. Desaturation of 16:0 FAs by fungal enzymes (Wewer et al., 2014) leads to accumulation of lipids containing specific 16:1 $\omega$ 5 FAs. Mal-CoA, Malonyl-Coenzyme A; FA, fatty acid; KAS,  $\beta$ -keto-acyl ACP synthase; GPAT, Glycerol-3-phosphate acyl transferase; PAM, periarbuscular membrane; LPA, lysophosphatic acid; MAG, monoacylglycerol; DAG, diacylglycerol; TAG, triacylglycerol; PA, phosphatidic acid; PC, phosphatidylcholine; PE, phosphatidylethanolamine; PS, phosphatidylserine; CDP-DAG, cytidine diphosphate diacylglycerol; PG, phosphatidylglycerol; PI, phosphatidylinositol. DOI: 10.7554/eLife.29107.043

phylogenetic divergence, *DIS* and the single copy housekeeping *KASI* gene of *Arabidopsis* are interchangeable (Figure 5). Therefore, the specificity of *DIS* to function in AM symbiosis is probably encoded in its promoter (Figure 2). In monocotyledons, the promoter of the housekeeping *KASI* gene may have acquired additional regulatory elements, sufficient for arbuscocyte-specific activation, thus making *DIS* dispensable.

We provide several pieces of complementary evidence that lipids synthesized by *DIS* and *RAM2* in the arbuscocyte are transferred from plants to AMF and are required for fungal development. We fed host plants with [U- $^{13}\text{C}_6$ ]glucose and subsequently determined the isotopolog profile of freshly synthesized 16:0 and 16:1 $\omega$ 5 FAs in roots and associated fungal extraradical mycelia (Figure 8). This showed that: (1) AMF were unable to incorporate  $^{13}\text{C}$  into FAs when fed with [U- $^{13}\text{C}_6$ ]glucose in absence of the host plant. (2) When associated with a wild-type host, the fungal extraradical mycelium accumulated  $^{13}\text{C}$  labelled 16:0 FAs and the isotopolog profile of these 16:0 FAs was almost identical with the host profile. (3) The 16:0 FA isotopolog fingerprint differed strongly between two different wild-type plant systems (*Lotus* seedling and carrot hairy root) but for each of them the fungal mycelium recapitulated the isotopolog profile. Therefore clearly, the plant dominates the profile of the fungus, because it is impossible that the fungus by itself generates the same FA isotopolog pattern as the plant – especially in the absence of cytosolic FA synthase. Therefore, this result provides compelling evidence for interkingdom transfer of 16:0 FAs from plants to AMF. (4) In agreement, the isotopolog profile of fungus-specific 16:1 $\omega$ 5 FAs inside and outside the root also resembled the plant 16:0 FA profile. (5) Colonized *dis* and *ram2* mutant roots resembled the 16:0 FA isotopolog profile of *L. japonicus* wild-type roots. However, the 16:0 FA profile of the fungal extraradical mycelium and the 16:1 $\omega$ 5 FA profile inside the roots showed a very different pattern, consistent with very low transport of labelled FAs to the fungus when associated with the mutants. (6) *DIS* and *RAM2* are specifically required for the synthesis of 16:0  $\beta$ -MAG (Figure 7) and the predominant FA chain length found in AM fungi is precisely 16. (7) *dis* and *ram2* roots do not allow the formation of lipid-containing fungal vesicles and accumulate very low levels of fungal signature lipids (Figure 5 and figure supplements). Together this strongly supports the idea that *DIS* and *RAM2* are required to provide lipids for transfer to the fungus. Consequently, in the mutants, the fungus is deprived of lipids.

The *L. japonicus* mutants were originally identified due to their defective arbuscule branching (Groth et al., 2013). The promoters of *DIS* and *RAM2* are active in arbusocytes and already during PPA formation, the earliest visible stage of arbuscocyte development. Together with the stunted arbuscule phenotype of *dis*, *ram2* and *fatm* mutants (Figure 1 [Bravo et al., 2017]) this suggests that plant lipids are needed for arbuscule growth, probably to provide material for the extensive plasma-membrane of the highly branched fungal structure. It also indicates that the arbuscule dictates development of the AMF as a whole, since lipid uptake at the arbuscule is required for vesicle formation, full exploration of the root and development of extraradical mycelia and spores. Defective arbuscule development was also observed for the different and phylogenetically distantly related AMF *Gigaspora rosea* (Groth et al., 2013), which similar to *R. irregularis* lacks genes encoding cytosolic FA synthase from their genomes (Wewer et al., 2014; Tang et al., 2016). Hence the dependence on plant lipids delivered at the arbuscule is likely a common phenomenon among AMF and a hallmark of AMF obligate biotrophy.

Despite the obvious central importance of lipid uptake by the arbuscule, the fungus can initially colonize the mutant roots with a low amount of intraradical hyphae and stunted arbuscules (Figure 1, Figure 5—figure supplement 4). The construction of membranes for this initial colonization may be supported by the large amounts of lipids stored in AMF spores. This would be consistent with the frequent observation that in wild-type roots, at initial stages of root colonization, AMF form

arbuscules immediately after reaching the inner cortex and before colonizing longer distances, possibly as a strategy to acquire lipids quickly after the reserves in the spore have been depleted. Alternatively, it is possible that plant housekeeping enzymes provide lipids to intraradical hyphae before arbuscule formation. Activity of the housekeeping KASI may also be responsible for slightly higher colonization levels observed for *dis* in some experiments as compared to other mutants.

It has recently been reported that photosynthetic wild-type nurse plants can restore arbuscule-branching in *Medicago ram2* and *str* mutants (Jiang et al., 2017; Luginbuehl et al., 2017), suggesting that lipids can be supplied to arbuscules via the extraradical hyphal network and intraradical hyphae through this route support arbuscule fine-branching. Based on four observations, we favor an alternative scenario, in which lipids need to be provided cell-autonomously by the arbuscocyte to support arbuscule fine-branching. However, we cannot exclude that our observations differ from the reported observations due to growth conditions or plant species. (1) Presence of nurse carrot hairy roots did not restore arbuscule branching in *dis*, *ram2* and *str* (Figure 8—figure supplement 1C–F). (2) *dis* and *ram2* were found in a forward genetics screen based on their stunted arbuscule phenotype. In this screen, the fungal inoculum was provided via chive nurse plants (Groth et al., 2013). (3) Map-based cloning of *Lotus dis*, *ram2* and *str* (Kojima et al., 2014) was performed with segregating mutant populations grown in the same pot, in which the wild-type and heterozygous siblings acted as nurse plants on the homozygous mutants. In this system, the stunted arbuscule phenotype was easily observable. (4) Arbuscule branching in a rice *str* mutant was not restored by wild type nurse plants (Gutjahr et al., 2012).

It still remains to be shown, which types of lipids are transported from the plant arbuscocyte to the fungal arbuscule and how. RAM2 is the most downstream acting enzyme in arbuscocyte-specific lipid biosynthesis known to date (Figure 9). It is predicted to synthesize  $\beta$ -MAG and we and others have shown that 16:0  $\beta$ -MAGs are indeed reduced in colonized roots of *dis*, *fatm* and *ram2* mutants, providing evidence that this is likely the case (Figure 7, [Bravo et al., 2017]). Although, we cannot exclude that a downstream metabolite of 16:0  $\beta$ -MAG is transported to the fungus, 16:0  $\beta$ -MAG as transport vehicle for 16:0 FAs to the fungus is a good candidate because conceptually this molecule may bear certain advantages. It has been shown in *Arabidopsis* that  $\beta$ -MAGs are not used for plant storage or membrane lipid biosynthesis but rather as pre-cursors for cuticle formation (Li et al., 2007). The production of  $\beta$ -MAGs could therefore, be a way, to withdraw FAs from the plants own metabolism to make them available to the fungus. In addition,  $\beta$ -MAGs are small and amphiphilic and could diffuse across the short distance of the hydrophilic apoplastic space between plant and fungal membrane. At the newly growing arbuscule branches the distance between the plant and fungal membrane is indeed very small and has been measured to be 80–100 nm on TEM images of high-pressure freeze-substituted samples (Bonfante, 2001). However, we could not detect fungus-specific 16:1 $\omega$ 5  $\beta$ -MAGs in colonized roots. This could mean that the fungus metabolizes them before desaturation of the 16:0 FAs to synthesize membrane and storage lipids. Alternatively,  $\beta$ -MAGs may not be taken up by the fungus.  $\beta$ -MAGs are known to isomerize to  $\alpha$ -MAGs in acid or basic conditions (Iqbal and Hussain, 2009). It is therefore, possible that they isomerize in the acidic periarbuscular space (Guttenberger, 2000) before being taken up by the arbuscule.

How are MAGs transported across the peri-arbuscular membrane? Good candidates for MAG transporters are the ABCG half transporters STR and STR2. Similar ABCG transporters have been implicated genetically in cuticle formation, which also requires  $\beta$ -MAGs (Pighin et al., 2004; Panikashvili et al., 2011; Yeats et al., 2012). The half ABCG transporters STR and STR2 are both independently required for arbuscule branching and they need to interact to form a full transporter (Zhang et al., 2010). We found that colonized roots of a *L. japonicus str* mutant, did not allow the formation of fungal vesicles and had the same lipid profile as *dis* and *ram2* (Figure 5 and figure supplements). Furthermore, our  $^{13}\text{C}$  labelling experiment demonstrated that *str* mutants do not transfer lipids to the fungus (Figure 8—figure supplement 2). Although these are encouraging indications, strong evidence for the role of STR in lipid transport across the periarbuscular membrane is still lacking and the substrate of STR remains to be determined. Therefore, currently, it cannot be excluded that mutation of *str* has an indirect effect on lipid transport and alternative mechanisms for example lipid translocation via vesicle fission and fusion are possible. Nevertheless, also in AMF, several ABC transporter genes are expressed in planta (Tisserant et al., 2012; Tang et al., 2016). They are not characterized, but if lipid transport via ABC transporters instead of other mechanisms would play a role, some of them could be involved in uptake of lipids into the fungal cytoplasm.

We found that mutants in the GRAS gene *RAM1* are impaired in AM-specific lipid accumulation in colonized roots and in AM-mediated activation of *DIS* and the single copy gene *KASIII* (Figure 6), in addition to *FatM*, *RAM2* and *STR* (Wang et al., 2012; Park et al., 2015; Pimprikar et al., 2016; Luginbuehl et al., 2017). This suggests that plants have evolved an AM-specific regulatory module for lipid production in arbuscules and delivery to the fungus. It remains to be shown, whether *RAM1* regulates lipid biosynthesis genes directly and how this occurs mechanistically.

Our finding that plants transfer lipids to AMF completely changes the previous view that the fungus receives only sugars from the plant (Pfeffer et al., 1999; Trépanier et al., 2005). It will now be interesting to determine the relative contributions of sugar and lipid transfer to AMF, and whether this may be a determinant of variation in root length colonization and extraradical mycelium formation depending on the plant-fungal genotype combination (Sawers et al., 2017). An interesting question refers to why AMF have lost the genes encoding cytosolic FA synthase to depend on the lipid biosynthesis machinery of the host. FA biosynthesis consumes more energy than biosynthesis of carbohydrates and organic carbon provided by the plant needs to be transported in fungal hyphae over long distances from the inside of the root to the extremities of the extraradical mycelium. Therefore, it is conceivable that supply of plant lipids to the fungus plus fungal lipid transport is more energy efficient for the symbiosis as a whole than fungal carbohydrate transport plus fungal lipid biosynthesis. Hence, inter-organismic lipid transfer followed by loss of fungal FA biosynthesis genes may have been selected for during evolution because it likely optimized the symbiosis for most rapid proliferation of extraradical mycelium, thus ensuring efficient mineral nutrient acquisition from the soil for supporting the plant host. Lipid transfer across kingdoms has also been observed in human parasites or symbiotic bacteria of insects (Caffaro and Boothroyd, 2011; Elwell et al., 2011; Herren et al., 2014). It will be interesting to learn whether this is a more widespread phenomenon among biotrophic inter-organismic interactions.

## Materials and methods

### Plant growth and inoculation with AM fungi

*Lotus japonicus* ecotype Gifu wild-type, *ram1-3*, *ram1-4*, *dis-1*, *dis-4*, *dis-like-5*, *ram2-1*, *ram2-2* and ecotype MG-20 wild-type and *str* mutant (kindly provided by Tomoko Kojima (NARO, Tochigi, Japan) seeds were scarified and surface sterilized with 1% NaClO. Imbibed seeds were germinated on 0.8% Bacto Agar (Difco) at 24°C for 10–14 days. Seedlings were cultivated in pots containing sand/vermiculite (2/1 vol.) as substrate. For colonization with *Rhizophagus irregularis* roots were inoculated with 500 spores (SYMPLANTA, Munich, Germany or Agronutrition, Toulouse, France) per plant. Plants were harvested 5 weeks post inoculation (wpi); except for *dis-1* complementation in Figure 1A, which was harvested at 4 wpi. *Arabidopsis thaliana* seeds of Col-0 wild-type, *kasI* mutant in the Col-0 background and the transgenically complemented *kasI* mutant were surface sterilized with 70% EtOH +0.05% Tween 20% and 100% EtOH, germinated on MS-Medium for 48 hr at 4°C in the dark followed by 5–6 days at 22°C (8 hr light/dark).

### Identification of *DIS* by map-based cloning and next generation sequencing

The *L. japonicus dis* mutant (line SL0154, [Groth et al., 2013]) resulting from an EMS mutagenesis program (Perry et al., 2003, 2009) was backcrossed to ecotype Gifu wild-type and outcrossed to the polymorphic mapping parent ecotype MG-20. The *dis* locus segregated as a recessive monogenic trait and was previously found to be linked to marker TM2249 on chromosome 4 (Groth et al., 2013). We confirmed the monogenic segregation as 26 of 110 individuals originating from the cross to MG-20 ( $\chi^2$ : P(3:1)=0.74) and 32 of 119 individuals originating from the cross to Gifu ( $\chi^2$ : P(3:1)=0.63) exhibited the mutant phenotype. To identify SL0154-specific mutations linked to the *dis* locus, we employed a genome re-sequencing strategy. Nuclear DNA of Gifu wild-type and the SL0154 mutant was subjected to paired end sequencing (2 × 100 bp) of a 300–500 bp insert library, on an Illumina Hi-Seq 2000 instrument resulting in between 16.7 and 19.5 Gigabases per sample, equivalent to roughly 35–41 fold coverage assuming a genome size of 470 Megabases. Reads were mapped to the reference genome of MG-20 v2.5 (Sato et al., 2008) and single nucleotide polymorphisms identified using CLC genomics workbench (CLC bio, Aarhus, Denmark). SL0154-specific

SNPs were identified by subtracting Gifu/MG-20 from SL0154/MG-20 polymorphisms. 19 potentially EMS induced (11x G->A, 8x C->T) SNPs called consistently in all mapped reads from SL0514 but not in Gifu were identified between the markers TM0046/TM1545, the initial *dis* target region (**Figure 1—figure supplement 1A**). In a screen for recombination events flanking the *dis* locus, 63 mutants out of 254 total F2 individuals of a cross MG-20 x SL0154 were genotyped with markers flanking the *dis* locus (**Figure 1—figure supplement 1B**). Interrogating recombinant individuals with additional markers in the region narrowed down the target interval between TM2249 and BM2170 (2 cM according to markers; ca. 650 kb). In this interval, 3 SL0154-specific SNPs with typical EMS signature (G to A transition) remained, of which one was predicted to be located in exon 3 of CM0004.1640.r2 (reference position 40381558 in *L. japonicus* genome version 2.5; <http://www.kazusa.or.jp/lotus/>), a gene annotated as ketoacyl-(acyl carrier protein) synthase. This co-segregation together with phenotyping of one additional mutant allele obtained through TILLING (**Supplementary file 1**, [Perry et al., 2003, 2009]) as well as transgenic complementation (**Figure 1A**) confirmed the identification of the mutation causing the *dis* phenotype of the SL0514 line. The two remaining mutations in the target region were located in a predicted intron of chr4. CM0004.1570.r2.a, a cyclin-like F-box protein (reference position: 40356684) and in a predicted intergenic region (reference position: 40364479). Untranslated regions of *DIS* and *DIS-LIKE* were determined using the Ambion FirstChoice RLM RACE kit according to manufacturer's instructions (<http://www.ambion.de/>). *DIS* sequence information can be found under the NCBI accession number KX880396.

### Identification of *RAM2* by map-based cloning and Sanger sequencing

The *L. japonicus* Gifu mutant *reduced and degenerate arbuscules* (*red*, line SL0181-N) resulting from an EMS mutagenesis (Perry et al., 2003, 2009) was outcrossed to the ecotype MG-20 and previously reported to segregate for two mutations, one on chromosome 1 and one on chromosome 6 (Groth et al., 2013). They were separated by segregation and the mutation on chromosome 1 was previously found in the GRAS transcription factor gene *REDUCED ARBUSCULAR MYCORRHIZA 1* (*RAM1*) (Pimprikar et al., 2016). A plant from the F2 population, which showed wild-type phenotype but was heterozygous for the candidate interval on chromosome 6 and homozygous Gifu for the candidate interval on chromosome 1 was selfed for producing an F3. The F3 generation segregated for only one mutation as 38 out of 132 individuals exhibited the mutant phenotype ( $\chi^2$ : P(3:1)=0.68). A plant from the F3 population, which displayed wild-type phenotype but was heterozygous for the candidate interval on chromosome 6 was selfed for producing an F4. The F4 generation also segregated for only one mutation as 17 out of 87 individuals exhibited the mutant phenotype ( $\chi^2$ : P(3:1)=0.76). To identify the mutation on chromosome 6 linked to the previously identified interval (Groth et al., 2013), we employed additional markers for fine mapping in F3 segregating and F4 mutant populations. This positioned the causative mutation between TM0082 and TM0302 (**Figure 1—figure supplement 3A**). Due to a suppression of recombination in this interval we could not get closer to the mutation and also next generation sequencing (see [Pimprikar et al., 2016] for the methodology) failed to identify a causative mutation. The *Medicago truncatula ram2* mutant displays stunted arbuscules similar to our mutant (Wang et al., 2012). *L. japonicus RAM2* had not been linked to any chromosome but was placed on chromosome 0, which prevented identification of a *RAM2* mutation in the target interval on chromosome 6. Therefore, we sequenced the *RAM2* gene by Sanger sequencing. Indeed, mutants with stunted arbuscule phenotype in the F3 and F4 generation carried an EMS mutation at base 1663 from G to A leading to amino acid change from Glycine to Glutamic acid, which co-segregated with the mutant phenotype (**Figure 1—figure supplement 3B-C**). An additional allelic mutant *ram2-2* (**Figure 1—figure supplement 3B**) caused by a LORE1 retrotransposon insertion (Malolepszy et al., 2016) and transgenic complementation with the wild-type *RAM2* gene confirmed that the causative mutation affects *RAM2* (**Figure 1B**). Untranslated regions of *RAM2* were determined using the Ambion FirstChoice(R) RLM RACE kit according to manufacturer's instructions (<http://www.ambion.de/>). A 1345 bp long sequence upstream of ATG was available from the <http://www.kazusa.or.jp/lotus/blast.html>. To enable cloning a 2275 bp promoter fragment upstream of ATG of *RAM2* the remaining upstream sequence of 1047 bp was determined by primer walking on TAC Lj T46c08. *L. japonicus RAM2* sequence information can be found under the NCBI accession number KX823334 and the promoter sequence under the number KX823335.

## Plasmid generation

Genes and promoter regions were amplified using Phusion PCR according to standard protocols and using primers indicated in [Supplementary file 2](#). Plasmids were constructed as indicated in [Supplementary file 3](#). For localization of DIS in *L. japonicus* hairy roots the LIII tricolor plasmid ([Binder et al., 2014](#)) was used. The plasmid containing 35S:*RFP* for localization of free RFP in *Nicotiana benthamiana* leaves was taken from [Yano et al. \(2008\)](#).

## Induction of transgenic hairy roots in *L. japonicus*

Hypocotyls of *L. japonicus* were transformed with plasmids shown in [Supplementary file 3](#) for hairy root induction using transgenic *Agrobacterium rhizogenes* AR1193 as described ([Takeda et al., 2009](#)).

## Floral dipping and rosette growth assay of *Arabidopsis thaliana*

Five plants per pot were sown. One week before transformation the primary bolt was cut off to induce growth of secondary floral bolts. 5 ml LB culture of *A. tumefaciens* transformed with a binary vector was incubated at 28°C, 300 rpm over night. 500 µl of the preculture was added to 250 µl LB medium with appropriate antibiotics. This culture was incubated again at 28°C, 300 rpm over night until an OD<sub>600</sub> of 1.5 was reached. Plants were watered and covered by plastic bags the day before the dipping to ensure high humidity. The cells were harvested by centrifugation (10 min, 5000 rpm) and resuspended in infiltration medium (0.5 x MS medium, 5% sucrose). The resuspended cell culture was transferred to a box and Silwet L-77 was added (75 µl to 250 ml medium). The floral bolts of the plants were dipped into the medium for 5 s and put back into plastic bags and left in horizontal position for one night. After that, plants were turned upright, bags were opened and mature siliques were harvested. For rosette growth assays T3 plants were used. 31 days post sowing the rosettes were photographed and then cut and dried in an oven at 65°C for the determination of rosette dry weight.

## Spatial analysis of promoter activity

For promoter:GUS analysis *L. japonicus* hairy roots transformed with plasmids containing the *DIS* and *RAM2* promoter fused to the *uidA* gene and colonized by *R. irregularis* were subjected to GUS staining as described ([Takeda et al., 2009](#)). To correlate *DIS* and *RAM2* promoter activity precisely with the stage of arbuscule development two expression cassettes were combined in the same golden gate plasmid for simultaneous visualization of arbuscule stages and promoter activity. The fungal silhouette including all stages of arbuscule development and pre-penetration apparatus were made visible by expressing secretion peptide coupled *mCherry* under the control of the *SbtM1* promoter region comprising 704 bp upstream of the *SbtM1* gene ([Takeda et al., 2009](#)). Promoter activity was visualized using a YFP reporter fused to a nuclear localization signal (NLS).

## Transient transformation of *N. benthamiana* leaves

*N. benthamiana* leaves were transiently transformed by infiltration of transgenic *A. tumefaciens* AGL1 as described ([Yano et al., 2008](#)).

## Real time qRT-PCR

For analysis of transcript levels, plant tissues were rapidly shock frozen in liquid nitrogen. RNA was extracted using the Spectrum Plant Total RNA Kit ([www.sigmaaldrich.com](http://www.sigmaaldrich.com)). The RNA was treated with Invitrogen DNase I amp. grade ([www.invitrogen.com](http://www.invitrogen.com)) and tested for purity by PCR. cDNA synthesis was performed with 500 ng RNA using the Superscript III kit ([www.invitrogen.com](http://www.invitrogen.com)). qRT-PCR was performed with GoTaq G2 DNA polymerase (Promega), 5 x colorless GoTaq Buffer (Promega) and SYBR Green I (Invitrogen S7563, 10.000x concentrated, 500 µl) - diluted to 100x in DMSO. Primers ([Supplementary file 2](#)) were designed with primer3 (58). The qPCR reaction was run on an iCycler (Biorad, [www.bio-rad.com/](http://www.bio-rad.com/)) according to manufacturer's instructions. Thermal cycler conditions were: 95°C 2 min, 45 cycles of 95°C 30 s, 60°C/62°C 30 s and 72°C 20 s followed by dissociation curve analysis. Expression levels were calculated according to the  $\Delta\Delta C_t$  method ([Rozen and Skaletsky, 2000](#)). For each genotype and treatment three to four biological replicates were tested and each sample was represented by two to three technical replicates.

## Sequence alignment and phylogeny

*L. japonicus* KASI, DIS, DIS-LIKE, RAM2, Lj1g3v2301880.1 (GPAT6) protein sequences were retrieved from Lotus genome V2.5 and V3.0 respectively (<http://www.kazusa.or.jp/lotus/>) and *A. thaliana* KASI, *E. coli* KASI, *E. coli* KASII, *M. truncatula* RAM2 and Medtr7g067380 (GPAT6) were obtained from NCBI (<http://www.ncbi.nlm.nih.gov>). The sequences from *L. japonicus* were confirmed with a genome generated by next generation sequencing in house. Protein alignment for DIS was performed by CLC Main Workbench (CLC bio, Aarhus, Denmark). The Target Peptide was predicted using TargetP 1.0 Server ([www.cbs.dtu.dk/services/TargetP-1.0/](http://www.cbs.dtu.dk/services/TargetP-1.0/)). RAM2 Protein alignment was performed by MEGA7 using ClustalW. The percentage identity matrix was obtained by Clustal Omega (<http://www.ebi.ac.uk/Tools/msa/clustalo/>).

To collect sequences for phylogeny construction corresponding to potential DIS orthologs, *Lotus* DIS and KASI (outgroup) protein sequences were searched in genome and transcriptome datasets using BLASTp and tBLASTn respectively. The list of species and the databases used are indicated in **Figure 3—source data 1**. Hits with an e-value  $>10^{-50}$  were selected for the phylogenetic analysis. Collected sequences were aligned using MAFFT (<http://mafft.cbrc.jp/alignment/server/>) and the alignment manually checked with Bioedit. Phylogenetic trees were generated by Neighbor-joining implemented in MEGA5 ([Tamura et al., 2011](#)). Partial gap deletion (95%) was used together with the JTT substitution model. Bootstrap values were calculated using 500 replicates.

## Synteny analysis

A ~200 kb sized region in the *L. japonicus* genome containing the *DIS* locus (CM00041640.r2.a) was compared to the syntenic region in *A. thaliana* (Col-0) using CoGe Gevo (<https://genomeevolution.org/CoGe/GEvo.pl>) - ([Lyons et al., 2008](#)) as described in [Delaux et al. \(2014\)](#). Loci encompassing *DIS* orthologs from *Medicago truncatula*, *Populus trichocarpa*, *Carica papaya*, *Phaseolus vulgaris* and *Solanum lycopersicum* were added as controls.

## AM staining and quantification

*Rhizophagus irregularis* in colonized *L. japonicus* roots was stained with acid ink ([Vierheilig et al., 1998](#)). Root length colonization was quantified using a modified gridline intersect method ([McGonigle et al., 1990](#)). For confocal laser scanning microscopy (CLSM) fungal structures were stained with 1  $\mu$ g WGA Alexa Fluor 488 (Molecular Probes, <http://www.lifetechnologies.com/>) ([Panchuk-Voloshina et al., 1999](#)).

## Microscopy

For quantification of AM colonization in *L. japonicus* roots a light microscope (Leica) with a 20x magnification was used. For observation of GUS-staining in *L. japonicus* hairy roots an inverted microscope (Leica DMI6000 B) was used with 10x and 20x magnification. Transformed roots were screened by stereomicroscope (Leica MZ16 FA) using an mCherry fluorescent transformation marker or the pSbtM1:mCherry marker for fungal colonization (for **Figure 2A and B**). Confocal microscopy (Leica SP5) for WGA-AlexaFluor488 detection using 20x and 63x magnification was performed as described ([Groth et al., 2010](#)). Transgenic roots showing mCherry fluorescence signal due to *SbtM1* promoter activity linked with fungal colonization were cut into pieces immediately after harvesting. The living root pieces were placed on a glass slide with a drop of water, covered by a cover slip and immediately subjected to imaging. Sequential scanning for the YFP and RFP signal was carried out simultaneously with bright field image acquisition. YFP was excited with the argon ion laser 514 nm and the emitted fluorescence was detected from 525 to 575 nm; RFP was excited with the Diode-Pumped Solid State laser at 561 nm and the emitted fluorescence was detected from 580 to 623 nm. Images were acquired using LAS AF software. Several z-optical sections were made per area of interest and assembled to a z-stack using Fiji. The z-stack movies and 3D projections were produced using the 3D viewer function in Fiji ([Schindelin et al., 2012](#)).

## Extraction and purification of phospho- and glyco- and triacylglycerols

Approximately 50–100 mg of root or leaf material was harvested, weighed and immediately frozen in liquid nitrogen to avoid lipid degradation. The frozen samples were ground to a fine powder

before extraction with organic solvents. Total lipids were extracted as described previously (Wewer *et al.*, 2011, 2014). Briefly, 1 mL chloroform/methanol/formic acid (1:1:0.1, v/v/v) was added and the sample was shaken vigorously. At this point the internal standards for TAG and fatty acid analysis were added. Phase separation was achieved after addition of 0.5 mL 1M KCl/0.2 M H<sub>3</sub>PO<sub>4</sub> and subsequent centrifugation at 4000 rpm for 5 min. The lipid-containing chloroform phase was transferred to a fresh glass tube and the sample was re-extracted twice with chloroform. The combined chloroform phases were dried under a stream of air and lipids were re-dissolved in 1 mL chloroform to yield the total lipid extract.

For phospho- and glycerolipid analysis 20 µl of the total lipid extract were mixed with 20 µl of the internal standard mix and 160 µl of methanol/chloroform/300 mM ammonium acetate (665:300:35, v/v/v) (Walti *et al.*, 2002). For triacylglycerol analysis 500 µl of the total lipid extract were purified by solid phase extraction on Strata silica columns (1 ml bed volume; Phenomenex) as described (Wewer *et al.*, 2011). TAGs were eluted from the silica material with chloroform, dried under a stream of air and re-dissolved in 1 mL methanol/chloroform/300 mM ammonium acetate (665:300:35, v/v/v).

### Extraction and purification of free fatty acids and monoacylglycerol (MAG)

Total lipids were extracted into chloroform and dried as described above. 15–0 FA and a mixture of 15–0 α-MAG and β-MAG were added as internal standard before the extraction. Dried extracts were resuspended in 1 ml n-hexane and applied to silica columns for solid-phase extraction with a n-hexane:diethylether gradient. Free fatty acids were eluted with a mixture of 92:8 (v/v) n-hexane:diethylether as described before (Gasulla *et al.*, 2013) and pure diethylether were used for elution of MAG.

### Analysis of total fatty acids and free fatty acids by GC-FID

For measurement of total fatty acids, 100 µl of the total lipid extract were used. For measurement of free fatty acids, the SPE-fraction containing free fatty acids was used. Fatty acid methyl esters (FAMES) were generated from acyl groups of total lipids and free fatty acids by addition of 1 mL 1N methanolic HCL (Sigma) to dried extracts and incubation at 80°C for 30 min (Browse *et al.*, 1986). Subsequently, FAMES were extracted by addition of 1 mL n-hexane and 1 mL of 0.9% (w/v) NaCl and analyzed on a gas chromatograph with flame-ionization detector (GC-FID, Agilent 7890A PlusGC). FAMES were separated on an SP 2380 fused silica GC column (Supelco, 30 mx 0.53 mm, 0.20 µm film) as described (Wewer *et al.*, 2013), with a temperature -gradient starting at 100°C, increased to 160°C with 25°C/min, then to 220°C with 10°C/min and reduced to 100°C with 25 °C/min. FAMES were quantified in relation to the internal standard pentadecanoic acid (15:0).

For MAG measurement, dried diethylether fractions were resuspended in 4:1 (v/v %) pyridine:*N*-Methyl-*N*-(trimethylsilyl)trifluoroacetamide (MSTFA), incubated at 80°C for 30 min, dried and re-suspended in hexane prior to application on an Agilent 7890A Plus gas chromatography-mass spectrometer. MAGs were quantified by extracted ion monitoring, using [M+ - 103] for α-MAGs and [M+ - 161] for β-MAGs as previously reported for 16:0 MAG (Destailats *et al.*, 2010) and 24:0 MAG (Li *et al.*, 2007).

### Quantification of glycerolipids by Q-TOF MS/MS

Phosphoglycerolipids (PC, PE, PG, PI, PS), glycerolipids (MGDG, DGDG, SQDG) and triacylglycerol (TAG) were analyzed in positive mode by direct infusion nanospray Q-TOF MS/MS on an Agilent 6530 Q-TOF instrument as described previously (Lippold *et al.*, 2012; Gasulla *et al.*, 2013). A continuous flow of 1 µl/min methanol/chloroform/300 mM ammonium acetate (665:300:35, v/v/v) (Walti *et al.*, 2002) was achieved using a nanospray infusion ion source (HPLC/chip MS 1200 with infusion chip). Data are displayed as X:Y, where X gives the number of C atoms of the fatty acid chain and Y the amount of desaturated carbo-carbon bonds inside that fatty acid chain.

### Internal standards

Internal standards for phospho- and glycerolipid analysis were prepared as described previously (Gasulla *et al.*, 2013; Wewer *et al.*, 2014). The following standards were dissolved in 20 µl of

chloroform/methanol (2:1, v/v): 0.2 nmol of each di14:0-PC, di20:0-PC, di14:0-PE, di20:0-PE, di14:0-PG, di20:0-PG, di14:0-PA and di20:0-PA; 0.03 nmol of di14:0-PS and di20:0-PS; 0.3 nmol of 34:0-PI; 0.15 nmol of 34:0-MGDG, 0.10 nmol of 36:0-MGDG; 0.2 nmol of 34:0-DGDG, 0.39 nmol of 36:0-DGDG and 0.4 nmol of 34:0-SQDG. 1 nmol each of tridecanoin (tri-10:0) and triundecenoin (tri-11:1), and 2 nmol each of triarachidin (tri-20:0) and trierucin (tri22:1) were used as internal standards for TAG quantification (Lippold et al., 2012). For quantification of total fatty acids and free fatty acids 5 µg of pentadecanoic acid (FA 15:0) was added to the samples (Wewer et al., 2013).

## Cultivation and <sup>13</sup>C-Labeling of *L. japonicus* and *Daucus carota* hairy roots

To determine lipid transfer from *L. japonicus* to the fungus we used the carrot root organ culture system (Bécard et al., 1988) to obtain sufficient amounts of fungal material for isotopolog profiling. (On petri dishes this was not possible with *L. japonicus* and in particular the lipid mutants alone). One compartment (carrot compartment) of the 2-compartmented petri dish system (Trépanier et al., 2005) was filled with MSR-medium (3% gelrite) containing 10% sucrose to support the shoot-less carrot root, and the other compartment (*Lotus* compartment) was filled with MSR-medium (3% gelrite) without sucrose. *Ri T-DNA* transformed *Daucus carota* hairy roots were placed in the carrot compartment. 1 week later, roots were inoculated with *R. irregularis*. Petri dishes were incubated at constant darkness and 30°C. Within 5 weeks *R. irregularis* colonized the carrot roots and its extraradical mycelium spread over both compartments of the petri dish and formed spores. At this stage two 2 week old *L. japonicus* seedlings (WT, *dis-1*, *ram2-1*) were placed into the *Lotus* compartment (Figure 8—figure supplement 1).

The plates were incubated at 24°C (16 hr light/8 hr dark). To keep the fungus and root in the dark the petri dishes were covered with black paper. 3 weeks after *Lotus* seedlings were placed into the petri dish [U-<sup>13</sup>C<sub>6</sub>]glucose (100 mg diluted in 2 ml MSR-medium) (Sigma-Aldrich) was added to the *Lotus* compartment. Therefore, only *Lotus* roots but not the carrot roots took up label. For transfer experiments with carrot roots no *Lotus* plant was placed into the *Lotus* compartment and the [U-<sup>13</sup>C<sub>6</sub>]glucose was added to the carrot compartment. 1 week after addition of [U-<sup>13</sup>C<sub>6</sub>]glucose the roots were harvested. The extraradical mycelium was extracted from the agar using citrate buffer pH 6 and subsequent filtration, after which it was immediately shock-frozen in liquid nitrogen.

## Isotopolog profiling of <sup>13</sup>C-labelled 16:0 and 16:1ω5 fatty acids

Root and fungal samples were freeze dried and subsequently derivatised with 500 µl MeOH containing 3 M HCl (Sigma-Aldrich) at 80°C for 20 hr. MeOH/HCL was removed under a gentle stream of nitrogen and the methyl esters of the fatty acids were solved in 100 µl dry hexane.

Gas chromatography mass spectrometry was performed on a GC-QP 2010 plus (Shimadzu, Duisburg, Germany) equipped with a fused silica capillary column (equity TM-5; 30 m by 0.25 mm, 0.25-µm film thickness; Supelco, Bellafonte, PA). The mass detector worked in electron ionization (EI) mode at 70 eV. An aliquot of the solution was injected in split mode (1:5) at an injector and interface temperature of 260°C. The column was held at 170°C for 3 min and then developed with a temperature gradient of 2 °C/min to a temperature of 192°C followed by a temperature gradient of 30°C/min to a final temperature of 300°C. Samples were analyzed in SIM mode (m/z values 267 to 288) at least three times. Retention times for fatty acids 16:1ω5 (unlabeled m/z 268) and 16:0 (unlabeled m/z 270) are 12.87 min and 13.20 min, respectively. Data were collected with LabSolution software (Shimadzu, Duisburg, Germany). The overall <sup>13</sup>C enrichment and the isotopolog compositions were calculated according to (Lee et al., 1991) and (Ahmed et al., 2014). The software package is open source and can be downloaded by the following link: [http://www.tr34.uni-wuerzburg.de/software\\_developments/isotopo/](http://www.tr34.uni-wuerzburg.de/software_developments/isotopo/).

Four independent labeling experiments were performed. Overall excess (o.e.) is an average value of <sup>13</sup>C atoms incorporated into 16:0/16:1ω5 fatty acids.

## Data availability

*Lunularia cruciata*: For this species, the raw RNAseq reads have been previously deposited to NCBI under the accession number SRR1027885. It is annotated with *Rhizophagus irregularis* (10% of sequences) as the transcriptome was partly prepared from *Lunularia* plant tissue colonized by the

fungus *Rhizophagus irregularis*. The corresponding *Lunularia* transcriptomic assembly is available at [www.polebio.lrsv.ups-tlse.fr/Luc\\_v1/](http://www.polebio.lrsv.ups-tlse.fr/Luc_v1/)

## Statistics

All statistical analyses (**Source code 1**) were performed and all boxplots were generated in R ([www.r-project.org](http://www.r-project.org)).

## Acknowledgements

We are grateful to Tomoko Kojima (NARO, Tochigi, Japan) for providing *Lotus japonicus str* mutant seeds and to LotusBase for providing LORE1 insertion lines. We thank Julia Mayer for help with setting up carrot hairy root systems, Samy Carbonnel, David Chiasson, Michael Paries and José Antonio Villaécija-Aguilar for contributing a golden gate module.

## Additional information

### Funding

Funder	Grant reference number	Author
Deutsche Forschungsgemeinschaft	SFB924 B03 Function of the GRAS protein RAM1 in arbuscule development	Caroline Gutjahr
Deutsche Forschungsgemeinschaft	Emmy Noether program GU1423/1-1	Caroline Gutjahr
Deutsche Forschungsgemeinschaft	PA493/7-1 Plant genes required for arbuscular mycorrhiza symbiosis	Martin Parniske
Deutsche Forschungsgemeinschaft	SFB924 B03 Genetic dissection of arbuscular mycorrhiza development	Martin Parniske
Deutsche Forschungsgemeinschaft	SPP1212	Peter Dörmann
Deutsche Forschungsgemeinschaft	Research Training Group GRK 2064 Do520/15-1	Peter Dörmann
Hans Fischer Gesellschaft e. V.		Wolfgang Eisenreich
Biotechnology and Biological Sciences Research Council		Trevor L Wang

The funders had no role in study design, data collection and interpretation, or the decision to submit the work for publication.

### Author contributions

AK, Conceptualization, Data curation, Formal analysis, Investigation, Visualization, Writing - contributed method description and figure legends; PP, Conceptualization, Data curation, Formal analysis, Investigation, Visualization; VW, Conceptualization, Investigation, Methodology; CH, Data curation, Investigation, Writing - contributed method description; MB, Data curation, Investigation, Methodology, Writing - contributed method description; SLB, VK, Investigation; P-MD, Formal analysis, Investigation; EvR-L, Investigation, generation of important preliminary data; TLW, Resources, Funding acquisition, Methodology; WE, Resources, Supervision, Funding acquisition; PD, Conceptualization, Supervision, Funding acquisition; MP, Conceptualization, Supervision, Funding acquisition, Investigation, Project administration, Writing—review and editing; CG, Conceptualization, Formal analysis, Supervision, Funding acquisition, Investigation, Writing—original draft, Project administration, Writing—review and editing

### Author ORCIDs

Andreas Keymer, <http://orcid.org/0000-0001-9933-3662>

Mathias Brands, <http://orcid.org/0000-0001-6548-1448>

Pierre-Marc Delaux, [ORCID](http://orcid.org/0000-0002-6211-157X) <http://orcid.org/0000-0002-6211-157X>

Peter Dörmann, [ORCID](http://orcid.org/0000-0002-5845-9370) <http://orcid.org/0000-0002-5845-9370>

Martin Parniske, [ORCID](http://orcid.org/0000-0001-8561-747X) <http://orcid.org/0000-0001-8561-747X>

Caroline Gutjahr, [ORCID](http://orcid.org/0000-0001-6163-745X) <http://orcid.org/0000-0001-6163-745X>

---

## Additional files

### Supplementary files

- Source code 1. Source code for ANOVA statistical test in R

DOI: [10.7554/eLife.29107.044](https://doi.org/10.7554/eLife.29107.044)

- Supplementary file 1. Mutations in *DIS* and *DIS-LIKE* identified by TILLING or in a LORE1 insertion collection.

DOI: [10.7554/eLife.29107.045](https://doi.org/10.7554/eLife.29107.045)

- Supplementary file 2. Primers used in this study.

DOI: [10.7554/eLife.29107.046](https://doi.org/10.7554/eLife.29107.046)

- Supplementary file 3. Plasmids used in this study were produced by classical cloning, Gateway cloning (Entry plasmids and Destination plasmids) and Golden Gate cloning (Level I, II and III). The Golden Gate toolbox is described in *Binder et al. (2014)*. EV, empty vector; HR, hairy root; trafo, transformation.

DOI: [10.7554/eLife.29107.047](https://doi.org/10.7554/eLife.29107.047)

- Supplementary file 4. Accession numbers for protein sequences used in the phylogenetic tree (*Figure 3*).

DOI: [10.7554/eLife.29107.048](https://doi.org/10.7554/eLife.29107.048)

---

## References

- Ahmed Z, Zeeshan S, Huber C, Hensel M, Schomburg D, Münch R, Eylert E, Eisenreich W, Dandekar T. 2014. 'Isotopo' a database application for facile analysis and management of mass isotopomer data. *Database* **2014**: bau077. doi: [10.1093/database/bau077](https://doi.org/10.1093/database/bau077), PMID: [25204646](https://pubmed.ncbi.nlm.nih.gov/25204646/)
- Bago B, Zipfel W, Williams RM, Jun J, Arreola R, Lammers PJ, Pfeffer PE, Shachar-Hill Y. 2002. Translocation and utilization of fungal storage lipid in the arbuscular mycorrhizal symbiosis. *Plant Physiology* **128**:108–124. doi: [10.1104/pp.010466](https://doi.org/10.1104/pp.010466), PMID: [11788757](https://pubmed.ncbi.nlm.nih.gov/11788757/)
- Bago B, Pfeffer PE, Abubaker J, Jun J, Allen JW, Brouillette J, Douds DD, Lammers PJ, Shachar-Hill Y. 2003. Carbon export from arbuscular mycorrhizal roots involves the translocation of carbohydrate as well as lipid. *Plant Physiology* **131**:1496–1507. doi: [10.1104/pp.102.007765](https://doi.org/10.1104/pp.102.007765), PMID: [12644699](https://pubmed.ncbi.nlm.nih.gov/12644699/)
- Bentivenga SP, Morton JB. 1996. Congruence of fatty acid methyl ester profiles and morphological characters of arbuscular mycorrhizal fungi in *Gigasporaceae*. *PNAS* **93**:5659–5662. doi: [10.1073/pnas.93.11.5659](https://doi.org/10.1073/pnas.93.11.5659), PMID: [11607684](https://pubmed.ncbi.nlm.nih.gov/11607684/)
- Binder A, Lambert J, Morbitzer R, Popp C, Ott T, Lahaye T, Parniske M. 2014. A modular plasmid assembly kit for multigene expression, gene silencing and silencing rescue in plants. *PLoS One* **9**:e88218. doi: [10.1371/journal.pone.0088218](https://doi.org/10.1371/journal.pone.0088218), PMID: [24551083](https://pubmed.ncbi.nlm.nih.gov/24551083/)
- Bonfante P. 2001. At the interface between mycorrhizal fungi and plants: the structural organization of cell wall, plasma membrane and cytoskeleton. In: Hock B (Ed). *The Mycota IX*. Heidelberg: Springer Verlag. doi: [10.1007/978-3-662-07334-6\\_4](https://doi.org/10.1007/978-3-662-07334-6_4)
- Bravo A, York T, Pumplin N, Mueller LA, Harrison MJ. 2016. Genes conserved for arbuscular mycorrhizal symbiosis identified through phylogenomics. *Nature Plants* **2**:15208. doi: [10.1038/nplants.2015.208](https://doi.org/10.1038/nplants.2015.208), PMID: [27249190](https://pubmed.ncbi.nlm.nih.gov/27249190/)
- Bravo A, Brands M, Wewer V, Dörmann P, Harrison MJ. 2017. Arbuscular mycorrhiza-specific enzymes FatM and RAM2 fine-tune lipid biosynthesis to promote development of arbuscular mycorrhiza. *New Phytologist* **214**: 1631–1645. doi: [10.1111/nph.14533](https://doi.org/10.1111/nph.14533), PMID: [28380681](https://pubmed.ncbi.nlm.nih.gov/28380681/)
- Browse J, McCourt PJ, Somerville CR. 1986. Fatty acid composition of leaf lipids determined after combined digestion and fatty acid methyl ester formation from fresh tissue. *Analytical Biochemistry* **152**:141–145. doi: [10.1016/0003-2697\(86\)90132-6](https://doi.org/10.1016/0003-2697(86)90132-6), PMID: [3954036](https://pubmed.ncbi.nlm.nih.gov/3954036/)
- Bécard G, Fortin JA, Ja F. 1988. Early events of vesicular-arbuscular mycorrhiza formation on Ri T-DNA transformed roots. *New Phytologist* **108**:211–218. doi: [10.1111/j.1469-8137.1988.tb03698.x](https://doi.org/10.1111/j.1469-8137.1988.tb03698.x)
- Caffaro CE, Boothroyd JC. 2011. Evidence for host cells as the Major contributor of lipids in the intravacuolar network of *Toxoplasma*-infected cells. *Eukaryotic Cell* **10**:1095–1099. doi: [10.1128/EC.00002-11](https://doi.org/10.1128/EC.00002-11), PMID: [21685319](https://pubmed.ncbi.nlm.nih.gov/21685319/)

- Delaux PM**, Varala K, Edger PP, Coruzzi GM, Pires JC, Ané JM. 2014. Comparative phylogenomics uncovers the impact of symbiotic associations on host genome evolution. *PLoS Genetics* **10**:e1004487. doi: [10.1371/journal.pgen.1004487](https://doi.org/10.1371/journal.pgen.1004487), PMID: [25032823](https://pubmed.ncbi.nlm.nih.gov/25032823/)
- Delaux PM**, Radhakrishnan GV, Jayaraman D, Cheema J, Malbreil M, Volkening JD, Sekimoto H, Nishiyama T, Melkonian M, Pokorny L, Rothfels CJ, Sederoff HW, Stevenson DW, Surek B, Zhang Y, Sussman MR, Dunand C, Morris RJ, Roux C, Wong GK, et al. 2015. Algal ancestor of land plants was preadapted for symbiosis. *PNAS* **112**:13390–13395. doi: [10.1073/pnas.1515426112](https://doi.org/10.1073/pnas.1515426112), PMID: [26438870](https://pubmed.ncbi.nlm.nih.gov/26438870/)
- Destaillets F**, Cruz-Hernandez C, Nagy K, Dionisi F. 2010. Identification of monoacylglycerol regio-isomers by gas chromatography-mass spectrometry. *Journal of Chromatography A* **1217**:1543–1548. doi: [10.1016/j.chroma.2010.01.016](https://doi.org/10.1016/j.chroma.2010.01.016), PMID: [20097347](https://pubmed.ncbi.nlm.nih.gov/20097347/)
- Elwell CA**, Jiang S, Kim JH, Lee A, Wittmann T, Hanada K, Melancon P, Engel JN. 2011. *Chlamydia trachomatis* co-opts GBF1 and CERT to acquire host sphingomyelin for distinct roles during intracellular development. *PLoS Pathogens* **7**:e1002198. doi: [10.1371/journal.ppat.1002198](https://doi.org/10.1371/journal.ppat.1002198), PMID: [21909260](https://pubmed.ncbi.nlm.nih.gov/21909260/)
- Fabre G**, Garroum I, Mazurek S, Daraspe J, Mucciolo A, Sankar M, Humbel BM, Nawrath C. 2016. The ABCG transporter PEC1/ABCG32 is required for the formation of the developing leaf cuticle in Arabidopsis. *New Phytologist* **209**:192–201. doi: [10.1111/nph.13608](https://doi.org/10.1111/nph.13608), PMID: [26406899](https://pubmed.ncbi.nlm.nih.gov/26406899/)
- Favre P**, Bapaume L, Bossolini E, Delorenzi M, Falquet L, Reinhardt D. 2014. A novel bioinformatics pipeline to discover genes related to arbuscular mycorrhizal symbiosis based on their evolutionary conservation pattern among higher plants. *BMC Plant Biology* **14**:333. doi: [10.1186/s12870-014-0333-0](https://doi.org/10.1186/s12870-014-0333-0), PMID: [25465219](https://pubmed.ncbi.nlm.nih.gov/25465219/)
- Gasulla F**, Vom Dorp K, Dombink I, Zähringer U, Gisch N, Dörmann P, Bartels D. 2013. The role of lipid metabolism in the acquisition of desiccation tolerance in *Craterostigma plantagineum*: a comparative approach. *The Plant Journal* **75**:726–741. doi: [10.1111/tpj.12241](https://doi.org/10.1111/tpj.12241), PMID: [23672245](https://pubmed.ncbi.nlm.nih.gov/23672245/)
- Gaude N**, Bortfeld S, Duensing N, Lohse M, Krajinski F. 2012a. Arbuscule-containing and non-colonized cortical cells of mycorrhizal roots undergo extensive and specific reprogramming during arbuscular mycorrhizal development. *The Plant Journal* **69**:510–528. doi: [10.1111/j.1365-313X.2011.04810.x](https://doi.org/10.1111/j.1365-313X.2011.04810.x), PMID: [21978245](https://pubmed.ncbi.nlm.nih.gov/21978245/)
- Gaude N**, Schulze WX, Franken P, Krajinski F. 2012b. Cell type-specific protein and transcription profiles implicate periarbuscular membrane synthesis as an important carbon sink in the mycorrhizal symbiosis. *Plant Signaling & Behavior* **7**:461–464. doi: [10.4161/psb.19650](https://doi.org/10.4161/psb.19650), PMID: [22499167](https://pubmed.ncbi.nlm.nih.gov/22499167/)
- Genre A**, Chabaud M, Faccio A, Barker DG, Bonfante P. 2008. Prepenetration apparatus assembly precedes and predicts the colonization patterns of arbuscular mycorrhizal fungi within the root cortex of both *Medicago truncatula* and *Daucus carota*. *The Plant Cell Online* **20**:1407–1420. doi: [10.1105/tpc.108.059014](https://doi.org/10.1105/tpc.108.059014), PMID: [18515499](https://pubmed.ncbi.nlm.nih.gov/18515499/)
- Gobbato E**, Marsh JF, Vernié T, Wang E, Maillet F, Kim J, Miller JB, Sun J, Bano SA, Ratet P, Mysore KS, Dénarié J, Schultze M, Oldroyd GE. 2012. A GRAS-type transcription factor with a specific function in mycorrhizal signaling. *Current Biology* **22**:2236–2241. doi: [10.1016/j.cub.2012.09.044](https://doi.org/10.1016/j.cub.2012.09.044), PMID: [23122845](https://pubmed.ncbi.nlm.nih.gov/23122845/)
- Gobbato E**, Wang E, Higgins G, Bano SA, Henry C, Schultze M, Oldroyd GE. 2013. *RAM1* and *RAM2* function and expression during arbuscular mycorrhizal symbiosis and *Aphanomyces euteiches* colonization. *Plant Signaling & Behavior* **8**:e26049. doi: [10.4161/psb.26049](https://doi.org/10.4161/psb.26049), PMID: [24270627](https://pubmed.ncbi.nlm.nih.gov/24270627/)
- Graham JH**, Hodge NC, Morton JB. 1995. Fatty Acid methyl ester profiles for characterization of glomalean fungi and their endomycorrhizae. *Applied and Environmental Microbiology* **61**:58–64. PMID: [16534923](https://pubmed.ncbi.nlm.nih.gov/16534923/)
- Groth M**, Takeda N, Perry J, Uchida H, Dräxl S, Brachmann A, Sato S, Tabata S, Kawaguchi M, Wang TL, Parniske M. 2010. *NENA*, a *Lotus japonicus* homolog of *Sec13*, is required for rhizodermal infection by arbuscular mycorrhiza fungi and rhizobia but dispensable for cortical endosymbiotic development. *The Plant Cell Online* **22**:2509–2526. doi: [10.1105/tpc.109.069807](https://doi.org/10.1105/tpc.109.069807), PMID: [20675572](https://pubmed.ncbi.nlm.nih.gov/20675572/)
- Groth M**, Kosuta S, Gutjahr C, Haage K, Hardel SL, Schaub M, Brachmann A, Sato S, Tabata S, Findlay K, Wang TL, Parniske M. 2013. Two *Lotus japonicus* symbiosis mutants impaired at distinct steps of arbuscule development. *The Plant Journal* **75**:117–129. doi: [10.1111/tpj.12220](https://doi.org/10.1111/tpj.12220), PMID: [23627596](https://pubmed.ncbi.nlm.nih.gov/23627596/)
- Gutjahr C**, Radovanovic D, Geoffroy J, Zhang Q, Siegler H, Chiapello M, Casieri L, An K, An G, Guiderdoni E, Kumar CS, Sundaresan V, Harrison MJ, Paszkowski U. 2012. The half-size ABC transporters *STR1* and *STR2* are indispensable for mycorrhizal arbuscule formation in rice. *The Plant Journal* **69**:906–920. doi: [10.1111/j.1365-313X.2011.04842.x](https://doi.org/10.1111/j.1365-313X.2011.04842.x), PMID: [22077667](https://pubmed.ncbi.nlm.nih.gov/22077667/)
- Guttenberger M**. 2000. Arbuscules of vesicular-arbuscular mycorrhizal fungi inhabit an acidic compartment within plant roots. *Planta* **211**:299–304. doi: [10.1007/s004250000324](https://doi.org/10.1007/s004250000324), PMID: [10987547](https://pubmed.ncbi.nlm.nih.gov/10987547/)
- Helber N**, Wippel K, Sauer N, Schaarschmidt S, Hause B, Requena N. 2011. A versatile monosaccharide transporter that operates in the arbuscular mycorrhizal fungus *Glomus* sp is crucial for the symbiotic relationship with plants. *The Plant Cell* **23**:3812–3823. doi: [10.1105/tpc.111.089813](https://doi.org/10.1105/tpc.111.089813), PMID: [21972259](https://pubmed.ncbi.nlm.nih.gov/21972259/)
- Herren JK**, Paredes JC, Schüpfer F, Arafah K, Bulet P, Lemaître B. 2014. Insect endosymbiont proliferation is limited by lipid availability. *eLife* **3**:e02964. doi: [10.7554/eLife.02964](https://doi.org/10.7554/eLife.02964), PMID: [25027439](https://pubmed.ncbi.nlm.nih.gov/25027439/)
- Hwang JU**, Song WY, Hong D, Ko D, Yamaoka Y, Jang S, Yim S, Lee E, Khare D, Kim K, Palmgren M, Yoon HS, Martinoia E, Lee Y. 2016. Plant ABC transporters enable many unique aspects of a terrestrial plant's lifestyle. *Molecular Plant* **9**:338–355. doi: [10.1016/j.molp.2016.02.003](https://doi.org/10.1016/j.molp.2016.02.003), PMID: [26902186](https://pubmed.ncbi.nlm.nih.gov/26902186/)
- Iqbal J**, Hussain MM. 2009. Intestinal lipid absorption. *AJP: Endocrinology and Metabolism* **296**:E1183–E1194. doi: [10.1152/ajpendo.90899.2008](https://doi.org/10.1152/ajpendo.90899.2008), PMID: [19158321](https://pubmed.ncbi.nlm.nih.gov/19158321/)
- Ivanov S**, Harrison MJ. 2014. A set of fluorescent protein-based markers expressed from constitutive and arbuscular mycorrhiza-inducible promoters to label organelles, membranes and cytoskeletal elements in *Medicago truncatula*. *The Plant Journal* **80**:1151–1163. doi: [10.1111/tpj.12706](https://doi.org/10.1111/tpj.12706), PMID: [25329881](https://pubmed.ncbi.nlm.nih.gov/25329881/)

- Javot H**, Penmetsa RV, Terzaghi N, Cook DR, Harrison MJ. 2007. A *Medicago truncatula* phosphate transporter indispensable for the arbuscular mycorrhizal symbiosis. *PNAS* **104**:1720–1725. doi: [10.1073/pnas.0608136104](https://doi.org/10.1073/pnas.0608136104), PMID: [17242358](https://pubmed.ncbi.nlm.nih.gov/17242358/)
- Jiang Y**, Wang W, Xie Q, Liu N, Liu L, Wang D, Zhang X, Yang C, Chen X, Tang D, Wang E. 2017. Plants transfer lipids to sustain colonization by mutualistic mycorrhizal and parasitic fungi. *Science* **356**:1172–1175. doi: [10.1126/science.aam9970](https://doi.org/10.1126/science.aam9970), PMID: [28596307](https://pubmed.ncbi.nlm.nih.gov/28596307/)
- Jones A**, Davies HM, Voelker TA. 1995. Palmitoyl-acyl carrier protein (ACP) thioesterase and the evolutionary origin of plant acyl-ACP thioesterases. *The Plant Cell Online* **7**:359–371. doi: [10.1105/tpc.7.3.359](https://doi.org/10.1105/tpc.7.3.359), PMID: [7734968](https://pubmed.ncbi.nlm.nih.gov/7734968/)
- Kojima T**, Saito K, Oba H, Yoshida Y, Terasawa J, Umehara Y, Suganuma N, Kawaguchi M, Ohtomo R. 2014. Isolation and phenotypic characterization of *Lotus japonicus* mutants specifically defective in arbuscular mycorrhizal formation. *Plant and Cell Physiology* **55**:928–941. doi: [10.1093/pcp/pcu024](https://doi.org/10.1093/pcp/pcu024), PMID: [24492255](https://pubmed.ncbi.nlm.nih.gov/24492255/)
- Lee WN**, Byerley LO, Bergner EA, Edmond J. 1991. Mass isotopomer analysis: theoretical and practical considerations. *Biological Mass Spectrometry* **20**:451–458. doi: [10.1002/bms.1200200804](https://doi.org/10.1002/bms.1200200804), PMID: [1768701](https://pubmed.ncbi.nlm.nih.gov/1768701/)
- Lee JY**, Kinch LN, Borek DM, Wang J, Wang J, Urbatsch IL, Xie XS, Grishin NV, Cohen JC, Otwinowski Z, Hobbs HH, Rosenbaum DM. 2016. Crystal structure of the human sterol transporter ABCG5/ABCG8. *Nature* **533**:561–564. doi: [10.1038/nature17666](https://doi.org/10.1038/nature17666), PMID: [27144356](https://pubmed.ncbi.nlm.nih.gov/27144356/)
- Li Y**, Beisson F, Ohlrogge J, Pollard M. 2007. Monoacylglycerols are components of root waxes and can be produced in the aerial cuticle by ectopic expression of a suberin-associated acyltransferase. *Plant Physiology* **144**:1267–1277. doi: [10.1104/pp.107.099432](https://doi.org/10.1104/pp.107.099432), PMID: [17496107](https://pubmed.ncbi.nlm.nih.gov/17496107/)
- Li-Beisson Y**, Shorrosh B, Beisson F, Andersson MX, Arondel V, Bates PD, Baud S, Bird D, Debono A, Durrett TP, Franke RB, Graham IA, Katayama K, Kelly AA, Larson T, Markham JE, Miquel M, Molina I, Nishida I, Rowland O, et al. 2010. Acyl-lipid metabolism. *The Arabidopsis Book* **8**:e0133. doi: [10.1199/tab.0133](https://doi.org/10.1199/tab.0133), PMID: [22303259](https://pubmed.ncbi.nlm.nih.gov/22303259/)
- Lippold F**, vom Dorp K, Abraham M, Hölzl G, Wewer V, Yilmaz JL, Lager I, Montandon C, Besagni C, Kessler F, Stymne S, Dörmann P. 2012. Fatty acid phytyl ester synthesis in chloroplasts of *Arabidopsis*. *The Plant Cell* **24**:2001–2014. doi: [10.1105/tpc.112.095588](https://doi.org/10.1105/tpc.112.095588), PMID: [22623494](https://pubmed.ncbi.nlm.nih.gov/22623494/)
- Lohse S**, Schliemann W, Ammer C, Kopka J, Strack D, Fester T. 2005. Organization and metabolism of plastids and mitochondria in arbuscular mycorrhizal roots of *Medicago truncatula*. *Plant Physiology* **139**:329–340. doi: [10.1104/pp.105.061457](https://doi.org/10.1104/pp.105.061457), PMID: [16126866](https://pubmed.ncbi.nlm.nih.gov/16126866/)
- Luginbuehl LH**, Menard GN, Kurup S, Van Erp H, Radhakrishnan GV, Breakspear A, Oldroyd GED, Eastmond PJ. 2017. Fatty acids in arbuscular mycorrhizal fungi are synthesized by the host plant. *Science* **356**:1175–1178. doi: [10.1126/science.aan0081](https://doi.org/10.1126/science.aan0081), PMID: [28596311](https://pubmed.ncbi.nlm.nih.gov/28596311/)
- Lyons E**, Pedersen B, Kane J, Alam M, Ming R, Tang H, Wang X, Bowers J, Paterson A, Lisch D, Freeling M. 2008. Finding and comparing syntenic regions among *Arabidopsis* and the outgroups papaya, poplar, and grape: coge with rosids. *Plant Physiology* **148**:1772–1781. doi: [10.1104/pp.108.124867](https://doi.org/10.1104/pp.108.124867), PMID: [18952863](https://pubmed.ncbi.nlm.nih.gov/18952863/)
- Madan R**, Pankhurst C, Hawke B, Smith S. 2002. Use of fatty acids for identification of AM fungi and estimation of the biomass of AM spores in soil. *Soil Biology and Biochemistry* **34**:125–128. doi: [10.1016/S0038-0717\(01\)00151-1](https://doi.org/10.1016/S0038-0717(01)00151-1)
- Malolepszy A**, Mun T, Sandal N, Gupta V, Dubin M, Urbański D, Shah N, Bachmann A, Fukai E, Hirakawa H, Tabata S, Nadzieja M, Markmann K, Su J, Umehara Y, Soyano T, Miyahara A, Sato S, Hayashi M, Stougaard J, et al. 2016. The LORE1 insertion mutant resource. *The Plant Journal* **88**:306–317. doi: [10.1111/tbj.13243](https://doi.org/10.1111/tbj.13243), PMID: [27322352](https://pubmed.ncbi.nlm.nih.gov/27322352/)
- McGonigle TP**, Miller MH, Evans DG, Fairchild GL, Swan JA. 1990. A new method which gives an objective measure of colonization of roots by vesicular-arbuscular mycorrhizal fungi. *New Phytologist* **115**:495–501. doi: [10.1111/j.1469-8137.1990.tb00476.x](https://doi.org/10.1111/j.1469-8137.1990.tb00476.x)
- Panchuk-Voloshina N**, Haugland RP, Bishop-Stewart J, Bhalgat MK, Millard PJ, Mao F, Leung WY, Haugland RP. 1999. Alexa dyes, a series of new fluorescent dyes that yield exceptionally bright, photostable conjugates. *Journal of Histochemistry & Cytochemistry* **47**:1179–1188. doi: [10.1177/002215549904700910](https://doi.org/10.1177/002215549904700910), PMID: [10449539](https://pubmed.ncbi.nlm.nih.gov/10449539/)
- Panikashvili D**, Shi JX, Schreiber L, Aharoni A. 2011. The *Arabidopsis* ABCG13 transporter is required for flower cuticle secretion and patterning of the petal epidermis. *New Phytologist* **190**:113–124. doi: [10.1111/j.1469-8137.2010.03608.x](https://doi.org/10.1111/j.1469-8137.2010.03608.x), PMID: [21232060](https://pubmed.ncbi.nlm.nih.gov/21232060/)
- Park HJ**, Floss DS, Levesque-Tremblay V, Bravo A, Harrison MJ. 2015. Hyphal Branching during Arbuscule Development Requires Reduced Arbuscular Mycorrhiza1. *Plant Physiology* **169**:2774–2788. doi: [10.1104/pp.15.01155](https://doi.org/10.1104/pp.15.01155), PMID: [26511916](https://pubmed.ncbi.nlm.nih.gov/26511916/)
- Perry JA**, Wang TL, Welham TJ, Gardner S, Pike JM, Yoshida S, Parniske M. 2003. A TILLING reverse genetics tool and a web-accessible collection of mutants of the legume *Lotus japonicus*. *Plant Physiology* **131**:866–871. doi: [10.1104/pp.102.017384](https://doi.org/10.1104/pp.102.017384), PMID: [12644638](https://pubmed.ncbi.nlm.nih.gov/12644638/)
- Perry J**, Brachmann A, Welham T, Binder A, Charpentier M, Groth M, Haage K, Markmann K, Wang TL, Parniske M. 2009. TILLING in *Lotus japonicus* identified large allelic series for symbiosis genes and revealed a Bias in functionally defective ethyl methanesulfonate alleles toward glycine replacements. *Plant Physiology* **151**:1281–1291. doi: [10.1104/pp.109.142190](https://doi.org/10.1104/pp.109.142190), PMID: [19641028](https://pubmed.ncbi.nlm.nih.gov/19641028/)
- Pfeffer PE**, Douds DD, Becard G, Shachar-Hill Y. 1999. Carbon uptake and the metabolism and transport of lipids in an arbuscular mycorrhiza. *Plant Physiology* **120**:587–598. doi: [10.1104/pp.120.2.587](https://doi.org/10.1104/pp.120.2.587), PMID: [10364411](https://pubmed.ncbi.nlm.nih.gov/10364411/)
- Pighin JA**, Zheng H, Balakshin LJ, Goodman IP, Western TL, Jetter R, Kunst L, Samuels AL. 2004. Plant cuticular lipid export requires an ABC transporter. *Science* **306**:702–704. doi: [10.1126/science.1102331](https://doi.org/10.1126/science.1102331), PMID: [15499022](https://pubmed.ncbi.nlm.nih.gov/15499022/)

- Pimprikar P**, Carbonnel S, Paries M, Katzer K, Klingl V, Bohmer MJ, Karl L, Floss DS, Harrison MJ, Parniske M, Gutjahr C. 2016. A CCaMK-CYCLOPS-DELLA complex activates transcription of RAM1 to regulate Arbuscule branching. *Current Biology* **26**:987–998. doi: [10.1016/j.cub.2016.01.069](https://doi.org/10.1016/j.cub.2016.01.069), PMID: 27020747
- Ropars J**, Toro KS, Noel J, Pelin A, Charron P, Farinelli L, Marton T, Krüger M, Fuchs J, Brachmann A, Corradi N. 2016. Evidence for the sexual origin of heterokaryosis in arbuscular mycorrhizal fungi. *Nature Microbiology* **1**:16033. doi: [10.1038/nmicrobiol.2016.33](https://doi.org/10.1038/nmicrobiol.2016.33), PMID: 27572831
- Rozen S**, Skaletsky H. 2000. Primer3 on the WWW for general users and for biologist programmers. In: Krawets S, Misener S (Eds). *Bioinformatics Methods and Protocols: Methods in Molecular Biology*. Totwana: Humana Press. p. 365–386.
- Salas JJ**, Ohlrogge JB. 2002. Characterization of substrate specificity of plant FatA and FatB acyl-ACP thioesterases. *Archives of Biochemistry and Biophysics* **403**:25–34. doi: [10.1016/S0003-9861\(02\)00017-6](https://doi.org/10.1016/S0003-9861(02)00017-6), PMID: 12061798
- Salvioli A**, Ghignone S, Novero M, Navazio L, Venice F, Bagnaresi P, Bonfante P. 2016. Symbiosis with an endobacterium increases the fitness of a mycorrhizal fungus, raising its bioenergetic potential. *The ISME Journal* **10**:130–144. doi: [10.1038/ismej.2015.91](https://doi.org/10.1038/ismej.2015.91), PMID: 26046255
- Sato S**, Nakamura Y, Kaneko T, Asamizu E, Kato T, Nakao M, Sasamoto S, Watanabe A, Ono A, Kawashima K, Fujishiro T, Katoh M, Kohara M, Kishida Y, Minami C, Nakayama S, Nakazaki N, Shimizu Y, Shinpo S, Takahashi C, et al. 2008. Genome structure of the legume, *Lotus japonicus*. *DNA Research* **15**:227–239. doi: [10.1093/dnares/dsn008](https://doi.org/10.1093/dnares/dsn008), PMID: 18511435
- Sawers RJ**, Svane SF, Quan C, Grønlund M, Wozniak B, Gebreselassie MN, González-Muñoz E, Chávez Montes RA, Baxter I, Goudet J, Jakobsen I, Paszkowski U. 2017. Phosphorus acquisition efficiency in arbuscular mycorrhizal maize is correlated with the abundance of root-external hyphae and the accumulation of transcripts encoding PHT1 phosphate transporters. *New Phytologist* **214**:632–643. doi: [10.1111/nph.14403](https://doi.org/10.1111/nph.14403), PMID: 28098948
- Schindelin J**, Arganda-Carreras I, Frise E, Kaynig V, Longair M, Pietzsch T, Preibisch S, Rueden C, Saalfeld S, Schmid B, Tinevez JY, White DJ, Hartenstein V, Eliceiri K, Tomancak P, Cardona A. 2012. Fiji: an open-source platform for biological-image analysis. *Nature Methods* **9**:676–682. doi: [10.1038/nmeth.2019](https://doi.org/10.1038/nmeth.2019), PMID: 22743772
- Shachar-Hill Y**, Pfeffer PE, Doups D, Osman SF, Doner LW, Ratcliffe RG. 1995. Partitioning of intermediary carbon metabolism in vesicular-arbuscular mycorrhizal leek. *Plant Physiology* **108**:7–15. doi: [10.1104/pp.108.1.7](https://doi.org/10.1104/pp.108.1.7), PMID: 12228450
- Smith S**, Read D. 2008. *Mycorrhizal Symbiosis*. Academic Press London.
- Stumpe M**, Carsjens JG, Stenzel I, Göbel C, Lang I, Pawlowski K, Hause B, Feussner I. 2005. Lipid metabolism in arbuscular mycorrhizal roots of *Medicago truncatula*. *Phytochemistry* **66**:781–791 <https://doi.org/10.1016/j.phytochem.2005.01.020>, PMID: 15797604
- Takeda N**, Sato S, Asamizu E, Tabata S, Parniske M. 2009. Apoplastic plant subtilases support arbuscular mycorrhiza development in *Lotus japonicus*. *The Plant Journal* **58**:766–777. doi: [10.1111/j.1365-3113.2009.03824.x](https://doi.org/10.1111/j.1365-3113.2009.03824.x), PMID: 19220794
- Takeda N**, Maekawa T, Hayashi M. 2012. Nuclear-localized and deregulated calcium- and calmodulin-dependent protein kinase activates rhizobial and mycorrhizal responses in *Lotus japonicus*. *The Plant Cell Online* **24**:810–822. doi: [10.1105/tpc.111.091827](https://doi.org/10.1105/tpc.111.091827), PMID: 22337918
- Tamura K**, Peterson D, Peterson N, Stecher G, Nei M, Kumar S. 2011. MEGA5: molecular evolutionary genetics analysis using maximum likelihood, evolutionary distance, and maximum parsimony methods. *Molecular Biology and Evolution* **28**:2731–2739. doi: [10.1093/molbev/msr121](https://doi.org/10.1093/molbev/msr121), PMID: 21546353
- Tang N**, San Clemente H, Roy S, Bécard G, Zhao B, Roux C. 2016. A survey of the Gene repertoire of *Gigaspora rosea* unravels conserved features among Glomeromycota for Obligate Biotrophy. *Frontiers in Microbiology* **7**:233. doi: [10.3389/fmicb.2016.00233](https://doi.org/10.3389/fmicb.2016.00233), PMID: 26973612
- Tisserant E**, Kohler A, Dozolme-Seddas P, Balestrini R, Benabdellah K, Colard A, Croll D, Da Silva C, Gomez SK, Koul R, Ferrol N, Fiorilli V, Formey D, Franken P, Helber N, Hijri M, Lanfranco L, Lindquist E, Liu Y, Malbreil M, et al. 2012. The transcriptome of the arbuscular mycorrhizal fungus *Glomus intraradices* (DAOM 197198) reveals functional tradeoffs in an obligate symbiont. *New Phytologist* **193**:755–769. doi: [10.1111/j.1469-8137.2011.03948.x](https://doi.org/10.1111/j.1469-8137.2011.03948.x), PMID: 22092242
- Trépanier M**, Bécard G, Moutoglou P, Willemot C, Gagné S, Avis TJ, Rioux JA. 2005. Dependence of arbuscular-mycorrhizal fungi on their plant host for palmitic acid synthesis. *Applied and Environmental Microbiology* **71**:5341–5347. doi: [10.1128/AEM.71.9.5341-5347.2005](https://doi.org/10.1128/AEM.71.9.5341-5347.2005), PMID: 16151123
- Vierheilig H**, Coughlan AP, Wyss U, Piche Y. 1998. Ink and vinegar, a simple staining technique for arbuscular-mycorrhizal fungi. *Applied and Environmental Microbiology* **64**:5004–5007. PMID: 9835596
- Volpe V**, Dell'Aglio E, Giovannetti M, Ruberti C, Costa A, Genre A, Guether M, Bonfante P. 2013. An AM-induced, MYB-family gene of *Lotus japonicus* (*LjMAMI*) affects root growth in an AM-independent manner. *The Plant Journal* **73**:442–455. doi: [10.1111/tpj.12045](https://doi.org/10.1111/tpj.12045), PMID: 23051146
- Wang J**, Grishin N, Kinch L, Cohen JC, Hobbs HH, Xie XS. 2011. Sequences in the nonconsensus nucleotide-binding domain of ABCG5/ABCG8 required for sterol transport. *Journal of Biological Chemistry* **286**:7308–7314. doi: [10.1074/jbc.M110.210880](https://doi.org/10.1074/jbc.M110.210880), PMID: 21209088
- Wang E**, Schornack S, Marsh JF, Gobbato E, Schwessinger B, Eastmond P, Schultze M, Kamoun S, Oldroyd GE. 2012. A common signaling process that promotes mycorrhizal and oomycete colonization of plants. *Current Biology* **22**:2242–2246. doi: [10.1016/j.cub.2012.09.043](https://doi.org/10.1016/j.cub.2012.09.043), PMID: 23122843
- Welti R**, Li W, Li M, Sang Y, Biesiada H, Zhou HE, Rajashekar CB, Williams TD, Wang X. 2002. Profiling membrane lipids in plant stress responses. role of phospholipase D alpha in freezing-induced lipid changes in

- Arabidopsis*. *The Journal of Biological Chemistry* **277**:31994–32002. doi: [10.1074/jbc.M205375200](https://doi.org/10.1074/jbc.M205375200), PMID: [12077151](https://pubmed.ncbi.nlm.nih.gov/12077151/)
- Wewer V**, Dombrink I, vom Dorp K, Dörmann P. 2011. Quantification of sterol lipids in plants by quadrupole time-of-flight mass spectrometry. *Journal of Lipid Research* **52**:1039–1054. doi: [10.1194/jlr.D013987](https://doi.org/10.1194/jlr.D013987), PMID: [21382968](https://pubmed.ncbi.nlm.nih.gov/21382968/)
- Wewer V**, Dörmann P, Hölzl G. 2013. Analysis and quantification of plant membrane lipids by thin-layer chromatography and gas chromatography. In: Munnik T, Heilmann I (Eds). *Plant Lipid Signaling Protocols*. Totowa: Humana Press. p. 69–78. doi: [10.1007/978-1-62703-401-2\\_8](https://doi.org/10.1007/978-1-62703-401-2_8)
- Wewer V**, Brands M, Dörmann P. 2014. Fatty acid synthesis and lipid metabolism in the obligate biotrophic fungus *rhizophagus irregularis* during mycorrhization of *Lotus japonicus*. *The Plant Journal* **79**:398–412. doi: [10.1111/tpj.12566](https://doi.org/10.1111/tpj.12566), PMID: [24888347](https://pubmed.ncbi.nlm.nih.gov/24888347/)
- Wittenburg H**, Carey MC. 2002. Biliary cholesterol secretion by the twinned sterol half-transporters ABCG5 and ABCG8. *Journal of Clinical Investigation* **110**:605–609. doi: [10.1172/JCI0216548](https://doi.org/10.1172/JCI0216548), PMID: [12208859](https://pubmed.ncbi.nlm.nih.gov/12208859/)
- Wu GZ**, Xue HW. 2010. *Arabidopsis*  $\beta$ -ketoacyl-[acyl carrier protein] synthase i is crucial for fatty acid synthesis and plays a role in chloroplast division and embryo development. *The Plant Cell* **22**:3726–3744. doi: [10.1105/tpc.110.075564](https://doi.org/10.1105/tpc.110.075564), PMID: [21081696](https://pubmed.ncbi.nlm.nih.gov/21081696/)
- Xue L**, Cui H, Buer B, Vijayakumar V, Delaux PM, Junkermann S, Bucher M. 2015. Network of GRAS transcription factors involved in the control of arbuscule development in *Lotus japonicus*. *Plant Physiology* **167**:854–871. doi: [10.1104/pp.114.255430](https://doi.org/10.1104/pp.114.255430), PMID: [25560877](https://pubmed.ncbi.nlm.nih.gov/25560877/)
- Yang W**, Pollard M, Li-Beisson Y, Beisson F, Feig M, Ohlrogge J. 2010. A distinct type of glycerol-3-phosphate acyltransferase with sn-2 preference and phosphatase activity producing 2-monoacylglycerol. *PNASUSA* **107**:12040–12045. doi: [10.1073/pnas.0914149107](https://doi.org/10.1073/pnas.0914149107), PMID: [20551224](https://pubmed.ncbi.nlm.nih.gov/20551224/)
- Yang W**, Simpson JP, Li-Beisson Y, Beisson F, Pollard M, Ohlrogge JB. 2012. A land-plant-specific glycerol-3-phosphate acyltransferase family in *Arabidopsis*: substrate specificity, sn-2 preference, and evolution. *Plant Physiology* **160**:638–652. doi: [10.1104/pp.112.201996](https://doi.org/10.1104/pp.112.201996), PMID: [22864585](https://pubmed.ncbi.nlm.nih.gov/22864585/)
- Yano K**, Yoshida S, Müller J, Singh S, Banba M, Vickers K, Markmann K, White C, Schuller B, Sato S, Asamizu E, Tabata S, Murooka Y, Perry J, Wang TL, Kawaguchi M, Imaizumi-Anraku H, Hayashi M, Parniske M. 2008. CYCLOPS, a mediator of symbiotic intracellular accommodation. *PNAS* **105**:20540–20545. doi: [10.1073/pnas.0806858105](https://doi.org/10.1073/pnas.0806858105), PMID: [19074278](https://pubmed.ncbi.nlm.nih.gov/19074278/)
- Yeats TH**, Martin LB, Viart HM, Isaacson T, He Y, Zhao L, Matas AJ, Buda GJ, Domozych DS, Clausen MH, Rose JK. 2012. The identification of cutin synthase: formation of the plant polyester cutin. *Nature Chemical Biology* **8**:609–611. doi: [10.1038/nchembio.960](https://doi.org/10.1038/nchembio.960), PMID: [22610035](https://pubmed.ncbi.nlm.nih.gov/22610035/)
- Zhang Q**, Blaylock LA, Harrison MJ. 2010. Two *Medicago truncatula* half-ABC transporters are essential for arbuscule development in arbuscular mycorrhizal symbiosis. *The Plant Cell Online* **22**:1483–1497. doi: [10.1105/tpc.110.074955](https://doi.org/10.1105/tpc.110.074955), PMID: [20453115](https://pubmed.ncbi.nlm.nih.gov/20453115/)
- van Aarle IM**, Olsson PA. 2003. Fungal lipid accumulation and development of mycelial structures by two arbuscular mycorrhizal fungi. *Applied and Environmental Microbiology* **69**:6762–6767. doi: [10.1128/AEM.69.11.6762-6767.2003](https://doi.org/10.1128/AEM.69.11.6762-6767.2003), PMID: [14602638](https://pubmed.ncbi.nlm.nih.gov/14602638/)

Figure 1 –figure Supplements 1

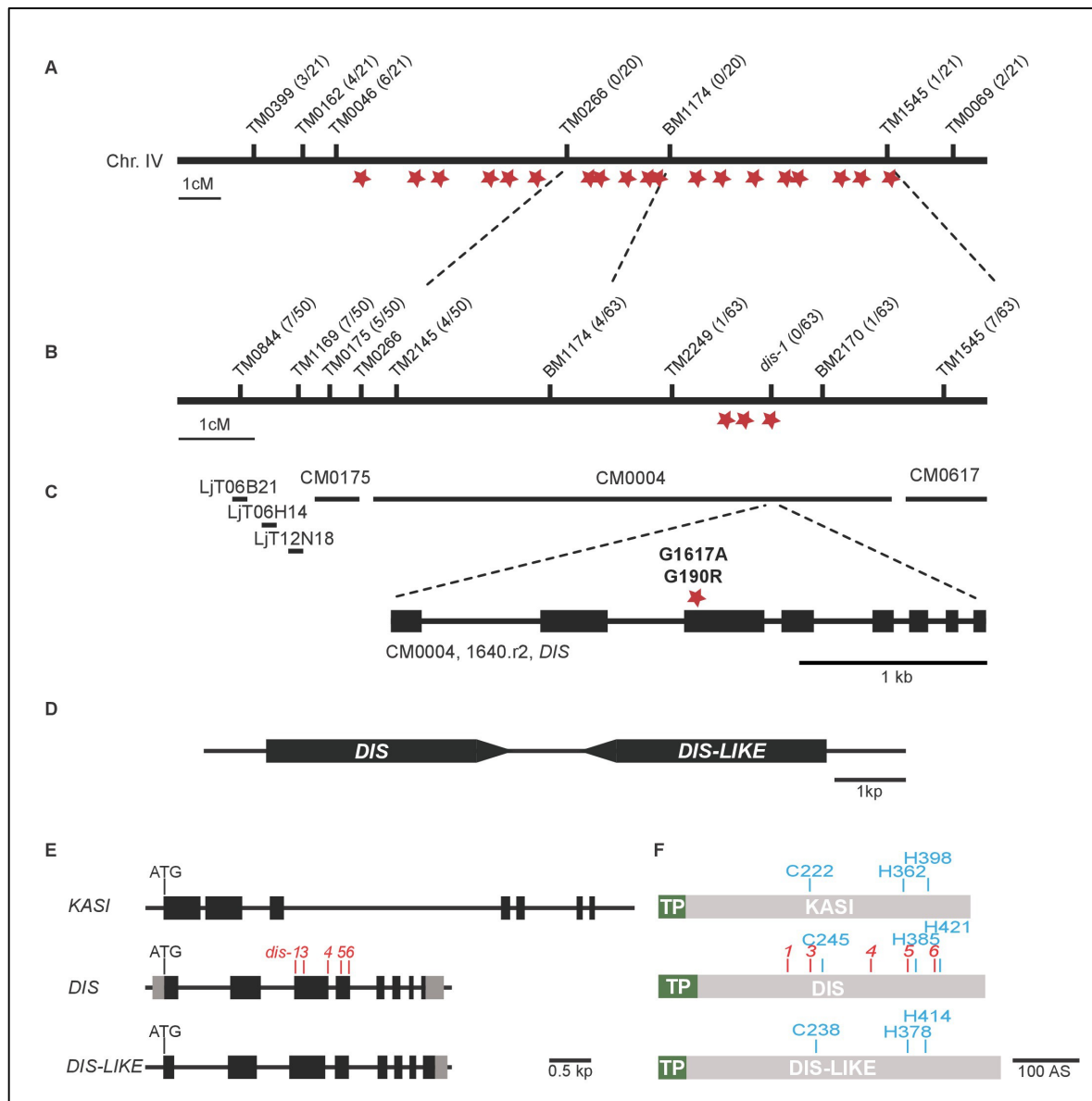


Figure 1 –figure Supplements 2

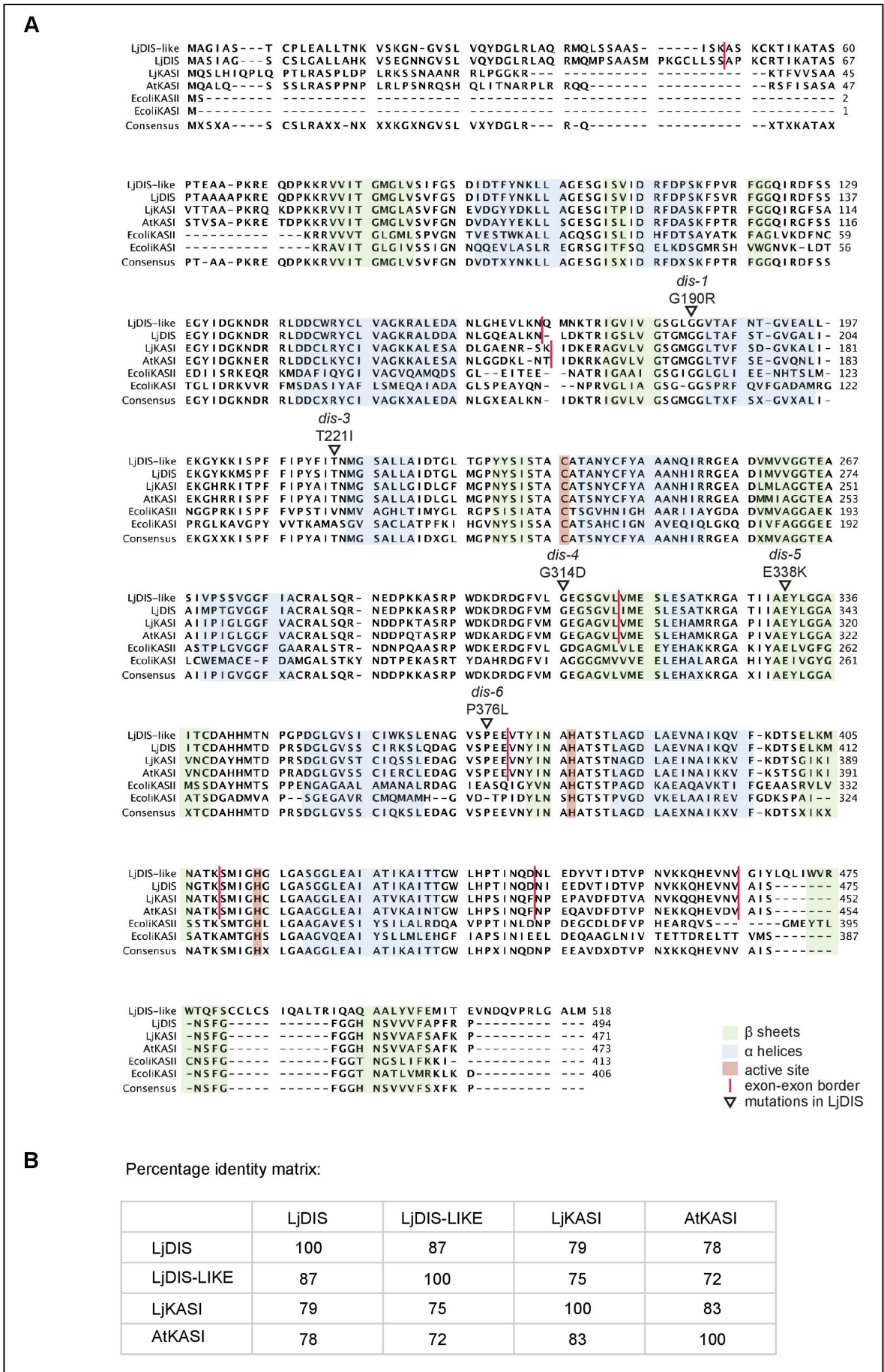


Figure 1 –figure Supplements 3

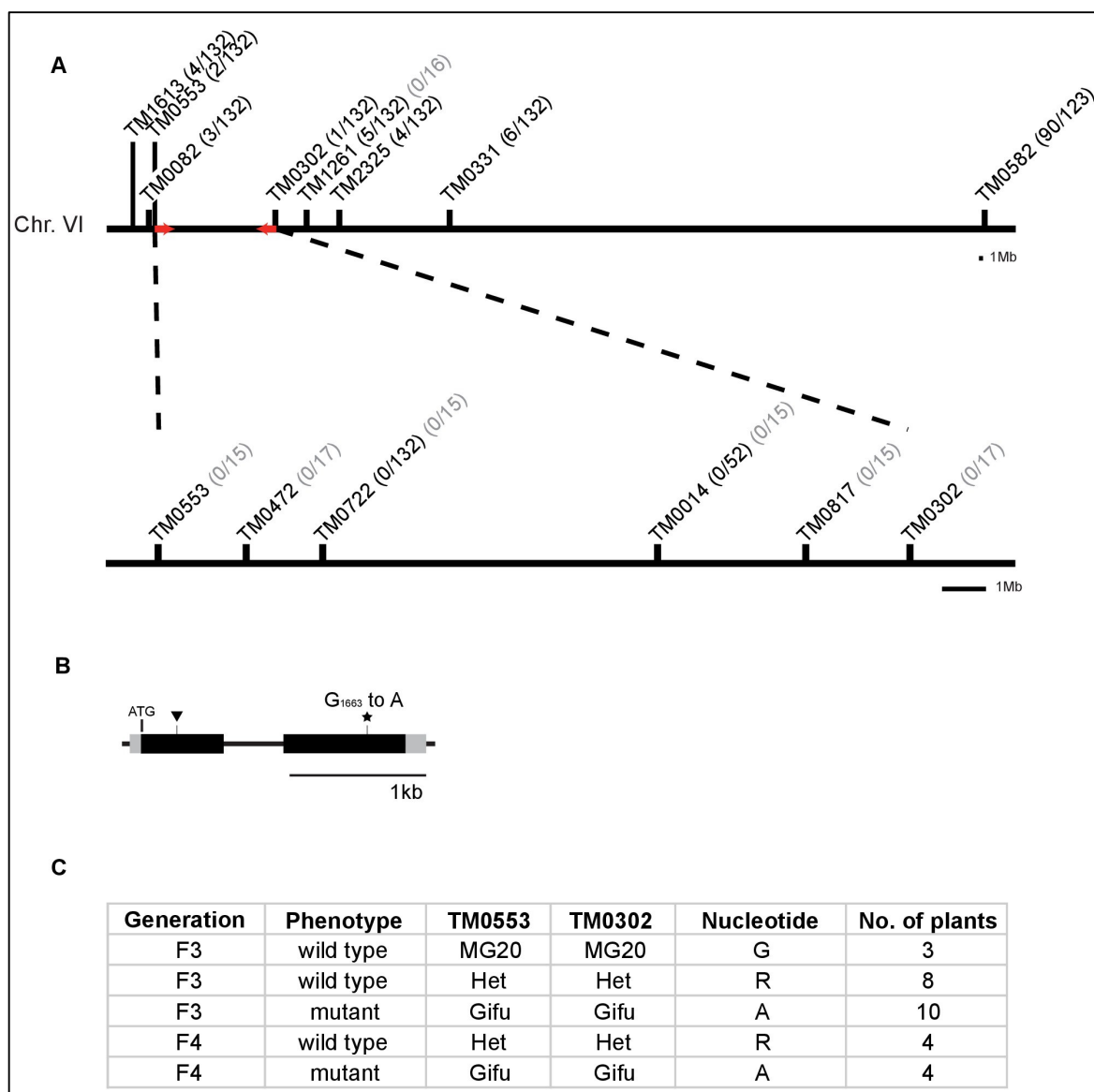


Figure 1 –figure Supplements 4

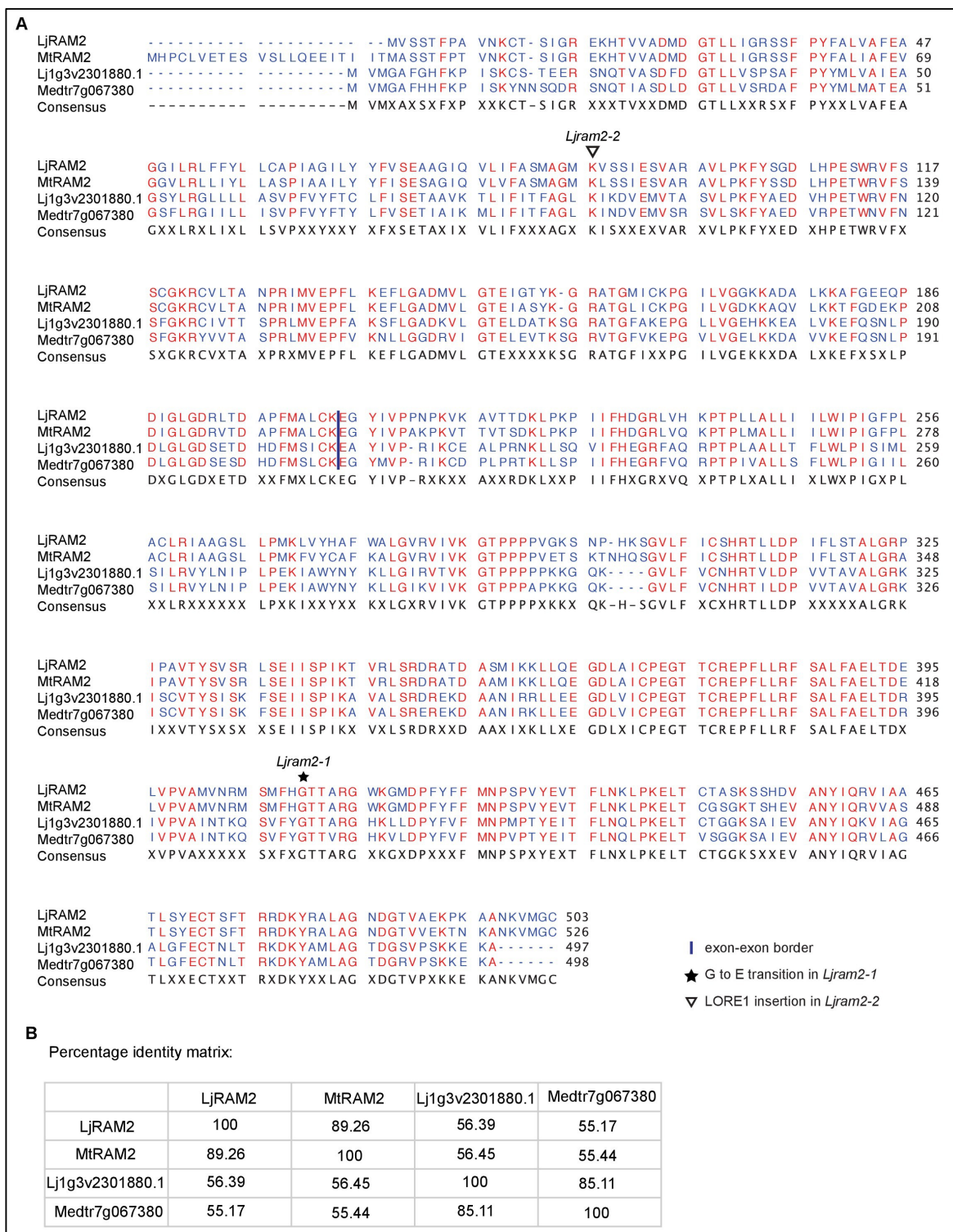


Figure 2 –figure Supplements 1

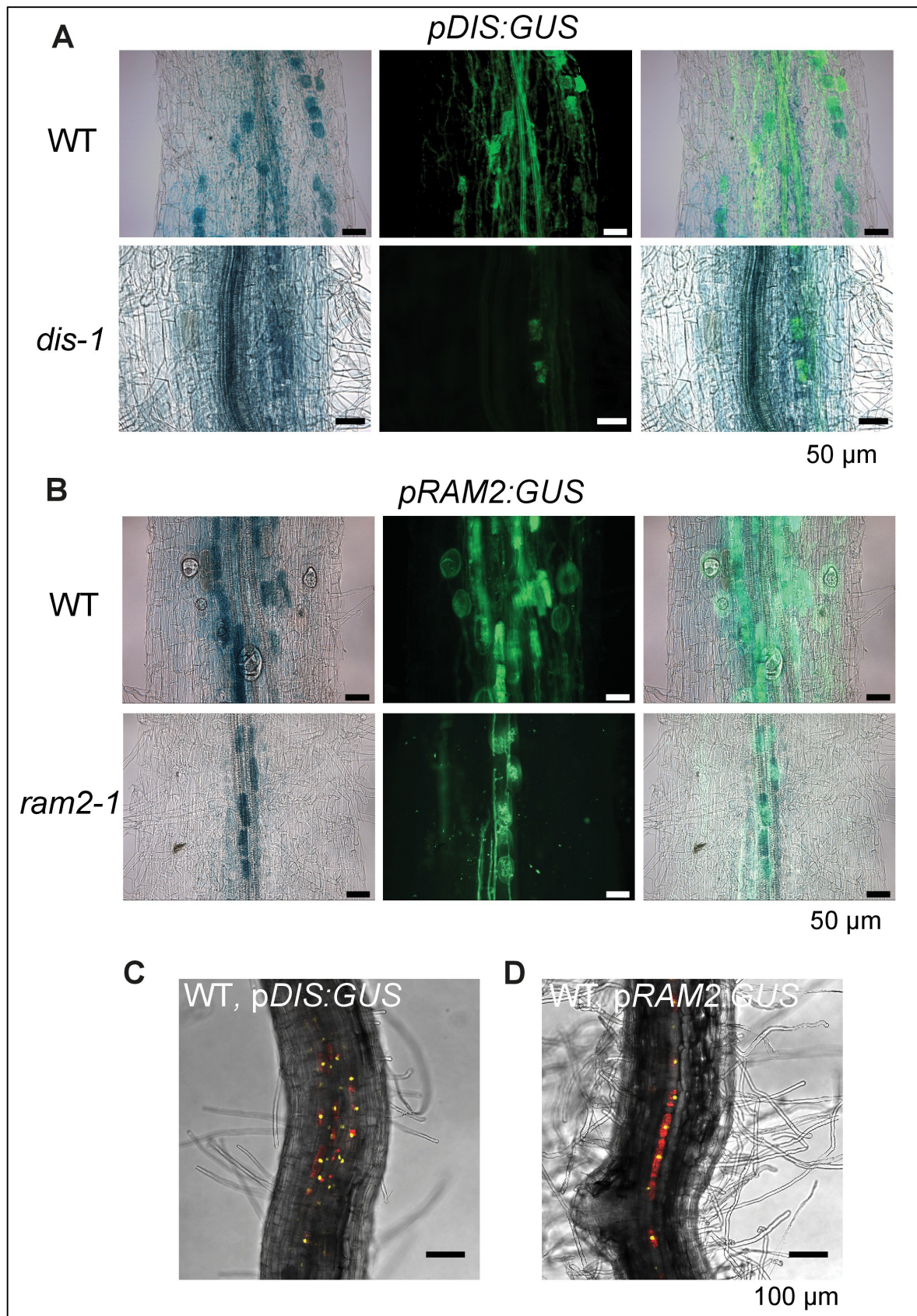


Figure 3 –figure Supplements 1

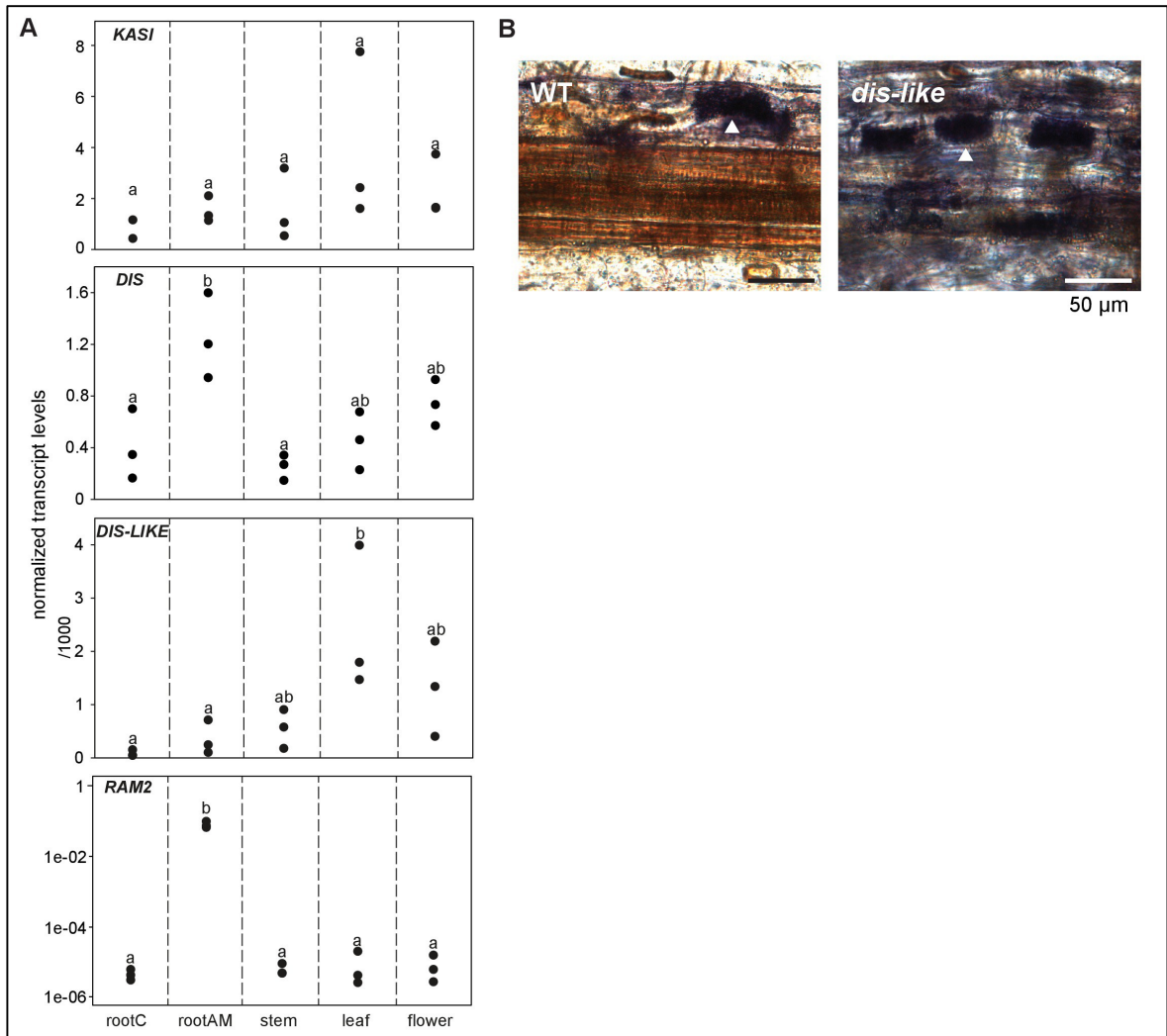


Figure 3 –figure Supplements 2

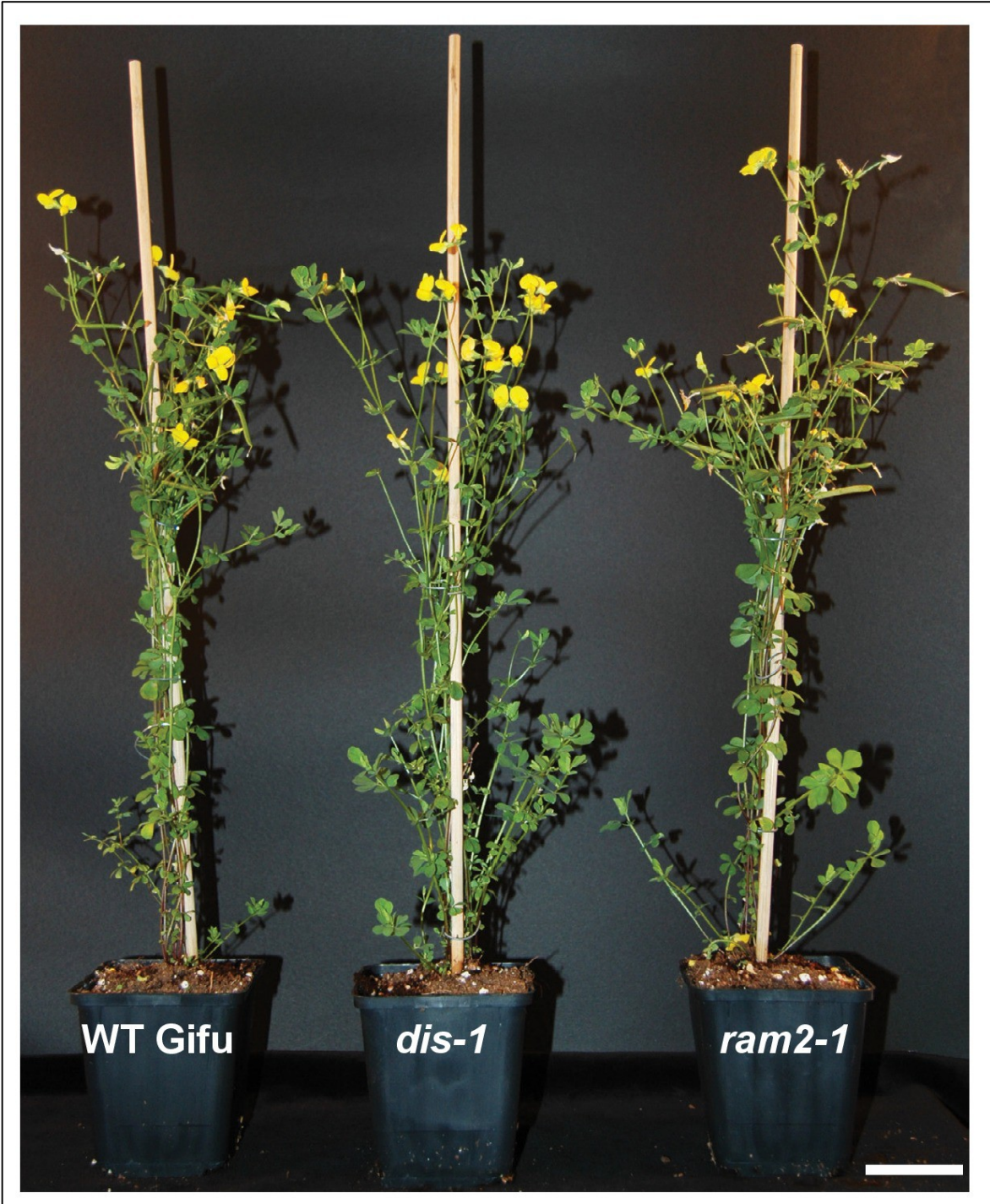


Figure 3 –figure Supplements 3

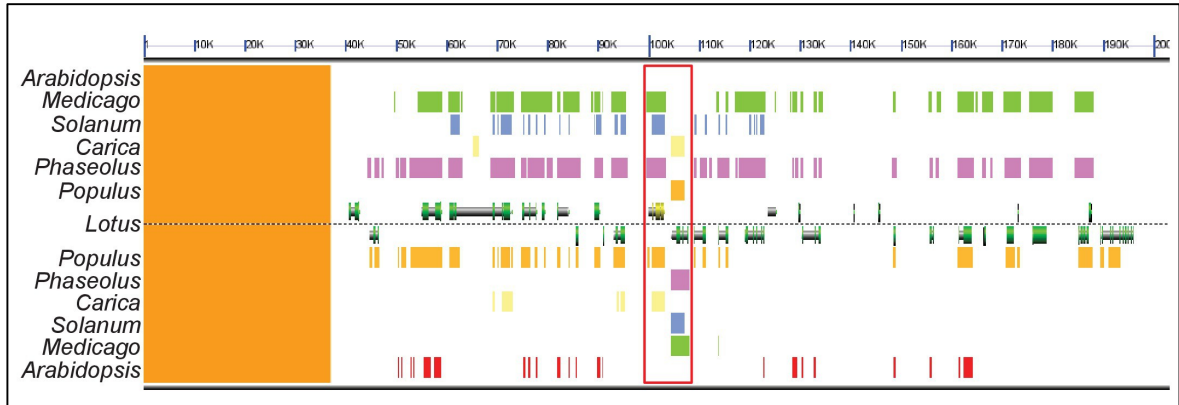


Figure 5 –figure Supplements 1

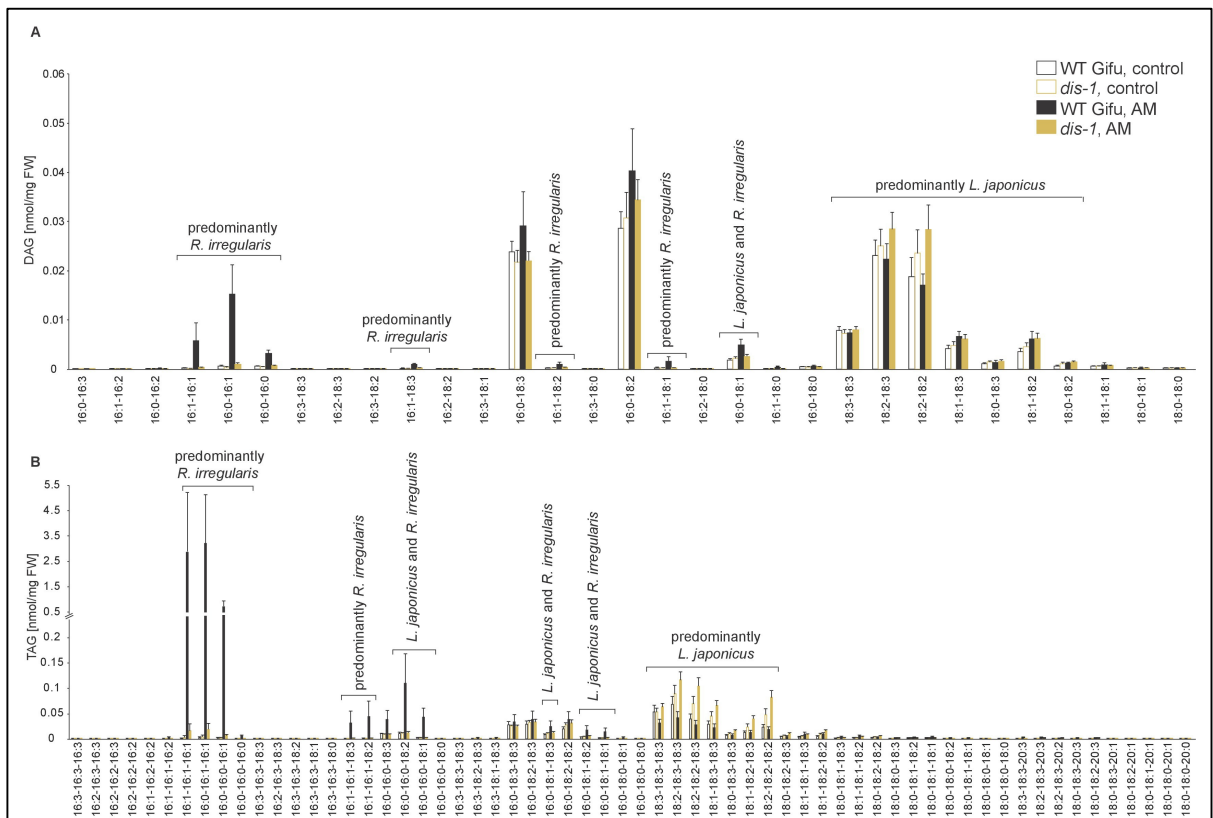


Figure 5 –figure Supplements 2

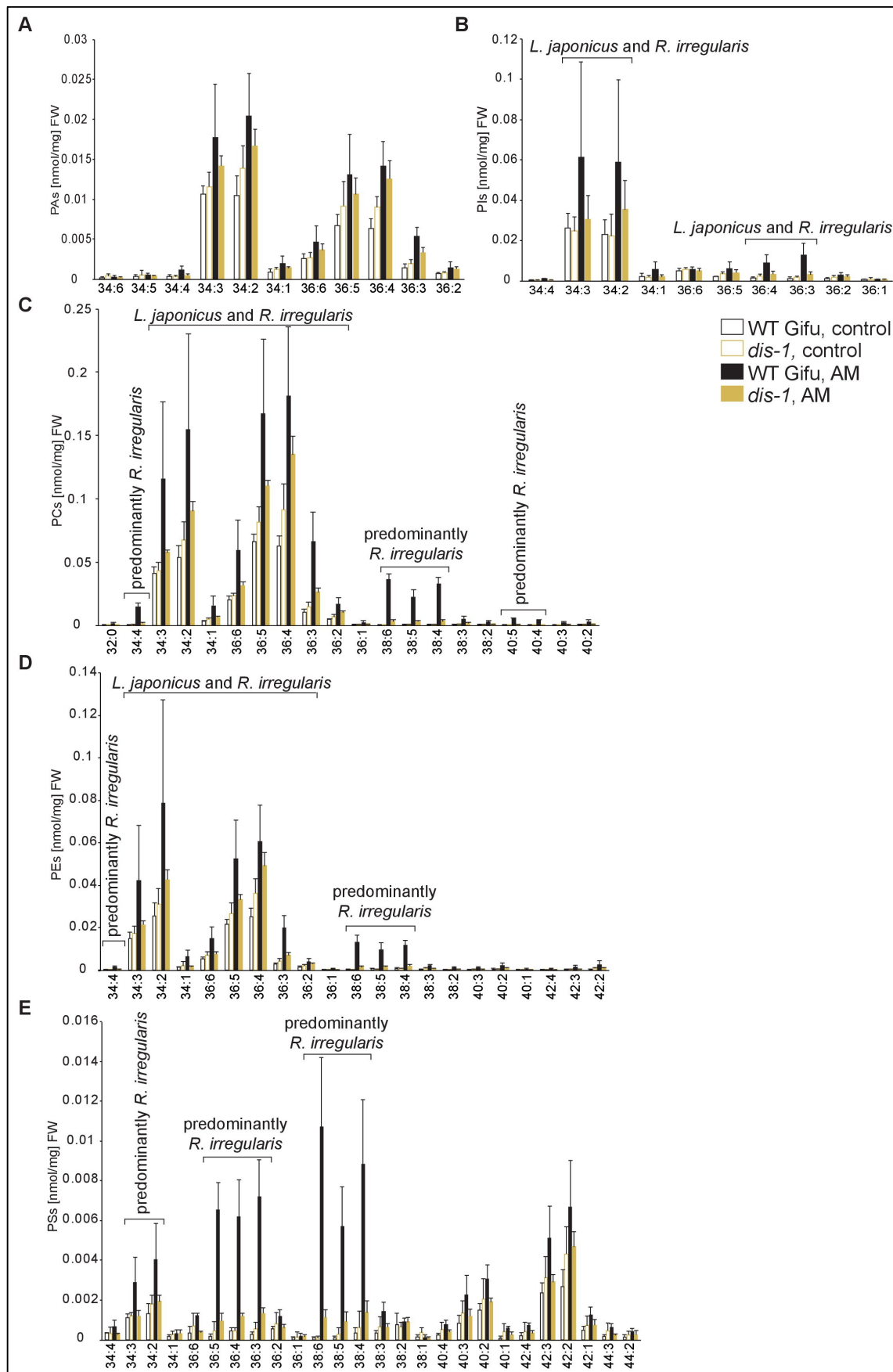


Figure 5 –figure Supplements 3

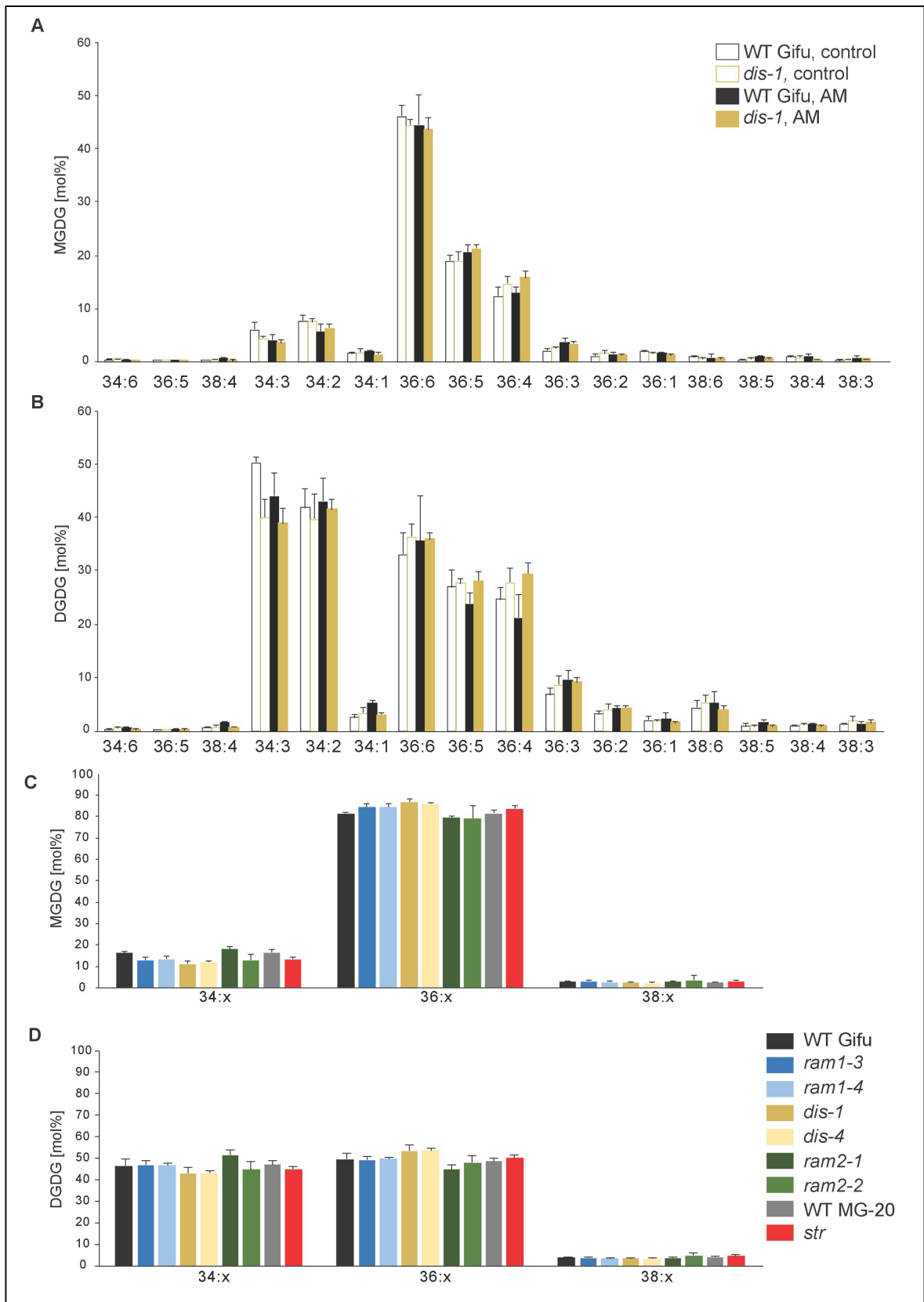


Figure 5 –figure Supplements 4

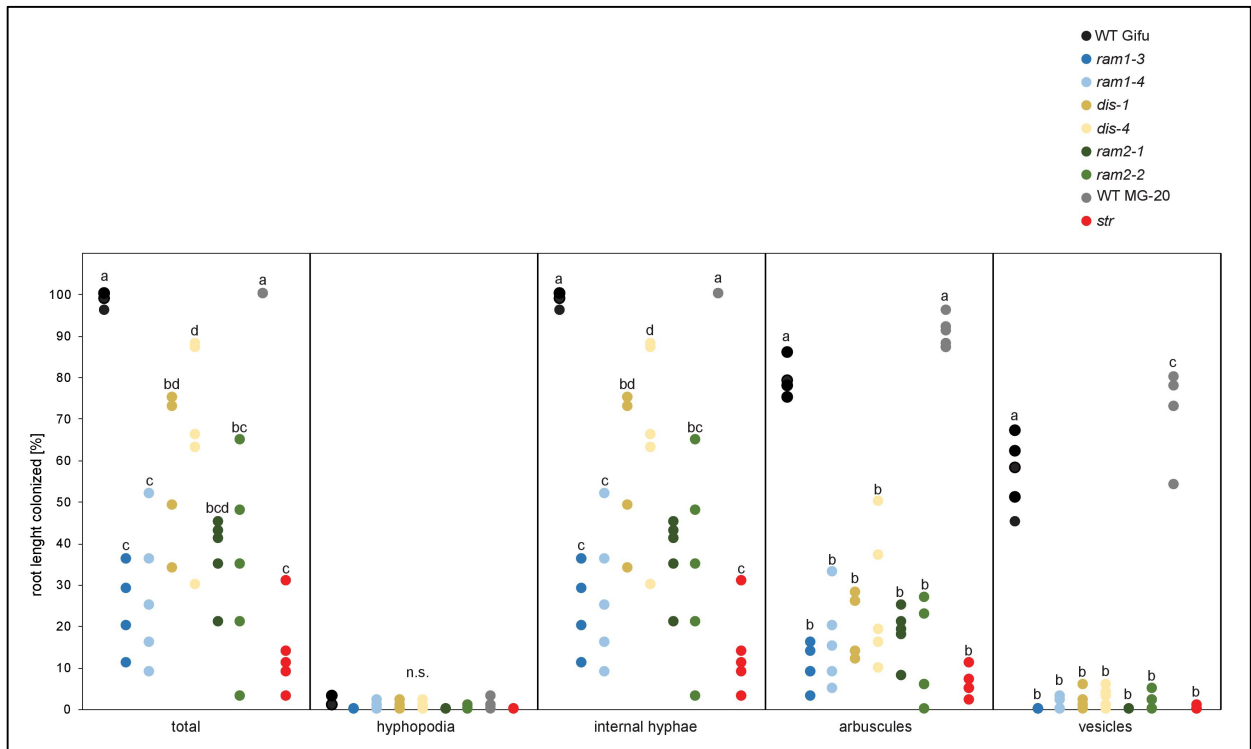


Figure 5 –figure Supplements 5

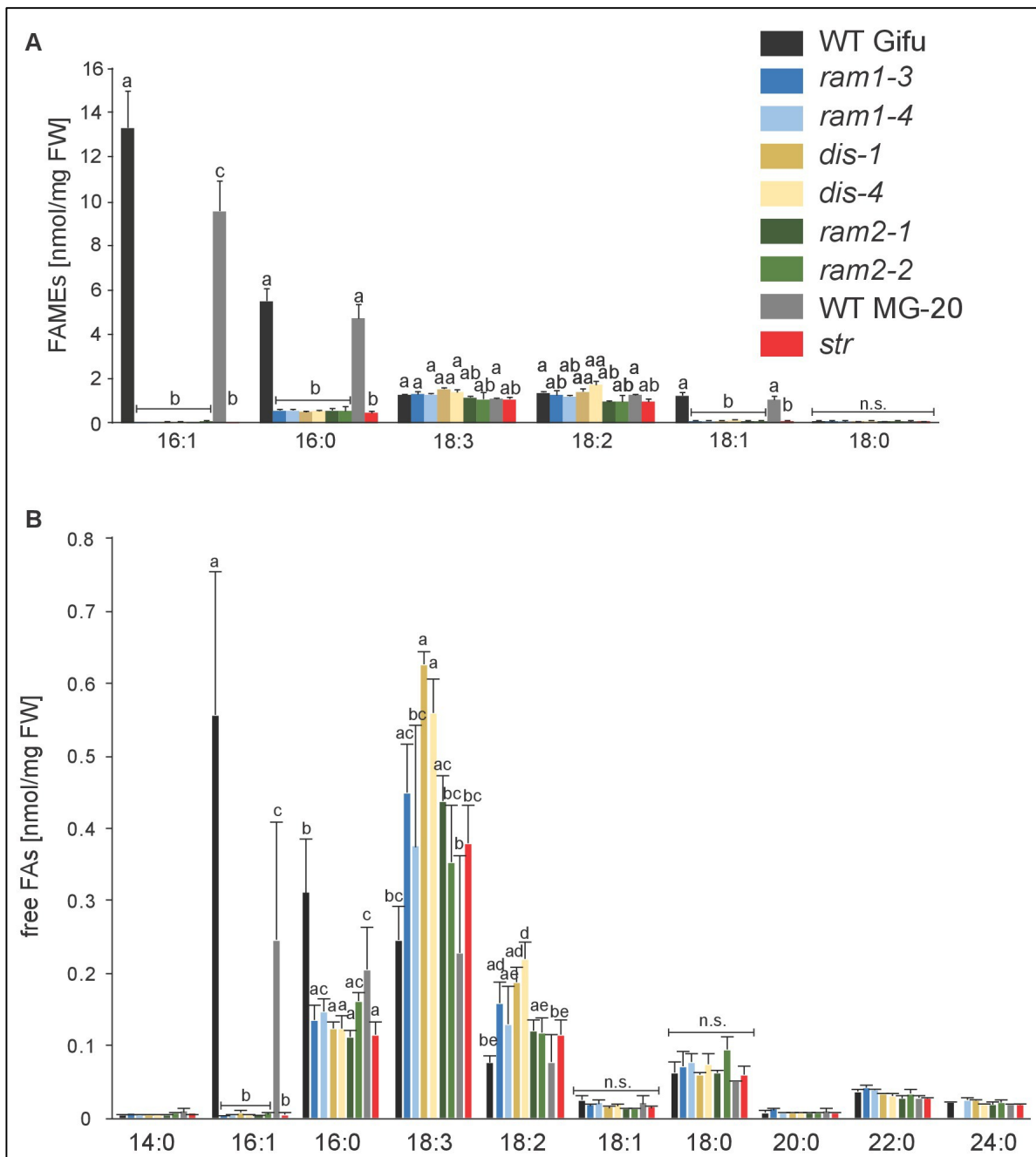


Figure 5 –figure Supplements 6

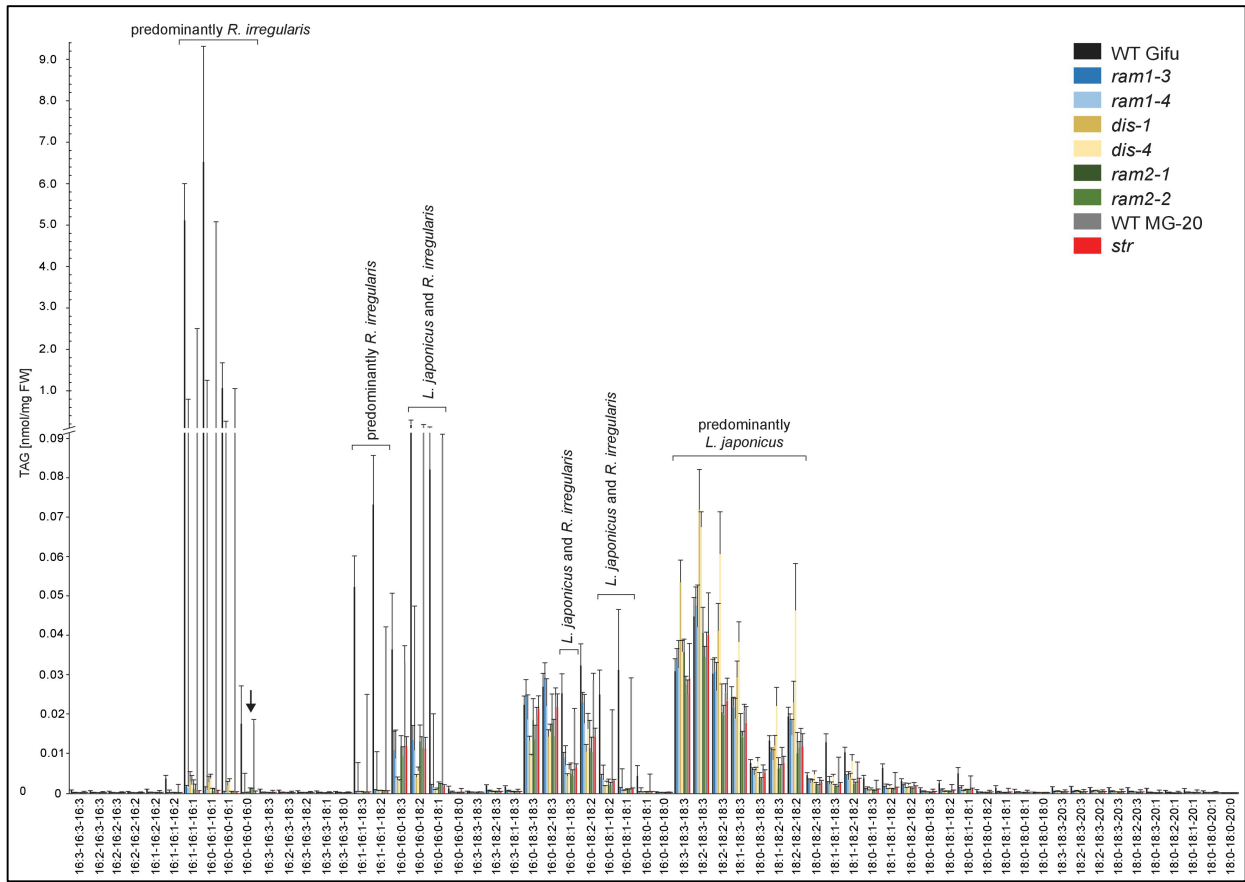


Figure 5 –figure Supplements 7

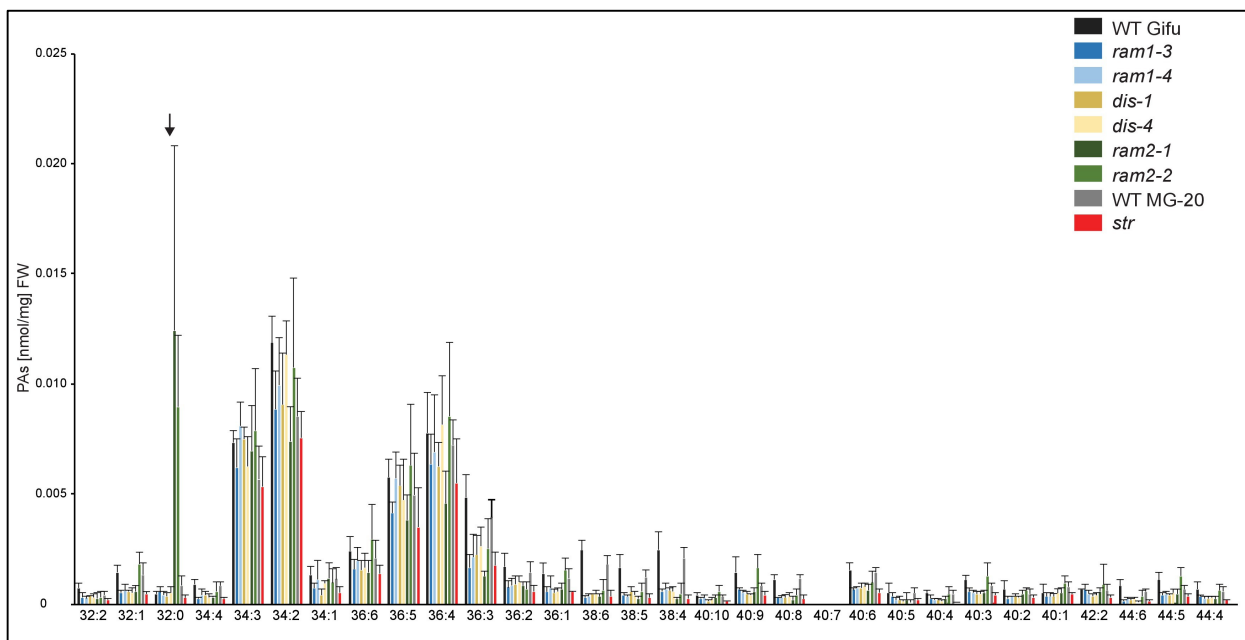


Figure 5 –figure Supplements 8

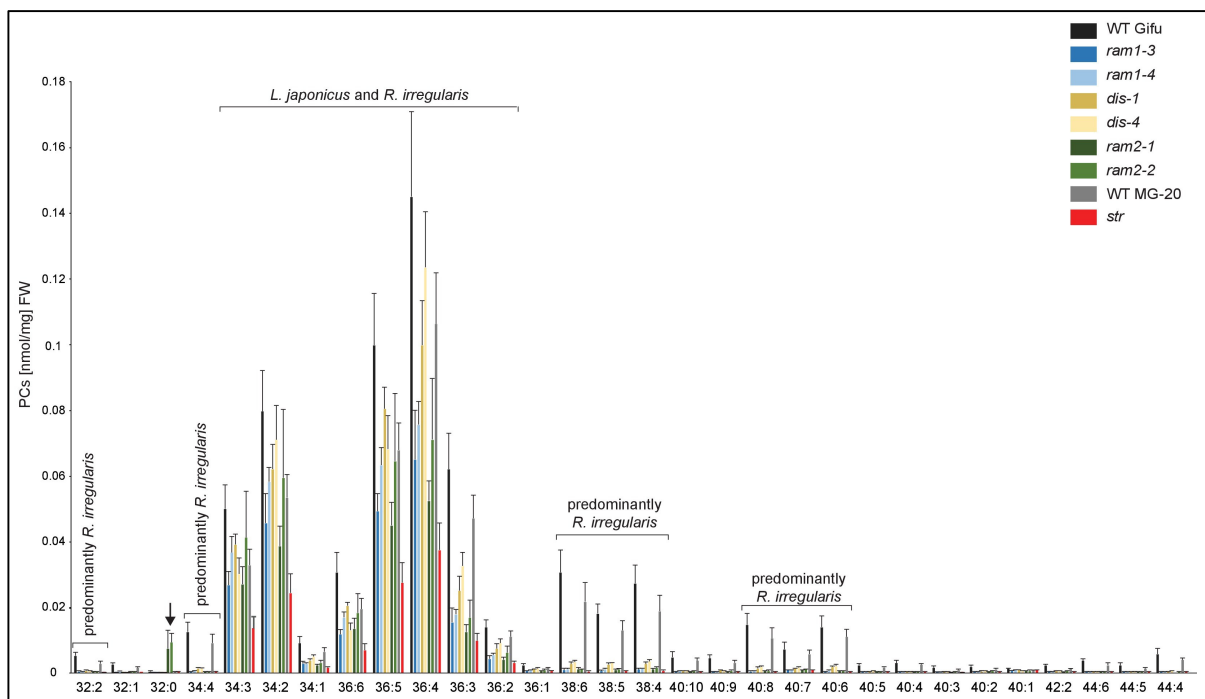


Figure 5 –figure Supplement 9

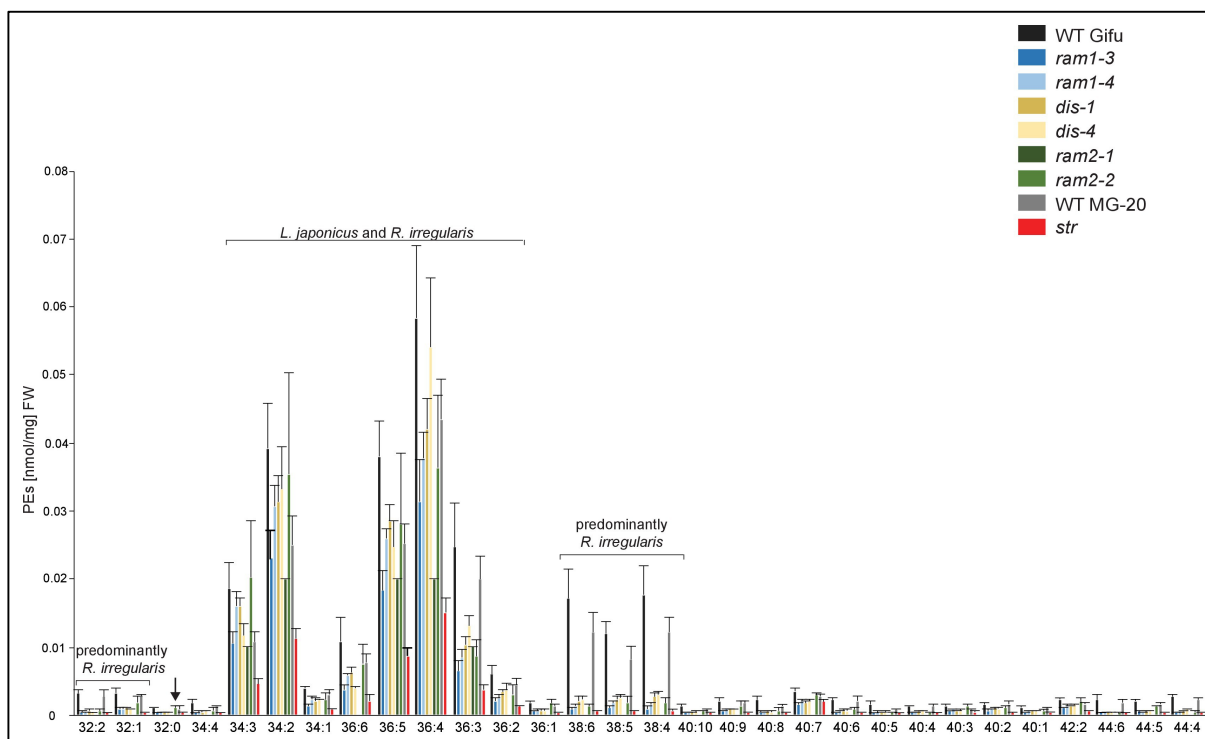


Figure 5 –figure Supplements 10

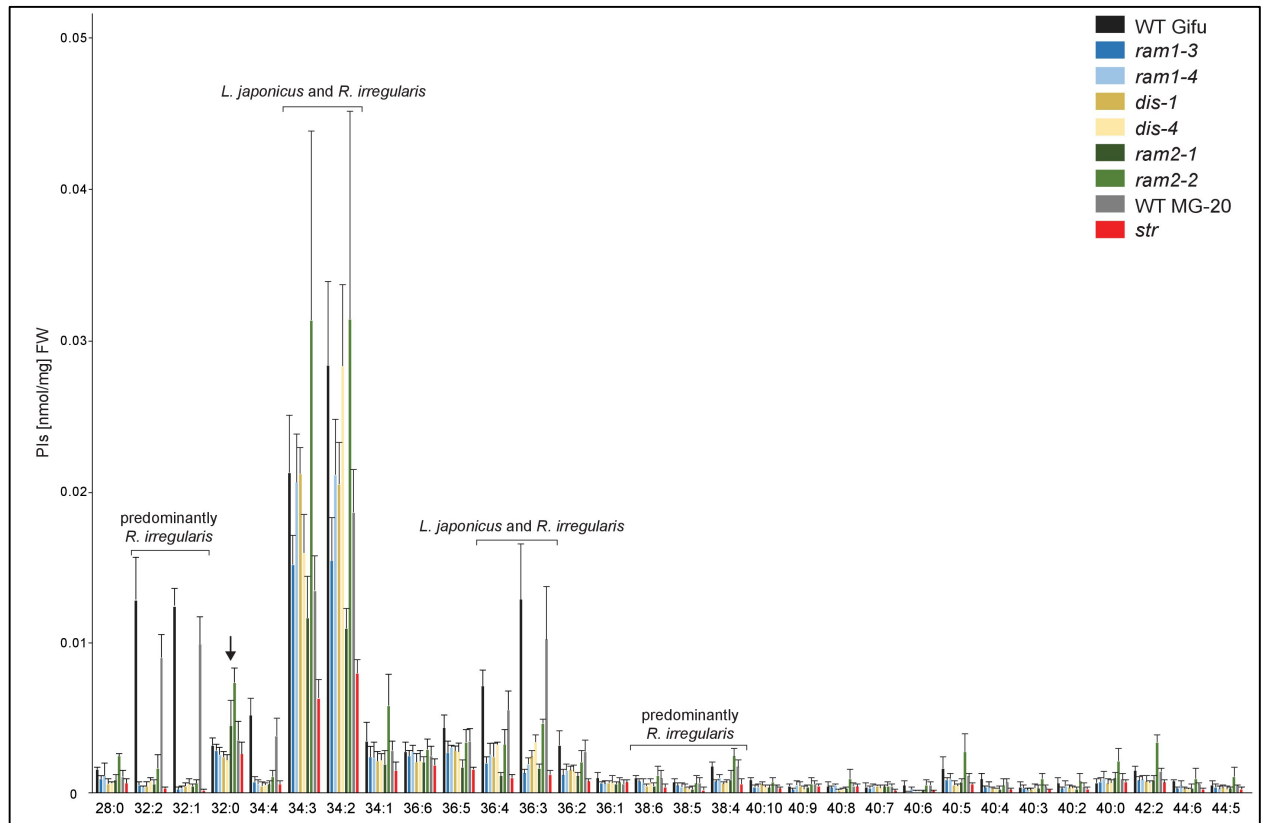


Figure 5 –figure Supplements 11

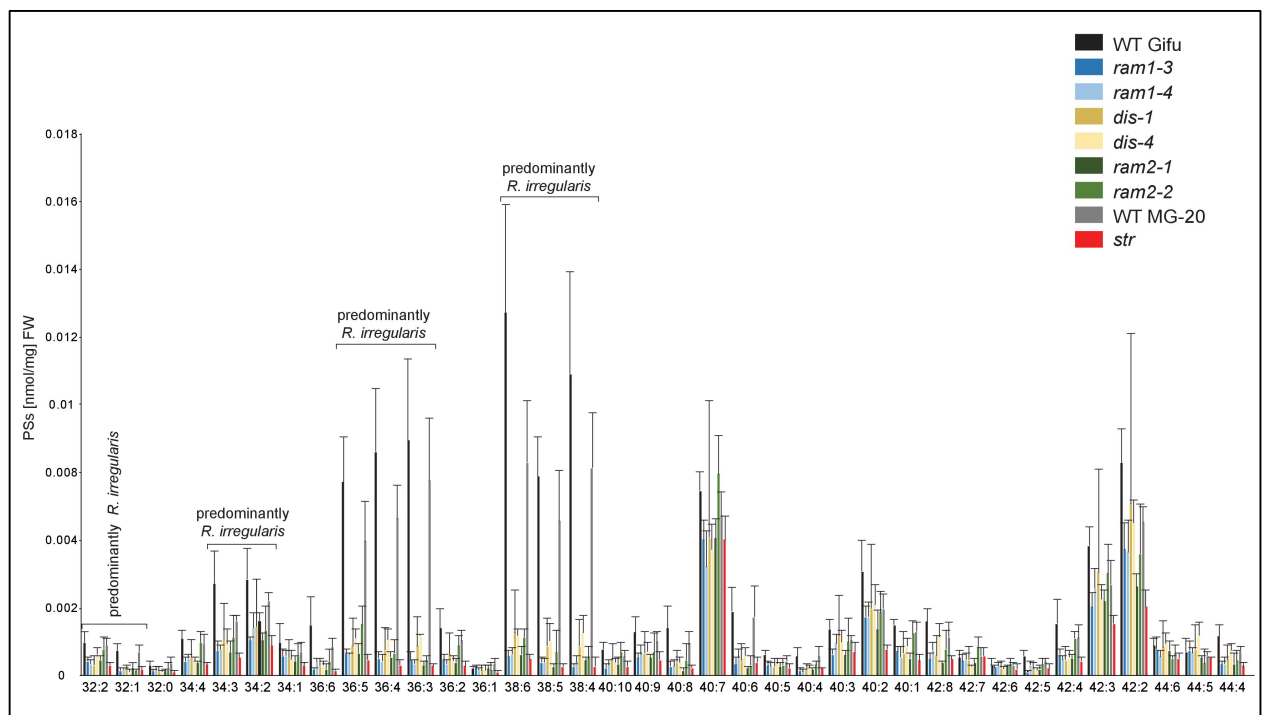


Figure 8 –figure Supplements 1

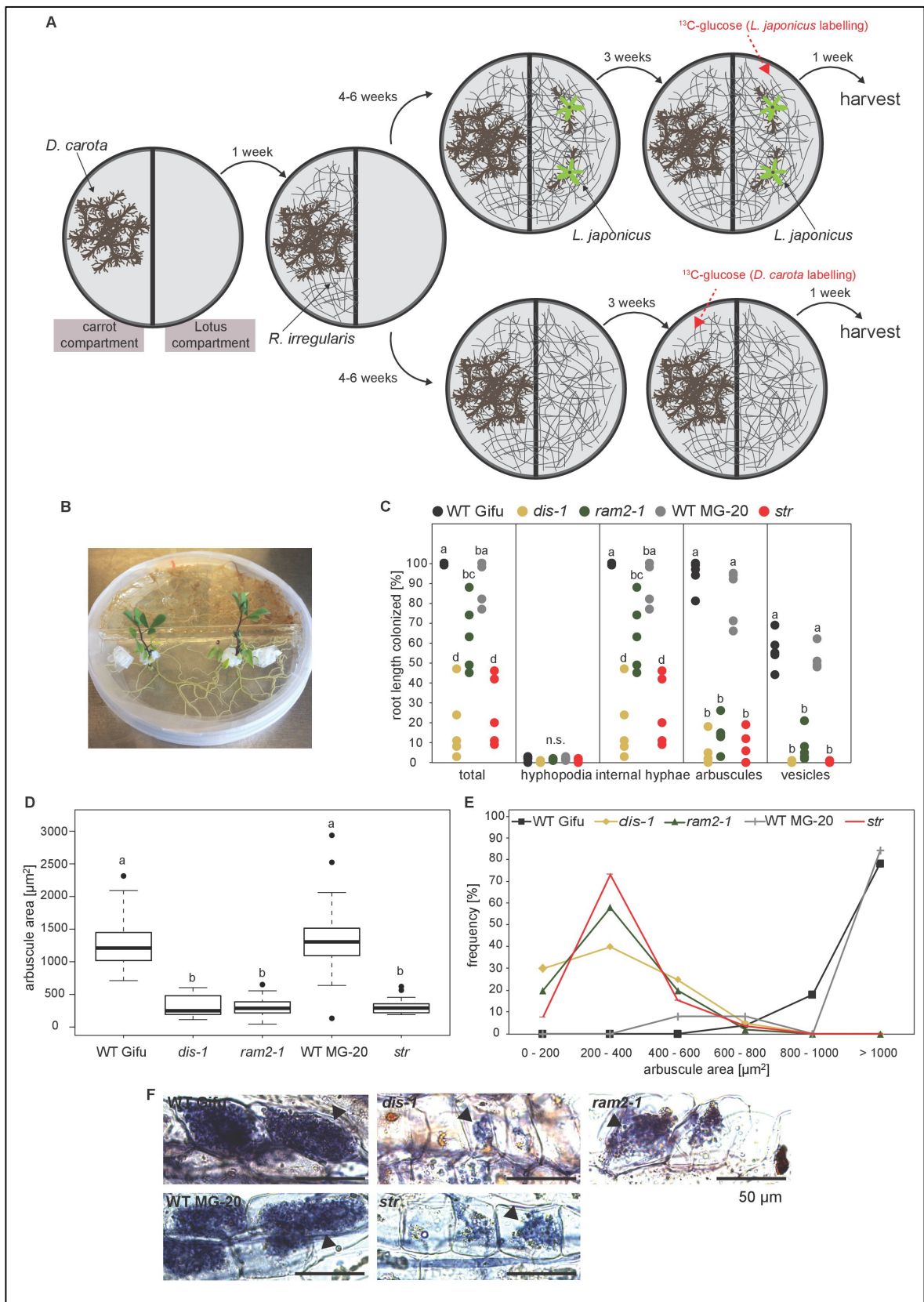


Figure 8 –figure Supplements 2

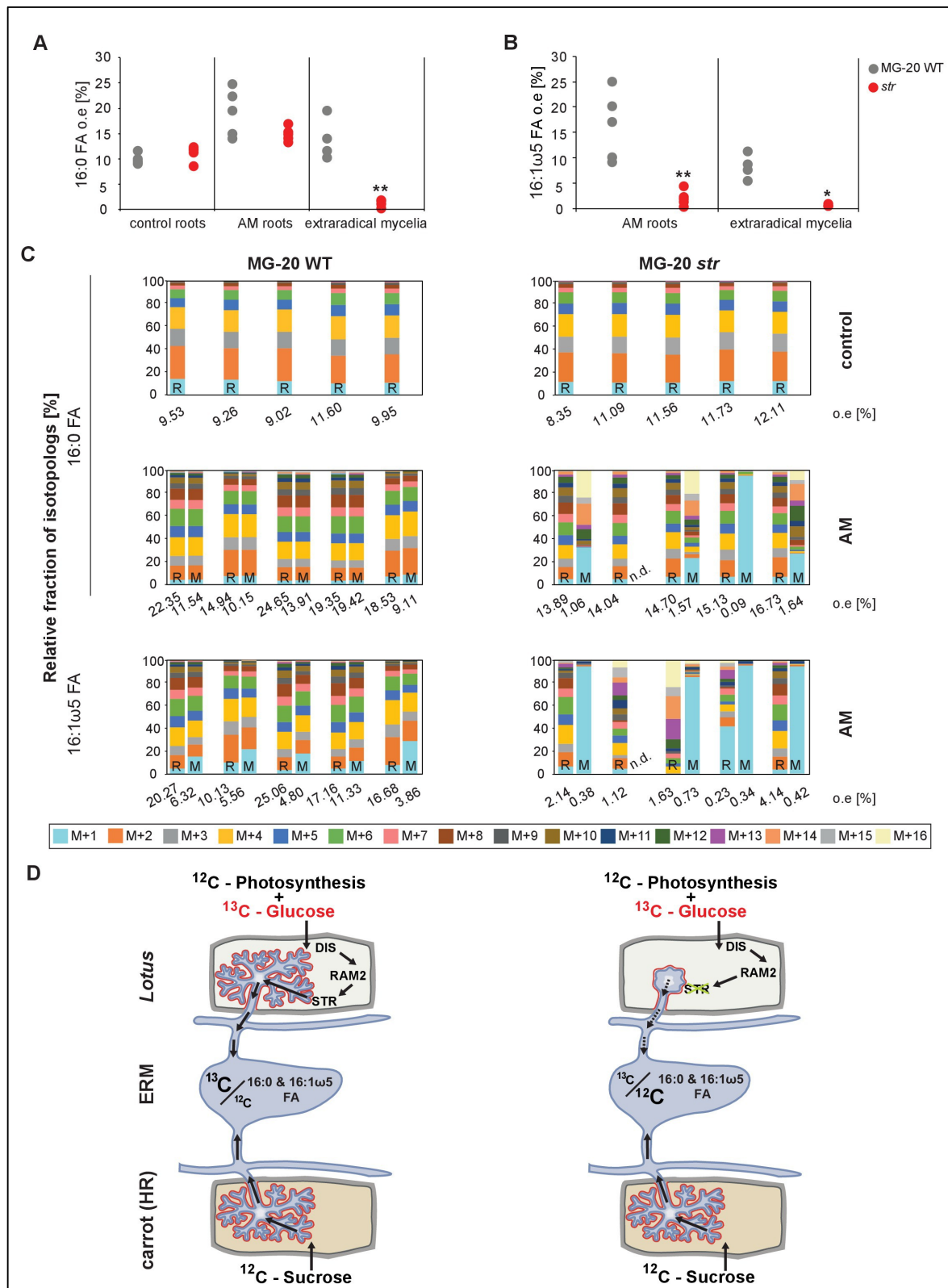


Figure 8 –figure Supplements 3

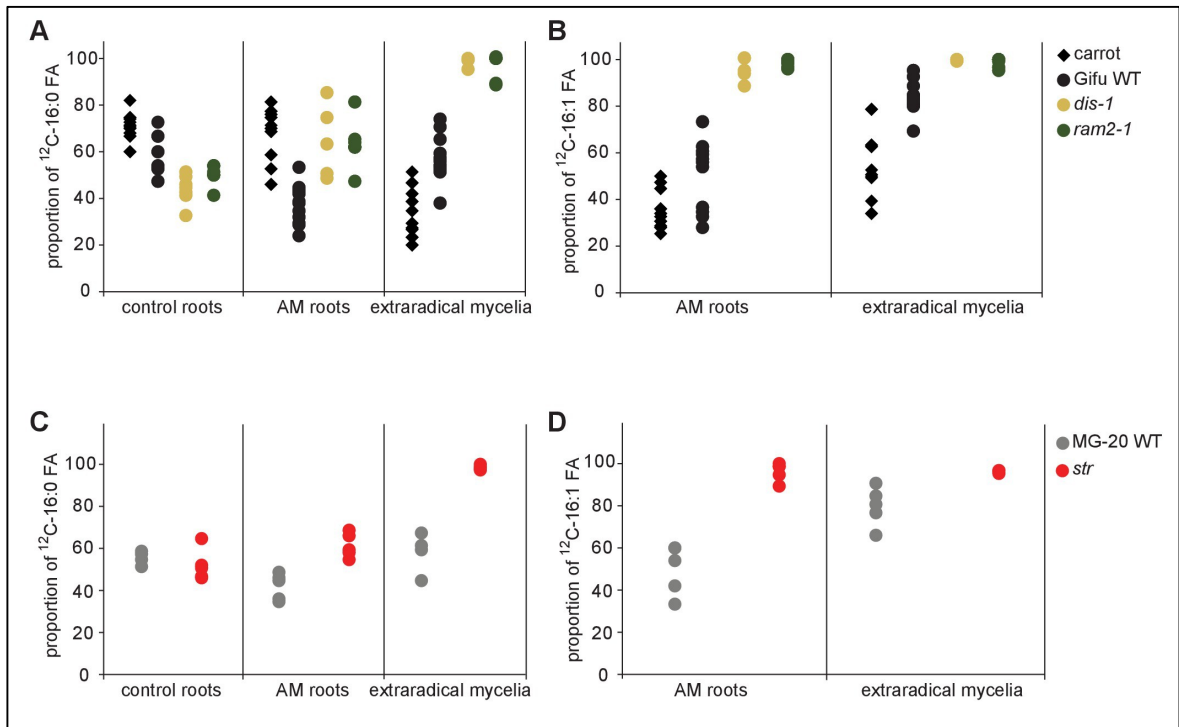
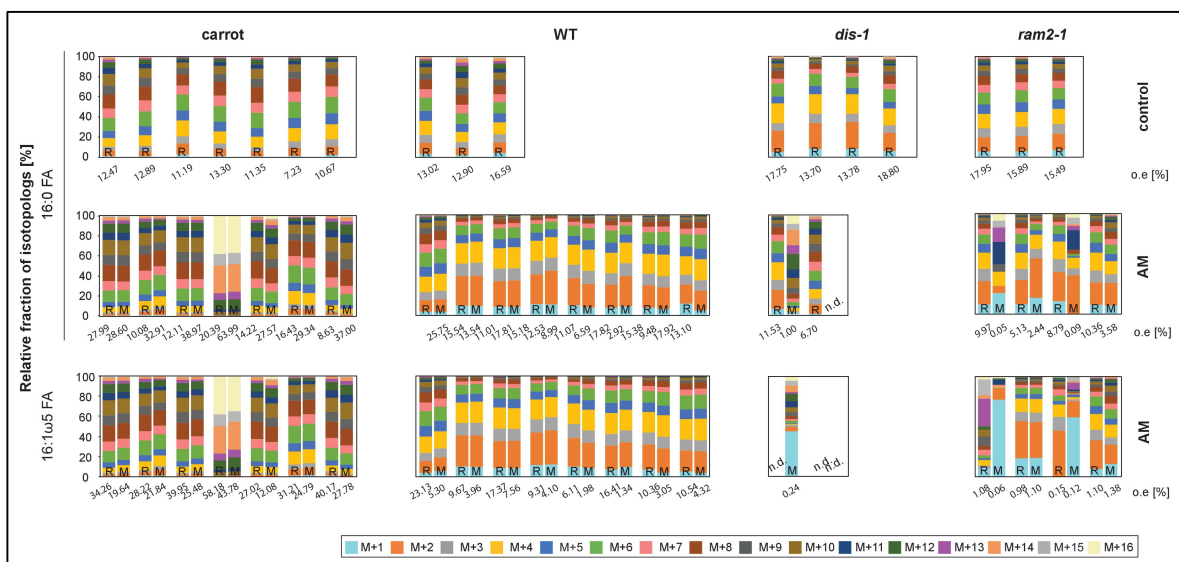


Figure 8 –figure Supplements 4



**Supplementary table S1. Mutations in *DIS* and *DIS-LIKE* identified by TILLING or in a LORE1 insertion collection.**

Allele	Line ID	aa change / insertion	Source
<i>dis-1</i>	SL0154-N	G190R	(Groth et al., 2013)
<i>dis-2</i>	30035849	LORE1 intron 2 insertion	(Małolepszy et al., 2016)
<i>dis-3</i>	SL4113-1	T221I	RevGen, UK
<i>dis-4</i>	SL0614-1	G314D	RevGen, UK
<i>dis-5</i>	SL5510-1	E338K	RevGen, UK
<i>dis-6</i>	SL0494-1	P376L	RevGen, UK
<i>disl-1</i>	SL3509-1	P61S	RevGen, UK
<i>disl-2</i>	30034395	LORE1 exon 2 insertion	(Małolepszy et al., 2016)
<i>disl-3</i>	SL1481-1	D109N	RevGen, UK
<i>disl-4</i>	SL5555-1	G176E	RevGen, UK
<i>disl-5</i>	SL1474-1	G180E	RevGen, UK
<i>disl-6</i>	SL4156-1	V193M	RevGen, UK

Groth M, Kosuta S, Gutjahr C, Haage K, Hardel SL, Schaub M, Brachmann A, Sato S, Tabata S, Findlay K, et al. 2013. Two *Lotus japonicus* symbiosis mutants impaired at distinct steps of arbuscule development. *The Plant Journal* 75: 117-129. 10.1111/tpj.12220.

Małolepszy A, Mun T, Sandal N, Gupta V, Dubin M, Urbański D, Shah N, Bachmann A, Fukai E, Hirakawa H, et al. 2016. The LORE1 insertion mutant resource. *Plant Journal*: DOI: 10.1111/tpj.13243. 10.1111/tpj.13243.

**Supplementary table S2. Primers used in this study.**

Purpose	Name	Sequence
<i>gDIS</i> cloning for <i>pDIS:gDIS</i>	SH71 SH72	CACCGGAACGGGACAAAAGACTCC TTAGGGCCTGAATGGAGCAAAGACAA
<i>pDIS</i> cloning for <i>pDIS:GUS</i>	SH94 SH104	ATTTAAGCTTGGAACGGGACAAAAGACTCC AATCAGGATCCTGTTCAATGTGTCTGTGGCA
<i>DIS</i> cloning for <i>DIS-RFP</i> localization in <i>N. benthamiana</i>	SH93 SH92	CACCATGGCAAGCATTGCTGGTTC GGGCCTGAATGGAGCAAAGACAAC

pLjPT4 cloning for pPT4:DIS	CG466 CG467	TTTGGTCTCTGCGGGGACTCAAGAAACCATGCTATC TTTGGTCTCTCAGACTTGAACGATGTCGATTTAGTTTG
DIS/dis-1 frag.1 cloning for pPT4:DIS/dis-1	SH124 SH125	ATGAAGACTTTACGGGTCTCACACCATGGCAAGCATT GCTGGTTC TTGAAGACTTTTTCGATTTTCAGGGCTCTCTTTGTTACCTG ATGACAACAAGCACCCTTTTGG
DIS/dis-1 frag.1 cloning for pPT4:DIS/dis-1	SH126 SH127	TTGAAGACTTCGAAACCCTGATGATTATT ATGAAGACTTCAGAGGTCTCACCTTGGGCCTGAATGG AGCAA
pDIS cloning for pDIS:AtKASI	SH122 SH123	ATGAAGACTTTACGGGTCTCAGCGGGGAACGGGACAA AAGACTCC ATGAAGACTTCAGAGGTCTCAGGTGTGTTCAATGTGTC TGTGG
pAtKASI cloning for pAtKASI:LjDIS	SH113 SH109	TTGGTCTCACACCGAGTCACAAAGATGCTATCG GGTCTCACCATGGTGGATCCAGAAATTGAGAG
3'UTR AtKASI cloning for pAtKASI:LjDIS	SH118 SH119	TGAGGTCTCGTTTCTTCATACCTTTTAGATTCT TGAGGTCTCGCCTTCAGTATAAATCTAATTTCTTC
gDIS frag.1 cloning for pAtKASI:LjDIS	SH110 SH114	TGAGGTCTCTATGGCAAGCATTGCTGGTTCATG TGAGGTCTCTTTTCGATTTTCAGGGCTCTCT
gDIS frag.2 cloning for pAtKASI:LjDIS	SH115 SH117	TTGGTCTCACGAAACCCTGATGATTATTAG TGAGGTCTCGGAAATTAGGGCCTGAATGGAGC
AtKASI frag.1 cloning for pDIS:AtKASI	CG455 CG456	ATGAAGACTTTACGGGTCTCACACCATGCAAGCTCTTC AATCTTCATCTCT ATGAAGACTTGTCGCAAAGGTCGCGCATTG
AtKASI frag.2 cloning for pDIS:AtKASI	CG457 CG458	ATGAAGACTTCGACGACAACAACGTTCCCTTCA ATGAAGACTTGAGTCCCATAACCAGTAATGACAAC
AtKASI frag.3 cloning for pDIS:AtKASI	CG459 CG460	ATGAAGACTTACTCGTCTCTGTGTTTGGTAACG ATGAAGACTTTGGCTCTCTCCAAAACAAAATGTCA
AtKASI frag.4 cloning for pDIS:AtKASI	CG461 CG462	ATGAAGACTTGCCACTAATTGTTGTATGCCCTAATAG ATGAAGACTTCAGAGGTCTCACCTTTCAGGGTTTGAAG GCAGAGAAGGC
qPCR of LjEF1alpha	EF1alpha_F EF1alpha_R	GCAGGTCTTTGTGTCAAGTCTT CGATCCAGAACCCAGTTCT
qPCR of LjKASI	LjKASI_qPCR_F LjKASI_qPCR_R	TCCCAACGCTAACTTCAAGC CCCTGCATCATTGAGGCTAT

qPCR of <i>LjKASII</i>	AK42 AK43	CGAGAAAGACTTGATCTCCCCAG CGTGGTTACATCACTTGGTCATG
qPCR of <i>LjKASIII</i>	AK44 AK45	GATTTGCATAGTAATGGTGATGG GCATGAATATGAGGACTGCTTGG
qPCR of <i>LjDIS</i>	qPCR_DIS4_F qPCR_DIS4_R	CATTCATTGATTTCCGGGACA CCAAACACAGAAGCAGATCAGA
qPCR of <i>LjDIS-like</i>	qPCR_DISL4_F qPCR_DISL4_R	CATGTTATCGATTTGTGTTTGG TGACTACTACCCATTTGCTGAAAG
qPCR of <i>LjUbiquitin</i>	qPCR_F_LjUbi qPCR_R_LjUbi	ATGCAGATCTTCGTCAAGACCTT ACCTCCCCTCAGACGAAG
qPCR of <i>LjRAM2</i>	PP101 PP102	ATCCTATGAGTGCCTAGCTTTACTAGAAG AACGAGCAAATTAATACTGAAAGAGAGTAC
qPCR for <i>LjSbtM1</i>		CACGTTGTTAGGACCCCAAT TTGAGCAGCACCCCTCTCTATC
qPCR for <i>LjBCP1</i>		TCATCTGTCCTTGGGGTCAT CAGCTGCAGAAGTTGCATTT
qPCR for <i>LjPT4</i>		GAATAAAGGGGCCAAAATCG GCTGTATCCTATCCCCATGC
qPCR for <i>LjAMT2.2</i>		TGGTTCAACTTTTCGTCCA CTTATCACCCCTGACCCCAAGA
qPCR for <i>LjSTR</i>		CTATATTGGTGACGAGGGAAGG GTCCTGAGGTAGGTTTCATCCAG
pRAM2_1a cloning for pRAM2:gRAM2 and pRAM2:GUS	PP103 PP104	ATGAAGACTTTACGGGTCTCAGCGGGATTGAAAGCTT CCCCATAG TAGAAGACAAATCTTCTCCTAGTATTTTTTTTTTAAAG
pRAM2_1b cloning for pRAM2:gRAM2 and pRAM2:GUS	PP105 PP106	ATGAAGACTTAGATCATTCCACGGAGGAG ATGAAGACTTCAGAGGTCTCACAGAGGTGAATGCACT TGTTGTTACTC
gRAM2 cloning for pPT4:gRAM2/ram2-1	AK20 AK21	ATGAAGACTTTACGGGTCTCACACCATGGTGTGCATCA ACG ATGAAGACTTCAGAGGTCTCACCTTGCAACCCATGAC TTTGTTTG

pRAM2 primer walking using TAC Lj T46c08	PP132	GTCGTTTTAGAGAATAATTTTTTG
pRAM2 primer walking using TAC Lj T46c08	PP133	AGGATAGGCTCAATACTTTGA
pRAM2 primer walking using TAC Lj T46c08	PP134	ATGGGTGAAAGTGGTAAGATGG
pRAM2 primer walking using TAC Lj T46c08	PP135	GCGTGACAAACATGGAAGG
pRAM2 primer walking using TAC Lj T46c08	PP136	AGCAAAGTTGGGGGAGAAAT
pRAM2 primer walking using TAC Lj T46c08	PP137	AGGTGGGTATTGGAGGTGGA
pRAM2 primer walking using TAC Lj T46c08	PP138	ACACTTAAAAAAGAACGGAG
pRAM2 primer walking using TAC Lj T46c08	PP139	CTCTAACAATCCACTATCTTG
pRAM2 primer walking using TAC Lj T46c08	PP140	CACACAAGAACTTCATGCAC
pRAM2 primer walking using TAC Lj T46c08	PP141	GAGCTTGATCACCTACTAATTAT
pRAM2 primer walking using TAC Lj T46c08	PP142	CTTGTATGCCAGCAGCCTCAGAG
pSbtM1 frag.1 cloning for pSbtM1:SPP-mCherry	JAVA-23 JAVA-24	ATGAAGACTTTACGGGTCTCAGCGGAACATTGAGGAC AGATTAAGG TAGAAGACAATTGCCTTCATTTGTGCCAAA
pSbtM1 frag.2 cloning for pSbtM1:SPP-mCherry	JAVA-25 JAVA-26	TAGAAGACAAGCAAATAAACCGTCCAAGGC ATGAAGACTTCAGAGGTCTCTCAGAGCTCCATCTTTAA TTGGAATTTGATG

<i>SbtM1</i> secretion signal peptide cloning for p <i>SbtM1</i> :SPP-mCherry	SC278 SC279	TATGGTCTCATCTGATGGAGCAAACCAAGTATAGGA TATGGTCTCAGGTGTCATGCTCTTGGCCTTCCT
---	----------------	---

### Supplementary table S3: Plasmids used in this study

Produced by classical cloning, Gateway cloning (Entry plasmids and Destination plasmids) and Golden Gate cloning (Level I, II and III). The Golden Gate toolbox is described in (48).

EV, empty vector; HR, hairy root; trafo, transformation

Purpose	Name	Description
<i>dis-1</i> transgenic complementation (Fig. 1A)	Entry: pENTR-p <i>DIS</i> :g <i>DIS</i>	PCR amplification of <i>DIS</i> promoter and gene with primers SH71 + SH72 and subcloning into pENTR/D-TOPO.
	HR Trafo: p <i>DIS</i> :g <i>DIS</i>	LR clonase (Invitrogen) recombination of ENTR-p <i>DIS</i> :g <i>DIS</i> with pK7RWG2.0 w/o 35S promoter (56).
	HR Trafo: EV	Removal of Gateway cassette from pK7RWG2.0 w/o 35S promoter (Antolín-Llovera et al., 2014) by EcoRV digest and religation.
Localization of <i>DIS</i> promoter activity (Fig. 2_S1)	p <i>DIS</i> -GUS	PCR amplification of 1.5 kb <i>DIS</i> promoter region with primers SH94 + SH104 and insertion into the HindIII and BamHI restriction sites of pBI101 (Jefferson et al., 1987).
Cross species complementation of <i>Arabidopsis kasI</i> mutant with <i>LjDIS</i> (Fig. 4C)	Entry: pENTR-p <i>AtKASI</i> : <i>DIS</i> :3' UTR <i>AtKASI</i> (pCG92)	Assembled from L0 p <i>AtKASI</i> , L0 <i>DIS</i> , L0 3' UTR <i>KASI</i> and pENTR-BsaI (BB04) by BsaI cut ligation
	Entry: pENTR-p <i>AtKASI</i> : <i>DIS</i> :3' UTR <i>AtKASI</i> (pCG93)	Assembled from L0 p <i>AtKASI</i> , L0 <i>dis-1</i> , L0 3' UTR <i>KASI</i> and pENTR-BsaI (BB04) by BsaI cut ligation
	<i>Arabidopsis</i> Trafo: p <i>KASI</i> : <i>DIS</i> (pCG94)	LR clonase (Invitrogen) recombination of pCG92 with pMDC99 (Curtis & Grossniklaus, 2003).
	<i>Arabidopsis</i> Trafo: p <i>KASI</i> : <i>dis-1</i> (pCG95)	LR clonase (Invitrogen) recombination of pCG93 with pMDC99 (Curtis & Grossniklaus, 2003).
Localization of <i>DIS</i> in <i>N. benthamiana</i> leaves (Fig. 4F)	Entry: pENTR- <i>DIS</i> w/o stop	PCR amplification of <i>DIS</i> gene with primers SH93 + SH92 and subcloning into pENTR/D-TOPO.
	<i>N. benthamiana</i> Trafo: p35S: <i>DIS</i> :RFP	LR clonase (Invitrogen) recombination of ENTR-pENTR- <i>DIS</i> w/o stop with pK7RWG2.0 (Karimi et al., 2002).
	<i>N. benthamiana</i> Trafo: p35S: <i>AtLhcb1.3</i> :YFP	

		LR clonase (Invitrogen) recombination of pENTR/D-TOPO- <i>AtLhcb1.3</i> w/o stop (kind gift from Jürgen Soll) with pB7FWG2.0 (Karimi et al., 2002).
Golden Gate level 0 and I (L0, LI) elements		
	L0 p <i>AtKASI</i>	PCR amplification of <i>AtKASI</i> 1.3 kb promoter fragment with SH113 + SH109 and assembly by <i>StuI</i> cut ligation into L0 pUC57 plasmid (BB01).
	L0 <i>DIS</i> and L0 <i>dis-1</i>	Assembled by <i>StuI</i> cut ligation into L0 pUC57 plasmid (BB01) from 2 PCR fragments amplified from genomic DNA of <i>L. japonicus</i> Gifu wild type ( <i>DIS</i> ) and <i>dis-1</i> mutant ( <i>dis-1</i> ). Primers:  Fragment 1: SH110 + SH 114  Fragment 2: SH115 + SH117
	L0 3' UTR <i>AtKASI</i>	3' UTR of <i>AtKASI</i> (343 bp) was PCR amplified with primers SH118 + SH119 and assembled by <i>StuI</i> cut ligation into L0 pUC57 plasmid (BB01).
	L0 p <i>RAM2A</i>	PCR amplification of 906 bp fragment <i>L. japonicus</i> Gifu genomic DNA with primers PP103+PP104. Assembly by <i>SmaI</i> cut ligation into LI-Amp (BB01)
	L0 p <i>RAM2B</i>	PCR amplification of 1434 bp fragment <i>L. japonicus</i> Gifu genomic DNA with primers PP105+PP106. Assembly by <i>SmaI</i> cut ligation into LI-Amp (BB01)
	LI A-C p <i>DIS</i> (pCG124)	PCR amplification of 1.5 kb <i>DIS</i> promoter from <i>L. japonicus</i> Gifu genomic DNA with primers SH122 + SH123 and <i>BpiI</i> cut ligation into LI- <i>BpiI</i> (BB03) plasmid.
	LI C-D <i>AtKASI</i> (pCG125)	Assembled 4 PCR fragments amplified from <i>A. thaliana</i> Col-0 gDNA by <i>BpiI</i> cut ligation into LI- <i>BpiI</i> plasmid (BB03). Primers:  Fragment 1: CG455 + CG456  Fragment 2: CG457 + CG458  Fragment 3: CG459 + CG460  Fragment 4: CG461 + CG462
	LI A-B p <i>PT4</i>	PCR amplification of 2.2 kb <i>PT4</i> promoter region from <i>L. japonicus</i> Gifu genomic DNA with primers CG466 + CG467 and assembly by <i>BpiI</i> cut ligation into LI- <i>BpiI</i> plasmid (BB03).

	LI C-D <i>DIS</i> LI C-D <i>dis-1</i>	Assembled from two PCR amplified fragments from genomic DNA of <i>L. japonicus</i> Gifu wild type ( <i>DIS</i> ) and <i>dis-1</i> mutant ( <i>dis-1</i> ). Assembly by BpiI cut ligation into LI-BpiI plasmid (BB03). Primers:  Fragment 1: SH124 + SH138  Fragment 2: SH126 + SH127
	LI A-B <i>pRAM2</i>	Assembled by BpiI cut ligation from: L0 <i>pRAM2A</i> + L0 <i>pRAM2B</i> + LI-BpiI (BB03)
	LI C-D <i>RAM2</i> LI C-D <i>ram2-1</i>	PCR amplification of 1998 bp fragment <i>L. japonicus</i> Gifu genomic DNA with primers AK20 + AK21. Assembled by SmaI blunt end cut ligation: pUC57 (BB02) + Fragment: AK20 + AK21
	LI C-D <i>GUS</i>	(Pimprikar et al., 2016)
	LI A-B <i>pSbtM1</i>	PCR amplification of 559 bp fragment with primers JAVA-23 + JAVA-24 and of 211 bp fragment with primers JAVA-25 + JAVA-26 from <i>pENTR D-TOPO pSbtM1</i> . Assembled by BpiI cut ligation from 559 bp fragment + 211 bp fragment + LI-BpiI (BB03)
	LI B-C SSP ( <i>SbtM1</i> secretion signal peptide)	PCR amplification of 135 bp fragment <i>L. japonicus</i> Gifu genomic DNA with primers SC278 + SC279. Assembly by SmaI cut ligation into LI-pUC57 (BB02)
Golden Gate level II (LII) plasmids		
	LII R 3-4 <i>p35S:mCherry</i> (selection marker for HR)	Assembled by BsaI cut ligation from:  LI A-C <i>p35S</i> (G009) + LI C-D <i>mCherry</i> (G057) + LI dy D-E (B008) + LI E-F 35S-T (G059) + LI dy F-G (BB09) + LII R 3-4
	LII F 1-2 <i>pDIS:AtKASI</i> (pCG126)	Assembled by BsaI cut ligation from:  LI A-C <i>pDIS</i> + LI C-D <i>AtKASI</i> + LI dy D-E (BB08) + LI E-F nos-T(G006) + LI dy F-G (BB09) + LIIc F 1-2 (BB30)
	LII F 1-2 <i>pDIS:EV</i> (pCG127)	Assembled by BsaI cut ligation from:  LI A-C <i>pDIS</i> + LI dy C-D (BB07) + LI dy D-E (BB08) + LI E-F nos-T(G006) + LI dy F-G (BB09) + LIIc F 1-2 (BB30)
	LII F 1-2 <i>pPT4:DIS</i> (pCG130)	Assembled by BsaI cut ligation from:  LI A-B <i>pPT4</i> + LI dy B-C (BB06) + LI C-D <i>DIS</i> + LI E-F nos-T(G006) + LI dy F-G (BB09) + LIIc F 1-2 (BB30)
	LII F 1-2 <i>pPT4:dis-1</i> (pCG131)	Assembled by BsaI cut ligation from:

		LI A-B pPT4 + LI dy B-C (BB06) + LI C-D <i>dis-1</i> + LI E-F nos-T(G006) + LI dy F-G (BB09) + LIc F 1-2 (BB30)
	LIc F 1-2 pRAM2:gRAM2 pPP106	Assembled by BsaI cut ligation from: LI A-B pRAM2 + LI B-C dy (BB06) + LI C-D RAM2 + LI D-E dy (BB08) + LI E-F nos-T (G006) + LI F-G dy (BB09) + LIc F 1-2 (BB30)
	LII F 3-4 pPT4:gRAM2 (pAK12)	Assembled by BsaI cut ligation from: LI A-B pPT4 + LI dy B-C (BB06) + LI C-D RAM2 + LI E-F nos-T(G006) + LI dy F-G (BB09) + LIc F 3-4 (BB34)
	LII F 3-4 pPT4:gram2-1 (pAK13)	Assembled by BsaI cut ligation from: LI A-B pPT4 + LI dy B-C (BB06) + LI C-D <i>ram2</i> + LI E-F nos-T(G006) + LI dy F-G (BB09) + LIc F 3-4 (BB34)
	LIc F 1-2 pRAM2:GUS pPP107	Assembled by BsaI cut ligation from: LI A-B pRAM2 + LI B-C dy (BB06) + LI C-D GUS + LI D-E dy (BB08) + LI E-F nos-T (G006) + LI F-G dy (BB09) + LIc F 1-2 (BB30)
	LIc R 3-4 pUbi:mCherry (pPP101)	(Pimprikar et al., 2016)
	LIIβ F 5-6 pPOI:NLS-2XYFP:NosT (pGC134)	Assembled by BsaI cut ligation from: LI A-B Esp3I- <i>lacZ</i> dy (G082) + LI B-C NLS (G60) + LI C-D YFP (G54) + LI D-E YFP (G12) + LI E-F Nos-T (G006) + LI F-G dy (BB09) + LIIβ F 5-6 (BB28)
	LIc F 1-2 pSbtM1:SPP-mCherry: HspT (pPP137)	Assembled by BsaI cut ligation from: LI A-B pSbtM1 + LI B-C SPP + LI C-D <i>mCherry</i> + LI D-E dy (BB08) + LI E-F Hsp-T (G045) + LI F-G dy (BB09) + LIc F 1-2 (BB30)
Golden Gate level III (LIII) plasmids for plant transformation		
<i>ram2-1</i> transgenic complementation (Fig. 1A)	LIIIβ F A-B pRAM2:RAM2 (pPP162)	Assembled by BpiI cut ligation from: LIc F 1-2 pRAM2:RAM2 + LII 2-3 ins (BB43) + LIc R 3-4 pUbi:mCherry + LII 4-6 dy (BB41) + LIIIβ F A-B (BB53)
Localization of <i>DIS</i> promoter activity (Fig 2_S1)	LIIIβ F A-B pDIS:GUS (pMP2)	Assembled by Esp3I Cut-Ligation. PCR product of pDIS + pPP170 [LIc F 1-2 pRAM1:GUS + LII 2-3 ins (BB43) + LIc R 3-4 pUbi:mCherry + LII 4-6 dy (BB41) + LIIIβ F A-B (BB53)] (Pimprikar et al., 2016).
Localization of RAM2 promoter activity (Fig 2_S1)	LIIIβ F A-B pRAM2:GUS (pPP163)	Assembled by BpiI cut ligation from: LIc F 1-2 pRAM2:GUS + LII 2-3 ins (BB43) + LIc R 3-4 pUbi:mCherry + LII 4-6 dy (BB41) + LIIIβ F A-B (BB53)

<p>Cross species complementation of <i>dis-1</i> mutant with <i>Arabidopsis</i> KASI (Fig. 2C)</p>	<p>LIIIβ F A-B pDIS:AtKASI (pCG128)</p> <p>LIIIβ F A-B pDIS:EV (pCG129)</p>	<p>Assembled by BpiI cut ligation from:</p> <p>LII F 1-2 pDIS:AtKASI + LII ins 2-3 (BB43) + LII R 3-4 p35S:mCherry + L II dy 4-6 (BB41) + LIIIβ F A-B</p> <p>Assembled by BpiI cut ligation from:</p> <p>LII F 1-2 pDIS:EV + LII ins 2-3 (BB43) + LII R 3-4 p35S:mCherry + L II dy 4-6 (BB41) + LIIIβ F A-B</p>
<p><i>dis-1</i> transgenic complementation with pPT4:DIS (Fig. 2C)</p>	<p>LIIIβ F A-B pPT4:DIS (pCG132)</p> <p>LIIIβ F A-B pPT4:dis-1 (pCG133)</p>	<p>Assembled by BpiI cut ligation from:</p> <p>LII F 1-2 pPT4:DIS + LII ins 2-3 (BB43) + LII R 3-4 p35S:mCherry + L II dy 4-6 (BB41) + LIIIβ F A-B</p> <p>Assembled by BpiI cut ligation from:</p> <p>LII F 1-2 pPT4:dis-1 + LII ins 2-3 (BB43) + LII R 3-4 p35S:mCherry + L II dy 4-6 (BB41) + LIIIβ F A-B</p>
<p><i>ram2-1</i> transgenic complementation with pPT4:RAM2 (Fig. 2C)</p>	<p>LIIIβ F A-B pPT4:RAM2 (pAK14)</p> <p>LIIIβ F A-B pPT4:ram2-1 (pAK15)</p>	<p>Assembled by BpiI cut ligation from:</p> <p>LII F 1-2 pUbi:mCherry + LII ins 2-3 (BB43) + LII F 3-4 pPT4:gRAM2 + L II dy 4-6 (BB41) + LIIIβ F A-B</p> <p>Assembled by BpiI cut ligation from:</p> <p>LII F 1-2 pUbi:mCherry + LII ins 2-3 (BB43) + LII F 3-4 pPT4:ram2-1 + L II dy 4-6 (BB41) + LIIIβ F A-B</p>
<p>Esp3I compatible destination backbone for Localization of promoter activity</p>	<p>Esp3I cut ligation compatible backbone: LIIIβ F A-B pSbtM1:SP-mCherry_pPOI:NLS-2XYFP (pPP217)</p>	<p>Assembled by BpiI cut ligation from: LIIC F 1-2 pSbtM1:SP-mCherry: HspT + LII 2-3 ins (BB43) + LII 3-4 dy (BB64) + LII 4-5 ins (BB44) + LIIβ F 5-6 pPOI:NLS-2XYFP:NosT + LIIIβ F A-B (BB53)</p>
<p>BsaI compatible destination backbone for Localization of promoter activity</p>	<p>BsaI cut ligation compatible backbone: LIIIβ F A-B pSbtM1:SP-mCherry_pPOI:NLS-2XYFP (pPP218)</p>	<p>Assembled by Esp3I cut ligation from: LIIIβ F A-B pSbtM1:SP-mCherry_pPOI:NLS-2XYFP + LI A-B Esp3I-ccdB dy (G084)</p>
<p>Localization of promoter activity of pDIS (Fig 2A)</p>	<p>LIIIβ F A-B pSbtM1:SSP:mCherry+pDIS:NLS-2xYFP (pPP241)</p>	<p>Assembled by BsaI cut ligation from:</p> <p>LI A-B pDIS + LIIIβ F A-B pSbtM1:SP-mCherry_pPOI:NLS-2XYFP (pPP218)</p>
<p>Localization of promoter activity of pRAM2 (Fig 2B)</p>	<p>LIIIβ F A-B pSbtM1:SSP:mCherry+pRAM2:NLS-2xYFP (pPP238)</p>	<p>Assembled by BsaI cut ligation from:</p> <p>LI A-B pRAM2 + LIIIβ F A-B pSbtM1:SP-mCherry_pPOI:NLS-2XYFP (pPP218)</p>

## References

- Antolín-Llovera M, Ried Martina K, Parniske M. 2014. Cleavage of the SYMBIOSIS RECEPTOR-LIKE KINASE ectodomain promotes complex formation with Nod Factor Receptor 5. *Current Biology* **24**(4): 422-427. 10.1016/j.cub.2013.12.053.
- Curtis MD, Grossniklaus U. 2003. A gateway cloning vector set for high-throughput functional analysis of genes *in planta*. *Plant Physiology* **133**(2): 462-469. 10.1104/pp.103.027979.
- Jefferson RA, Kavanagh TA, Bevan MW. 1987. GUS fusions: beta-glucuronidase as a sensitive and versatile gene fusion marker in higher plants. *EMBO J* **6**: 3901-3907.
- Karimi M, Inzé D, Depicker A. 2002. GATEWAY™ vectors for *Agrobacterium*-mediated plant transformation. *Trends in Plant Science* **7**(5): 193-195. 10.1016/S1360-1385(02)02251-3.
- Pimprikar P, Carbonnel S, Paries M, Katzer K, Klingl V, Bohmer M, Karl L, Floss D, Harrison M, Parniske M, et al. 2016. A CCaMK-CYCLOPS-DELLA complex regulates transcription of RAM1, a central regulator of arbuscule branching. *Current Biology* **26**: 987-998. 10.1016/j.cub.2016.01.069.

**Supplementary Table 4:** Accession numbers for protein sequences used in the phylogenetic tree (Figure 3)

Species	Gene	Accession numbers	Database
<i>Arabidopsis lyrata</i>	KA SI	494344	<a href="http://www.phytozome.com">www.phytozome.com</a>
<i>Arabidopsis thaliana</i>	KA SI	AT5G46290.3	<a href="http://www.phytozome.com">www.phytozome.com</a>
<i>Beta vulgaris</i>	KA SI	21760 ecdj.t1	<a href="http://bvseq.molgen.mpg.de/index.shtml">http://bvseq.molgen.mpg.de/index.shtml</a>
<i>Brachypodium distachyon</i>	KA SI	Bradi1g19190.1 / Bradi1g46610.1	<a href="http://www.phytozome.com">www.phytozome.com</a>
<i>Brassica rapa</i>	KA SI	Bra025025 / Bra017565 / Bra022029	<a href="http://www.phytozome.com">www.phytozome.com</a>
<i>Capsella rubella</i>	KA SI	Carubv1002634 4m	<a href="http://www.phytozome.com">www.phytozome.com</a>
<i>Carica papaya</i>	KA SI	evm.model.sup ercontig 166.28	<a href="http://www.phytozome.com">www.phytozome.com</a>
<i>Carica papaya</i>	DI S	evm.model.sup ercontig 79.6	<a href="http://www.phytozome.com">www.phytozome.com</a>
<i>Cunninghamia lanceolata</i>	KA SI	JU992615.1	NCBI
<i>Cunninghamia lanceolata</i>	DI S	JU992615.1	NCBI
<i>Cuscuta sativa</i>	KA SI	GAQC01004821 .1	NCBI
<i>Glycine max</i>	KA SI	Glyma08g08910 .1 /	<a href="http://www.phytozome.com">www.phytozome.com</a>

		Glyma05g25970 .1	
<i>Glycine max</i>	DI S	Glyma08g02850 .1 / Glyma18g10220 .1 / Glyma05g36690 .2	<a href="http://www.phytozome.com">www.phytozome.com</a>
<i>Gossipium raimondii</i>	KA SI	Gorai.009G1564 00.1 / Gorai.010G1656 00.1	<a href="http://www.phytozome.com">www.phytozome.com</a>
<i>Gossipium raimondii</i>	DI S	Gorai.004G1318 00.1	<a href="http://www.phytozome.com">www.phytozome.com</a>
<i>Lotus japonicus</i>	KA SI	chr4.CM0007.85 0.r2.d	<a href="http://www.kazusa.or.jp/lotus/blast.html">http://www.kazusa.or.jp/lotus/blast.html</a>
<i>Lotus japonicus</i>	DI S / DI S- like	chr4.CM0004.16 40.r2.a / chr4.CM0004.16 50.r2.a	<a href="http://www.kazusa.or.jp/lotus/blast.html">http://www.kazusa.or.jp/lotus/blast.html</a>
<i>Lunularia cruciata</i>	DI S- KA SI	contig3372	<a href="http://www.polebio.lrsv.upstlse.fr/Luc_v1/Luc_v1.fa">http://www.polebio.lrsv.upstlse.fr/Luc_v1/Luc_v1.fa</a>
<i>Lupinus albus</i>	KA SI	25301	NCBI
<i>Lupinus albus</i>	DI S	32493	NCBI
<i>Lupinus angustifolius</i>	DI S	AOCW0116011 0.1	NCBI
<i>Medicago truncatula</i>	KA SI	Medtr4g096690. 1	<a href="http://www.phytozome.com">www.phytozome.com</a>
<i>Medicago truncatula</i>	DI S	Medtr8g099695. 1	<a href="http://www.phytozome.com">www.phytozome.com</a>
<i>Mimulus guttatus</i>	KA SI	mgv1a005817m	<a href="http://www.phytozome.com">www.phytozome.com</a>
<i>Mimulus guttatus</i>	DI S	mgv1a006855m / mgv1a024999m / mgv1a005480m	<a href="http://www.phytozome.com">www.phytozome.com</a>
<i>Oryza sativa</i>	KA SI	Os06g09630.1	<a href="http://www.phytozome.com">www.phytozome.com</a>
<i>Panicum virgatum</i>	KA SI	Pavirv00002168 m / Pavirv00070739	<a href="http://www.phytozome.com">www.phytozome.com</a>

		m / Pavirv00049911 m	
<i>Phaeseolus vulgaris</i>	KA SI	Phvul.002G1943 00.1	<a href="http://www.phytozome.com">www.phytozome.com</a>
<i>Phaeseolus vulgaris</i>	DI S	Phvul.002G3004 00.1	<a href="http://www.phytozome.com">www.phytozome.com</a>
<i>Physcomitrella patens</i>	DI S- KA SI	XP_001762687.1 / XP_001762048.1 / XP_001776124.1	NCBI
<i>Pohlia nutans</i>	DI S- KA SI	GACA01011151 .1	NCBI
<i>Populus trichocarpa</i>	KA SI	XP_002305334.1 / XP_002316735.1	NCBI
<i>Populus trichocarpa</i>	DI S	XP_002303661.2 / XP_002299456.1	NCBI
<i>Selaginella moellendorffii</i>	DI S- KA SI	XP_002960175.1 / XP_002964698.1 / XP_002961627.1	NCBI
<i>Setaria italica</i>	KA SI	Si033275m / Si039166m / Si006383m	<a href="http://www.phytozome.com">www.phytozome.com</a>
<i>Solanum lycopersicum</i>	KA SI	Solyc08g016170. 2.1	<a href="http://www.phytozome.com">www.phytozome.com</a>
<i>Solanum lycopersicum</i>	DI S	Solyc08g082620. 2.1	<a href="http://www.phytozome.com">www.phytozome.com</a>
<i>Solanum tuberosum</i>	KA SI	PGSC0003DMP 400014579	<a href="http://www.phytozome.com">www.phytozome.com</a>
<i>Solanum tuberosum</i>	DI S	PGSC0003DMP 400021710	<a href="http://www.phytozome.com">www.phytozome.com</a>
<i>Sorghum bicolor</i>	KA SI	Sb02g041620.1 / Sb10g006430.1	<a href="http://www.phytozome.com">www.phytozome.com</a>
<i>Thellungiella halophila</i>	KA SI	Thhalv10000874 m	<a href="http://www.phytozome.com">www.phytozome.com</a>
<i>Theobroma cacao</i>	KA SI	Thecc1EG02951 3t1	<a href="http://www.phytozome.com">www.phytozome.com</a>
<i>Theobroma cacao</i>	DI S	Thecc1EG01649 8t1	<a href="http://www.phytozome.com">www.phytozome.com</a>

<i>Utricularia giba</i>	KA SI	Scf00389.g16797 .t1	<a href="http://genomeevolution.org/CoGe/OrganismView.pl?oid=36222">http://genomeevolution.org/CoGe/OrganismView.pl?oid=36222</a>
<i>Vitis vinifera</i>	KA SI	XP_002272874.2	NCBI
<i>Vitis vinifera</i>	DI S	XP_002265207.1	NCBI
<i>Zea mays</i>	KA SI	GRMZM2G012 863 / GRMZM2G135 498	<a href="http://www.phytozome.com">www.phytozome.com</a>

<i>Lunularia cruciata</i>	D I S - K A S I	contig 3372	<a href="http://www.polebi.o.lrsv.ups-tlse.fr/Luc_v1/Luc_v1.fa">http:// www. polebi o.lrsv. ups- tlse.fr/ Luc_v 1/Luc v1.fa</a>	MAATSAVVGASFQGLRAVDGRAVSEVSVLRGSRVSKPS AQHRFARELSQNGARAMAATTTAPKRETDPKKRVVITG MGVVSVFGNDVDIFYDKLLEGQSGISLIDRFDASTFPTKF GGQIRGFSSQGYIDGKNDRRLDDCLRYCLVSGQKGLEH AGLGGEKLNVEVDKQRVGVLVGTGMGGLSVFSDGVQAL IEKGYKRITPFFIPYAITNMA SALLAIELGLMGP NYSISTA CATSNYCFYAAANHIRRGEADIMVAGGTEAAIIPVGLG GFVACRALSTRNDDPQTASRPWDKDREGFVMGEGAGV LVMESLEHALKRGAPILAEYLGGAVNCDAYHMTDPRA DGLGVSTCIERSLEDAGVSPEEVNYINAHATSTIVGDLAE VNALKKVKFDGSEIKMNATKSMIGHCLGAAGGLEAIAT IQAIN TGWLHPTINQFNPEEAVTFDTVANVKKQHVN GISNSFGFGGHNSCVVFGPYNG*
-------------------------------	--------------------------------------	----------------	---	---

## IX. General discussion

The major benefit of arbuscular mycorrhiza symbiosis for both partners is the exchange of nutrients (MacLean et al. 2017). The nutrients are trafficked across the PAM which encapsulates every hypha of arbuscule formed in the inner cortical cell of the host. Thus, the degree of arbuscule branching determines the surface area of the symbiotic interface and thereby the rate of the nutrient transfer. Despite the importance of arbuscule development for AM symbiosis, most regulatory molecular mechanism governing arbuscule branching and transcriptional complexes inducing AM-specific genes are still elusive. Transcriptomic analysis revealed that the largest number of transcript accumulated specifically in the cells containing arbuscules (Hogekamp and Küster 2013). The majority of transcripts accumulating during AM development encode putative transcription factors, indicating complex transcriptional networks (Xue et al. 2015). The *L. japonicus* Gifu red (*reduced and degenerate arbuscule*) mutant found in forward genetics screen carried two mutations causative for the arbuscule phenotype (Groth et al. 2013). We separated the two mutations by segregation and the single homozygous mutants obtained were used for the following studies. The first mutation was found in the *RAM1* gene on chromosome 1. *RAM1* encodes a GRAS-type transcription factor family protein, which is essential for arbuscule branching. On the contrary, *RAM1* was previously found to be essential for the early stage of interaction during AM development, as the deletion mutant *ram1-1* in *M. truncatula* showed absence of root length colonization with significant reduction in hyphopodia formation (Gobbato et al. 2012). A set of genes induced by Myc-LCO were shown to be dependent on *RAM1* (Hohnjec et al. 2015), supporting the role of *RAM1* in early stage of AM development. However, two other reports from *L. japonicus* and *P. hybrida* indicated role of *RAM1* in arbuscule branching and not in hyphopodia formation (Rich et al. 2015, Xue et al. 2015). Likewise, a weak mutant allele of *RAM1* in *Medicago* displayed stunted arbuscule in rare cases where the fungus was able to colonize the inner cortex of the root (Gobbato et al. 2013). However, it is possible that certain growth or inoculation conditions caused the reduction in hyphopodium formation on the root surface of *Medicago ram1-1* mutant reported in Gobbato et al., (2012). For example, AM colonization is reduced in low red and far red light condition or at high phosphate concentration (Javot et al. 2007a, Nagata et al. 2015). Re-analysis of AM phenotype in the *ram1-1* mutant in *Medicago* in various condition by Park and co-worker from another lab revealed that *RAM1* is not necessary for hyphopodium formation or hyphal entry into the host root but for arbuscule branching (Park et al. 2015). Thus, *RAM1* was re-assigned to play a major role in arbuscule branching and

development. In addition to the arbuscule branching phenotype, *ram1* mutants in *L. japonicus*, *M. truncatula*, and *P. hybrida* also displayed significantly reduced root length colonization (Park et al. 2015, Rich et al. 2015, Xue et al. 2015, Pimprikar et al. 2016). Decreased root length colonization might be a consequence of stunted arbuscule formation inhibiting the AM fungus to spread in the root. Additionally, RAM1 may play a minor role in the pre-contact stage ultimately resulting in less colonized roots. Therefore, the role of RAM1 in the pre-symbiotic phase needs to be re-investigated carefully.

The *L. japonicus ram1-3* and *ram1-4* mutants in this study showed absence of induction of *AMT2.2* and *DIS* upon colonization. Conversely, *ram1* mutants in *M. truncatula* were perturbed in the induction of genes such as *BCP1*, *PT4*, *RAM2*, *STR*, *AMT2.4*, *AMT2.5*, *Vapyrin* (Park et al. 2015, Luginbuehl et al. 2017). Also, *ram1* mutant in *P. hybrida* did not display induction of genes such as *BCP1*, *PT4*, *PT5*, *RAM2*, *STR*, *STR2*, *AMT2*, *Vapyrin* upon colonization (Rich et al. 2015, Rich et al. 2017a). The differential set of *RAM1*-dependent genes in *Medicago* and *Petunia* as compared to *Lotus* might be due to species-specific genetic redundancy at the level of *RAM1*. Phylogenetic analysis of GRAS-type transcription factor from *L. japonicus*, *M. truncatula*, and *O. sativa* indicated that the closest homolog of *RAM1* is *RAD1* (Xue et al. 2015, Pimprikar et al. 2016). Promoter activity of *RAD1* specifically in colonized root is similar to the promoter activity of *RAM1* in *L. japonicus* (Xue et al. 2015, Pimprikar et al. 2016). Most importantly *RAD1* is also essential for arbuscule development in *L. japonicus* as *rad1* mutant displayed stunted arbuscule (Xue et al. 2015), supporting the hypothesis that *RAD1* and *RAM1* might be partially redundant in function. However, in *M. truncatula*, *rad1* mutants show a weaker phenotype, with reduce root length colonization but normally developed arbuscule (Park et al. 2015). Thus, it appears that the relative importance of *RAM1* and *RAD1* in supporting arbuscule formation differs between *Lotus* and *Medicago*. This may also explain the different effects of the *RAM1* mutation on induction of genes required for AM development in the two species. Interestingly, *RAD1* is shown to interact with *RAM1* and *NSP2* in Y2H, BiFC and CoIP in *L. japonicus* and *M. truncatula* (Park et al. 2015, Xue et al. 2015). Additionally, *RAM1* was shown to form a complex with *NSP2* using BiFC (Gobbato et al. 2012). Thus, it is possible that *RAM1*, *NSP2* and *RAD1* forms heterocomplexes and co-regulate certain set of genes. However, formation and biological relevance of this dimeric or trimeric complexes need to be analyzed *in vivo*. It was proposed that *RAM1* and *NSP2* act together to regulate the expression of genes required for AM development analogous to the *NSP1-NSP2* complex in root nodule symbiosis (Gobbato et al. 2012). Thus, it is possible that different GRAS transcription factor complexes

regulate different sets of genes during AM symbiosis. Nevertheless, the putative partially redundant factor at the level of RAM1 in *L. japonicus* was unable to induce *AMT2.2* and *DIS* indicating RAM1 is essential to regulate genes co-regulated with *AMT2.2* and *DIS* (Pimprikar et al. 2016).

Although the CCaMK-CYCLOPS complex and DELLA are indispensable for AM development, their direct targets in AM were not known until I started my doctoral thesis. The specific induction upon colonization (Gobbato et al. 2012, Park et al. 2015, Xue et al. 2015, Pimprikar et al. 2016) and the AM-specific promoter activity of *RAM1* suggested an AM-induced spatial and temporal regulatory mechanism governing its activation. Epistatic analysis carried out in this thesis, placed *RAM1* downstream of CCaMK and *CYCLOPS*, as *RAM1* induction was absent in *ccamk* and *cyclops* AM colonized *L. japonicus* roots and ectopic expression of *RAM1* could restore arbuscule formation in *cyclops* mutants (Pimprikar et al. 2016). *CYCLOPS* is shown to bind the promoter and activate transcription of the nodulation specific gene *NIN* upon phosphorylation by CCaMK (Singh et al. 2014). Transcriptional activation of *RAM1* by ectopic expression of auto-active NLS-CCaMK<sup>314</sup> (containing solely kinase domain) in absence of AM fungus in wild-type (Takeda et al. 2015, Pimprikar et al. 2016) but not in *cyclops* (Pimprikar et al. 2016), indicated that *RAM1* activation via CCaMK<sup>314</sup> is dependent on *CYCLOPS*. Further, transactivation assay in *N. benthamiana* indicated that *CYCLOPS* phosphorylation by CCaMK is also a pre-requisite for *RAM1* transcriptional activation as reporter activity under the *RAM1* promoter was only detected in presence of both CCaMK<sup>314</sup> and *CYCLOPS*. A deletion series and mutational analysis of the *RAM1* promoter by transactivation assays in *N. benthamiana* indicated that *CYCLOPS* acts via a palindromic *cis*-element named *AMCYC-RE* upon phosphorylation by NLS-CCaMK<sup>314</sup> (Pimprikar et al. 2016). The palindromic *AMCYC-RE* found in the *RAM1* promoter in this study, was already reported to be present in several AM-specific induced genes via computational analysis (Favre et al. 2014). Presence of *AMCYC-RE* in several AM-induced genes suggests that *CYCLOPS* might play a role in activating these genes. Using EMSA, we showed that *CYCLOPS* binds directly to the *AMCYC-RE* element in a sequence-specific manner (Pimprikar et al. 2016). Similarly, *CYCLOPS* was presented to bind *cis*-elements, which differ from the *AMCYC-RE* in the *NIN* and *ERN1* promoter using EMSA (Table 1, Singh et al. 2014, Pimprikar et al. 2016, Cerri et al. 2017). Though, the *CYCLOPS* binding *cis*-element in *RAM1*, *NIN* and *ERN1* promoter differs in sequence from each other, they are all rich in GC content.

Table 1: Known CYCLOPS bound *cis*-elements

Gene	CYC-RE element sequence	Base number	GC content (%)
<i>RAM1</i>	ATGGGCCCGGCCCAA	14	71.4
<i>NIN</i>	TTGCCATGTGGCAC	14	57.14
<i>ERN1</i>	CCTCCATGTGGCAG	14	64.28

The *cis*-element in the *RAM1* promoter bound by CYCLOPS is a perfect palindromic sequence whereas in *NIN*, the palindrome is separated by two nucleotide bases. Often, presence of a palindromic *cis*-element in a promoter indicates formation of a dimer. This hypothesis is consistent with CYCLOPS forming homodimers in BiFC assays (Yano et al. 2008). Thus, it is possible that CYCLOPS forms a homodimer to activate *RAM1*. The diversity in *cis*-elements bound by CYCLOPS indicates that CYCLOPS is able to bind diverse DNA sequences rich in GC content. Deviation from the consensus sequence in *cis*-regulatory elements may allow formation of multiple different transcription factor complexes, resulting in differential transcriptional responses (Ramos and Barolo 2013) for the establishment of AM or root nodule symbiosis. Thus, to generate specific response, it is possible that CYCLOPS interacts with different transcription factors. Ectopic expression of degradation insensitive *DELLA* induced AM-specific genes such as *BCP1* in *Medicago* and *RAM1* in *Lotus* in absence of AM fungi (Floss et al. 2016, Pimprikar et al. 2016), indicating that *DELLA* acts as a transcriptional activator during AM development. Several other experimental outcomes in this thesis indicate that *DELLA* and CYCLOPS both participate in the transcriptional activation of *RAM1*. In this study, we show that *DELLA* interacts with CYCLOPS in Y2H, BiFC and CoIP but not with CCaMK in Y2H and participates in transcriptional activation of *RAM1*. *DELLA* belongs to a GRAS-type transcription factor family which have been exclusively detected in plants (Bolle 2004). Based on electrophoresis mobility shift gel assays (EMSA), NODULATION SIGNALING PATHWAY 1 (NSP1) from *M. truncatula* and SCARECROW-LIKE 7 (SCL7) from rice belonging to the GRAS-type transcription factor family, have so far been suggested to bind DNA (Hirsch et al. 2009, Li et al. 2016). However, no evidence for DNA-binding is present for *DELLA* and other GRAS-type transcription factors except NSP1 and SCL7. *DELLA* is shown to act as a transcriptional modifier via interaction with DNA-binding transcription factors such as C2H2 zinc finger transcription factors of the INDETERMINATE DOMAIN (IDD) proteins family (Fukazawa et al. 2014, Yoshida et al. 2014, Fukazawa et al. 2017). Also, SHORT-ROOT (SHR) and SCARECROW (SCR) belonging to the GRAS-type family bind to IDD10 called JACKDAW (JKD) (Hirano et al. 2017). The crystal structure of the trimeric complex of SCR-SHR-JKD

confirmed that SHR and SCR do not contain a DNA-binding domain and that the DNA binding is mediated via the JKD (Hirano et al. 2017). The CYCLOPS-DELLA interaction was confirmed by another study, in which IPD3, an ortholog of CYCLOPS in *M. truncatula* was shown to interact with DELLA1, -2 and -3 in Y2H, BiFC and CoIP (Jin et al. 2016). The formation of CYCLOPS-DELLA complex was also evident from transactivation assays in *N. benthamiana*, in which addition of DELLA to CYCLOPS and CCaMK enhanced the activation of the *RAM1* promoter. Similarly, Jin and co-worker showed that presence of DELLA in addition to CCaMK and CYCLOPS in yeast three-hybrid assays, results in increased activation of the reporter. Presence of CCaMK in this experiment enhanced the interaction between IPD3 and DELLA in yeast (Jin et al. 2016). Using *in vitro kinase* assay they showed that CCaMK phosphorylates CYCLOPS but not DELLA and presence of DELLA protein enhanced the intensity of phosphorylation of IPD3 by CCaMK (Jin et al. 2016). It has been shown that CCaMK phosphorylates CYCLOPS at position S50 and S154, which is essential for establishment of both RNS and AM symbiosis as mutated CYCLOPS with a serine replacement to alanine failed to complement *cyclops-3* mutant roots for AM and root nodule symbiosis (Singh et al. 2014). Interestingly, the serine replacement to aspartate at position S50 and S154 resulted in gain-of-function phenotype leading to formation of spontaneous nodules even in absence of rhizobia bacteria in root nodule symbiosis (Singh et al. 2014). The phosphoablative mutant version of CYCLOPS protein did not interact with DELLA in the yeast three hybrid assay (Jin et al. 2016), indicating that phosphorylation of CYCLOPS at position S50 and S154 by CCaMK might be a prerequisite for interaction with DELLA. Based on these results, it can be hypothesized that CCaMK upon activation, phosphorylates CYCLOPS at specific residues, which enables interaction with DELLA. In summary, I demonstrated that *RAM1* is transcriptionally activated by a CCaMK-CYCLOPS-DELLA complex via direct binding of CYCLOPS to the *AMCYC-RE* element in the *RAM1* promoter. DELLA was shown to interact with other GRAS-type transcription factors; NSP2, MIG1, RAD1, DELLA INTERACTING PROTEIN 1 (DIP1) and Myb family protein MYB1 in Y2H, BiFC or CoIP (Yu et al. 2013, Floss et al. 2016, Fonouni-Farde et al. 2016, Heck et al. 2016, Jin et al. 2016, Floss et al. 2017), important for AM development. DELLA appear to act at multiple stages of arbuscule development as it interact with protein required for different stages during arbuscule development (Floss et al. 2016, Fonouni-Farde et al. 2016, Heck et al. 2016, Jin et al. 2016, Pimprikar et al. 2016, Floss et al. 2017). However, these interaction of DELLA with different transcription factors might be responsible for generating specific responses enabling progression from one developmental stage of arbuscule to the next. Here, we assume an

additional DNA-binding transcription factor interacting with DELLA protein, involved in transcriptional activation of *RAM1*. As *RAM1* was transcriptionally activated upon treatment with Paclobutrazol (PAC) in absence of AM fungi in *ccamk* and *cyclops* roots. Further, expression of *della1-Δ18* and PAC treatment restored wild-type arbuscule formation in *cyclops*. In addition, we showed that CYCLOPS-DELLA complex activate transcription of *RAM1* by CYCLOPS binding to DNA directly. Thus, together these results indicates that DELLA can transcriptionally activate *RAM1* even in absence of CYCLOPS (Pimprikar et al. 2016). Thus, this dilemma can be resolved by assuming an additional DNA-binding protein X, which also interact with DELLA and becomes sufficient in the absence of CYCLOPS when DELLA is stabilized. We showed for the first time that *RAM1* as an entry point into AM-specific transcriptional activation downstream of common symbiotic signaling components CYCLOPS and DELLA.

The second mutation in the *red* mutant was found in a lipid biosynthesis gene named *REDUCED ARBUSCULAR MYCORRHIZA 2* (*RAM2*). The *L. japonicus* *RAM2* locus was not associated with any chromosome but was placed on chromosome 0. Our mapping analysis showed that the second mutation in *red* is linked to chromosome 6. Confirmation that the mutation in *RAM2* is causative for the *red* phenotype, indicated that the *RAM2* gene is located on chromosome 6. *RAM2* encodes a glycerol 3-phosphate acyl transferase 6 (GPAT6). In *Arabidopsis* and *Medicago*, GPAT6 was shown to specifically produce *sn*-2-monoacylglycerol ( $\beta$ -MAG) for cutin biosynthesis by acetylating the *sn*-2 position of glycerol-3-phosphate with a fatty acid and cleaves the phosphate from the lysophosphatidic acid (Yang et al. 2010, Luginbuehl et al. 2017). *RAM2* is essential for arbuscule development in *L. japonicus* as *ram2* mutants (segregants from the *red* mutant containing only one mutation in *RAM2* on chromosome 6) in *Lotus* displayed stunted arbuscules. In addition, the *ram2* mutant showed a significant reduction in root length colonization and blocked the formation of lipid-containing vesicles of the AM fungus *Rhizophagus irregularis* (Keymer et al. 2017). In contrast, in a previous publication, a *ram2* mutant in *Medicago* showed significant reduction in hyphopodia number and root length colonization (Wang et al. 2012). However, when the AM fungus managed to enter the root, it displayed stunted arbuscules (Wang et al. 2012). External supply of the C16 aliphatic fatty acids associated with cutin restored the number of hyphopodia to the level of wild-type (Wang et al. 2012), supporting role of *RAM2* in the production of cutin monomers and thus essential for early contact phase (Wang et al. 2012). Cutin monomers are predicted to act as chemical signaling molecules required for hyphopodia formation, as for appressorium formation of pathogenic fungi on the leaf surface (Murray et al. 2013). However,

subsequent studies, reported that the *ram2* mutant in *Medicago* displays aberrant arbuscules but no hyphopodium phenotype (Bravo et al. 2017, Keymer et al. 2017). Furthermore, another PhD thesis (Andreas Keymer) reports that the *ram2* mutant can be complemented by transgenic expression of *RAM2* under control of the *PT4* promoter, which is only active in cells containing arbuscule (Keymer et al. 2017). Thus, the difference in the *ram2* phenotype in the previous report (Wang et al. 2012) as compared to others reports (Bravo et al. 2017, Jiang et al. 2017, Keymer et al. 2017, Luginbuehl et al. 2017) needs to be carefully re-examined.

Ectopic expression of *RAM1* in absence of fungus, induced AM-specific genes including *RAM2*, *SbtM1*, *PT4*, and *AMT2.2* in wild-type, *ccamk*, and *cyclops* mutant roots in *L. japonicus*. However, these genes were still induced in *ram1* mutant root in *L. japonicus* upon colonization except *AMT2.2* indicating that *RAM1* is sufficient but not required for induction of *RAM2*, *SbtM1* and *PT4* downstream of *CCaMK* and *CYCLOPS*. In contrast, *RAM2* induction was absent in *ram1* mutant of *M. truncatula* and *P. hybrida* (Park et al. 2015, Rich et al. 2015, Xue et al. 2015, Pimprikar et al. 2016, Luginbuehl et al. 2017, Rich et al. 2017a), indicating species-specific redundancy at level of *RAM1* for regulation of *RAM2*. In addition, overexpression of *NLS-CCaMK<sup>314</sup>* under the 35S promoter in wild-type *Lotus* hairy roots, transcriptionally activate the AM-marker genes *SbtM1* and *RAM2* in addition to *RAM1* in absence of the AM fungi (Takeda et al. 2015). Taken together, these results indicate that *CYCLOPS* upon phosphorylation by *CCaMK* transcriptionally activate *RAM1* and *RAM1* may be involved in activation of *RAM2* downstream of *CCaMK-CYCLOPS* complex. However, to activate the transcription of genes, it is likely that *RAM1* interacts with DNA-binding transcription factors. *RAM1* was shown to bind *RAM2* promoter in a Chromatin immunoprecipitation-polymerase chain reaction (ChIP-PCR) assay using antibodies against native *RAM1* protein from wild-type but not from *ram1* mutant colonized roots in *Medicago* (Gobbato et al. 2012). It remains to be investigated, whether *RAM1* directly binds to DNA as ChIP involving crosslinking steps can fix protein complexes. Thus, this evidence fails to rule out the possibility that *RAM1* does not interact with another DNA-binding transcription factor. Furthermore, transcriptomic analysis in *Medicago* indicated that *RAM1* is required for induction of genes associated with lipid and carbohydrate metabolism during AM colonization (Luginbuehl et al. 2017). Many plant lipid biosynthesis genes are specifically induced during arbuscule formation (Gomez et al. 2009, Gaude et al. 2012, Hogeekamp and Küster 2013). Several of these genes are AM-specific duplications of housekeeping lipid biosynthesis genes and are conserved exclusively in plants that establish AM symbiosis (Bravo et al. 2016). Recently, it has been shown that plant genes involved in lipid biosynthesis

including *RAM2* are essential for arbuscule development (Bravo et al. 2017, Jiang et al. 2017, Keymer et al. 2017, Luginbuehl et al. 2017). Overexpression or knockdown of lipid biosynthesis genes results in respectively increased or decreased root length colonization in *Medicago* (Jiang et al. 2017). Further, mutations in several lipid biosynthesis genes lead to under-developed arbuscules indicating that lipids are required for arbuscule development (Bravo et al. 2017, Jiang et al. 2017, Keymer et al. 2017, Luginbuehl et al. 2017). Thus, it is possible that a major role of *RAM1* in arbuscule development is to activate the transcription of lipid biosynthetic genes. Consistent with this hypothesis, overexpression of *RAM1* induced the lipid biosynthesis gene *FatM* in addition to *RAM2* in absence of AM fungi in *Medicago* (Luginbuehl et al. 2017). *RAM1* was also essential for transcriptional activation of two more lipid biosynthetic genes *KASIII* and *DIS* (Keymer et al. 2017). *KASIII* is a single copy gene in *L. japonicus* and encodes  $\beta$ -keto-acyl ACP synthase III, which produces precursors for DISORGANIZED ARBUSCULES/KASI (DIS/KASI) by catalyzing fatty acyl chain elongation from C2:0-ACP to C4:0-ACP (Keymer et al. 2017). In the frame of another Ph.D. thesis work (unfinished), Simone Bucerius and co-workers found an additional AM specific lipid biosynthetic gene *DIS* required for arbuscule development through forward genetics. *DIS* encodes a  $\beta$ -keto-acyl ACP synthase I (KASI) (Keymer et al. 2017). This gene was further characterized by Andreas Keymer (doctoral thesis to be completed). According to its homology with *Arabidopsis* KASI, *DIS* is predicted to catalyze condensation reactions from C4:0-ACP to C16:0-ACP during fatty acyl chain elongation (Li-Beisson et al. 2010). It was observed that *ram2* but not *dis* over-accumulates C16:0 fatty acids containing phospholipids and triacylglycerol. This observation indicates that *RAM2* uses C16:0 fatty acids synthesized by *DIS* as substrates for synthesis of  $\beta$ -MAG (Keymer et al. 2017). Congruously, *RAM2* (*GPAT6*) was shown to have substrate specificity for C16:0 fatty acids (Yang et al. 2012, Luginbuehl et al. 2017). Together, these results suggest that *RAM2* acts downstream of *DIS* in same lipid biosynthesis pathway. Genetics and phenotyping approaches integrated with lipidomics and isotopolog profiling of roots, intraradical and extraradical AM fungal hyphae revealed that plant lipids synthesized by *DIS* and *RAM2* in the arbuscule containing cells are supplied to the fatty acid auxotrophic AM fungi (Jiang et al. 2017, Keymer et al. 2017, Luginbuehl et al. 2017). Thus, all together we demonstrated that plants provide not only carbohydrate but also lipid to the AM fungi during symbiosis. However, it is still not well understood how lipids are transported from plants to fungi. Potential candidates which might be involved in lipid export are the two half ABCG transporters *STR* and *STR2*. *STR* could be implicated in lipid export from the arbuscule-containing cell based on analogy with the function of other ABCG

transporter family members (Zhang et al. 2010, Gutjahr et al. 2012, Lee et al. 2016). *STR* and *STR2* are individually essential for arbuscule development as the half ABCG transporter *STR* and *STR2* interact to form a full transporter (Zhang et al. 2010). Consistent with its predicted role in lipid export during arbuscule development, the *STR* protein localizes to the PAM (Zhang et al. 2010). Ectopic expression of *RAM1* induces *STR* in absence of AM fungi (Pimprikar et al. 2016). The *ram1*, *ram2*, *dis* and *str* mutant in *L. japonicus* showed strong reduction in accumulation of AM-specific lipids in colonized roots (Keymer et al. 2017). Thus, *RAM1* is sufficient for transcriptional activation of lipid biosynthesis and export genes, which likely act in a pathway, which is crucial for arbuscule development.

Due to simultaneous presence of different stages of AM development in the same root, it is challenging to attribute transcriptional changes to specific stage of AM development. Pharmacological application of synthetic fungal molecules to non-colonized roots, and separation of cells containing specific fungal structures using laser microdissection, partially revealed transcriptional changes during different AM developmental stages (Balestrini et al. 2007, Gomez et al. 2009, Czaja et al. 2012, Gaude et al. 2012, Hogenkamp and Küster 2013, Miyata et al. 2014, Camps et al. 2015, Giovannetti et al. 2015, Gutjahr et al. 2015, Hohnjec et al. 2015). Similarly, arbuscule development takes place in a step-wise manner but is an asynchronous process such that all stages (stage 0 to stage V, as shown in the introduction) are simultaneously present in the root (Gutjahr and Parniske 2013). Protein products of the genes required for these stages must precisely guide the step-wise development of the arbuscule. Transcriptional changes during arbuscule development likely occur in a successive but overlapping manner (Gutjahr and Parniske 2013). The transcriptome of arbuscule containing cells was investigated in detail using laser microdissection of cells containing arbuscules followed by qPCR or microarray hybridization (Fiorilli et al. 2009, Gomez et al. 2009, Gaude et al. 2012, Hogenkamp and Küster 2013). However, this method failed to correlate the transcriptional changes in arbuscule containing cells to particular developmental stage(s) of arbuscule. In addition, this approach could not analyze cells forming a PPA (stage 0 of arbuscule development) due to absence of a visible fungal structure. Until now it was not possible to trace the arbuscule developmental stages in live roots. The staining methods used to stain the fungal structure inside the roots, killed the roots. In this thesis, I designed a construct, which will help to correlate promoter activity to different developmental stages of AM and arbuscule including cells undergoing early cellular changes in live roots. Using the same construct, I could co-visualize arbuscule-developmental stages and promoter activity in living roots to show that *DIS* and *RAM2* promoters are active prior to and during arbuscule development but

promoter activity is absent during arbuscule degeneration (Keymer et al. 2017). In addition, *DIS* promoter activity was visible in the cortical cells of non-colonized but inoculated roots. Thus, activity of *RAM2* and *DIS* promoters indicates that cells prior to and during arbuscule development are engaged in production of lipids which is subsequently supplied to the fungus. Thus, the construct I designed is not only useful for localizing the promoter activity in live roots but also enable to follow micro-activity of promoter during arbuscule development.

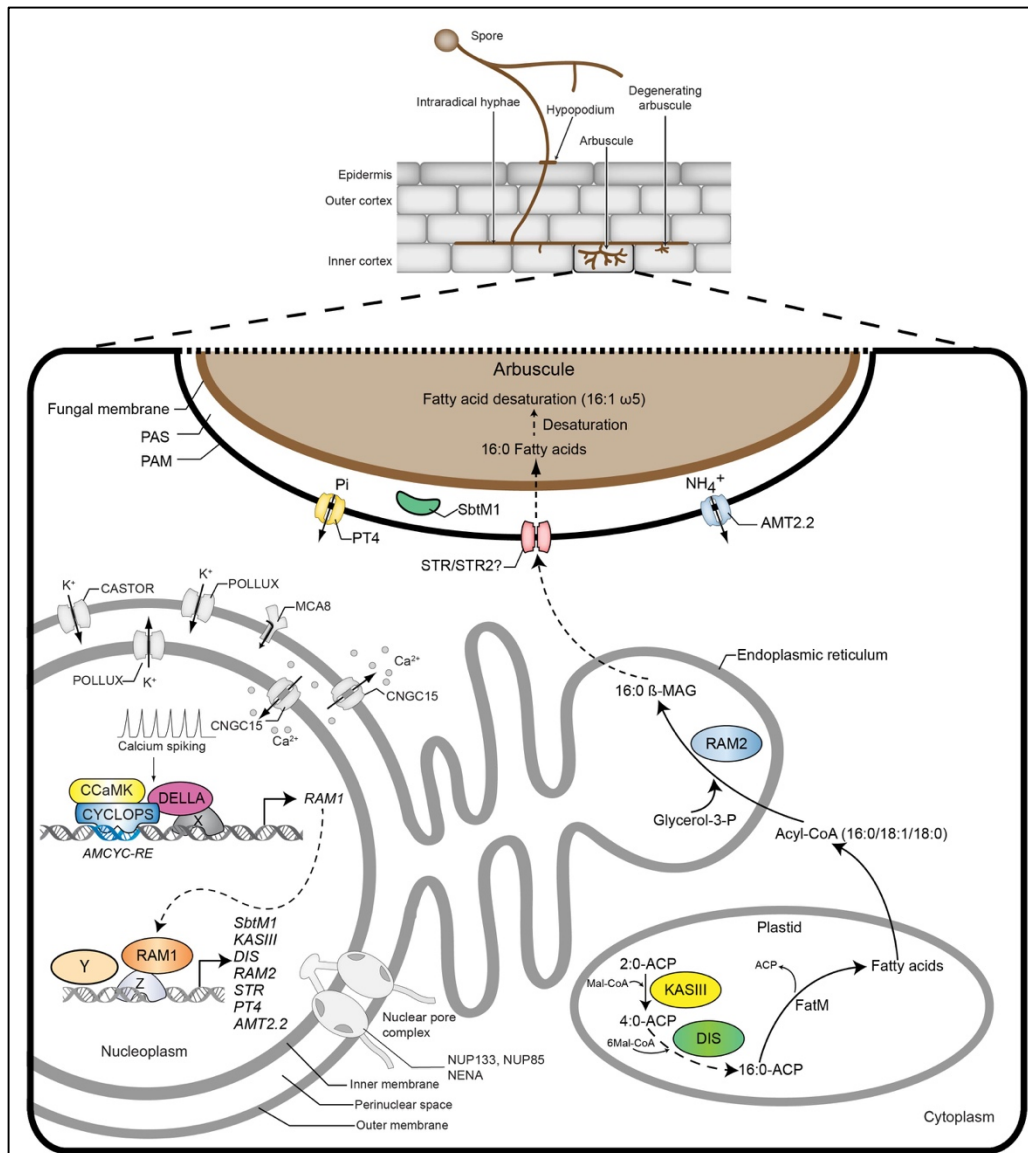


**Figure 5: RAM1 is a central regulator of arbuscule development (strongly modified from Singh and Parniske, 2012).** Model summarizing transcriptional regulation of *RAM1*, targets of *RAM1* and their predicted function in *L. japonicus*. Nuclear calcium spiking generated upon Myc Factor perception by the calcium spiking machinery (CASTOR, POLLUX, MCA8, NUP85, NUP133, NENA,

CNGC15s) is decoded by CCaMK (Calcium and Calmodulin dependent Kinase) which then interacts and phosphorylate CYCLOPS (Levy et al. 2004, Mitra et al. 2004, Kistner et al. 2005, Messinese et al. 2007, Gutjahr et al. 2008, Yano et al. 2008, Singh and Parniske 2012, Singh et al. 2014, Pimprikar et al. 2016). The CCaMK-CYCLOPS-DELLA complex activates the transcription of *REDUCED ARBUSCULAR MYCORRHIZA 1 (RAM1)* by direct binding of CYCLOPS to *AMCYC-RE* in the *RAM1* promoter. We hypothesize that an unknown DNA-binding transcription factor X also interacts with DELLA in addition to CYCLOPS to activate the transcription of *RAM1*. *RAM1* likely interacts with an unknown DNA binding transcription factor Z, which leads to the activation of the genes *SbtM1*, *PT4*, *AMT2.2*, *STR*, *KASIII*, *DIS* and *RAM2*. The unknown partially redundant factor Y acts at the level of *RAM1* in the activation of *SbtM1*, *PT4*, *STR* and *RAM2* in *L. japonicus*. The predicted subtilase (SbtM1) with unknown function localizes to the peri-arbuscular space (PAS) (Takeda et al. 2009). The PHOSPHATE TRANSPORTER 4 (PT4) and the AMMONIUM TRANSPORTER 2.2 (AMT2.2) are localized to the peri-arbuscular membrane (PAM) and are required for phosphate and nitrogen uptake from the peri-arbuscular space (PAS) delivered by the arbuscule (Harrison et al. 2002, Pumplin and Harrison 2009, Kobae et al. 2010, Breuillin-Sessoms et al. 2015). *KASIII* ( $\beta$ -KETO-ACYL ACP SYNTHASE III) in *L. japonicus* produces a precursor for DISORGANIZED ARBUSCULES (*DIS*,  $\beta$ -KETO-ACYL ACP SYNTHASE I) activity by catalyzing fatty acyl chain elongation from C2 to C4 (Keymer et al. 2017). *DIS* catalyzes condensation reactions from C4:0-ACP to C16:0-ACP during fatty acyl chain elongation (Keymer et al. 2017). *REDUCED ARBUSCULAR MYCORRHIZA 2 (RAM2)* acts downstream of *DIS* to synthesizes  $\beta$ -MAG using C16:0-ACP (Keymer et al. 2017). *STR* localizes to the PAM and is predicted to export lipids synthesized by *RAM2* to the arbuscule (Zhang et al. 2010, Jiang et al. 2017, Keymer et al. 2017, Luginbuehl et al. 2017). The exported lipids are then desaturated by fungal enzymes leading to accumulation of fungus-specific lipids containing 16:1  $\omega$ 5 fatty acids (Luginbuehl and Oldroyd 2017, MacLean et al. 2017, Rich et al. 2017b). ACP, ACYL-CARRIER PROTEIN; Ca<sup>2+</sup>, calcium ions; CoA, Coenzyme A; K<sup>+</sup>, potassium ions; Mal-CoA, Malonyl-Coenzyme A; MAG, monoacylglycerol; NH<sub>4</sub><sup>+</sup>, ammonium; Pi, phosphate.

## X. Outlook

Several experiments in *L. japonicus* and *M. truncatula* indicated that RAM1 is essential for AM-specific activation of a whole cohort of genes encoding proteins with diverse function, required for arbuscule development (Park et al. 2015, Rich et al. 2015, Xue et al. 2015, Pimprikar et al. 2016, Keymer et al. 2017, Luginbuehl et al. 2017). Thus, identifying all targets of RAM1 will help to understand the biology of complex arbuscule development and function. One of the approaches for identifying RAM1 targets would be to compare the transcriptome of colonized and non-colonized wild-type and *ram1* mutant roots by RNAseq in *L. japonicus*. A similar approach in *M. truncatula* and *P. hybrid* indicated AM induced genes were dependent on RAM1 (Luginbuehl et al. 2017, Rich et al. 2017a). However, RAM1 requirement for the induction of AM-specific genes varies within *L. japonicus*, *M. truncatula* and *P. hybrida* (Park et al. 2015, Rich et al. 2015, Xue et al. 2015, Pimprikar et al. 2016, Keymer et al. 2017, Luginbuehl et al. 2017) and therefore comparative studies for targets of RAM1 will increase our understanding of micro-diversification of gene regulatory network within closely related species such as legumes *L. japonicus* and *M. truncatula*. Understanding the role of the targets of RAM1 via reverse genetics will be next step towards increasing our current knowledge about arbuscule development. Many GRAS-type transcription factor family proteins are predicted to lack the ability to bind to the DNA directly and probably activate the transcription of gene via interaction with other DNA-binding transcription factor (Fukazawa et al. 2014, Yoshida et al. 2014, Fukazawa et al. 2017, Hirano et al. 2017). As RAM1 is also a GRAS-type transcription factor (Gobbato et al. 2012), it is possible that RAM1 interacts with proteins binding to DNA directly to activate transcription of genes required for arbuscule development. Therefore, it will be interesting to reveal RAM1 interacting partners and thereby the transcription factor complexes involved in the activation of RAM1 targets. RAM1 interacting partners can be identified by a Y2H screen of a cDNA library from AM colonized wild-type roots using RAM1 as a bait or by pull-down of protein complexes from colonized *ram1* transgenic hairy roots transformed with a construct expressing tagged RAM1 followed by protein identification via mass spectrometry. Furthermore, the identification of *cis*-regulatory elements in the promoter of the RAM1-target genes required for their activation via RAM1-containing transcription factor complexes will guide us to understand, which other genes could be regulated via same transcriptional complexes. AM development is tightly regulated by physiological and nutritional status of plants, likely via plant hormones. For example, high phosphate level or far-red light inhibit AM development (Breuillin et al. 2010,

Nagata et al. 2015). Also, in my thesis I showed that the GA regulated DELLA protein is required for activation of *RAM1*. Therefore, investigating whether other plant hormones participate in the transcriptional regulation of *RAM1* (for example activation) will be a step toward understanding how plants regulate AM symbiosis depending on their physiological and nutritional status.

## XI. References

- Akiyama, K., Matsuzaki, K. & Hayashi, H. (2005) Plant sesquiterpenes induce hyphal branching in arbuscular mycorrhizal fungi. *Nature*. 435: 824-827.
- Alexander, T., Toth, R., Meier, R. & Weber, H. C. (1989) Dynamics of arbuscule development and degeneration in onion, bean, and tomato with reference to vesicular–arbuscular mycorrhizae in grasses. *Can. J. Bot.* 67: 2505-2513.
- Ane, J.-M., Kiss, G. B., Riely, B. K., Penmetsa, R. V., Oldroyd, G. E. D., Ayax, C., Levy, J., Debelle, F., Baek, J.-M., Kalo, P., Rosenberg, C., Roe, B. A., Long, S. R., Denarie, J. & Cook, D. R. (2004) *Medicago truncatula* DMI1 required for bacterial and fungal symbioses in legumes. *Science*. 303: 1364-1367.
- Antolín-Llovera, M., Ried, M. K., Binder, A. & Parniske, M. (2012) Receptor kinase signaling pathways in plant-microbe interactions. *Ann. Rev. Phytopathol.* 50: 451-473.
- Antolín-Llovera, M., Ried, Martina k. & Parniske, M. (2014) Cleavage of the SYMBIOSIS RECEPTOR-LIKE KINASE ectodomain promotes complex formation with Nod Factor Receptor 5. *Curr. Biol.* 24: 422-427.
- Augé, R. M. (2001) Water relations, drought and vesicular-arbuscular mycorrhizal symbiosis. *Mycorrhiza*. 11: 3-42.
- Bago, B., Pfeffer, P. & Shachar-Hill, Y. (2000) Carbon metabolism and transport in arbuscular mycorrhizas. *Plant Physiol.* 124: 949-957.
- Balestrini, R., Berta, G. & Bonfante, P. (1992) The plant nucleus in mycorrhizal roots: positional and structural modifications. *Biol Cell.* 75: 235-243.
- Balestrini, R., Gómez-Ariza, J., Lanfranco, L. & Bonfante, P. (2007) Laser microdissection reveals that transcripts for five plant and one fungal phosphate transporter genes are contemporaneously present in arbusculated cells. *Mol. Plant-Microbe Interact.* 20: 1055-1062.
- Balzergue, C., Puech-Pagès, V., Bécard, G. & Rochange, S. F. (2010) The regulation of arbuscular mycorrhizal symbiosis by phosphate in pea involves early and systemic signalling events. *Journal of Experimental Botany.* 62: 1049-1060.
- Bentivenga, S. P. & Morton, J. B. (1996) Congruence of fatty acid methyl ester profiles and morphological characters of arbuscular mycorrhizal fungi in Gigasporaceae. *Proceedings of the National Academy of Sciences.* 93: 5659-5662.
- Besserer, A., Bécard, G., Jauneau, A., Roux, C. & Séjalon-Delmas, N. (2008) GR24, a synthetic analog of strigolactones, stimulates the mitosis and growth of the arbuscular mycorrhizal fungus *Gigaspora rosea* by boosting its energy metabolism. *Plant Physiol.* 148: 402-413.
- Besserer, A., Puech-Pagès, V. & Kiefer, P., Gomez-Roldan, V, Jauneau, a, Roy, S, Portais, Jc, Roux, C, Bécard, G, Séjalon-Delmas, N. (2006) Strigolactones stimulate arbuscular mycorrhizal fungi by activating mitochondria. *PLoS Biology.* 4: e226.
- Bialeski, R. (1973) Phosphate pools, phosphate transport, and phosphate availability. *Annual review of plant physiology.* 24: 225-252.

- Binder, A. & Parniske, M. (2013) The nuclear pore complex in symbiosis and pathogen defence. *Annual Plant Reviews: Plant Nuclear Structure, Genome Architecture and Gene Regulation, Volume 46*. 229-254.
- Blancaflor, E., Zhao, L. & Harrison, M. (2001) Microtubule organization in root cells of *Medicago trunculata* during development of an arbuscular mycorrhizal symbiosis with *Glomus versiforme*. *Protoplasma*. 217: 154-165.
- Bolle, C. (2004) The role of GRAS proteins in plant signal transduction and development. *Planta*. 218: 683-692.
- Bonfante, P. & Genre, A. (2008) Plants and arbuscular mycorrhizal fungi: an evolutionary-developmental perspective. *Trends Plant Sci*. 13: 492-498.
- Bonfante, P., Genre, A., Faccio, A., Martini, I., Schauser, L., Stougaard, J., Webb, J. & Parniske, M. (2000) The *Lotus japonicus* *LjSym4* gene is required for the successful symbiotic infection of root epidermal cells. *Mol. Plant-Microbe Interact*. 13: 1109-1120.
- Bravo, A., Brands, M., Wewer, V., Dörmann, P. & Harrison, M. J. (2017) Arbuscular mycorrhiza-specific enzymes FatM and RAM2 fine-tune lipid biosynthesis to promote development of arbuscular mycorrhiza. *New Phytol*. 214: 1631-1645.
- Bravo, A., York, T., Pumplin, N., Mueller, L. & Harrison, M. (2016) Genes conserved for arbuscular mycorrhizal symbiosis identified through phylogenomics. *Nature Plants*. 2 15208
- Breuillin, F., Schramm, J., Hajirezaei, M., Ahkami, A., Favre, P., Druège, U., Hause, B., Bucher, M., Kretschmar, T., Bossolini, E., Kuhlemeier, C., Martinoia, E., Franken, P., Scholz, U. & Reinhardt, D. (2010) Phosphate systemically inhibits development of arbuscular mycorrhiza in *Petunia hybrida* and represses genes involved in mycorrhizal functioning. *Plant J*. 64: 1002-1017.
- Breuillin-Sessoms, F., Floss, D. S., Gomez, S. K., Pumplin, N., Ding, Y., Levesque-Tremblay, V., Noar, R. D., Daniels, D. A., Bravo, A., Eaglesham, J. B., Benedito, V. A., Udvardi, M. K. & Harrison, M. J. (2015) Suppression of arbuscule degeneration in *Medicago truncatula phosphate transporter4* mutants is dependent on the ammonium transporter 2 family protein AMT2;3. *Plant Cell*. 27: 1352-1366.
- Brown, M. & King, E. (1982) Morphology and histology of vesicular-arbuscular mycorrhizae. A. Anatomy and cytology. *Methods and principles of mycorrhizal research. Amer. Phytopath. Soc.: St Paul*. 15-21.
- Buée, M., Rossignol, M., Jauneau, A., Ranjeva, R. & Bécard, G. (2000) The pre-symbiotic growth of arbuscular mycorrhizal fungi is induced by a branching factor partially purified from from plant root exsudates. . *Mol. Plant-Microbe Interact*. 13: 693-698.
- Buendia, L., Wang, T., Girardin, A. & Lefebvre, B. (2016) The LysM receptor-like kinase SILYK10 regulates the arbuscular mycorrhizal symbiosis in tomato. *New Phytol*. 210: 184-195.
- Camps, C., Jardinaud, M. F., Rengel, D., Carrère, S., Hervé, C., Debellé, F., Gamas, P., Bensmihen, S. & Gough, C. (2015) Combined genetic and transcriptomic

- analysis reveals three major signalling pathways activated by Myc-LCOs in *Medicago truncatula*. *New Phytol.* 208: 224-240.
- Capoen, W., Sun, J., Wysham, D., Otegui, M. S., Venkateshwaran, M., Hirsch, S., Miwa, H., Downie, J. A., Morris, R. J., Ané, J.-M. & Oldroyd, G. E. D. (2011) Nuclear membranes control symbiotic calcium signaling of legumes. *Proc. Natl. Acad. Sci. USA.* 108: 14348-14353.
- Carbonnel, S. & Gutjahr, C. (2014) Control of arbuscular mycorrhiza development by nutrient signals. *Front. Plant Sci.* 5.
- Carotenuto, G., Chabaud, M., Miyata, K., Capozzi, M., Takeda, N., Kaku, H., Shibuya, N., Nakagawa, T., Barker, D. G. & Genre, A. (2017) The rice LysM receptor-like kinase OsCERK1 is required for the perception of short-chain chitin oligomers in arbuscular mycorrhizal signaling. *New Phytol.* 214: 1440-1446.
- Cerri, M. R., Wang, Q., Stolz, P., Folgmann, J., Frances, L., Katzer, K., Li, X., Heckmann, A. B., Wang, T. L. & Downie, J. A. (2017) The *ERN1* transcription factor gene is a target of the CCaMK/CYCLOPS complex and controls rhizobial infection in *Lotus japonicus*. *New Phytologist.* 215: 323-337.
- Chabaud, M., Genre, A., Sieberer, B. J., Faccio, A., Fournier, J., Novero, M., Barker, D. G. & Bonfante, P. (2011) Arbuscular mycorrhizal hyphopodia and germinated spore exudates trigger Ca<sup>2+</sup> spiking in the legume and nonlegume root epidermis. *New Phytol.* 189: 347-355.
- Charpentier, M., Bredemeier, R., Wanner, G., Takeda, N., Schleiff, E. & Parniske, M. (2008) *Lotus japonicus* CASTOR and POLLUX are ion channels essential for perinuclear calcium spiking in legume root endosymbiosis. *Plant Cell.* 20: 3467-3479.
- Charpentier, M., Sun, J., Martins, T. V., Radhakrishnan, G. V., Findlay, K., Soumpourou, E., Thouin, J., Véry, A.-A., Sanders, D. & Morris, R. J. (2016) Nuclear-localized cyclic nucleotide-gated channels mediate symbiotic calcium oscillations. *Science.* 352: 1102-1105.
- Cook, C., Whichard, L. P., Wall, M., Egley, G. H., Coggon, P., Luhan, P. A. & Mcphail, A. (1972) Germination stimulants. II. Structure of strigol, a potent seed germination stimulant for witchweed (*Striga lutea*). *Journal of the American Chemical Society.* 94: 6198-6199.
- Cook, C. E., Whichard, L. P., Turner, B., Wall, M. E. & Egley, G. H. (1966) Germination of witchweed (*Striga lutea* Lour.): Isolation and properties of a potent stimulant. *Science.* 154: 1189-1190.
- Couzigou, J.-M., Lauressergues, D., André, O., Gutjahr, C., Guillotin, B., Bécard, G. & Combier, J.-P. (2017) Positive gene regulation by a natural protective miRNA enables arbuscular mycorrhizal symbiosis. *Cell host & microbe.* 21: 106-112.
- Cox, G. & Sanders, F. (1974) Ultrastructure of the host-fungus interface in a vesicular-arbuscular mycorrhiza. *New Phytol.* 73: 901-912.
- Cruz, C., Egsgaard, H., Trujillo, C., Ambus, P., Requena, N., Martins-Loução, M. A. & Jakobsen, I. (2007) Enzymatic evidence for the key role of arginine in

- nitrogen translocation by arbuscular mycorrhizal fungi. *Plant physiology*. 144: 782-792.
- Cutler, S. R., Ehrhardt, D. W., Griffiths, J. S. & Somerville, C. R. (2000) Random GFP::cDNA fusions enable visualization of subcellular structures in cells of *Arabidopsis* at a high frequency. *Proceedings of the National Academy of Sciences*. 97: 3718-3723.
- Czaja, L. F., Hogeekamp, C., Lamm, P., Maillet, F., Martinez, E. A., Samain, E., Dénarié, J., Küster, H. & Hohnjec, N. (2012) Transcriptional responses toward diffusible signals from symbiotic microbes reveal MtNFP- and MtDMI3-dependent reprogramming of host gene expression by arbuscular mycorrhizal fungal lipochitooligosaccharides. *Plant Physiol*. 159: 1671-1685.
- Davière, J.-M. & Achard, P. (2013) Gibberellin signaling in plants. *Development*. 140: 1147-1151.
- Davière, J.-M. & Achard, P. (2016) A pivotal role of DELLAs in regulating multiple hormone signals. *Mol. Plant*. 9: 10-20.
- Delaux, P.-M., Bécard, G. & Combier, J.-P. (2013) NSP1 is a component of the Myc signaling pathway. *New Phytol.*: DOI: 10.1111/nph.12340.
- Demchenko, K., Winzer, T., Stougaard, J., Parniske, M. & Pawlowski, K. (2004) Distinct roles of *Lotus japonicus* SYMRK and SYM15 in root colonization and arbuscule formation. *New Phytol*. 163: 381-392.
- Dickson, S. (2004) The Arum-Paris continuum of mycorrhizal symbioses. *New Phytol*. 163: 187-200.
- El Ghachtouli, N., Martin-Tanguy, J., Paynot, M. & Gianinazzi, S. (1996) First-report of the inhibition of arbuscular mycorrhizal infection of *Pisum sativum* by specific and irreversible inhibition of polyamine biosynthesis or by gibberellic acid treatment. *FEBS letters*. 385: 189-192.
- Endre, G., Kereszt, A., Kevei, Z. & Mihacea, S. (2002) A receptor kinase gene regulating symbiotic nodule development. *Nature*. 417: 962.
- Engstrom, E. M., Andersen, C. M., Gumulak-Smith, J., Hu, J., Orlova, E., Sozzani, R. & Bowman, J. (2010) Arabidopsis homologs of the petunia hairy meristem gene are required for maintenance of shoot and root indeterminacy. *Plant Physiol.*: pp. 110.168757.
- Ezawa, T., Smith, S. E. & Smith, F. A. (2002) P metabolism and transport in AM fungi. *Plant and Soil*. 244: 221-230.
- Favre, P., Bapaume, L., Bossolini, E., Delorenzi, M., Falquet, L. & Reinhardt, D. (2014) A novel bioinformatics pipeline to discover genes related to arbuscular mycorrhizal symbiosis based on their evolutionary conservation pattern among higher plants. *BMC Plant Biol*. 14: 333.
- Feddermann, N., Duvvuru Muni, R. R., Zeier, T., Stuurman, J., Ercolin, F., Schorderet, M. & Reinhardt, D. (2010) The PAM1 gene of petunia, required for intracellular accommodation and morphogenesis of arbuscular mycorrhizal fungi, encodes a homologue of VAPYRIN. *Plant J*. 64: 470-481.
- Fester, T., Strack, D. & Hause, B. (2001) Reorganization of tobacco root plastids during arbuscule development. *Planta*. 213: 864-868.

- Fiorilli, V., Catoni, M., Miozzi, L., Novero, M., Accotto, G. P. & Lanfranco, L. (2009) Global and cell-type gene expression profiles in tomato plants colonized by an arbuscular mycorrhizal fungus. *New Phytol.* 184: 975-987.
- Fleet, C. M. & Sun, T.-P. (2005) A DELLAcate balance: the role of gibberellin in plant morphogenesis. *Curr. Opin. Plant Biol.* 8: 77-85.
- Floss, D. S., Gomez, S. K., Park, H.-J., Maclean, A. M., Müller, L. M., Bhattarai, K. K., Lévesque-Tremblay, V., Maldonado-Mendoza, I. E. & Harrison, M. J. (2017) A transcriptional program for arbuscule degeneration during AM symbiosis is regulated by MYB1. *Current Biology.* 27: 1206-1212.
- Floss, D. S., Lévesque-Tremblay, V., Park, H.-J. & Harrison, M. J. (2016) DELLA proteins regulate expression of a subset of AM symbiosis-induced genes in *Medicago truncatula*. *Plant Signaling & Behavior.* 11: e1162369.
- Floss, D. S., Levy, J. G., Lévesque-Tremblay, V., Pumplun, N. & Harrison, M. J. (2013) DELLA proteins regulate arbuscule formation in arbuscular mycorrhizal symbiosis. *Proc. Natl. Acad. Sci. USA.* 110: E5025-E5034.
- Fonouni-Farde, C., Tan, S., Baudin, M., Brault, M., Wen, J., Mysore, K. S., Niebel, A., Frugier, F. & Diet, A. (2016) DELLA-mediated gibberellin signalling regulates Nod factor signalling and rhizobial infection. *Nature communications.* 7.
- Foo, E., Ross, J. J., Jones, W. T. & Reid, J. B. (2013) Plant hormones in arbuscular mycorrhizal symbioses: an emerging role for gibberellins. *Ann. Bot.* 111: 769-779.
- Frenzel, A., Manthey, K., Perlick, A. M., Meyer, F., Pühler, A., Küster, H. & Krajinski, F. (2005) Combined transcriptome profiling reveals a novel family of arbuscular mycorrhizal-specific *Medicago truncatula* lectin genes. *Molecular plant-microbe interactions.* 18: 771-782.
- Fukazawa, J., Mori, M., Watanabe, S., Miyamoto, C., Ito, T. & Takahashi, Y. (2017) DELLA-GAF1 Complex is a Main Component in Gibberellin Feedback Regulation of GA20ox2 in Arabidopsis. *Plant Physiol.*: pp. 00282.2017.
- Fukazawa, J., Teramura, H., Murakoshi, S., Nasuno, K., Nishida, N., Ito, T., Yoshida, M., Kamiya, Y., Yamaguchi, S. & Takahashi, Y. (2014) DELLAs function as coactivators of GAI-ASSOCIATED FACTOR1 in regulation of gibberellin homeostasis and signaling in *Arabidopsis*. *Plant Cell.* 26: 2920-2938.
- Gaude, N., Bortfeld, S., Duensing, N., Lohse, M. & Krajinski, F. (2012) Arbuscule-containing and non-colonized cortical cells of mycorrhizal roots undergo extensive and specific reprogramming during arbuscular mycorrhizal development. *Plant J.* 69: 510-528.
- Genre, A. & Bonfante, P. (1998) Actin versus tubulin configuration in arbuscule-containing cells from mycorrhizal tobacco roots. *New Phytol.* 140: 745-752.
- Genre, A., Chabaud, M., Balzergue, C., Puech-Pages, V., Novero, M., Rey, T., Fournier, J., Rochange, S., Becard, G., Bonfante, P. & Barker, D. (2013) Short-chain chitin oligomers from arbuscular mycorrhizal fungi trigger nuclear Ca(2+) spiking in *Medicago truncatula* roots and their production is enhanced by strigolactone. *New Phytol.* 198: 190-202.

- Genre, A., Chabaud, M., Faccio, A., Barker, D. G. & Bonfante, P. (2008) Prepenetration apparatus assembly precedes and predicts the colonization patterns of arbuscular mycorrhizal fungi within the root cortex of both *Medicago truncatula* and *Daucus carota*. *Plant Cell*. 20: 1407-1420.
- Genre, A., Chabaud, M. & Timmers, T., Bonfante, P, Barker, Dg. (2005) Arbuscular mycorrhizal fungi elicit a novel intracellular apparatus in *Medicago truncatula* root epidermal cells before infection. *Plant Cell*. 17: 3489-3499.
- Genre, A., Ivanov, S., Fendrych, M., Faccio, A., Zarsky, V., Bisseling, T. & Bonfante, P. (2012) Multiple exocytotic markers accumulate at the sites of perifungal membrane biogenesis in arbuscular mycorrhizas. *Plant Cell Physiol*. 53: 244-255.
- Genre, A., Ortu, G., Bertoldo, C., Martino, E. & Bonfante, P. (2009) Biotic and abiotic stimulation of root epidermal cells reveals common and specific responses to arbuscular mycorrhizal fungi. *Plant Physiol*. 149: 1424-1434.
- Gianinazzi, S., Gollotte, A., Binet, M.-N., Tuinen, D., Redecker, D. & Wipf, D. (2010) Agroecology: the key role of arbuscular mycorrhizas in ecosystem services. *Mycorrhiza*. 20: 519-530.
- Giovannetti, M., Mari, A., Novero, M. & Bonfante, P. (2015) Early *Lotus japonicus* root transcriptomic responses to symbiotic and pathogenic fungal exudates. *Front. Plant Sci*. 6.
- Gobbato, E., Marsh, J., Vernié, T., Wang, E., Maillet, F., Kim, J., Miller, J., Sun, J., Bano, S., Ratet, P., Mysore, K., Dènarié, J., Schultze, M. & Oldroyd, G. (2012) A GRAS-type transcription factor with a specific function in mycorrhizal signaling. *Curr. Biol*. 22: 2236-2241.
- Gobbato, E., Wang, E., Higgins, G., Bano, S. A., Henry, C., Schultze, M. & Oldroyd, G. E. D. (2013) *RAM1* and *RAM2* function and expression during arbuscular mycorrhizal symbiosis and *Aphanomyces euteiches* colonization. *Plant Signaling & Behavior*. 8: e26049.
- Göhre, V. & Paszkowski, U. (2006) Contribution of the arbuscular mycorrhizal symbiosis to heavy metal phytoremediation. *Planta*. 223: 1115-1122.
- Gomez, S. K., Javot, H., Deewatthanawong, P., Torres-Jerez, I., Tang, Y., Blancaflor, E., Udvardi, M. & Harrison, M. (2009) *Medicago truncatula* and *Glomus intraradices* gene expression in cortical cells harboring arbuscules in the arbuscular mycorrhizal symbiosis. *BMC Plant Biol*. 9: 10.
- Govindarajulu, M., Pfeffer, P., Jin, H. & Abubaker, J., Douds, Dd, Allen, Jw, Bücking, H, Lammers, Pj, Shachar-Hill, Y. (2005) Nitrogen transfer in the arbuscular mycorrhizal symbiosis. *Nature*. 435: 819-823.
- Graham, J. H., Hodge, N. C. & Morton, J. B. (1995) Fatty Acid methyl ester profiles for characterization of glomalean fungi and their endomycorrhizae. *Applied and environmental microbiology*. 61: 58-64.
- Groth, M., Kosuta, S., Gutjahr, C., Haage, K., Hardel, S. L., Schaub, M., Brachmann, A., Sato, S., Tabata, S., Findlay, K., Wang, T. L. & Parniske, M. (2013) Two *Lotus japonicus* symbiosis mutants impaired at distinct steps of arbuscule development. *Plant J*. 75: 117-129.

- Groth, M., Takeda, N., Perry, J., Uchida, H., Draxl, S., Brachmann, A., Sato, S., Tabata, S., Kawaguchi, M., Wang, T. L. & Parniske, M. (2010) NENA, a *Lotus japonicus* homolog of Sec13, is required for rhizodermal infection by arbuscular mycorrhiza fungi and rhizobia but dispensable for cortical endosymbiotic development. *Plant Cell*. 22: 2509-2526.
- Guether, M., Balestrini, R., Hannah, M., He, J., Udvardi, M. & Bonfante, P. (2009a) Genome-wide reprogramming of regulatory networks, transport, cell wall and membrane biogenesis during arbuscular mycorrhizal symbiosis in *Lotus japonicus*. *New Phytol*. 182: 200-212.
- Guether, M., Neuhauser, B., Balestrini, R., Dynowski, M., Ludewig, U. & Bonfante, P. (2009b) A mycorrhizal-specific ammonium transporter from *Lotus japonicus* acquires nitrogen released by arbuscular mycorrhizal fungi. *Plant Physiol*. 150: 73-83.
- Güimil, S., Chang, H. & Zhu, T., Sesma, a, Osbourn, a, Roux, C, Ioannidis, V, Oakeley, Ej, Docquier, M, Descombes, P, Briggs, Sp, Paszkowski, U. (2005) Comparative transcriptomics of rice reveals an ancient pattern of response to microbial colonization. *Proc. Natl. Acad. Sci. USA*. 102: 8066-8070.
- Gutjahr, C., Banba, M., Croset, V., An, K., Miyao, A., An, G., Hirochika, H., Imaizumi-Anraku, H. & Paszkowski, U. (2008) Arbuscular mycorrhiza-specific signaling in rice transcends the common symbiosis signaling pathway. *Plant Cell*. 20: 2989-3005.
- Gutjahr, C., Gobbato, E., Choi, J., Riemann, M., Johnston, M. G., Summers, W., Carbonnel, S., Mansfield, C., Yang, S.-Y., Nadal, M., Acosta, I., Takano, M., Jiao, W.-B., Schneeberger, K., Kelly, K. A. & Paszkowski, U. (2015) Rice perception of symbiotic arbuscular mycorrhizal fungi requires the karrikin receptor complex. *Science*. 350: 1521-1524.
- Gutjahr, C., Novero, M., Guether, M., Montanari, O., Udvardi, M. & Bonfante, P. (2009) Presymbiotic factors released by the arbuscular mycorrhizal fungus *Gigaspora margarita* induce starch accumulation in *Lotus japonicus* roots. *New Phytol*. 183: 53-61.
- Gutjahr, C. & Parniske, M. (2013) Cell and developmental biology of the arbuscular mycorrhiza symbiosis. *Ann. Rev. Cell Dev. Biol*. 29: 593-617.
- Gutjahr, C. & Parniske, M. (2017) Cell Biology: Control of partner lifetime in a plant-fungus relationship. *Curr. Biol*. 27: R420-R423.
- Gutjahr, C., Radovanovic, D., Geoffroy, J., Zhang, Q., Siegler, H., Chiapello, M., Casieri, L., An, K., An, G., Guiderdoni, E., Kumar, C. S., Sundaresan, V., Harrison, M. J. & Paszkowski, U. (2012) The half-size ABC transporters STR1 and STR2 are indispensable for mycorrhizal arbuscule formation in rice. *Plant J*. 69: 906-920.
- Handa, Y., Nishide, H., Takeda, N., Suzuki, Y., Kawaguchi, M. & Saito, K. (2015) RNA-seq transcriptional profiling of an arbuscular mycorrhiza provides insights into regulated and coordinated gene expression in *Lotus japonicus* and *Rhizophagus irregularis*. *Plant Cell Physiol*. 56: 1490-1511.

- Hans, J., Hause, B., Strack, D. & Walter, M. H. (2004) Cloning, characterization, and immunolocalization of a mycorrhiza-inducible 1-deoxy-d-xylulose 5-phosphate reductoisomerase in arbuscule-containing cells of maize. *Plant Physiol.* 134: 614-624.
- Harrison, M., Dewbre, G. & Liu, J. (2002) A phosphate transporter of *Medicago truncatula* involved in the acquisition of phosphate released by arbuscular mycorrhizal fungi. *Plant Cell.* 14: 2413-2429.
- Hauvermale, A. L., Ariizumi, T. & Steber, C. M. (2012) Gibberellin signaling: a theme and variations on DELLA repression. *Plant physiology.* 160: 83-92.
- Hayashi, T., Banba, M., Shimoda, Y., Kouchi, H., Hayashi, M. & Imaizumi-Anraku, H. (2010) A dominant function of CCaMK in intracellular accommodation of bacterial and fungal endosymbionts. *Plant J.* 63: 141-154.
- Heck, C., Kuhn, H., Heidt, S., Walter, S., Rieger, N. & Requena, N. (2016) Symbiotic fungi control plant root cortex development through the novel GRAS transcription factor MIG1. *Curr. Biol.* 26: 2770-2778.
- Hedden, P. & Thomas, S. G. (2012) Gibberellin biosynthesis and its regulation. *Biochemical Journal.* 444: 11-25.
- Helber, N., Wippel, K., Sauer, N., Schaarschmidt, S., Hause, B. & Requena, N. (2011) A versatile monosaccharide transporter that operates in the arbuscular mycorrhizal fungus *Glomus* sp is crucial for the symbiotic relationship with plants. *Plant Cell.* 23: 3812-3823.
- Held, M., Hossain, M. S., Yokota, K., Bonfante, P., Stougaard, J. & Szczyglowski, K. (2010) Common and not so common symbiotic entry. *Trends in plant science.* 15: 540-545.
- Hirano, Y., Nakagawa, M., Suyama, T., Murase, K., Shirakawa, M., Takayama, S., Sun, T. & Hakoshima, T. (2017) Structure of the SHR-SCR heterodimer bound to the BIRD/IDD transcriptional factor JKD. *Nature plants.* 3: 17010.
- Hirsch, S., Kim, J., Muñoz, A., Heckmann, A. B., Downie, J. A. & Oldroyd, G. E. (2009) GRAS proteins form a DNA binding complex to induce gene expression during nodulation signaling in *Medicago truncatula*. *Plant Cell.* 21: 545-557.
- Hodge, A., Campbell, C. D. & Fitter, A. H. (2001) An arbuscular mycorrhizal fungus accelerates decomposition and acquires nitrogen directly from organic material. *Nature.* 413: 297-299.
- Hofferek, V., Mendrinna, A., Gaude, N., Krajinski, F. & Devers, E. A. (2014) MiR171h restricts root symbioses and shows like its target *NSP2* a complex transcriptional regulation in *Medicago truncatula*. *BMC Plant Biol.* 14: 199.
- Hogekamp, C. & Küster, H. (2013) A roadmap of cell-type specific gene expression during sequential stages of the arbuscular mycorrhiza symbiosis. *BMC Genom.* 14.
- Hohnjec, N., Czaja-Hasse, L. F., Hogekamp, C. & Küster, H. (2015) Pre-announcement of symbiotic guests: transcriptional reprogramming by mycorrhizal lipochitoooligosaccharides shows a strict co-dependency on the GRAS transcription factors *NSP1* and *RAM1*. *BMC genomics.* 16: 994.

- Hohnjec, N., Vieweg, M., Pühler, A., Becker, A. & Küster, H. (2005) Overlaps in the transcriptional profiles of *Medicago truncatula* roots inoculated with two different *Glomus* fungi provide insights in the genetic program activated during arbuscular mycorrhiza. *Plant Physiol.* 137: 1283-1301.
- Imaizumi-Anraku, H., Takeda, N., Charpentier, M. & Perry, J., Miwa, H, Umehara, Y, Kouchi, H, Murakami, Y, Mulder, L, Vickers, K, Pike, J, Downie, Ja, Wang, T, Sato, S, Asamizu, E, Tabata, S, Yoshikawa, M, Murooka, Y, Wu, G, Kawaguchi, M, Kawasaki, S, Parniske, M, Hayashi, M. (2005) Plastid proteins crucial for symbiotic fungal and bacterial entry into plant roots. *Nature.* 433: 527 - 531.
- Ivanov, S., Fedorova, E. E., Limpens, E., De Mita, S., Genre, A., Bonfante, P. & Bisseling, T. (2012) Rhizobium–legume symbiosis shares an exocytotic pathway required for arbuscule formation. *Proc. Natl. Acad. Sci. USA.* 109: 8316-8321.
- Ivanov, S. & Harrison, M. J. (2014) A set of fluorescent protein-based markers expressed from constitutive and arbuscular mycorrhiza-inducible promoters to label organelles, membranes and cytoskeletal elements in *Medicago truncatula*. *Plant J.* 80: 1151-1163.
- Javot, H., Penmetsa, R. V., Breuillin, F., Bhattarai, K. K., Noar, R. D., Gomez, S. K., Zhang, Q., Cook, D. R. & Harrison, M. J. (2011) *Medicago truncatula mtpt4* mutants reveal a role for nitrogen in the regulation of arbuscule degeneration in arbuscular mycorrhizal symbiosis. *Plant J.* 68: 954-965.
- Javot, H., Pumplin, N. & Harrison, M. (2007a) Phosphate in the arbuscular mycorrhizal symbiosis: transport properties and regulatory roles. *Plant Cell Environ.* 30: 310-322.
- Javot, H., Varma Penmetsa, R., Terzaghi, N., Cook, D. R. & Harrison, M. J. (2007b) A *Medicago truncatula* phosphate transporter indispensable for the arbuscular mycorrhizal symbiosis. *Proc. Natl. Acad. Sci. USA.* 104: 1720-1725.
- Jiang, Y., Wang, W., Xie, Q., Liu, N., Liu, L., Wang, D., Zhang, X., Yang, C., Chen, X. & Tang, D. (2017) Plants transfer lipids to sustain colonization by mutualistic mycorrhizal and parasitic fungi. *Science.* eaam9970.
- Jin, Y., Liu, H., Luo, D., Yu, N., Dong, W., Wang, C., Zhang, X., Dai, H., Yang, J. & Wang, E. (2016) DELLA proteins are common components of symbiotic rhizobial and mycorrhizal signalling pathways. *Nature communications.* 7.
- Kaló, P., Gleason, C., Edwards, A., Marsh, J., Mitra, R., Hirsch, S., Jakab, J., Sims, S., Long, S., Rogers, J., Kiss, G., Downie, J. & Oldroyd, G. (2005) Nodulation signaling in legumes requires NSP2, a member of the GRAS family of transcriptional regulators. *Science.* 308: 1786-1789.
- Kanamori, N., Madsen, L. H., Radutoiu, S., Frantescu, M., Quistgaard, E. M., Miwa, H., Downie, J. A., James, E. K., Felle, H. H. & Haaning, L. L. (2006) A nucleoporin is required for induction of Ca<sup>2+</sup> spiking in legume nodule development and essential for rhizobial and fungal symbiosis. *Proc. Natl. Acad. Sci. USA.* 103: 359-364.

- Karandashov, V. & Bucher, M. (2005) Symbiotic phosphate transport in arbuscular mycorrhizas. *Trends in plant science*. 10: 22-29.
- Kevei, Z., Loughon, G., Mergaert, P., Horváth, G. V., Kereszt, A., Jayaraman, D., Zaman, N., Marcel, F., Regulski, K. & Kiss, G. B. (2007) 3-Hydroxy-3-methylglutaryl coenzyme A reductase1 interacts with NORK and is crucial for nodulation in *Medicago truncatula*. *Plant Cell*. 19: 3974-3989.
- Keymer, A., Pimprikar, P., Wewer, V., Huber, C., Brands, M., Bucerius, S. L., Delaux, P. M., Klingl, V., Ropenack-Lahaye, E. V., Wang, T. L., Eisenreich, W., Dormann, P., Parniske, M. & Gutjahr, C. (2017) Lipid transfer from plants to arbuscular mycorrhiza fungi. *Elife*. 6.
- Kistner, C. & Parniske, M. (2002) Evolution of signal transduction in intracellular symbiosis. *Trends Plant Sci*. 7.
- Kistner, C., Winzer, T. & Pitzschke, A., Mulder, L., Sato, S, Kaneko, T, Tabata, S, Sandal, N, Stougaard, J, Webb, K, Szczyglowski, K, Parniske, M. (2005) Seven *Lotus japonicus* genes required for transcriptional reprogramming of the root during fungal and bacterial symbiosis. *Plant Cell*. 17: 2217-2229.
- Kobae, Y. & Hata, S. (2010) Dynamics of periarbuscular membranes visualized with a fluorescent phosphate transporter in arbuscular mycorrhizal roots of rice. *Plant Cell Physiol*. 51: 341-353.
- Kobae, Y., Tamura, Y., Takai, S., Banba, M. & Hata, S. (2010) Localized expression of arbuscular mycorrhiza-inducible ammonium transporters in soybean. *Plant Cell Physiol*. 51: 1411-1415.
- Kosuta, S., Chabaud, M., Loughon, G., Gough, C., Dénarié, J., Barker, D. & Becard, G. (2003) A diffusible factor from arbuscular mycorrhizal fungi induces symbiosis-specific *MtENOD11* expression in roots of *Medicago truncatula*. *Plant Physiol*. 131: 952-962.
- Kosuta, S., Hazledine, S., Sun, J., Miwa, H., Morris, R. J., Downie, J. A. & Oldroyd, G. E. D. (2008) Differential and chaotic calcium signatures in the symbiosis signaling pathway of legumes. *Proc. Natl. Acad. Sci. USA*. 105: 9823-9828.
- Kretschmar, T., Kohlen, W., Sasse, J., Borghi, L., Schlegel, M., Bachelier, J. B., Reinhardt, D., Bours, R., Bouwmeester, H. J. & Martinoia, E. (2012) A petunia ABC protein controls strigolactone-dependent symbiotic signalling and branching. *Nature*. 483: 341-344.
- Kuhn, H., Küster, H. & Requena, N. (2010) Membrane steroid-binding protein 1 induced by a diffusible fungal signal is critical for mycorrhization in *Medicago truncatula*. *New Phytol*. 185: 716-733.
- Lauressergues, D., Delaux, P.-M., Formey, D., Lelandais-Brière, C., Fort, S., Cottaz, S., Bécard, G., Niebel, A., Roux, C. & Combier, J.-P. (2012) The microRNA miR171h modulates arbuscular mycorrhizal colonization of *Medicago truncatula* by targeting NSP2. *Plant J*. 72: 512-522.
- Lee, J.-Y., Kinch, L. N., Borek, D. M., Wang, J., Wang, J., Urbatsch, I. L., Xie, X.-S., Grishin, N. V., Cohen, J. C. & Otwinowski, Z. (2016) Crystal structure of the human sterol transporter ABCG5/ABCG8. *Nature*. 533: 561-564.

- Levy, J., Bres, C., Geurts, R., Chalhoub, B., Kulikova, O., Duc, G., Journet, E.-P., Ane, J.-M., Lauber, E., Bisseling, T., Denarie, J., Rosenberg, C. & Debelle, F. (2004) A putative Ca<sup>2+</sup> and calmodulin-dependent protein kinase required for bacterial and fungal symbioses. *Science*. 303: 1361-1364.
- Li, S., Zhao, Y., Zhao, Z., Wu, X., Sun, L., Liu, Q. & Wu, Y. (2016) Crystal Structure of the GRAS Domain of SCARECROW-LIKE7 in *Oryza sativa*. *The Plant Cell Online*. 28: 1025-1034.
- Li-Beisson, Y., Shorrosh, B., Beisson, F., Andersson, M. X., Arondel, V., Bates, P. D., Baud, S., Bird, D., Debono, A., Durrett, T. P., Franke, R. B., Graham, I. A., Katayama, K., Kelly, A. A., Larson, T., Markham, J. E., Miquel, M., Molina, I., Nishida, I., Rowland, O., Samuels, L., Schmid, K. M., Wada, H., Welti, R., Xu, C., Zallot, R. & Ohlrogge, J. (2010) Acyl-Lipid Metabolism. *The Arabidopsis Book*. e0133.
- Liu, J., Blaylock, L., Endre, G., Cho, J., Town, C., Vandenbosch, K. & Harrison, M. (2003) Transcript profiling coupled with spatial expression analysis reveals genes involved in distinct developmental stages of the arbuscular mycorrhizal symbiosis. *Plant Cell*. 15: 2106-2123.
- Liu, J., Maldonado-Mendoza, I., Lopez-Meyer, M., Cheung, F., Town, C. D. & Harrison, M. J. (2007) Arbuscular mycorrhizal symbiosis is accompanied by local and systemic alterations in gene expression and an increase in disease resistance in the shoots. *Plant J*. 50: 529-544.
- Liu, W., Kohlen, W., Lillo, A., Op Den Camp, R., Ivanov, S., Hartog, M., Limpens, E., Jamil, M., Smaczniak, C., Kaufmann, K., Yang, W.-C., Hooiveld, G. J. E. J., Charnikhova, T., Bouwmeester, H. J., Bisseling, T. & Geurts, R. (2011) Strigolactone biosynthesis in *Medicago truncatula* and rice requires the symbiotic GRAS-type transcription factors NSP1 and NSP2. *Plant Cell*. 23: 3853-3865.
- Lohse, S., Schliemann, W., Ammer, C., Kopka, J., Strack, D. & Fester, T. (2005) Organization and metabolism of plastids and mitochondria in arbuscular mycorrhizal roots of *Medicago truncatula*. *Plant Physiol*. 139: 329-340.
- López-Pedrosa, A., González-Guerrero, M., Valderas, A., Azcón-Aguilar, C. & Ferrol, N. (2006) *GintAMT1* encodes a functional high-affinity ammonium transporter that is expressed in the extraradical mycelium of *Glomus intraradices*. *Fungal Genetics and Biology*. 43: 102-110.
- Lota, F., Wegmüller, S., Buer, B., Sato, S., Bräutigam, A., Hanf, B. & Bucher, M. (2013) The *cis*-acting CTTC-P1BS module is indicative for gene function of *LjVTI12*, a Qb-SNARE protein gene, required for arbuscule formation in *Lotus japonicus*. *Plant J*. 74: 280-293.
- Luginbuehl, L. H., Menard, G. N., Kurup, S., Van Erp, H., Radhakrishnan, G. V., Breakspear, A., Oldroyd, G. E. & Eastmond, P. J. (2017) Fatty acids in arbuscular mycorrhizal fungi are synthesized by the host plant. *Science*. eaan0081.
- Luginbuehl, L. H. & Oldroyd, G. E. (2017) Understanding the arbuscule at the heart of endomycorrhizal symbioses in plants. *Curr. Biol*. 27: R952-R963.

- Maclean, A. M., Bravo, A. & Harrison, M. J. (2017) Plant signaling and metabolic pathways enabling arbuscular mycorrhizal symbiosis. *The Plant Cell*. 29: 2319-2335.
- Madan, R., Pankhurst, C., Hawke, B. & Smith, S. (2002) Use of fatty acids for identification of AM fungi and estimation of the biomass of AM spores in soil. *Soil Biology and Biochemistry*. 34: 125-128.
- Maillet, F., Poinso, V., Andre, O., Puech-Pages, V., Haouy, A., Gueunier, M., Cromer, L., Giraudet, D., Formey, D., Niebel, A., Martinez, E. A., Driguez, H., Becard, G. & Denarie, J. (2011) Fungal lipochitooligosaccharide symbiotic signals in arbuscular mycorrhiza. *Nature*. 469: 58-63.
- Messinese, E., Mun, J., Yeun, L., Jayaraman, D., Rougé, P., Barre, A., Lougnon, G., Schornack, S., Bono, J., Cook, D. & Ané, J. (2007) A novel nuclear protein interacts with the symbiotic DMI3 calcium and calmodulin dependent protein kinase of *Medicago truncatula*. *Mol. Plant-Microbe Interact.* 20: 912-921.
- Miller, J. B., Pratap, A., Miyahara, A., Zhou, L., Bornemann, S., Morris, R. J. & Oldroyd, G. E. D. (2013) Calcium/calmodulin-dependent protein kinase is negatively and positively regulated by calcium, providing a mechanism for decoding calcium responses during symbiosis signaling. *Plant Cell*. 25: 5053-5066.
- Mitra, R. M., Gleason, C. A., Edwards, A., Hadfield, J., Downie, J. A., Oldroyd, G. E. D. & Long, S. R. (2004) From The Cover: A Ca<sup>2+</sup>/calmodulin-dependent protein kinase required for symbiotic nodule development: Gene identification by transcript-based cloning. *Proc. Natl. Acad. Sci. USA*. 101: 4701-4705.
- Miyata, K., Kozaki, T., Kouzai, Y., Ozawa, K., Ishii, K., Asamizu, E., Okabe, Y., Umehara, Y., Miyamoto, A. & Kobae, Y. (2014) The bifunctional plant receptor, OsCERK1, regulates both chitin-triggered immunity and arbuscular mycorrhizal symbiosis in rice. *Plant Cell Physiol*. 55: 1864-1872.
- Mukherjee, A. & Ané, J.-M. (2010) Germinating spore exudates from arbuscular mycorrhizal fungi: molecular and developmental responses in plants and their regulation by ethylene. *Mol. Plant-Microbe Interact.* 24: 260-270.
- Murray, J. D., Cousins, D. R., Jackson, K. J. & Liu, C. (2013) Signaling at the root surface: the role of cutin monomers in mycorrhization. *Molecular plant*. 6: 1381.
- Murray, J. D., Muni, R. R. D., Torres-Jerez, I., Tang, Y., Allen, S., Andriankaja, M., Li, G., Laxmi, A., Cheng, X., Wen, J., Vaughan, D., Schultze, M., Sun, J., Charpentier, M., Oldroyd, G., Tadege, M., Ratet, P., Mysore, K. S., Chen, R. & Udvardi, M. K. (2011) Vapyrin, a gene essential for intracellular progression of arbuscular mycorrhizal symbiosis, is also essential for infection by rhizobia in the nodule symbiosis of *Medicago truncatula*. *Plant J*. 65: 244-252.
- Nagahashi, G. & Douds, D. D. (1997) Appressorium formation by AM fungi on isolated cell walls of carrot roots. *New Phytol*. 136: 299-304.

- Nagata, M., Yamamoto, N., Shigeyama, T., Terasawa, Y., Anai, T., Sakai, T., Inada, S., Arima, S., Hashiguchi, M., Akashi, R., Nakayama, H., Ueno, D., Hirsch, A. M. & Suzuki, A. (2015) Red/far red light controls arbuscular mycorrhizal colonization via jasmonic acid and strigolactone signaling. *Plant Cell Physiol.* 56: 2100-2109.
- Navazio, L., Moscatiello, R. & Genre, A., Novero, M, Baldan, B, Bonfante, P, Mariani, P. (2007) A diffusible signal from arbuscular mycorrhizal fungi elicits a transient cytosolic calcium elevation in host plant cells. *Plant Physiol.* 114: 673-681.
- Olah, B., Brière, C., Bécard, G., Dénarié, J. & Gough, C. (2005) Nod factors and a diffusible factor from arbuscular mycorrhizal fungi stimulate lateral root formation in *Medicago truncatula* via the DMI1/DMI2 signalling pathway. *Plant J.* 44: 195-207.
- Oldroyd, G. E. & Downie, J. A. (2004) Calcium, kinases and nodulation signalling in legumes. *Nature Reviews Molecular Cell Biology.* 5: 566-576.
- Op Den Camp, R., Streng, A., De Mita, S., Cao, Q., Polone, E., Liu, W., Ammiraju, J. S. S., Kudrna, D., Wing, R., Untergasser, A., Bisseling, T. & Geurts, R. (2011) LysM-type mycorrhizal receptor recruited for rhizobium symbiosis in nonlegume *Parasponia*. *Science.* 331: 909-912.
- Ortu, G., Balestrini, R., Pereira, P. A., Becker, J. D., Küster, H. & Bonfante, P. (2012) Plant genes related to gibberellin biosynthesis and signaling are differentially regulated during the early stages of AM fungal interactions. *Mol. Plant.* 5: 951-4.
- Pan, H., Oztas, O., Zhang, X., Wu, X., Stonoha, C., Wang, E., Wang, B. & Wang, D. (2016) A symbiotic SNARE protein generated by alternative termination of transcription. *Nature plants.* 2: 15197.
- Park, H.-J., Floss, D. S., Levesque-Tremblay, V., Bravo, A. & Harrison, M. J. (2015) Hyphal branching during arbuscule development requires RAM1. *Plant Physiol.* 169: 2774-2788.
- Parniske, M. (2008) Arbuscular mycorrhiza: the mother of plant root endosymbioses. *Nat. Rev. Microbiol.* 6: 763-775.
- Pfeffer, P. E., Douds, D. D., Bécard, G. & Shachar-Hill, Y. (1999) Carbon uptake and the metabolism and transport of lipids in an arbuscular mycorrhiza. *Plant Physiol.* 120: 587-598.
- Pimprikar, P., Carbonnel, S., Paries, M., Katzer, K., Klingl, V., Bohmer, M., Karl, L., Floss, D., Harrison, M., Parniske, M. & Gutjahr, C. (2016) A CCaMK-CYCLOPS-DELLA complex regulates transcription of RAM1, a central regulator of arbuscule branching. *Curr. Biol.* 26: 987-998.
- Pimprikar, P. & Gutjahr, C. (2018) Transcriptional regulation of arbuscular mycorrhiza development. *Plant Cell Physiol.*: pcy024-psy024.
- Pumplin, N. & Harrison, M. J. (2009) Live-cell imaging reveals periarbuscular membrane domains and organelle location in *Medicago truncatula* roots during arbuscular mycorrhizal symbiosis. *Plant Physiol.* 151: 809-819.

- Pumplin, N., Mondo, S. J., Topp, S., Starker, C. G., Gantt, J. S. & Harrison, M. J. (2010) *Medicago truncatula* Vapyrin is a novel protein required for arbuscular mycorrhizal symbiosis. *Plant J.* 61: 482-494.
- Pumplin, N., Zhang, X., Noar, R. & Harrison, M. (2012) Polar localization of a symbiosis-specific phosphate transporter is mediated by a transient reorientation of secretion. *Proc. Natl. Acad. Sci. USA.* 109: E665 - 672.
- Ramos, A. I. & Barolo, S. (2013) Low-affinity transcription factor binding sites shape morphogen responses and enhancer evolution. *Phil. Trans. R. Soc. B.* 368: 20130018.
- Reddy, S., Schorderet, M., Feller, U. & Reinhardt, D. (2007) A petunia mutant affected in intracellular accommodation and morphogenesis of arbuscular mycorrhizal fungi. *Plant J.* 51: 739-750.
- Remy, W., Taylor, T. N., Hass, H. & Kerp, H. (1994) Four hundred-million-year-old vesicular arbuscular mycorrhizae. *Proc. Natl. Acad. Sci. USA.* 91: 11841-11843.
- Rich, M. K., Courty, P.-E., Roux, C. & Reinhardt, D. (2017a) Role of the GRAS transcription factor ATA/RAM1 in the transcriptional reprogramming of arbuscular mycorrhiza in *Petunia hybrida*. *BMC genomics.* 18: 589.
- Rich, M. K., Nouri, E., Courty, P.-E. & Reinhardt, D. (2017b) Diet of Arbuscular Mycorrhizal Fungi: Bread and Butter? *Trends in Plant Science.* 22: 652-660.
- Rich, M. K., Schorderet, M., Bapaume, L., Falquet, L., Morel, P., Vandenbussche, M. & Reinhardt, D. (2015) The *Petunia* GRAS transcription factor ATA/RAM1 regulates symbiotic gene expression and fungal morphogenesis in arbuscular mycorrhiza. *Plant Physiol.* 168: 788-797.
- Richardson, A. (1994) Soil microorganisms and phosphorus availability.
- Ropars, J., Toro, K. S., Noel, J., Pelin, A., Charron, P., Farinelli, L., Marton, T., Krüger, M., Fuchs, J., Brachmann, A. & Corradi, N. (2016) Evidence for the sexual origin of heterokaryosis in arbuscular mycorrhizal fungi. *Nature Microbiology.* 1: 16033.
- Roth, R. & Paszkowski, U. (2017) Plant carbon nourishment of arbuscular mycorrhizal fungi. *Current Opinion in Plant Biology.* 39: 50-56.
- Ruiz-Lozano, J. M. (2003) Arbuscular mycorrhizal symbiosis and alleviation of osmotic stress. New perspectives for molecular studies. *Mycorrhiza.* 13: 309-317.
- Saito, K., Yoshikawa, M., Yano, K., Miwa, H., Uchida, H., Asamizu, E., Sato, S., Tabata, S., Imaizumi-Anraku, H. & Umehara, Y. (2007) NUCLEOPORIN85 is required for calcium spiking, fungal and bacterial symbioses, and seed production in *Lotus japonicus*. *Plant Cell.* 19: 610-624.
- Salvioli, A., Ghignone, S., Novero, M., Navazio, L., Venice, F., Bagnaresi, P. & Bonfante, P. (2016) Symbiosis with an endobacterium increases the fitness of a mycorrhizal fungus, raising its bioenergetic potential. *ISME J.* 10: 130-144.
- Scannerini, S. & Bonfante-Fasolo, P. (1983) Comparative ultrastructural analysis of mycorrhizal associations. *Can. J. Bot.* 61: 917-943.
- Schaarschmidt, S., Gresshoff, P. M. & Hause, B. (2013) Analyzing the soybean transcriptome during autoregulation of mycorrhization identifies the

- transcription factors GmNF-YA1a/b as positive regulators of arbuscular mycorrhization. *Genome biology*. 14: R62.
- Schulze, S., Schäfer, B. N., Parizotto, E. A., Voinnet, O. & Theres, K. (2010) *LOST MERISTEMS* genes regulate cell differentiation of central zone descendants in *Arabidopsis* shoot meristems. *Plant J*. 64: 668-678.
- Shachar-Hill, Y., Pfeffer, P. E., Douds, D., Osman, S. F., Doner, L. W. & Ratcliffe, R. G. (1995) Partitioning of intermediary carbon metabolism in vesicular-arbuscular mycorrhizal leek. *Plant Physiol*. 108: 7-15.
- Siciliano, V., Genre, A., Balestrini, R., Cappellazzo, G., Dewit, P. J. G. M. & Bonfante, P. (2007) Transcriptome analysis of arbuscular mycorrhizal roots during development of the prepenetration apparatus. *Plant Physiol*. 144: 1455-1466.
- Sieberer, B. J., Chabaud, M., Fournier, J., Timmers, A. C. J. & Barker, D. G. (2012) A switch in Ca<sup>2+</sup> spiking signature is concomitant with endosymbiotic microbe entry into cortical root cells of *Medicago truncatula*. *Plant J*. 69: 822-830.
- Silverstone, A. L., Jung, H.-S., Dill, A., Kawaide, H., Kamiya, Y. & Sun, T.-P. (2001) Repressing a repressor: Gibberellin-induced rapid reduction of the RGA protein in *Arabidopsis*. *Plant Cell*. 13: 1555-1566.
- Singh, S., Katzer, K., Lambert, J., Cerri, M. & Parniske, M. (2014) CYCLOPS, a DNA-binding transcriptional activator, orchestrates symbiotic root nodule development. *Cell Host Microbe*. 15: 139-152.
- Singh, S. & Parniske, M. (2012) Activation of calcium- and calmodulin-dependent protein kinase (CCaMK), the central regulator of plant root endosymbiosis. *Curr. Opin. Plant Biol*. 15: 444-453.
- Smit, P., Raedts, J., Portyanko, V., Debelle, F., Gough, C., Bisseling, T. & Geurts, R. (2005) NSP1 of the GRAS protein family is essential for rhizobial Nod factor-induced transcription. *Science*. 308: 1789-1791.
- Smith, F. W. 2002. The phosphate uptake mechanism. *Food Security in Nutrient-Stressed Environments: Exploiting Plants' Genetic Capabilities*. Springer.
- Smith, S. & Read, D. 2008. *Mycorrhizal Symbiosis*, Academic Press London.
- Smith, S. E. & Smith, F. A. (2011) Roles of arbuscular mycorrhizas in plant nutrition and growth: new paradigms from cellular to ecosystem scales. *Ann. Rev. Plant Biol*. 62: 227-250.
- Spatafora, J. W., Chang, Y., Benny, G. L., Lazarus, K., Smith, M. E., Berbee, M. L., Bonito, G., Corradi, N., Grigoriev, I. & Gryganskyi, A. (2016) A phylum-level phylogenetic classification of zygomycete fungi based on genome-scale data. *Mycologia*. 108: 1028-1046.
- Stracke, S., Kistner, C., Yoshida, S., Mulder, L., Sato, S., Kaneko, T., Tabata, S., Sandal, N., Stougaard, J., Szczyglowski, K. & Parniske, M. (2002) A plant receptor-like kinase required for both bacterial and fungal symbiosis. *Nature*. 417: 959-962.
- Stuurman, J., Jäggi, F. & Kuhlemeier, C. (2002) Shoot meristem maintenance is controlled by a GRAS-gene mediated signal from differentiating cells. *Genes Dev*. 16: 2213-2218.

- Sun, J., Miller, J. B., Granqvist, E., Wiley-Kalil, A., Gobbato, E., Maillet, F., Cottaz, S., Samain, E., Venkateshwaran, M., Fort, S., Morris, R. J., Ané, J.-M., Dénarié, J. & Oldroyd, G. E. D. (2015) Activation of symbiosis signaling by arbuscular mycorrhizal fungi in legumes and rice. *Plant Cell*. 27: 823-838.
- Takeda, N., Haage, K., Sato, S., Tabata, S. & Parniske, M. (2011) Activation of a *Lotus japonicus* subtilase gene during arbuscular mycorrhiza is dependent on the common symbiosis genes and two *cis*-active promoter regions. *Mol. Plant-Microbe Interact.* 24: 662-670.
- Takeda, N., Handa, Y., Tsuzuki, S., Kojima, M., Sakakibara, H. & Kawaguchi, M. (2015) Gibberellins interfere with symbiosis signaling and gene expression and alter colonization by arbuscular mycorrhizal fungi in *Lotus japonicus*. *Plant Physiol.* 167: 545-557.
- Takeda, N., Maekawa, T. & Hayashi, M. (2012) Nuclear-localized and deregulated calcium- and calmodulin-dependent protein kinase activates rhizobial and mycorrhizal responses in *Lotus japonicus*. *Plant Cell*. 24: 810-822.
- Takeda, N., Sato, S., Asamizu, E., Tabata, S. & Parniske, M. (2009) Apoplastic plant subtilases support arbuscular mycorrhiza development in *Lotus japonicus*. *Plant J.* 58: 766-777.
- Takeda, N., Tsuzuki, S., Suzaki, T., Parniske, M. & Kawaguchi, M. (2013) CERBERUS and NSP1 of *Lotus japonicus* are common symbiosis genes that modulate arbuscular mycorrhiza development. *Plant Cell Physiol.* 54: 1711-1723.
- Tang, N., San Clemente, H., Roy, S., Bécard, G., Zhao, B. & Roux, C. (2016) A survey of the gene repertoire of *Gigaspora rosea* unravels conserved features among glomeromycota for obligate biotrophy. *Front. Microbiol.* 7.
- Tirichine, L., Imaizumi-Anraku, H., Yoshida, S., Murakami, Y., Madsen, L. H., Miwa, H., Nakagawa, T., Sandal, N., Albrektsen, A. S., Kawaguchi, M., Downie, A., Sato, S., Tabata, S., Kouchi, H., Parniske, M., Kawasaki, S. & Stougaard, J. (2006) Deregulation of a Ca<sup>2+</sup>/calmodulin-dependent kinase leads to spontaneous nodule development. *Nature*. 441: 1153-1156.
- Trépanier, M., Bécard, G., Moutoglis, P., Willemot, C., Gagné, S., Avis, T. & Rioux, J. (2005) Dependence of arbuscular-mycorrhizal fungi on their plant host for palmitic acid synthesis. *Appl. Environ. Microbiol.* 71: 5341-5347.
- Venkateshwaran, M., Cosme, A., Han, L., Banba, M., Satyshur, K. A., Schleiff, E., Parniske, M., Imaizumi-Anraku, H. & Ané, J.-M. (2012) The recent evolution of a symbiotic ion channel in the legume family altered ion conductance and improved functionality in calcium signaling. *Plant Cell*. 24: 2528-2545.
- Venkateshwaran, M., Jayaraman, D., Chabaud, M., Genre, A., Balloon, A. J., Maeda, J., Forshey, K., Den Os, D., Kwiecien, N. W. & Coon, J. J. (2015) A role for the mevalonate pathway in early plant symbiotic signaling. *Proc. Natl. Acad. Sci. USA*. 112: 9781-9786.
- Volpe, V., Dell'aglio, E., Giovannetti, M., Ruberti, C., Costa, A., Genre, A., Guether, M. & Bonfante, P. (2013) An AM-induced, MYB-family gene of *Lotus japonicus*

- (*LjMAMI*) affects root growth in an AM-independent manner. *Plant J.* 73: 442-455.
- Wang, E., Schornack, S., Marsh, J., Gobbato, E., Schwessinger, B., Eastmond, P., Schultze, M., Kamoun, S. & Oldroyd, G. (2012) A common signaling process that promotes mycorrhizal and oomycete colonization of plants. *Curr. Biol.* 22: 2242-2246.
- Waters, M. T., Gutjahr, C., Bennett, T. & Nelson, D. C. (2017) Strigolactone signaling and evolution. *Ann. Rev. Plant Biol.* 68: 291-322.
- Watt, M. & Evans, J. R. (1999) Proteoid roots. Physiology and development. *Plant Physiol.* 121: 317-323.
- Wewer, V., Brands, M. & Dörmann, P. (2014) Fatty acid synthesis and lipid metabolism in the obligate biotrophic fungus *Rhizophagus irregularis* during mycorrhization of *Lotus japonicus*. *Plant J.* 79: 398-412.
- Williamson, L. C., Ribrioux, S. P., Fitter, A. H. & Leyser, H. O. (2001) Phosphate availability regulates root system architecture in *Arabidopsis*. *Plant Physiol.* 126: 875-882.
- Willige, B. C., Ghosh, S., Nill, C., Zourelidou, M., Dohmann, E. M. N., Maier, A. & Schwechheimer, C. (2007) The DELLA domain of GA INSENSITIVE mediates the interaction with the GA INSENSITIVE DWARF1a gibberellin receptor of *Arabidopsis*. *Plant Cell.* 19: 1209-1220.
- Xue, L., Cui, H., Buer, B., Vijayakumar, V., Delaux, P.-M., Junkermann, S. & Bucher, M. (2015) Network of GRAS transcription factors involved in the control of arbuscule development in *Lotus japonicus*. *Plant Physiol.* 167: 854-871.
- Yamaguchi, S. (2008) Gibberellin metabolism and its regulation. *Annu. Rev. Plant Biol.* 59: 225-251.
- Yang, W., Pollard, M., Li-Beisson, Y., Beisson, F., Feig, M. & Ohlrogge, J. (2010) A distinct type of glycerol-3-phosphate acyltransferase with *sn*-2 preference and phosphatase activity producing 2-monoacylglycerol. *Proc. Natl. Acad. Sci. USA.* 107: 12040-12045.
- Yang, W., Simpson, J. P., Li-Beisson, Y., Beisson, F., Pollard, M. & Ohlrogge, J. B. (2012) A land-plant-specific glycerol-3-phosphate acyltransferase family in *Arabidopsis*: substrate specificity, *sn*-2 preference, and evolution. *Plant Physiology.* 160: 638-652.
- Yano, K., Yoshida, S., Müller, J., Singh, S., Banba, M., Vickers, K., Markmann, K., White, C., Schuller, B., Sato, S., Asamizu, E., Tabata, S., Murooka, Y., Perry, J., Wang, T., Kawaguchi, M., Imaizumi-Anraku, H., Hayashi, M. & Parniske, M. (2008) CYCLOPS, a mediator of symbiotic intracellular accommodation. *Proc. Natl. Acad. Sci. USA.* 105: 20540-20545.
- Yoneyama, K., Xie, X., Kim, H., Kisugi, T., Nomura, T., Sekimoto, H., Yokota, T. & Yoneyama, K. (2012) How do nitrogen and phosphorus deficiencies affect strigolactone production and exudation? *Planta.* 235: 1197-1207.
- Yoneyama, K., Xie, X., Kusumoto, D., Sekimoto, H., Sugimoto, Y., Takeuchi, Y. & Yoneyama, K. (2007) Nitrogen deficiency as well as phosphorus deficiency in sorghum promotes the production and exudation of 5-deoxystrigol, the

- host recognition signal for arbuscular mycorrhizal fungi and root parasites. *Planta*. 227: 125-132.
- Yoshida, H., Hirano, K., Sato, T., Mitsuda, N., Nomoto, M., Maeo, K., Koketsu, E., Mitani, R., Kawamura, M., Ishiguro, S., Tada, Y., Ohme-Takagi, M., Matsuoka, M. & Ueguchi-Tanaka, M. (2014) DELLA protein functions as a transcriptional activator through the DNA binding of the INDETERMINATE DOMAIN family proteins. *Proc. Natl. Acad. Sci. USA*. 111: 7861-7866.
- Yu, N., Luo, D., Zhang, X., Liu, J., Wang, W., Jin, Y., Dong, W., Liu, J., Liu, H., Yang, W., Zeng, L., Li, Q., He, Z., Oldroyd, G. E. D. & Wang, E. (2013) A DELLA protein complex controls the arbuscular mycorrhizal symbiosis in plants. *Cell Res*. 10.1038/cr.2013.167.
- Zhang, Q., Blaylock, L. A. & Harrison, M. J. (2010) Two *Medicago truncatula* half-ABC transporters are essential for arbuscule development in arbuscular mycorrhizal symbiosis. *Plant Cell*. 22: 1483-1497.
- Zhang, X., Dong, W., Sun, J., Feng, F., Deng, Y., He, Z., Oldroyd, G. E. & Wang, E. (2015a) The receptor kinase CERK1 has dual functions in symbiosis and immunity signalling. *Plant J*. 81: 258-267.
- Zhang, X., Pumplin, N., Ivanov, S. & Harrison, M. J. (2015b) EXO70I is required for development of a sub-domain of the periarbuscular membrane during arbuscular mycorrhizal symbiosis. *Curr. Biol*. 25: 2189-2195.

## **XII. List of Figures**

1. Schematic representation of cell and stage specific gene expression corresponding to AM developmental stages (p. 19)
2. Schematic representation of stages of arbuscule development (p. 20)
3. Nutrients transport and exchange between the two symbionts in AM symbiosis (p. 24)
4. Overview of signal transduction via common symbiosis signaling (p. 28)
5. A schematic representation of the GA perception (p. 30)
6. RAM1 is a central regulator of arbuscule development (p. 152)

## **XIII. List of Tables**

1. Known CYCLOPS bound *cis*-elements (p. 146)

#### **XIV. Acknowledgements**

I would like to thank all the people who supported and helped me during my Ph.D. thesis.

First of all, I would like to express my most profound gratitude and special thanks to my Ph.D. supervisor, Prof. Dr. Caroline Gutjahr, for her continuous support, intuitive comments, and encouragement throughout my thesis. Caroline has been a constant source of inspiration and ready for spontaneous discussion and help throughout my thesis period. Her immense knowledge in the field has always widened my research from various perspectives. I am thankful to her for giving me not only the freedom to pursue my scientific ideas but has also encouraged my participation in international scientific conferences. I would also like to thank her for training me in scientific writing and evaluating my Ph.D. thesis. Lastly, I would also like to thank for her valuable advice not only in research but also day-to-day life.

I especially want to thank Prof. Dr. Martin Parniske for all the exciting and fruitful comments and sharing new ideas on our research. I enjoyed the scientific discussion during the journal club and short breaks in the kitchen. I appreciate his effort to train all the students for good scientific practices. I would like to acknowledge him for his valuable attempt and implication of different methods to promote social and scientific activities in the lab. Lastly I would like to thank him for his time to evaluate my Ph.D. thesis.

I would like to thank the remaining Ph.D. thesis committee members PD. Dr. Cordelia Bolle, Prof. Dr. Angelika Böttger, Prof. Dr. Wolfgang Frank and Prof. Dr. Andreas Klingl for giving their valuable time and efforts to evaluate this research work.

I would like to thanks, Andreas Keymer for the co-operative and very friendly collaboration on the RAM2 project. I would also like to thank Andy for his last minute help in writing the German summary of this thesis.

I would like to thank Samy Carbonnel for his valuable time to critically correct my thesis. I enjoyed scientific discussion on various topic and was always amazed by his deep understanding. His innovative ideas and critical comments were always beneficial and helped the project to progress a lot.

I would like to thank my friend Dr. Bhushan Vishal for being there for me all the time and for correcting my thesis critically.

I would like to thank Samy Carbonnel and Michael Paries for their precious contribution on the RAM1 project, without their help it would have been tough to publish the RAM1 research within a short period and in a good journal due to intense competition. I would also like to thank my excellent Master and Bachelor students Monica Bohmer and Leonhard Karl for their valuable contribution to the RAM1 project. I would like to thank our technician Verena Klingl for hands-on experience in different research methods and participation in the RAM1 project.

It was a great pleasure to supervise Christina Spiessl, who was an excellent student helper and great assistance in the lab but also became a good friend of mine. Her vigilant nature and outstanding work in the lab in the last few months of my Ph.D. duration provided me relief from the lab work and gave me an opportunity to focus on my Ph.D. thesis and review writing.

I would like to especially thank Dr. Marion Cerri for her support, valuable advice and fruitful scientific discussion.

I would like to thank Dr. Andreas Binder, Dr. Jayne Lambert, Dr. Katja Katzer, Chloé Cathebras and Dr. David Chiasson for their help and answering all the questions.

I would like to express my heartfelt thanks to our green house and tobacco plant caretaker Anna Heuberger, without her it would have been impossible to perform all the transactivation assay experiment in *N. benthamiana*. I would also like to take the opportunity to thank our excellent genomics service members, Dr. Andreas Brachmann, Ute Bergmann and Gisela Brinkmann, for their patience and helpful nature all the time. I would like to thank Frau Sandra Buschsieweke, Frau Barbara Dollrieß and Frau Stephanie Wunderle for their helpful nature in administration and official documents, especially for the non-German speaking students.

I would like to thank all the group members of Prof. Dr. Caroline Gutjahr, for their help and support all the time. I particularly enjoyed having worked with Samy Carbonnel and José Villaécija Aguilar, who were fabulous lab colleagues, true friends and always helpful. I was delighted to share both funny moments and

difficult situation in daily Ph.D. and personal life with them. I would also like to thank them for sharing great ideas on different topics and research, for the exciting and fruitful discussion. I would like to thank Florian Berger for all his immense help and spontaneous German to English translator.

I am grateful for the help received from the former and present group leaders in the chair of Prof. Dr. Martin Parniske, Prof. Dr. Micheal Boshart, Dr. Andreas Brachmann, Dr. David Chiasson Dr. Macarena Marín and Dr. Arne Weiberg who made the lab a friendly and collaborative workplace. I would like to specially thank Florian Dunker for all the intense discussion on various topics and help and support.

I would like to thanks, Graduate School Life Science Munich (LSM) for all the support and help. I would especially like to thank Frau Francisca Rosa Mende for help and support in every kind of problem.

I would like to thank SFB924 for funding this project, financial support for attending the conference, soft skill courses and exciting Ph.D. student retreats. I am grateful to Prof. Dr. Claus Schwechheimer for his participation in my research topic and inviting me to DELLA mini-symposium. I would also like to thank him for his spontaneous kind help all the time.

Last but not the least, I am very grateful to all my friends for their love and support. Finally, I would like to express my most profound gratitude to my family, for their unconditional support and love. I am grateful to my parents Jyoti Pimprikar and Sunil Pimprikar for their immense support, sacrifices and hard struggle to bring me so far. I am lucky to have strong support and tremendous love for my two sisters Poonam and Teju and one brother Chetan, without them it would have been impossible for me to be what I am today. I would like to thanks also family members of Samy Carbonnel, who made me feel at home in Europe.

## XV. Curriculum Vitae



### **Priya Pimprikar, Doctoral student**

Faculty of Biology-Genetics

LMU Munich

Germany

Email: priya.pimprikar@bio.lmu.de

Date of birth: 24.07.1986

Citizenship: Indian

### **Academic Career**

- |                 |  |
|-----------------|--|
| 09/2012-present | Doctoral student at Faculty of Biology, Genetics, Ludwig-Maximilians University Munich, Germany under the supervision of Dr. Caroline Gutjahr.   |
| 09/2012-present | Student of Graduate School Life Science Munich (LSM), Germany.   |
| 06/2010-05/2012 | Master in Technology in Applied Botany at Indian Institute of Technology Kharagpur (IIT KGP), West Bengal, India; Grade: 9.72/10.  |
| 05/2005-05/2010 | Master in Science in Biotechnology (Five years integrated course) at Institute of Bioinformatics and Biotechnology, Savitribai Phule, University of Pune; Maharashtra, India; Grade 7.59/10. |
| 03/2004-04/2005 | Teaching Maths and Science subject to the higher secondary and secondary school students.  |

- 05/2002-02/2004 Higher secondary school at Modern College of Art, Science and Commerce, University of Pune, Maharashtra, India; Grade: 8.25/10.
- 03/2001-03/2002 Secondary school certificate examination, Maharashtra State Board of Secondary and Higher Secondary Education, Pune ; 8/10.

### **Awards**

- 2012 Best student award at Department of Agricultural & Food Engineering, Indian Institute of Technology Kharagpur (IIT KGP), West Bengal, India.
- 2012 Best thesis award in living organism Department of Agricultural & Food Engineering, Indian Institute of Technology Kharagpur (IIT KGP), West Bengal, India.
- 2016 Best paper award of the Life Science Munich (LSM) graduate school

### **Scholarship**

- 09/2011-05/2012 DAAD "Sandwich-Model" Scholarship Offer for M. Tech and M.S. student (Research).

### **Travel grants**

- 2016 Ko Shimamoto Travel Award to attend the International Society for Molecular Plant-Microbe Interaction (IS-MPMI) Congress 2016 (I could not attend this conference due to delay in approval of traveling document i.e, VISA by the US Embassy).

### **Teaching experience**

- Six years teaching experience to the students of higher secondary and secondary school students in India.
- Laboratory supervisor in the master module at Munich University called *Molecular Plant Microbe Interactions*. The course taught in genetics of root nodule and arbuscular mycorrhiza symbiosis, classical genetic mapping, mapping and analysis of re-sequenced mutant genome by NGS for identification of causal mutation, phenotyping of plant mutant perturbed in AMS and root nodule symbiosis, natural variation in *L. japonicus* Nod factor perception and Nod factor isolation.

### Supervision of students

- 10 weeks B.Sc thesis of Leonhard Karl on “A CCaMK-CYCLOPS-DELLA complex activates transcription of *RAM1* to regulate arbuscule branching” project.
- 6 months M.Sc thesis of Monica Bohmer on “A CCaMK-CYCLOPS-DELLA complex activates transcription of *RAM1* to regulate arbuscule branching” project.
- 6 months M.Sc thesis of Michael Paries on “A CCaMK-CYCLOPS-DELLA complex activates transcription of *RAM1* to regulate arbuscule branching” project.

### Research projects

- Lipid transfer from plants to arbuscular mycorrhiza fungi, Germany, 2012-present (Data published).
- A CCaMK-CYCLOPS-DELLA complex activates transcription of *RAM1* to regulate arbuscule branching, Germany, 2012-present (Data published).
- Identification (map-based cloning and NGS analysis) and characterization of *L. japonicus* plant mutant *RED*, required for arbuscular mycorrhiza development, Germany, 2012-present (Data published).
- Functional characterization of *Arabidopsis* AGC Kinases 3-PHOSPHOINOSITIDE DEPENDENT KINASE-1 (PDK1) and tumor suppressor UNICORN (UCN), Germany, 2011-2012.
- Genetic engineering of *Yarrowia lipolytica* for the production of URICASE and

TYROSINASE, India, 2009-2010 (Data published).

- Cloning and expression of biotechnology relevant enzymes PHYTASE and ESTERASE in *Yarrowia lipolytica*, India, 2009-2010.
- Studies on Nanoparticle synthesis using the yeast *Yarrowia lipolytica* NCIM 3589, India, 2007-2008 (Data published).

### Publications

- A. Keymer#, **P. Pimprikar**#, V. Wewer, C. Huber, M. Brands, SL. Bucerius, PM. Delaux, V. Klingl, E von Roepenack-Lahaye, TL. Wang, W. Eisenreich, P. Dörmann, M. Parniske, C. Gutjahr (2017). Lipid transfer from plants to arbuscular mycorrhiza fungi. **eLife**, 6. doi:10.7554/eLife.29107 (# **Equal contribution**).
- **P. Pimprikar**, S. Carbonnel, M. Paries, K. Katzer, V. Klingl, M. Bohmer, L. Karl, D S. Floss, M J. Harrison, M. Parniske, C. Gutjahr (2016). A CCaMK-CYCLOPS-DELLA complex activates transcription of *RAM1* to regulate arbuscule branching. **Current Biology**, 26: 987-998.
- A. Rao, **P. Pimprikar**, C. Bendigiri A. R. Kumar, S. S. Zinjarde (2011). Cloning and expression of a *tyrosinase* from *Aspergillus oryzae* in *Yarrowia lipolytica*: application in L- DOPA biotransformation. **Applied Microbiology and Biotechnology**, 92, 951-959.
- **P. Pimprikar**, S.S. Joshi, A.R. Kumar, S.S. Zinjarde, S.K. Kulkarni (2009). Influence of biomass and gold salt concentration on nanoparticle synthesis by the tropical marine yeast *Yarrowia lipolytica* NCMI 3589. **Colloids Surf. B: Biointerf**, 74, 309-316.

### Reviews

- **Pimprikar P**, Gutjahr C (2018). Transcriptional regulation of arbuscular mycorrhiza development. **Plant Cell Physiology**. doi.org/10.1093/pcp/pcy024

### Poster presentation

- SFB924 Conference, Germany, 2017.

- 2<sup>nd</sup> International Molecular Mycorrhiza Meeting (iMMM), United Kingdom, 2015.
- 36<sup>th</sup> New Phytologist Symposium, Germany, 2015.
- SFB924 Conference, Germany, 2013.

### **Oral presentation**

- SFB924 Progress report meeting, Germany, 2015.
- Symposium on DELLA and Gibberellin Dependent Plant Growth Regulation, Germany, 2015.
- SFB924 Progress report meeting, Germany, 2014.

### **Attended Workshops**

- Scientific writing and Communication skills
- Biovoxxel course for image processing using ImageJ software
- Phylogenetic analysis (MEGA, RAxML, MAFFT, others)
- Vector graphic files (Adobe Illustrator)
- Literature Management (Endnote, Mendeley)
- Protein structure analysis (SWISS MODEL)
- R-Programming

## **XVI. Permission for republishing**

## OXFORD UNIVERSITY PRESS LICENSE TERMS AND CONDITIONS

Feb 12, 2018

This Agreement between Ms. Priya Pimprikar ("You") and Oxford University Press ("Oxford University Press") consists of your license details and the terms and conditions provided by Oxford University Press and Copyright Clearance Center.

License Number	4286520363578
License date	Feb 12, 2018
Licensed content publisher	Oxford University Press
Licensed content publication	Plant and Cell Physiology
Licensed content title	Transcriptional regulation of arbuscular mycorrhiza development
Licensed content author	Pimprikar, Priya; Gutjahr, Caroline
Licensed content date	Feb 7, 2018
Type of Use	Thesis/Dissertation
Institution name	
Title of your work	Doctoral Student
Publisher of your work	Ludwig Maximilians Universität München
Expected publication date	Feb 2018
Permissions cost	0.00 EUR
Value added tax	0.00 EUR
Total	0.00 EUR
Requestor Location	Ms. Priya Pimprikar
	Germany Attn: Ms. Priya Pimprikar
Publisher Tax ID	GB125506730
Billing Type	Invoice
Billing Address	Ms. Priya Pimprikar
	Attn: Ms. Priya Pimprikar
Total	0.00 EUR
Terms and Conditions	

### STANDARD TERMS AND CONDITIONS FOR REPRODUCTION OF MATERIAL FROM AN OXFORD UNIVERSITY PRESS JOURNAL

1. Use of the material is restricted to the type of use specified in your order details.
2. This permission covers the use of the material in the English language in the following territory: world. If you have requested additional permission to translate this material, the terms and conditions of this reuse will be set out in clause 12.
3. This permission is limited to the particular use authorized in (1) above and does not allow you to sanction its use elsewhere in any other format other than specified above, nor does it apply to quotations, images, artistic works etc that have been reproduced from other sources which may be part of the material to be used.
4. No alteration, omission or addition is made to the material without our written consent. Permission must be re-cleared with Oxford University Press if/when you decide to reprint.
5. The following credit line appears wherever the material is used: author, title, journal, year, volume, issue number, pagination, by permission of Oxford University Press or the sponsoring society if the journal is a society journal. Where a journal is being published on behalf of a learned society, the details of that society must be included in the credit line.
6. For the reproduction of a full article from an Oxford University Press journal for whatever purpose, the corresponding author of the material concerned should be informed of the proposed use. Contact details for the corresponding authors of all Oxford University Press journal contact can be found alongside either the abstract or full text of the article concerned, accessible from [www.oxfordjournals.org](http://www.oxfordjournals.org) Should there be a problem clearing these rights, please contact [journals.permissions@oup.com](mailto:journals.permissions@oup.com)
7. If the credit line or acknowledgement in our publication indicates that any of the figures, images or photos was reproduced, drawn or modified from an earlier source it will be necessary for you to clear this permission with the original publisher as well. If this permission has not been obtained, please note that this material cannot be included in your publication/photocopies.
8. While you may exercise the rights licensed immediately upon issuance of the license at the end of the licensing process for the transaction, provided that you have disclosed complete and accurate details of your proposed use, no license is finally effective unless and until full payment is received from you (either by Oxford University Press or by Copyright Clearance Center (CCC)) as provided in CCC's Billing and Payment terms and conditions. If full payment is not received on a timely basis, then any license preliminarily granted shall be deemed automatically revoked and shall be void as if never granted. Further, in the event that you breach any of these terms and conditions or any of CCC's Billing and Payment terms and conditions, the license is automatically revoked and shall be void as if never granted. Use of materials as described in a revoked license, as well as any use of the materials beyond the scope of an unrevoked license, may constitute copyright infringement and Oxford University Press reserves the right to take any and all action to protect its copyright in the materials.
9. This license is personal to you and may not be sublicensed, assigned or transferred by you to any other person without Oxford University Press's written permission.
10. Oxford University Press reserves all rights not specifically granted in the combination of (i) the license details provided by you and accepted in the course of this licensing transaction, (ii) these terms and conditions and (iii) CCC's Billing and Payment terms and conditions.
11. You hereby indemnify and agree to hold harmless Oxford University Press and CCC, and their respective officers, directors, employs and agents, from and against any and all claims arising out of your use of the licensed material other than as specifically authorized pursuant to this license.
12. Other Terms and Conditions:  
v1.4

**Questions? [customer care@copyright.com](mailto:customer care@copyright.com) or +1-855-239-3415 (toll free in the US) or +1-978-646-2777.**

---

---

## SPRINGER NATURE LICENSE TERMS AND CONDITIONS

Jan 31, 2018

This Agreement between Ms. Priya Pimprikar ("You") and Springer Nature ("Springer Nature") consists of your license details and the terms and conditions provided by Springer Nature and Copyright Clearance Center.

License Number	4279330814509
License date	Jan 31, 2018
Licensed Content Publisher	Springer Nature
Licensed Content Publication	Nature Reviews Microbiology
Licensed Content Title	Arbuscular mycorrhiza: the mother of plant root endosymbioses
Licensed Content Author	Martin Parniske
Licensed Content Date	Oct 1, 2008
Licensed Content Volume	6
Licensed Content Issue	10
Type of Use	Thesis/Dissertation
Requestor type	academic/university or research institute
Format	print and electronic
Portion	figures/tables/illustrations
Number of figures/tables/illustrations	7
High-res required	no
Will you be translating?	no
Circulation/distribution	<501
Author of this Springer Nature content	no
Title	Doctoral Student
Instructor name	Prof. Dr. Caroline Gutjahr
Institution name	Ludwig Maximilians Universität München
Expected presentation date	Feb 2018
Portions	Figure number 7
Requestor Location	Ms. Priya Pimprikar
	Germany Attn: Ms. Priya Pimprikar
Billing Type	Invoice
Billing Address	Ms. Priya Pimprikar

Attn: Ms. Priya Pimprikar

Total 0.00 EUR

### Terms and Conditions

#### Springer Nature Terms and Conditions for RightsLink Permissions

**Springer Customer Service Centre GmbH (the Licensor)** hereby grants you a non-exclusive, world-wide licence to reproduce the material and for the purpose and requirements specified in the attached copy of your order form, and for no other use, subject to the conditions below:

1. The Licensor warrants that it has, to the best of its knowledge, the rights to license reuse of this material. However, you should ensure that the material you are requesting is original to the Licensor and does not carry the copyright of another entity (as credited in the published version).

If the credit line on any part of the material you have requested indicates that it was reprinted or adapted with permission from another source, then you should also seek permission from that source to reuse the material.

2. Where **print only** permission has been granted for a fee, separate permission must be obtained for any additional electronic re-use.
3. Permission granted **free of charge** for material in print is also usually granted for any electronic version of that work, provided that the material is incidental to your work as a whole and that the electronic version is essentially equivalent to, or substitutes for, the print version.
4. A licence for 'post on a website' is valid for 12 months from the licence date. This licence does not cover use of full text articles on websites.
5. Where '**reuse in a dissertation/thesis**' has been selected the following terms apply: Print rights for up to 100 copies, electronic rights for use only on a personal website or institutional repository as defined by the Sherpa guideline ([www.sherpa.ac.uk/romeo/](http://www.sherpa.ac.uk/romeo/)).
6. Permission granted for books and journals is granted for the lifetime of the first edition and does not apply to second and subsequent editions (except where the first edition permission was granted free of charge or for signatories to the STM Permissions Guidelines <http://www.stm-assoc.org/copyright-legal-affairs/permissions/permissions-guidelines/>), and does not apply for editions in other languages unless additional translation rights have been granted separately in the licence.
7. Rights for additional components such as custom editions and derivatives require additional permission and may be subject to an additional fee. Please apply to [Journalpermissions@springernature.com](mailto:Journalpermissions@springernature.com)/[bookpermissions@springernature.com](mailto:bookpermissions@springernature.com) for these rights.
8. The Licensor's permission must be acknowledged next to the licensed material in print. In electronic form, this acknowledgement must be visible at the same time as the figures/tables/illustrations or abstract, and must be hyperlinked to the journal/book's homepage. Our required acknowledgement format is in the Appendix below.
9. Use of the material for incidental promotional use, minor editing privileges (this does not include cropping, adapting, omitting material or any other changes that affect the meaning, intention or moral rights of the author) and copies for the disabled are permitted under this licence.

10. Minor adaptations of single figures (changes of format, colour and style) do not require the Licensor's approval. However, the adaptation should be credited as shown in Appendix below.

## **Appendix — Acknowledgements:**

### **For Journal Content:**

Reprinted by permission from [**the Licensor**]: [**Journal Publisher** (e.g. Nature/Springer/Palgrave)] [**JOURNAL NAME**] [**REFERENCE CITATION** (Article name, Author(s) Name), [**COPYRIGHT**] (year of publication)]

### **For Advance Online Publication papers:**

Reprinted by permission from [**the Licensor**]: [**Journal Publisher** (e.g. Nature/Springer/Palgrave)] [**JOURNAL NAME**] [**REFERENCE CITATION** (Article name, Author(s) Name), [**COPYRIGHT**] (year of publication), advance online publication, day month year (doi: 10.1038/sj.[**JOURNAL ACRONYM**].)]

### **For Adaptations/Translations:**

Adapted/Translated by permission from [**the Licensor**]: [**Journal Publisher** (e.g. Nature/Springer/Palgrave)] [**JOURNAL NAME**] [**REFERENCE CITATION** (Article name, Author(s) Name), [**COPYRIGHT**] (year of publication)]

### **Note: For any republication from the British Journal of Cancer, the following credit line style applies:**

Reprinted/adapted/translated by permission from [**the Licensor**]: on behalf of Cancer Research UK: : [**Journal Publisher** (e.g. Nature/Springer/Palgrave)] [**JOURNAL NAME**] [**REFERENCE CITATION** (Article name, Author(s) Name), [**COPYRIGHT**] (year of publication)]

### **For Advance Online Publication papers:**

Reprinted by permission from The [**the Licensor**]: on behalf of Cancer Research UK: [**Journal Publisher** (e.g. Nature/Springer/Palgrave)] [**JOURNAL NAME**] [**REFERENCE CITATION** (Article name, Author(s) Name), [**COPYRIGHT**] (year of publication), advance online publication, day month year (doi: 10.1038/sj.[**JOURNAL ACRONYM**].)]

### **For Book content:**

Reprinted/adapted by permission from [**the Licensor**]: [**Book Publisher** (e.g. Palgrave Macmillan, Springer etc)] [**Book Title**] by [**Book author(s)**] [**COPYRIGHT**] (year of publication)]

## **Other Conditions:**

Version 1.0

**Questions? [customercare@copyright.com](mailto:customercare@copyright.com) or +1-855-239-3415 (toll free in the US) or +1-978-646-2777.**



## ELSEVIER LICENSE TERMS AND CONDITIONS

Jan 31, 2018

This Agreement between Ms. Priya Pimprikar ("You") and Elsevier ("Elsevier") consists of your license details and the terms and conditions provided by Elsevier and Copyright Clearance Center.

License Number	4279340011214
License date	Jan 31, 2018
Licensed Content Publisher	Elsevier
Licensed Content Publication	Current Opinion in Plant Biology
Licensed Content Title	Activation of calcium- and calmodulin-dependent protein kinase (CCaMK), the central regulator of plant root endosymbiosis
Licensed Content Author	Sylvia Singh, Martin Parniske
Licensed Content Date	Aug 1, 2012
Licensed Content Volume	15
Licensed Content Issue	4
Licensed Content Pages	10
Start Page	444
End Page	453
Type of Use	reuse in a thesis/dissertation
Intended publisher of new work	other
Portion	figures/tables/illustrations
Number of figures/tables/illustrations	1
Format	both print and electronic
Are you the author of this Elsevier article?	No
Will you be translating?	No
Original figure numbers	Figure 1
Title of your thesis/dissertation	Doctoral Student
Publisher of new work	Ludwig Maximilians Universität München
Author of new work	Prof. Dr. Caroline Gutjahr
Expected completion date	Feb 2018
Estimated size (number of pages)	1
Requestor Location	Ms. Priya Pimprikar

Germany  
Attn: Ms. Priya Pimprikar

Publisher Tax ID GB 494 6272 12

Total 0.00 USD

[Terms and Conditions](#)

### INTRODUCTION

1. The publisher for this copyrighted material is Elsevier. By clicking "accept" in connection with completing this licensing transaction, you agree that the following terms and conditions apply to this transaction (along with the Billing and Payment terms and conditions established by Copyright Clearance Center, Inc. ("CCC"), at the time that you opened your Rightslink account and that are available at any time at <http://myaccount.copyright.com>).

### GENERAL TERMS

2. Elsevier hereby grants you permission to reproduce the aforementioned material subject to the terms and conditions indicated.

3. Acknowledgement: If any part of the material to be used (for example, figures) has appeared in our publication with credit or acknowledgement to another source, permission must also be sought from that source. If such permission is not obtained then that material may not be included in your publication/copies. Suitable acknowledgement to the source must be made, either as a footnote or in a reference list at the end of your publication, as follows:

"Reprinted from Publication title, Vol /edition number, Author(s), Title of article / title of chapter, Pages No., Copyright (Year), with permission from Elsevier [OR APPLICABLE SOCIETY COPYRIGHT OWNER]." Also Lancet special credit - "Reprinted from The Lancet, Vol. number, Author(s), Title of article, Pages No., Copyright (Year), with permission from Elsevier."

4. Reproduction of this material is confined to the purpose and/or media for which permission is hereby given.

5. Altering/Modifying Material: Not Permitted. However figures and illustrations may be altered/adapted minimally to serve your work. Any other abbreviations, additions, deletions and/or any other alterations shall be made only with prior written authorization of Elsevier Ltd. (Please contact Elsevier at [permissions@elsevier.com](mailto:permissions@elsevier.com)). No modifications can be made to any Lancet figures/tables and they must be reproduced in full.

6. If the permission fee for the requested use of our material is waived in this instance, please be advised that your future requests for Elsevier materials may attract a fee.

7. Reservation of Rights: Publisher reserves all rights not specifically granted in the combination of (i) the license details provided by you and accepted in the course of this licensing transaction, (ii) these terms and conditions and (iii) CCC's Billing and Payment terms and conditions.

8. License Contingent Upon Payment: While you may exercise the rights licensed immediately upon issuance of the license at the end of the licensing process for the transaction, provided that you have disclosed complete and accurate details of your proposed use, no license is finally effective unless and until full payment is received from you (either by publisher or by CCC) as provided in CCC's Billing and Payment terms and conditions. If full payment is not received on a timely basis, then any license preliminarily granted shall be deemed automatically revoked and shall be void as if never granted. Further, in the event that you breach any of these terms and conditions or any of CCC's Billing and Payment terms and conditions, the license is automatically revoked and shall be void as if never

granted. Use of materials as described in a revoked license, as well as any use of the materials beyond the scope of an unrevoked license, may constitute copyright infringement and publisher reserves the right to take any and all action to protect its copyright in the materials.

9. **Warranties:** Publisher makes no representations or warranties with respect to the licensed material.

10. **Indemnity:** You hereby indemnify and agree to hold harmless publisher and CCC, and their respective officers, directors, employees and agents, from and against any and all claims arising out of your use of the licensed material other than as specifically authorized pursuant to this license.

11. **No Transfer of License:** This license is personal to you and may not be sublicensed, assigned, or transferred by you to any other person without publisher's written permission.

12. **No Amendment Except in Writing:** This license may not be amended except in a writing signed by both parties (or, in the case of publisher, by CCC on publisher's behalf).

13. **Objection to Contrary Terms:** Publisher hereby objects to any terms contained in any purchase order, acknowledgment, check endorsement or other writing prepared by you, which terms are inconsistent with these terms and conditions or CCC's Billing and Payment terms and conditions. These terms and conditions, together with CCC's Billing and Payment terms and conditions (which are incorporated herein), comprise the entire agreement between you and publisher (and CCC) concerning this licensing transaction. In the event of any conflict between your obligations established by these terms and conditions and those established by CCC's Billing and Payment terms and conditions, these terms and conditions shall control.

14. **Revocation:** Elsevier or Copyright Clearance Center may deny the permissions described in this License at their sole discretion, for any reason or no reason, with a full refund payable to you. Notice of such denial will be made using the contact information provided by you. Failure to receive such notice will not alter or invalidate the denial. In no event will Elsevier or Copyright Clearance Center be responsible or liable for any costs, expenses or damage incurred by you as a result of a denial of your permission request, other than a refund of the amount(s) paid by you to Elsevier and/or Copyright Clearance Center for denied permissions.

### LIMITED LICENSE

The following terms and conditions apply only to specific license types:

15. **Translation:** This permission is granted for non-exclusive world **English** rights only unless your license was granted for translation rights. If you licensed translation rights you may only translate this content into the languages you requested. A professional translator must perform all translations and reproduce the content word for word preserving the integrity of the article.

16. **Posting licensed content on any Website:** The following terms and conditions apply as follows: Licensing material from an Elsevier journal: All content posted to the web site must maintain the copyright information line on the bottom of each image; A hyper-text must be included to the Homepage of the journal from which you are licensing at <http://www.sciencedirect.com/science/journal/xxxxx> or the Elsevier homepage for books at <http://www.elsevier.com>; Central Storage: This license does not include permission for a scanned version of the material to be stored in a central repository such as that provided by Heron/XanEdu.

Licensing material from an Elsevier book: A hyper-text link must be included to the Elsevier homepage at <http://www.elsevier.com> . All content posted to the web site must maintain the copyright information line on the bottom of each image.

**Posting licensed content on Electronic reserve:** In addition to the above the following

clauses are applicable: The web site must be password-protected and made available only to bona fide students registered on a relevant course. This permission is granted for 1 year only. You may obtain a new license for future website posting.

**17. For journal authors:** the following clauses are applicable in addition to the above:

**Preprints:**

A preprint is an author's own write-up of research results and analysis, it has not been peer-reviewed, nor has it had any other value added to it by a publisher (such as formatting, copyright, technical enhancement etc.).

Authors can share their preprints anywhere at any time. Preprints should not be added to or enhanced in any way in order to appear more like, or to substitute for, the final versions of articles however authors can update their preprints on arXiv or RePEc with their Accepted Author Manuscript (see below).

If accepted for publication, we encourage authors to link from the preprint to their formal publication via its DOI. Millions of researchers have access to the formal publications on ScienceDirect, and so links will help users to find, access, cite and use the best available version. Please note that Cell Press, The Lancet and some society-owned have different preprint policies. Information on these policies is available on the journal homepage.

**Accepted Author Manuscripts:** An accepted author manuscript is the manuscript of an article that has been accepted for publication and which typically includes author-incorporated changes suggested during submission, peer review and editor-author communications.

Authors can share their accepted author manuscript:

- immediately
  - via their non-commercial person homepage or blog
  - by updating a preprint in arXiv or RePEc with the accepted manuscript
  - via their research institute or institutional repository for internal institutional uses or as part of an invitation-only research collaboration work-group
  - directly by providing copies to their students or to research collaborators for their personal use
  - for private scholarly sharing as part of an invitation-only work group on commercial sites with which Elsevier has an agreement
- After the embargo period
  - via non-commercial hosting platforms such as their institutional repository
  - via commercial sites with which Elsevier has an agreement

In all cases accepted manuscripts should:

- link to the formal publication via its DOI
- bear a CC-BY-NC-ND license - this is easy to do
- if aggregated with other manuscripts, for example in a repository or other site, be shared in alignment with our hosting policy not be added to or enhanced in any way to appear more like, or to substitute for, the published journal article.

**Published journal article (JPA):** A published journal article (PJA) is the definitive final record of published research that appears or will appear in the journal and embodies all value-adding publishing activities including peer review co-ordination, copy-editing, formatting, (if relevant) pagination and online enrichment.

Policies for sharing publishing journal articles differ for subscription and gold open access articles:

**Subscription Articles:** If you are an author, please share a link to your article rather than the

full-text. Millions of researchers have access to the formal publications on ScienceDirect, and so links will help your users to find, access, cite, and use the best available version. Theses and dissertations which contain embedded PJAs as part of the formal submission can be posted publicly by the awarding institution with DOI links back to the formal publications on ScienceDirect.

If you are affiliated with a library that subscribes to ScienceDirect you have additional private sharing rights for others' research accessed under that agreement. This includes use for classroom teaching and internal training at the institution (including use in course packs and courseware programs), and inclusion of the article for grant funding purposes.

**Gold Open Access Articles:** May be shared according to the author-selected end-user license and should contain a [CrossMark logo](#), the end user license, and a DOI link to the formal publication on ScienceDirect.

Please refer to Elsevier's [posting policy](#) for further information.

18. **For book authors** the following clauses are applicable in addition to the above: Authors are permitted to place a brief summary of their work online only. You are not allowed to download and post the published electronic version of your chapter, nor may you scan the printed edition to create an electronic version. **Posting to a repository:** Authors are permitted to post a summary of their chapter only in their institution's repository.

19. **Thesis/Dissertation:** If your license is for use in a thesis/dissertation your thesis may be submitted to your institution in either print or electronic form. Should your thesis be published commercially, please reapply for permission. These requirements include permission for the Library and Archives of Canada to supply single copies, on demand, of the complete thesis and include permission for Proquest/UMI to supply single copies, on demand, of the complete thesis. Should your thesis be published commercially, please reapply for permission. Theses and dissertations which contain embedded PJAs as part of the formal submission can be posted publicly by the awarding institution with DOI links back to the formal publications on ScienceDirect.

### **Elsevier Open Access Terms and Conditions**

You can publish open access with Elsevier in hundreds of open access journals or in nearly 2000 established subscription journals that support open access publishing. Permitted third party re-use of these open access articles is defined by the author's choice of Creative Commons user license. See our [open access license policy](#) for more information.

#### **Terms & Conditions applicable to all Open Access articles published with Elsevier:**

Any reuse of the article must not represent the author as endorsing the adaptation of the article nor should the article be modified in such a way as to damage the author's honour or reputation. If any changes have been made, such changes must be clearly indicated.

The author(s) must be appropriately credited and we ask that you include the end user license and a DOI link to the formal publication on ScienceDirect.

If any part of the material to be used (for example, figures) has appeared in our publication with credit or acknowledgement to another source it is the responsibility of the user to ensure their reuse complies with the terms and conditions determined by the rights holder.

#### **Additional Terms & Conditions applicable to each Creative Commons user license:**

**CC BY:** The CC-BY license allows users to copy, to create extracts, abstracts and new works from the Article, to alter and revise the Article and to make commercial use of the Article (including reuse and/or resale of the Article by commercial entities), provided the user gives appropriate credit (with a link to the formal publication through the relevant DOI), provides a link to the license, indicates if changes were made and the licensor is not represented as endorsing the use made of the work. The full details of the license are available at <http://creativecommons.org/licenses/by/4.0>.

**CC BY NC SA:** The CC BY-NC-SA license allows users to copy, to create extracts,

abstracts and new works from the Article, to alter and revise the Article, provided this is not done for commercial purposes, and that the user gives appropriate credit (with a link to the formal publication through the relevant DOI), provides a link to the license, indicates if changes were made and the licensor is not represented as endorsing the use made of the work. Further, any new works must be made available on the same conditions. The full details of the license are available at <http://creativecommons.org/licenses/by-nc-sa/4.0>.

**CC BY NC ND:** The CC BY-NC-ND license allows users to copy and distribute the Article, provided this is not done for commercial purposes and further does not permit distribution of the Article if it is changed or edited in any way, and provided the user gives appropriate credit (with a link to the formal publication through the relevant DOI), provides a link to the license, and that the licensor is not represented as endorsing the use made of the work. The full details of the license are available at <http://creativecommons.org/licenses/by-nc-nd/4.0>.

Any commercial reuse of Open Access articles published with a CC BY NC SA or CC BY NC ND license requires permission from Elsevier and will be subject to a fee.

Commercial reuse includes:

- Associating advertising with the full text of the Article
- Charging fees for document delivery or access
- Article aggregation
- Systematic distribution via e-mail lists or share buttons

Posting or linking by commercial companies for use by customers of those companies.

## 20. Other Conditions:

v1.9

**Questions? [customercare@copyright.com](mailto:customercare@copyright.com) or +1-855-239-3415 (toll free in the US) or +1-978-646-2777.**